The Skin as a Window on Mechanisms of Neuropathy and Neuropathic Pain

By

Elspeth Jane Hutton

January 2016

A thesis submitted to University College London for the degree of Doctor of Philosophy

Declaration

I, Elspeth Jane Hutton, confirm that the work presented in this thesis is my own. Where information has been derived from other sources, I confirm that this has been indicated in the thesis.

25/1/2016

List of Figures

List of Tables

Abbreviations

ACE	angiotensin converting enzyme
ADM	abductor digiti minimi
AMH	A-mechanoheat sensitive afferent
ANA	antineuronal antibody
AP-1	activator protein-1, a family of dimeric basic leucine zipper (bZIP) transcription factors, comprising members of the Jun, Fos and activator transcription factor (ATF) subfamilies
APC	antigen presenting cell
ASIC	acid-sensing ion channel
ASIC3	acid-sensing ion channel 3
ATF	activating transcription factor
ATP	adenosine triphosphate
α-MSH	alpha-melanocyte stimulating hormone
BNaC	acid-sensing ion channel (see also ASIC)
BK	bradykinin
BM-DC	bone-marrow derived dendritic cell
BDNF	brain-derived neurotrophic factor
CaMKII	Ca^{2+}/calmodulin-dependent protein kinase II
cAMP	cyclic adenosine monophosphate
CCI	chronic constriction injury
CCL (2, 5, 17, 22)	chemokine (C-C motif) ligand
CD11c	cluster of differentiation 11c (Integrin, a dendritic cell marker)
CD1a	cluster of differentiation 1a (Langerhans cell marker)

CD4	cluster of differentiation 4 (Th subset cell marker (also monocyte, macrophage & dendritic cells)
CD8	cluster of differentiation 8 (Natural killer T-cell marker (also dendritic cells))
CD 45	cluster of differentiation 45 (leucocyte common antigen)
CD 68	cluster of differentiation 68 (monocyte / macrophage marker)
CD 207	cluster of differentiation 207 (Langerin, Langerhans cell marker)
CDT	cold detection threshold
c-Fos	human oncogene homologous to Finkel-Biskis-Jinkins (FBJ) murine osteosarcoma virus oncogene.
CGRP	calcitonin gene-related peptide
CIDP	chronic inflammatory demyelinating polyradiculoneuropathy
c-Jun	homolog of the oncogene v-Jun (putative transforming gene of avian sarcoma virus) 17
CMH	C-mechanoheat sensitive afferent
CM_iH_i	C-mechano and heat insensitive afferent
CMT	Charcot-Marie Tooth (disease)
COX-2	cyclooxygenase-2
CPT	cold pain threshold
CXCL (2, 3, 10)	chemokine (C-X-C motif) ligand
DAB	3,3’-Diaminobenzidine
DAG	diacylglycerol
DAMP	damage-associated molecular pattern
DC	dendritic cell
DFNS	Deutsches Forschunsnetz (German Research Network)
DMA	dynamic mechanical allodynia

DM	demyelination / demyelinating
DML	distal motor latency
DPX	dibutyl phthalate
DRG	dorsal root ganglion
dsDNA	double-stranded deoxyribonucleic acid
EDB	extensor digitorum brevis
ELISA	enzyme-linked immunosorbant assay
EMG	electromyography
ENA	extractable nuclear antigen
ERG2	early growth response gene 2 (human analog to Krox-20)
ERK 1/2	extracellular-signal-regulated kinase 1/2
ERT	enzyme-replacement therapy
FRAP	fluoride-resistant acid phosphatase
Gb3, GL-3	globotriaosylceramide
GBS	Guillain-Barré sydrome
GDNF	glial cell line-derived neurotrophic factor
GM-CSF	granulocyte macrophage colony stimulating factor
GTP	guanosine triphosphate
HaCaT	immortal keratinocyte cell line
HADS	Hospital Anxiety and Depression Scale
HPT	heat pain threshold

IB4	isolectin B4
IENFD	intraepidermal nerve fibre density
IFN-Y	interferon-gamma
IL (1β, 2, 3, 4, 6, 10, 12, 17, 21, 22)	interleukin (1β, 2, 3, 4, 6, 10, 12, 17, 21, 22)
iNOS	inducible nitrogen oxide synthetase
IP-10	interferon gamma-induced protein 10 (also known as CXCL10)
IP_3	inositol triphosphate
JNK	c-Jun N-terminal kinase
Krox-20	Murine homonolog of human EGR 2 (early growth response gene 2)
LC	Langerhans' cell
LLOQ	lower limit of quantification
LOB	limit of blank
LOD	limit of detection
MAPK	mitogen-activated protein kinase
MKP	MAPK phospholipase
MKK	MAPK kinase
MBP	myelin basic protein
MCP-1	monocyte chemoattractant protein-1 (also known as CCL2)
MCV	motor conduction velocity
mDC	monocyte-derived dendritic cell
MDT	mechanical detection threshold

MHCII	major histocompatibility complex class II
MMP-1	matrix metalloproteinase-1
MPS	mechanical pain sensitivity
MPT	mechanical pain threshold
mRNA	messenger ribonucleic acid
MSH	melanocyte stimulating hormone
МΦ	macrophage
NADA	*N*-arachidonoyl dopamine (a TRPV1 agonist)
NALP-1	NACHT, LRR and PYD domains-containing protein 1
NEP	neutral endopeptidase
NF-κB	nuclear factor kappa-light-chain-enhancer of activated B cells
NF200	neurofilament (200kDa subunit)
NGF	nerve growth factor
NGFβ	nerve growth factor (beta subunit)
NK_1	neurokinin 1 (substance P receptor)
NO	nitric oxide
NP	neuropathy
NPSI	neuropathic pain symptom inventory
NSF	*N*-ethylmaleimide sensitive fusion proteins
NT3	neurotrophin-3
OCT	optimal cutting temperature mounting medium
OX-40	CD134 (TNFRSF4, a member of the TNF receptor superfamily)
$P_2X(3, 4, 7)$	purinergic receptor type 2X (ligand-gated ion channel type)

P_2Y1	purinergic receptor type 2Y (G-protein-coupled receptor)
p38-MAPK	p38 mitogen-activated protein kinase
PBS	phosphate-buffered saline
PCR	polymerase chain reaction
PGE2	prostaglandin E2
PGP 9.5	protein gene-product 9.5
PHS	paradoxical heat sensation
PICK	proinflammatory cytokine
PIP_2	phosphatidylinositol 4,5-biphosphate
Pirt	phosphoinositide-interacting regulator of transient receptor potential channels
PKA	protein kinase A
PKC	protein kinase C
PLA_2	phospholipase A2
PLC	phospholipase C
PLP	proteolipid protein
PMP22	peripheral myelin protein 22
POEMS	syndrome of polyneuropathy, organomegaly, endocrinopathy, monocloncal paraprotein and skin changes
PPT	pressure pain threshold
RacGTP	subfamily of Rho guanosine triphosphatases
RANK	receptor activator of nuclear factor kappa B
RANKL	receptor activator of nuclear factor kappa B ligand
RANTES	regulated on activation, normal T-cell expressed and secreted (also known as CCL5)
Ret	rearranged during transfection (tyrosine kinase receptor for GDNF family ligands)

RF	receptive field
RhoA	Ras homolog gene family, member A (small GTPase)
RIA	radioimmuoassay
RP1	retinitis pigmentosa 1 protein
S-100	family of small, dimeric calcium and zinc binding proteins.
SAP	sensory action potential
SC	Schwann cell
SCV	sensory nerve conduction velocity
SFN	small fibre neuropathy
SG	substantia gelatinosa
SM	sensorimotor
SNARE	SNAP (soluble NSF attachment protein) receptor
SOM	somatostatin
SP	substance P
V-SNARE	vesicle SNARE
TBS	Tris-buffered saline
TGF	transforming growth factor
TGF-β	transforming growth factor beta
Th(1, 2, 17)	T-helper(1, 2, 17)
TLI	terminal latency index
TNF-α	tumour necrosis factor alpha
Tris	2-Amino-2-hydroxymethyl-propane-1,3-diol
TrkA	tropomyosin receptor kinase A (high affinity NGF receptor)
TRP	transient receptor potential channel

TRPA1	transient receptor potential ion channel (ankyrin)
TRPM8	transient receptor potential ion channel (melastatin)
TRPV	transient receptor potential ion channel (vanilloid)
TSL	thermal sensory limens
TTR	tranthyretin
TTX-R	tetrodotoxin resistant
TTX-S	tetrodotoxin sensitive
UVB	ultraviolet B
VAS	visual analogue scale
VD_3	Vitamin D_3
VDR	vitamin D receptor
VDT	vibration detection threshold
VIP	vasoactive intestinal peptide
VR1	transient receptor potential ion channel (vanilloid)
WDT	warm detection threshold
WUR	wind-up ratio

Ackowledgements

I would like to thank my supervisors, Prof Martin Koltzenburg and Dr Michael Lunn for their support and guidance in allowing me to develop and undertake this project. I would also like to thank Prof Mary Reilly, who supervised much of the c-Jun work, and has been an unfailing source of encouragement and guidance throughout the project.

Thanks to Dr Rosalind King for her kind donation of some of the nerve tissue used in the c-Jun study. Thanks to the clinicians who helped me to recruit the patients for the Anderson-Fabry study: Dr Robin Lachmann (National Hospital for Neurology and Neurosurgery, London), Prof Atul Mehta and Dr Derralynn Hughes (The Royal Free Hospital, London), and to all of the patients and volunteers who agreed to take part in these studies.

I would also like to thank Prof Michael Polydefkis, and particularly Peter Hauer at the Johns Hopkins Cutaneous Nerve Laboratory for all of their valued advice and guidance while I was establishing the IENFD skin biopsy technique. Thanks also to Dr Roman Rukwied and Prof Martin Schmelz at the University of Heidelberg, Mannheim for taking the time to teach me how to perform the dermal microdialysis technique. Thanks to Dr Dorren Pfau and Prof Walter Magerl at the University of Heidelberg, Mannheim for taking the time to teach me the DFNS quantitative sensory testing protocol. Thanks also to the Neuroimmunology Laboratory at the Institute of Neurology and Dr Elizabeth King at the London School of Hygiene and Tropical Medicine for their assistance in helping me set up and run the ELISAs.

Thanks to The Ipsen Fund, The BMA Vera Down Fellowship and the EFIC-Grunenthal Grant for funding my research, and to the UCLH Charities Clinical Research and Development committee research fund who provided funding for the c-Jun study. Without these bodies, it would not have been possible to undertake these studies.

Finally, unending thanks to my parents, for their unfailing encouragement and support through this project, and their endless proof-reading patience!

Table of Contents

The Skin as a Window on Mechanisms of Neuropathy and Neuropathic Pain

Abstract

Neuropathies are common, yet the pathogenic mechanisms of many remain incompletely understood. Animal and cell models have provided much useful information about disease mechanisms, and yet translation of this knowledge to clinical practice and disease therapies is often disappointing. One of the difficulties in studying human nerves is limited availability of tissue, due to the morbidity of peripheral nerve (usually sural nerve) biopsy. I sought to evaluate the utility of cutaneous nerves, both generally as a tool to assess the relevance of pathogenic mechanisms identified in animal studies in human disease, and also specifically in evaluating whether immune changes in the skin may play a role in the development of neuropathic pain.

Animal models have suggested that proinflammatory cytokines exert algesic effects on nerves, whilst anti-inflammatory cytokines have a counter-regulatory analgesic effect (Üçeyler et al., 2009). More recently, support for a link between variability in systemic and / or local cytokine balance and pain in neuropathy has begun to emerge (Üçeyler et al., 2007c, Üçeyler et al., 2010). Despite some support for a link between painful neuropathies and increased inflammatory and / or decreased anti-inflammatory cytokines, it remains unclear whether the immune changes reflect underlying neuropathological processes, a response to nociceptor activation, variability in individual immune response to nerve damage or are a biomarker of another factor indirectly modulating both pain and immune function. It is also unclear whether immune-nerve interactions are unidirectional or bidirectional:

does increased nociceptor firing modulate local immune function or does immune response to nerve damage modulate activity of remaining undamaged fibres, or is there a combination of these factors? I sought to understand the effect of acute nociceptor activation on skin immune profile, as well as whether changes in chronic neuropathy would be associated with the presence and intensity of pain.

Chapter 1: Introduction

The skin has important protective and homeostatic roles. It acts as a sensor and effector organ for initial immune responses to pathogens, autonomic regulatory responses, hormonal regulation, and physical sensing of the environment. Previously considered to be a simple inert barrier, recent research has elucidated a number of important bidirectional neuroimmune interactions which may be pertinent in understanding both neuropathic pain and the modulation of skin integrity by nerves, a key issue in preventing the ulceration and infection suffered by many patients with peripheral neuropathy. These include the role of neurogenic inflammation in chronic skin inflammatory conditions (Chapman and Moynihan, 2009), Langerhans cell function (Ding et al., 2008, Hosoi et al., 1993), wound healing (da Silva et al., 2010) and regulation of hair growth cycling (Hendrix et al., 2008). Conversely, cytokines (Üçeyler et al., 2009), growth factors (Pezet and McMahon, 2006), and purines (Dussor et al., 2009) released by skin cells modulate neural plasticity and function, with the potential to contribute to the persistence of neuropathic pain and itch.

Why study skin nerves?

Histological study of the skin is an attractive model in which to study human neuropathic mechanisms. It is easily accessible, with punch biopsy an easy technique with minimal morbidity and the ability to study changes over time. This provides a distinct advantage over sural nerve biopsy, which has hitherto been the only method available to examine nerve biology. Skin biopsies have been used for nearly 20 years to examine small fibre innervation density (McCarthy et al., 1995),

but the idea of exploring pathogenic mechanisms using epidermal and dermal nerves is in its infancy (Katona et al., 2009). There are also some exciting developments in the use of skin biopsy to diagnose CNS disease, such as synucleinopathies, tauopathies and neuronal intranuclear inclusion disease with leucoencephalopathy (Brennan et al., 2015, Jerath and Shy, 2015, Shy et al., 1996). In order to understand the pathogenic mechanisms in neuropathy, particularly the frequently 'idiopathic' small fibre neuropathy, the ability to study human pathology in a relatively non-invasive fashion would be of immense benefit in understanding disease mechanisms and developing treatment strategies. It may also allow better evaluation of the efficacy of therapies, which are often disappointing in their translation from animal to human models. Study of skin nerves could help bridge this gap.

How could skin nerves help us understand neuropathic pain?

Neuropathy, and particularly neuropathic pain, are conditions with significant morbidity, but very limited therapeutic options. Although pain is more commonly associated with particular types of neuropathy, we do not understand why different individuals with the same underlying disease vary widely in both the presence and intensity of pain that they suffer, but also in their pharmacological response. The skin is an attractive site to study both disease mechanisms in neuropathy, and potential biomechanisms in neuropathic pain for a number of reasons:

- It is readily accessible, and suitable for repeated studies over time. This is particularly important in pathological studies in humans, as other sources of

nerve tissue for study, such as sural nerve biopsy, involve morbidity and may only be studied once.

- It is the site of target action of many sensory nerves, allowing study of the fibres in the context of their terminal receptive field, and the factors in that field which may affect their function; and
- It allows correlation of pathological, biochemical and functional mechanisms through the use of quantitative sensory testing in combination with histological and biochemical techniques, providing a more complete understanding of the environment in which sensory nerves function.

This PhD project was designed to demonstrate the utility of skin nerves for studying mechanisms in neuropathy, and in particular to try to understand mechanisms affecting the genesis of pain in humans, with a view to potentially identify new approaches to treatment.

The focus of my thesis is to explore the utility of the skin as a window through which to study pathobiological process in neuropathy, and more particularly neuropathic pain, using methods with minimal patient morbidity. The skin is a readily accessible tissue, with rich innervation by several different fibre types and has potential as a window through which to examine neuropathological processes, both from a natural history and response to therapy perspective. Currently studies of cutaneous innervation have centred on studies of epidermal nerve fibre density as a measure of small fibre neuropathy. This is beginning to expand to include studies of myelinated fibres (Li et al., 2005, Katona et al., 2009) and methods to quantify autonomic innervation (Nolano et al., 2010, Sommer and Lauria, 2007).

There remains, however, much scope for using skin nerves to study mechanisms of disease, and in pain to try to elucidate mechanisms in order to develop new therapeutic options. In particular, a focussed study using a broader range of immunohistochemical and biologic methods, combined with functional and behavioural correlates offers potential for evaluating the pathogenic relevance of recently proposed immune pathways in human neuropathic pain.

The first part of the project explores the utility of dermal nerve fibres in understanding whether mechanisms recently identified in animal models of demyelination are also relevant in human disease. The second explores whether acute activation of nociceptors can evoke immune response in the skin. The final section examines whether cellular or humoral immune changes in the skin are linked with pain in a genetic human small fibre neuropathy, Fabry's disease.

Overall structure of PhD thesis

1. Use of cutaneous nerves to evaluate pathogenic mechanisms in neuropathy

This section of the project is a pilot study to establish whether nerves in human skin undergo changes in signalling kinases identified in animal research. c-Jun is a transcription factor recently identified as a key modulator of Schwann cell dedifferentiation and demyelination in injured nerves in animal studies (Jessen and Mirsky, 2008). This project used a combination of sural and dermal nerve biopsies to determine whether c-Jun expression was increased in human neuropathies, and whether these changes could be identified in dermal nerves as well as sural nerves. The work has recently been published in the Journal of the Peripheral Nervous System (Hutton et al., 2011).

2. Use of dermal microdialysis to determine the immune effect of acute nociceptor activation

The second part studied whether acute activation of cutaneous nociceptors by topical capsaicin would alter the skin's immune profile, which is the focus of this MPhil upgrade submission and will be discussed below. The aim of this section of the project was two-fold. Firstly, I wished to establish that dermal microdialysis in normal controls was able to detect the cytokines of interest, and to establish the operating range of the assay. Secondly, I wished to determine whether acute activation of nociceptors altered the levels of cutaneous cytokines, as this has not previously been established.

3. Neuropathologic, immune and functional study of patients with Anderson-Fabry disease: does pain in neuropathy correlate with changes in skin immune profile

The final part of the project is a detailed clinical, neurophysiological, immunological and anatomical study of subjects with Anderson-Fabry neuropathy, to determine whether patients with greater pain related to their neuropathy exhibit pro-inflammatory changes in cutaneous immune profile, examining soluble factors and changes in the intrinsic epidermal immune cell, the Langerhans cell.

PhD research site and duration:

The work presented in this thesis was carried out in laboratories at the Institute of Child Health (Neural Plasticity Laboratory), and The Institute of Neurology (Neuroimmunology Laboratory), London School of Hygiene and Tropical Medicine (Wolfson Cell Biology Facility (Luminex)) and the MRC Centre for Neuromuscular Diseases. The research work was conducted between January 2009 and May 2012.

Chapter 2: Background: Neuroimmune and cutaneous biology, and their possible links with neuropathic pain.

Skin Innervation

The skin is densely innervated by free and specialised sensory nerve endings in the epidermis and dermis that supply the blood vessels and sweat glands. These nerves and their accessory structures detect various types of environmental stimuli (mechanical, chemical, thermal) and control autonomic components that regulate vascular tone in arteries and arterioles and the secretion of sweat from sweat glands (Rice and Albrecht, 2008).

The innervation of human skin varies depending on location. Skin is divided into two main types, namely glabrous skin, found on the palms and soles of the feet, and hairy skin. Glabrous skin has a thick epidermis which is penetrated by dermal papillae and lacks hair follicles (Rice and Albrecht, 2008). It contains Meissner's corpuscles and Pacinian corpuscles, which are absent in hairy skin, and more frequent Merkel cells than hairy skin. It also contains a higher proportion of larger myelinated afferents (Li et al., 2005). Cutaneous nerves enter the skin from collateral branches of the major nerves, e.g. branches of the digital nerves in the hand. These branches form a deep plexus that lies superficial to the level of the sweat glands and Pacinian corpuscles. Branches pass more superficially to form the superficial dermal plexus, a network of fibres running parallel to the skin surface, just deep to the dermal-epidermal junction (Wang et al., 1990). Nerve fibres decrease in diameter from around 5 µm in the dermal plexus to around 3 µm as they enter the dermal papillae in glabrous skin.

From dermal networks, fibres innervate cutaneous structures such as sweat glands, hair follicles, specialised sensory organs and blood vessels, or penetrate the epidermis as free nerve endings to run vertically between the keratinocytes. Ninety per cent of the dermal nerve fibres are unmyelinated on electron microscopy, and all fibres lose their myelin sheath at the dermal-epidermal junction (Ebenezer et al., 2007, McGlone and Reilly, 2010). Large, deep dermal nerves have an intact perineurium, but smaller, superficial nerves often lack perineurium, and are instead associated with partially encircling fibroblast-like cells without a basal lamina. Remak bundles are surrounded by collagen fibres, with closely applied Remak basal lamina (Ebenezer et al., 2007). Figure 1 below illustrates some of the key features of glabrous and hairy skin innervation.

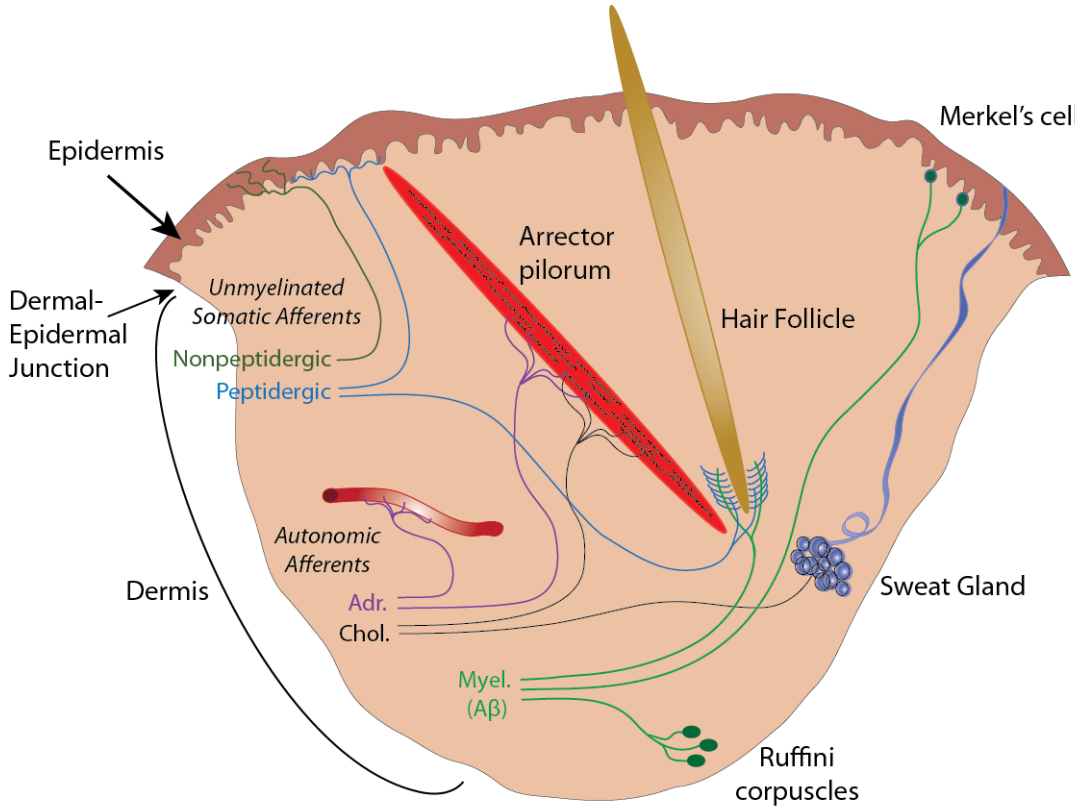

Figure 1A: Innervation of hairy skin

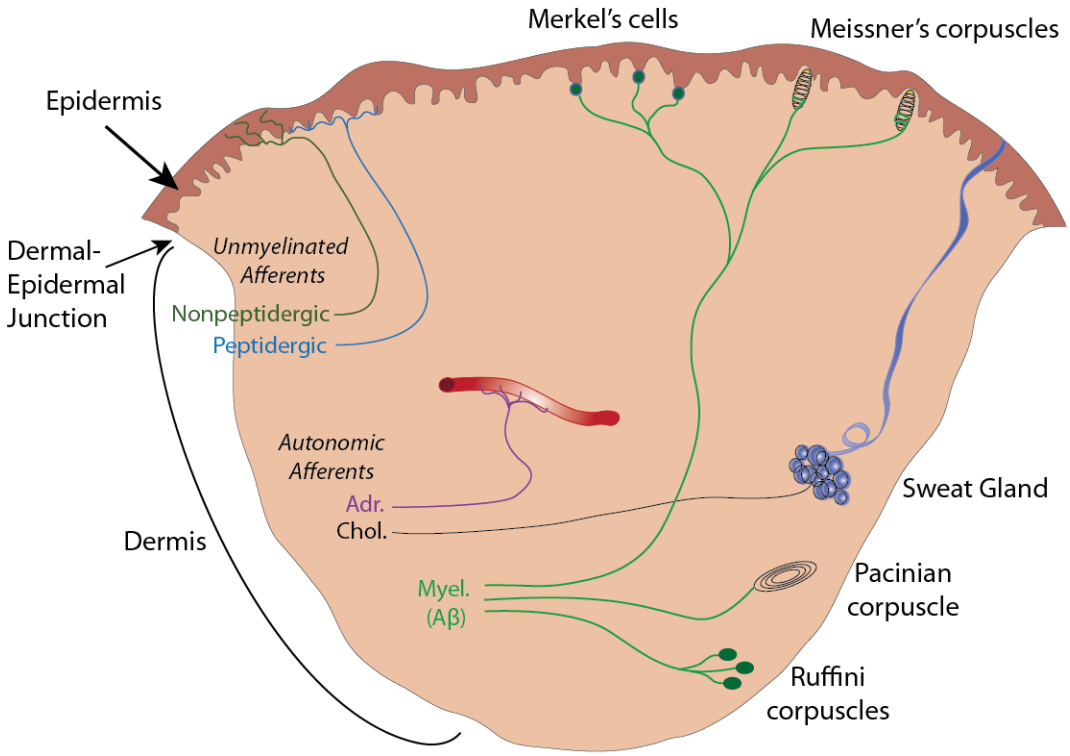

Figure 1B: Innervation of glabrous skin

Primary Sensory Afferents

Primary sensory afferents are specialised neurons that are activated by environmental stimuli rather than synaptic input from another nerve cell. Their cell bodies are located in the dorsal root ganglia with a process that bifurcates into an axon with a proximal and distal branch (pseudobipolar). These branches may both branch to form several central and peripheral connections for a single axon (Navarro et al., 2007, Schmidt and Rathjen, 2011). The proximal arm passes into the dorsal horn of the spinal cord, where some fibers form synapses with the neurons of the central nervous system, whilst others course caudally or rostrally to form synapses at other sites. The distal arm passes along the spinal and peripheral nerves to terminate as a free nerve ending or specialised sensory structure in the skin. As the skin is subject to a variety of sensory stimuli (mechanical, thermal and

chemical), normal sensory function is dependent on the ability to perceive and integrate a variety of sensory inputs in parallel. Within the skin, each ending responds to stimuli of its specialised modality over a defined area of skin, known as the receptive field. The size of the field varies with the type of sensory ending and the anatomical location (Rice and Albrecht, 2008, Bolton et al., 1966, Schmelz and Schmidt, 2010).

Sensory afferents may be classified according to neurophysiological, anatomical and biochemical characteristics, but there is often substantial overlap between subgroups. Fibres may share a common classification in one system of categorisation, but vary in other characteristics, precluding a clear subdivision of sensory neurons. Cutaneous sensory neurons are traditionally classified according to three key neurophysiological parameters: conduction velocity, the optimal modality for generation of an action potential, and rate of adaptation (time taken to stop responding to a continuously applied stimulus) (Rice and Albrecht, 2008). The large, myelinated Aβ are the fastest conducting sensory axons (35-75 ms^{-1}), followed by the smaller, thinly myelinated Aδ (5-30 ms^{-1}) with the thinnest, unmyelinated C fibres having the slowest conduction velocity (0.5 – 2 ms^{-1}). Figure 2 illustrates the central connections of the sensory afferents in different laminae of the dorsal horn.

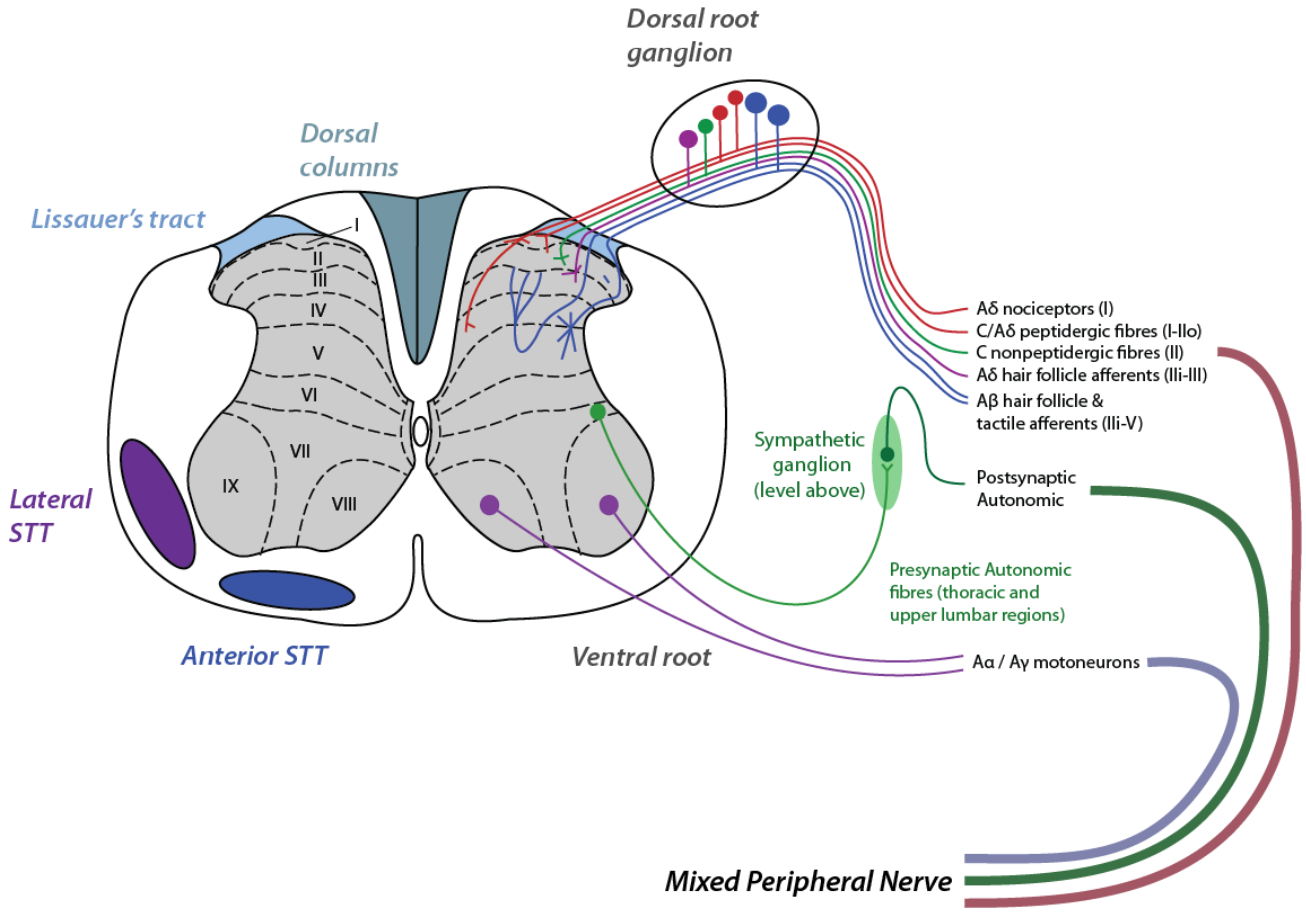

Figure 2: Central sensory connections and components of mixed peripheral nerves

Specialised transducers in the skin and other tissues translate sensory inputs into the electrical impulses transmitted to higher centres. Sensory neurons carry this information about mechanical force, change in temperature or chemical stimuli, with some responding selectively to low (mild) or high threshold stimuli (Scholzen et al., 1998). Chemical responses may be subdivided by the nature of the ligand, and include capsaicin, menthol, H^+, glutamate and ATP responsiveness, among others. Mechanical receptors may be divided by their response to the rate of application, duration and direction of the stimulus. Sensory neurons are classified as slowly adapting if they generate a prolonged train of action potentials in response to a sustained optimal stimulus, or as rapidly adapting if they generate a brief burst of action potentials when the stimulus is applied. Rapidly adapting afferents typically also generate a brief impulse train when the stimulus is removed (Gardner and Martin, 2000).

Nociceptors are defined as sensory nerve cells which make a response to noxious stimuli, with the resultant potential generating a perception of pain. These stimuli can be of the same modalities as those that generate nonnociceptive responses, but are considered to be of an intensity that has the potential to generate tissue damage. Nociception differs from other forms of sensation in a number of ways. Nociceptors are often polymodal, where other sensory modalities are specific or unimodal. Nociceptors often sensitise (that is increase their response) to repeated stimuli, whereas other sensory receptors typically adapt. Nociceptors are subdivided by stimulus response into thermal, chemical, mechanical or polymodal nociceptors. Another class of nociceptor, termed a metaboreceptor has been described near blood vessels in muscle. These co-express the acid-sensing ASIC3

receptor and CGRP and are thought to detect metabolic stress, triggering nociceptive signalling if there is insufficient oxygen to meet demand (Molliver et al., 2005).

Generally, low threshold mechanoreceptors tend to be faster conducting Aβ afferents, whilst high threshold mechanoreceptors, thermoreceptors, chemoreceptors and nociceptors tend to have afferents conducting in the Aδ or C fibre range (Rice and Albrecht, 2008). These divisions are not, however, absolute and the final perception of a tactile stimulus is a central product of the integration of a number of parallel inputs from individual fibre subtypes firing at variable intensities.

Free Nerve Endings

The majority of human cutaneous sensory neurons are unmyelinated free nerve endings, terminating primarily in the epidermis. These comprise the endings of a sensory axon in the target organ that lacks both a unique morphology and accompanying terminal glia or other accessory cells. Structurally, intraepidermal nerve fibres are unmyelinated, and their cytoskeletal composition is primarily of microtubules, with scant phosphorylated neurofilaments (Lauria et al., 2004). Fibres lose their Schwann cell wrapping at the dermal-epidermal junction, and are classified into two major subclasses, peptidergic and nonpeptidergic (McGlone and Reilly, 2010). The peptidergic fibres terminate in the deeper layers of the epidermis, whilst the nonpeptidergic fibres course between the keratinocytes to terminate more superficially (Zylka et al., 2005) (see figure 3).

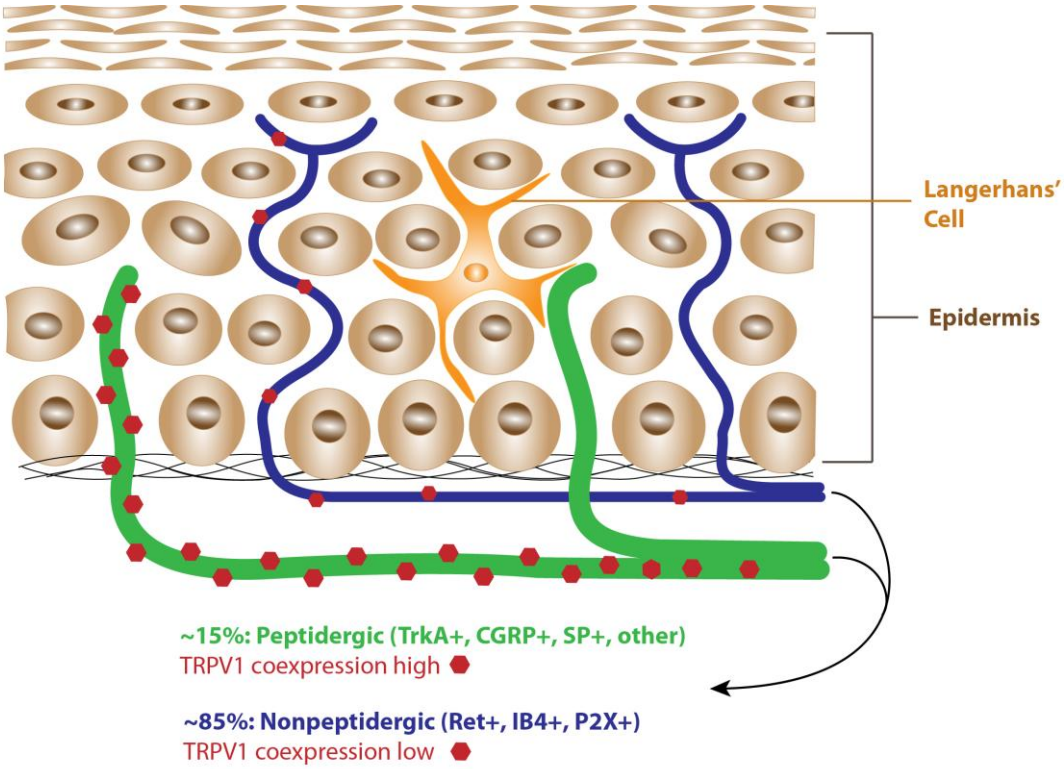

Figure 3: Epidermal termination of peptidergic and non-peptidergic fibres

Peptidergic and non-peptidergic innervation

Neuropeptides are small peptide molecules that mediate signalling between neurons, but also with other cell types and are often co-expressed with other neurotransmitters. They include several large families, but the ones most important in neurocutaneous biology are calcitonin gene-related peptide (CGRP) and substance P (SP). On depolarisation of peptidergic cutaneous nerves, neuropeptides are released from both the central terminal, to signal to dorsal horn neurons, and the peripheral collaterals, to exert local modulatory changes in the skin. These include mediation of the axonal flare reflex, as well as modulating the behaviour of keratinocytes, mast cells, Langerhans cells and other immune cells in the skin.

In the rat lumbar DRG, around 45% of cells are immunopositive for CGRP (compared to around 30% in the mouse), with a number co-expressing other neuropeptides,

such as substance P (SP) (Averill et al., 1995, Zwick et al., 2002). Most of these cells also express the NGF receptor, TrkA which labels around 45% of the total DRG population. The remaining cells (30% of DRG population) are composed of the small, isolectin B4 (IB4) / fluoride-resistant acid phosphatase (FRAP) positive population, most of which are peptide-negative, and cell bodies of larger, myelinated afferents (RT97 / NF200 positive), of which around 5% also express CGRP (Averill et al., 1995). Figure 4 illustrates the relative composition of DRG neurons based on rodent studies.

The innervation of the skin, mucosal surfaces and muscles differ in the relative proportions of peptidergic and nonpeptidergic fibres involved. In the rat, non-peptidergic fibres project predominantly to the skin and viscera, with few projections to skeletal muscle, whilst skeletal muscle and the viscera receive a higher proportion of CGRP-positive afferents (Bradbury et al., 1998, Perry and Lawson, 1998). Figure 5 illustrates the relative innervation of different target organs, based on data from rat studies, with the expression of neuropeptides and IB4 the same throughout the nerve fibre, from the DRG to the skin. The site of termination within the dorsal horn also varies, with nonpeptidergic afferents terminating in lamina II inner, whilst peptidergic ones terminate in lamina II outer and lamina I of the dorsal horn (see figure 2) (Basbaum and Bràz, 2010, Bradbury et al., 1998, Molliver et al., 1995).

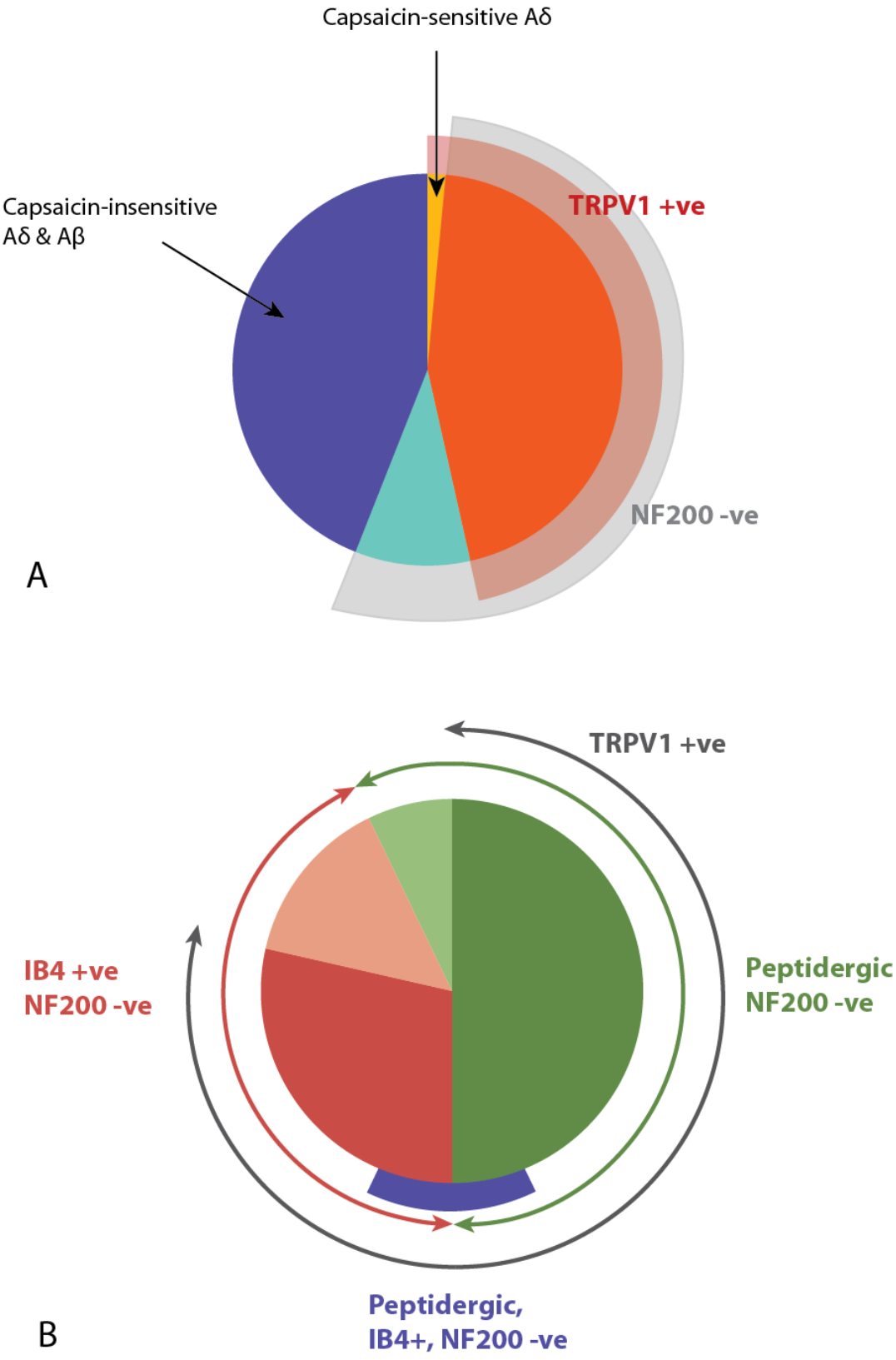

Figure 4: DRG neuron subgroups (based on rat studies):
A - Total DRG population
B - NF200 negative population (primarily unmyelinated fibres)
Adapted from: *Michaels & Priestley, J. Neurosci. 1999*

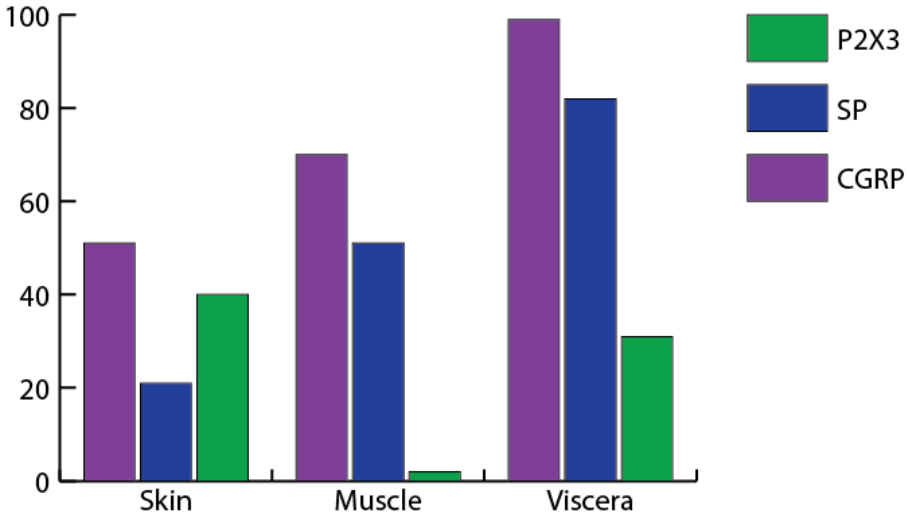

Figure 5: Variation in fibre subtypes by target organ innervation (in rat).
(Adapted from Perry & Lawson, 1998 and Bradbury et al, 1998)

The innervation of the epidermis and hair follicles is predominantly composed of non-peptidergic fibres, with CGRP positive fibres found mainly around blood vessels, sebaceous glands and sweat glands, with scant fibres terminating in the deep layers of the epidermis. There is limited data detailing epidermal CGRP innervation in humans, however a few studies in patients with pain or itch found CGRP innervation to comprise around 14% of the total fibre epidermal population (Wallengren and Sundler, 2004, Chao et al., 2007). The epidermal peptidergic fibres are thicker than their nonpeptidergic neighbours, with fewer branches but more varicosities, (Taylor et al., 2009). The nonpeptidergic fibres in the skin are predominantly P2X3 positive fibres, which largely overlap with the IB4 positive / GDNF-sensitive population of the DRG. Around 90% of IB4 positive neurons also show positive immunolabelling for P2X3. P2X3 is a cation-selective ligand-gated (ATP) channel, which generally exists as a dimer, either a homodimer or as a

heterodimer with P2X2 (Lewis et al., 1995, Bradbury et al., 1998, Zwick et al., 2002). TRPV1 is expressed on both peptidergic and non-peptidergic fibres, although there is more frequent expression on peptidergic fibres. Figure 3 illustrates epidermal innervation terminations of peptidergic and non-peptidergic fibres. Note that non-peptidergic fibres represent around 85% of epidermal innervation, and peptidergic 15%, but are not illustrated proportionately in order to demonstrate the termination levels in the epidermis.

Differences have been observed between peptidergic and non-peptidergic epidermal nerve fibres in the context of neuropathy. In a model of murine streptozotocin-induced diabetic neuropathy, early loss of the peptidergic population correlated with reduced mechanical, thermal and chemical sensitivity, with nonpeptidergic fibre loss occurring later, with no accompanying change in sensory phenotype (Johnson et al., 2008). Recovery of cutaneous innervation following chronic constriction injury in rats also showed greatly delayed recovery of myelinated and non-peptidergic fibres compared to peptidergic reinnervation (Peleshok and Ribeiro-da-Silva, 2011).

The peptides of unmyelinated nerve fibres in skin

1. CGRP

Calcitonin gene-related peptide (CGRP) has a variety of effects on the skin. It induces keratinocyte proliferation and production of cytokines (TNF-α, IL-1α, IL-8) and NGF (Takahashi et al., 1993, Yu et al., 2009, Dallos et al., 2006). CGRP positive fibres are closely apposed to other non-neural cells in the epidermis, with up to 80% of Langerhans' cell bodies found in relation to CGRP-IR nerve fibres (Hosoi et al.,

1993, Gaudillere et al., 1996). Possibly as a result Langerhans' cells alter with neural modifications. Langerhans cell numbers increase following peptidergic denervation, whether by nerve injury or selective denervation of the capsaicin-sensitive, primarily peptidergic population, reducing to previous levels with epidermal reinnervation (Stankovic et al., 1999, Hsieh et al., 1996, Beresford et al., 2004). Neuropeptides released by peptidergic fibres can also modulate Langerhans' cell function (Asahina et al., 1995, Ding et al., 2007, Ding et al., 2008). In this context, CGRP exerts a tonic anti-inflammatory effect by reducing Langerhans' cell (LC) density, suppressing antigen presentation and cell migration, as well as shifting LC cytokine production toward an anti-inflammatory Th2 profile. This results in reduced antigen presenting ability and a shift in cytokine and chemokine production, such that LCs secrete increased Th2 and decreased Th1 chemokines and cytokines. Close contacts exist between intraepidermal nerve fibres and LCs, and denervation, with loss of the tonic effect of CGRP, shifts their cytokine and chemokine profiles to a more inflammatory, Th1 profile. (Hosoi et al., 1993, Ding et al., 2007, Ding et al., 2008, Niizeki et al., 1997).

Mast cells also have close contacts with CGRP positive fibres (Botchkarev et al., 1997). CGRP increases TNF-α (Niizeki et al., 1997) and promotes release of histamine from mast cells, although less potently than SP (Piotrowski and Foreman, 1986).

Keratinocytes also express receptors for CGRP, with stimulation inducing cAMP and calcium mobilisation (Peters et al., 2006). CGRP also promotes melanogenesis, through stimulating keratinocyte α-MSH release (Toyoda et al., 1999).

Substance P

SP is produced in neurons of the peripheral and central nervous system. Substance P (SP) is an undecapeptide belonging to the tachykinin family, which on binding to its high affinity receptor NK1, can activate two key G-protein pathways: phospholipase C (PLC) activation, which cleaves PIP_2 (phosphatidylinositol 4,5-biphosphate) to DAG (diacyleglyceral) and IP_3 (inositol (1,4,5) triphosphate); and activation of adenylate cyclase to increase cAMP (Douglas and Leeman, 2011). SP is used as an excitatory neurotransmitter by nociceptors, where it is often colocalised with CGRP.

SP release also acts on the skin in a number of ways. It regulates wound healing, hair follicle cycling (Delgado et al., 2005, Peters et al., 2001), has effects on mast cells and modulates the cytokine profile of Langerhans' cells (Mathers et al., 2007). The effects of substance P are dose dependent, with lower concentrations (10^{-11}M) mediating trophic and immunomodulatory effects, higher concentrations (10^{-8}M) inducing plasma extravasation, but only the highest concentrations (10^{-5}M) causing mast cell degranulation (Weidner et al., 2000).

Mast cells are highly expressed at sites of exposure to external antigen, including the upper dermal skin, respiratory tract and bowel mucosa, as well as being prominent perivascularly and near neurons, with frequent close apposition to peptidergic nerve fibres observed (Harvima et al., 2010). Substance P-induced mast cell degranulation releases a variety of other inflammatory mediators, including histamine, TNF-α, chemotactic chemokines (MCP-1, IP-10, RANTES, IL-8) and IL-3. These mediators promote recruitment and activation of T-lymphocytes, eosinophils

and other inflammatory cells (Kulka et al., 2008, Ansel et al., 1993, Cocchiara et al., 1999, Maggi, 1993).

Langerhans' cells express the Substance P receptor, NK1. Activation of NK1 promotes a shift in Langerhans' cells to a more inflammatory, Th1 phenotype, with increased antigen presenting capability, MHC II expression, NF-κB activation, and inflammatory cytokine (IL-2, IL-12 and IFN-γ) production (Marriott and Bost, 2001, Lambrecht, 2001). Thus, SP acts on immune tone in Langerhans' cells in an opposite manner to CGRP.

Human keratinocytes (particularly in the deeper half of the epidermis) also express the substance P receptor, NK1 (Pincelli et al., 1993, Scholzen et al., 1998, Peters et al., 2006). Binding of SP activates keratinocytes through PLC, increasing inositol 1,4,5-triphosphate (IP_3), calcium mobilisation, and activation of activated protein C activation and NF-κB (Peters et al., 2006). Activation of keratinocytes increases release of IL-1α, IL-1β, IL-8, NGF and TNF-α (Dallos et al., 2006). In addition to increasing synthesis of pro-IL-1β, substance P also increase keratinocyte production of the NALP-1 inflammasome (nucleotide-binding domain, leucine-rich repeat-containing receptor protein) and caspase-1, which are necessary to cleave pro-IL-1β into its active form (Feldmeyer et al., 2010).

Neurogenic inflammation and the flare response

Activation of the terminal receptive field of nociceptors may produce a flare response, as well as sensitisation, which has both peripheral and central aspects.

Neurogenic inflammation

Neurogenic inflammation is the inflammatory response generated by antidromic depolarisation of local arborisation of the terminal branches of peptidergic nociceptors that occurs in addition to orthodromic central signalling. It is the mechanism underlying the neurogenic flare that may be recorded using laser Doppler imaging (see Chapter 4). Neuropeptide release (particularly substance P and CGRP) acts on blood vessels to cause vasodilatation and protein extravasation. SP induces a brief peak of vasodilation with a more prolonged increase in plasma extravasation, whilst CGRP induces greater and more sustained vasodilation, but not plasma extravasation (Weidner et al., 2000, Scholzen et al., 1998). Plasma extravasation is much less prominent in humans than in rodents (Sauerstein et al., 2000).

Antidromic axonal reflex activation and subsequent substance P release induces degranulation of mast cells, which in addition to releasing histamine, also release cellular stores of SP. Mast cell SP is particularly important in the production of the wheal element of the reaction. Nociceptor blockade by local anaesthetic or capsaicin inhibits the flare, but not the wheal (Cocchiara et al., 1999, Ansel et al., 1993, Foreman et al., 1983).

A potentially positively reinforcing cycle of peptidergic neuroinflammation is terminated by the action of peptidases, particularly angiotensin converting enzyme (ACE) and neutral endopeptidase (NEP), which are produced by keratinocytes, vascular endothelial cells and fibroblasts (Roosterman et al., 2006).

Nociceptor sensitisation

Following injury or nociceptor activation with heat or mechanical stimuli, changes in sensory response occur in the stimulated area and the surrounding skin. The area of initial nociceptor activation develops primary mechanical and thermal hyperalgesia, that is, a decrease in pain threshold (Treede et al., 1992). Primary hyperalgesia occurs to heat and mechanical stimuli, whilst secondary hyperalgesia is considered only to occur to mechanical stimuli (Treede et al., 1992). In primary hyperalgesia nociceptors are sensitised, with left-shift of the stimulus-response curve, reduced thresholds, an augmented response to suprathreshold stimuli and ongoing spontaneous activity (Meyer et al., 2006). The type and extent of sensitisation is dependent upon the tissue involved and the type of nociceptor. C-mechanoheat sensitive afferents (CMH) in hairy skin become sensitised to heat, whilst those in glabrous skin do not, with heat sensitisation occurring in Type I A-mechanoheat (AMH type I) sensitive afferents in glabrous skin (Campbell and LaMotte, 1983, Meyer and Campbell, 1981).

Secondary mechanical hyperalgesia develops in a zone around the area of injury or activation, and extends beyond the region of the flare response. Local anaesthetic blockade of myelinated fibres blocks development of the flare response, but not mechanical hyperalgesia, suggesting that while flare is dependent on local innervation, mechanical hyperalgesia is not (Klede et al., 2003). Secondary dynamic mechanical allodynia is prevented by compression block of larger myelinated afferents, indicating a myelinated-fibre dependent central modulation, while spontaneous pain, heat hyperalgesia and static pressure pain threshold are not affected by compression block, indicating dependence of peripheral unmyelinated

afferents (Koltzenburg et al., 1992). Cooling also reduces primary, but not secondary hyperalgesia, indicating a peripheral site of modulation (Koltzenburg et al., 1992). Figure 6 illustrates some of the key features of the flare response and regions of hyperalgesia following injury or nociceptor activation.

In humans, microneurography and microdialysis studies have confirmed that the flare response is mediated by C- fibre afferents that are not responsive to mechanical or heat stimulation (CM_iH_i). However these become responsive to these stimuli following sensitisation. They have a larger receptive field than C-mechanosensitive fibres, and are activated by pungent chemicals, such as capsaicin. Some fibres in this population mediate itch (Schmelz et al., 2000, Schmelz and Schmidt, 2010). In humans and pigs, the flare response is primarily mediated by CGRP-induced vasodilatation, with little SP induced plasma extravasation, while rats show a larger SP component to the flare (Schmelz et al., 2000, Schmelz et al., 1997).

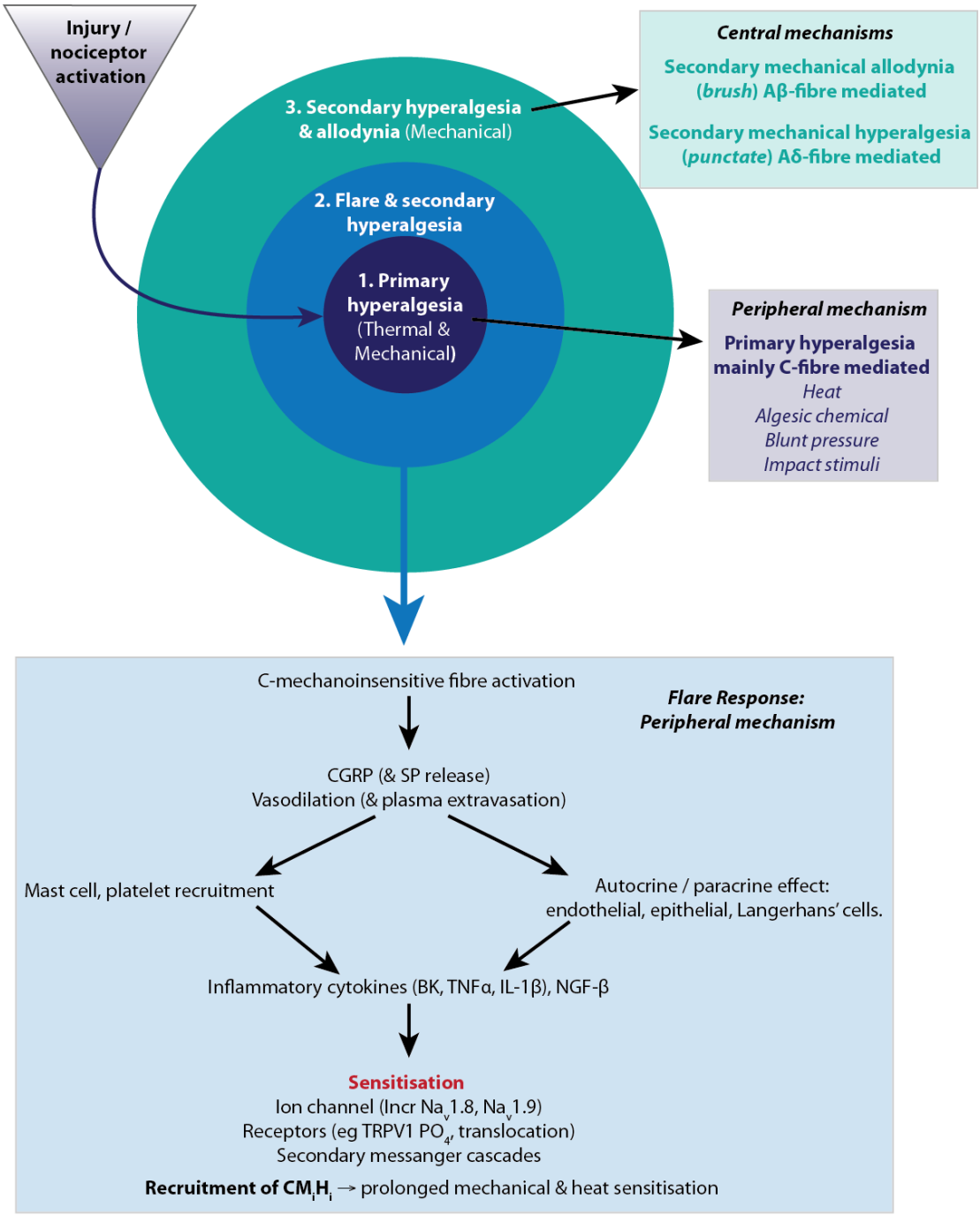

Figure 6: Key elements of cutaneous flare response and regions of sensitisation

Sensory Transduction

Sensory receptors transduce stimulus characteristics and induce the initial neural responses in the sensory system. In addition to their location, neurophysiological characteristics and morphology, the activation of sensory receptors is dependent

upon the combination of molecular transduction molecules that they express and these can be modified by the surrounding milieu. Normal sensory transduction of thermal, mechanical and chemical stimuli is mediated by a variety of ion channels and G-protein coupled receptors within the transducers themselves. These include the transient receptor potential channels (TRP), brain sodium channel / acid-sensing ion channels (BNaC/ASIC), purinergic receptors (P_2X, P_2Y) and others (Lumpkin and Caterina, 2007). These receptors and channels may be modulated by mediators released in pathological conditions, such as inflammation or nerve injury contributing to peripheral sensitisation.

Capsaicin & its receptor, TRPV1

Effects of capsaicin in models of pain

Capsaicin applied topically to the skin induces acute burning pain, and has been used as a model of acute sensitisation in normal healthy subjects. Topical capsaicin results in primary hyperalgesia over the treated area. Intracutaneous capsaicin elicits a dose dependent response, with increasing severity, pain duration and area of hyperalgesia with increasing dose from 0.1 – 100 µg (Simone et al., 1989). Surrounding the area of primary hyperalgesia, a region of secondary hyperalgesia develops.

Sensitisation techniques are useful to assess the functional changes associated with nociceptor activation, however they are less helpful in completely modelling neuropathic pain biology, as despite the ability to simulate some aspects of neuropathic pain (e.g. hyperalgesia), they are all limited in their inability to evoke ongoing, severe spontaneous pain, a characteristic of patients with neuropathic

pain. As such, our current human models can only partially mimic the clinical picture of neuropathic pain. Topical capsaicin is, however an established non-invasive method of robustly activating nociceptors, evoking axonal flare and visibly inflaming the skin without inducing tissue damage. Although the vascular and sensory components of neurogenic inflammation are well established, the effect of acute activation of nociceptors on the local immune profile has not been determined, and is explored further in chapter 4 of this thesis. This is of interest in light of recent studies suggesting immune activity may play a role in neuropathic pain.

Discovery of TRPV1

Capsaicin (trans-8-methyl-*N*-vanillyl-6-nonenamide) is a crystalline, lipophilic odourless alkaloid in the vanilloid family. Columbus made the first Western reports of the hot spicy effects of capsaicin in his journal in 1493. The active component, capsaicin (then called 'capsicol') was first crystallised in 1876 by Tresh, and its molecular structure was determined in 1919 by Dawson (Reyes-Escogido et al., 2011). A selective action of capsaicin on sensory neurons was proposed in 1878 by Hogyes (Caterina and Julius, 2001), but it was not until the 1950s that Jancsó et al. reported that in addition to stimulating nociceptors, capsaicin could also induce their desensitisation, rendering animals insensitive to painful stimuli (Szolcsányi, 1993). Caterina, Julius and colleagues identified the molecular target of capsaicin after finding a single DRG-derived cDNA clone that showed a robust response to capsaicin stimulation in transfected cells (Caterina et al., 1997). Further characterisation demonstrated this was a calcium-permeable, non-selective cation channel activated by capsaicin as well as heat, protons and resiniferatoxin, and blocked by the capsaicin antagonist capsazepine and ruthenium red. It also exhibits

desensitisation kinetics and cytotoxicity with prolonged stimulation. It was named vanilloid receptor type I (VR1) in recognition of the vanilloid moiety that forms the core of the capsaicin molecule.

VR1 was the first ion channel in the TRPV family to be identified and characterised. Structurally, it displays homology with the TRP family of channels in the *Drosophila* retina, so was renamed transient receptor potential vanilloid receptor type 1 (TRPV1) (Clapham et al., 2001, Montell et al., 2002). Polymorphisms of the TRPV1 receptor in humans have been associated with different phenotypes in patients with neuropathic pain (Binder et al., 2011).

Functional characteristics of TRPV1

Activation and modulation

TRPV1 is a multistate ion channel whose state (open, closed or refractory) may be modulated by a variety of factors, including temperature, voltage and certain agonists. TRPV1 is activated by noxious heat (>43°C), phosphorylation of the channel and a wide variety of endogenous and exogenous chemicals. These include protons, ethanol, lidocaine, capsaicin, piperine (black pepper), resiniferatoxin, ruthenium red, endogenous cannabinoids (anadamide, N-arachidonoyl-dopamine (NADA)), and a variety of inflammatory lipid metabolites (Szallasi and Blumberg, 2007, Vay et al., 2012). Low concentrations of capsaicin, heat, protons and other activating ligands may all shift the channel towards an open state even if they do not directly activate it in isolation (Rosenbaum and Simon, 2007).

The TRPV1 receptor usually exists in a balance between the open (activated) state and the closed (resting) state. TRPV1 exhibits two types of desensitisation: acute

desensitisation, the rapid loss of activity following agonist binding, mediated by conformational change; and tachyphylaxis, a gradual reduction in subsequent response with repeated administration of an agonist, mediated by activation of intracellular signalling pathways (Rosenbaum et al., 2004). Figure 7 illustrates TRPV1 structure and key binding sites, as well as summarising the key factors modulating its functional state.

The activation of TRPV1 on nociceptors triggers excitatory neurotransmitter release (glutamate, neuropeptides) from the central terminals of associated neurones in the dorsal horn of the spinal cord. It also stimulates local release of neuropeptides from the terminal branches of the stimulated fibre, contributing to neurogenic inflammation (Maggi, 1993) (see above).

A: TRPV1 structure and key binding sites

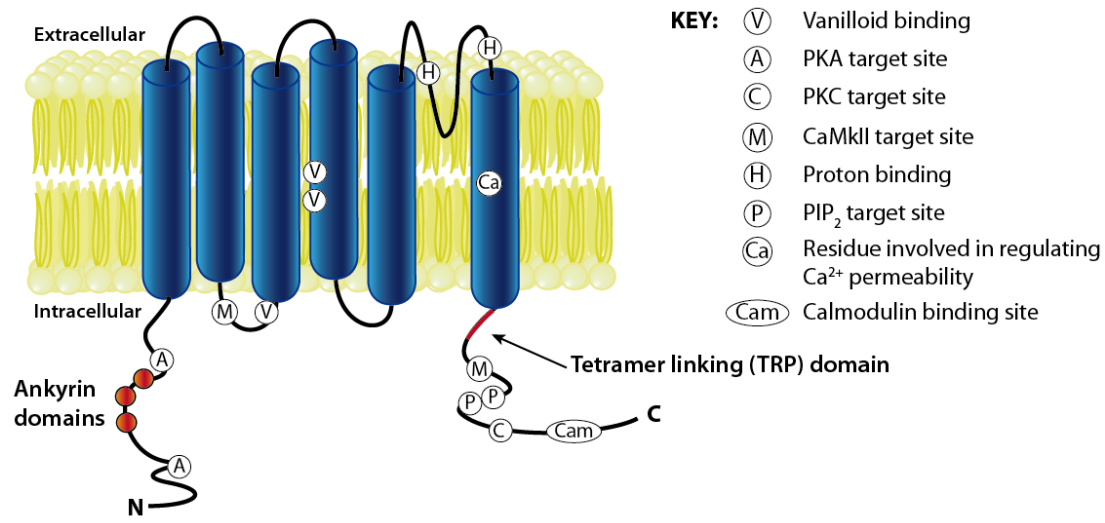

B: Summary of modulation of TRPV1 states by ligand binding and phosphorylation

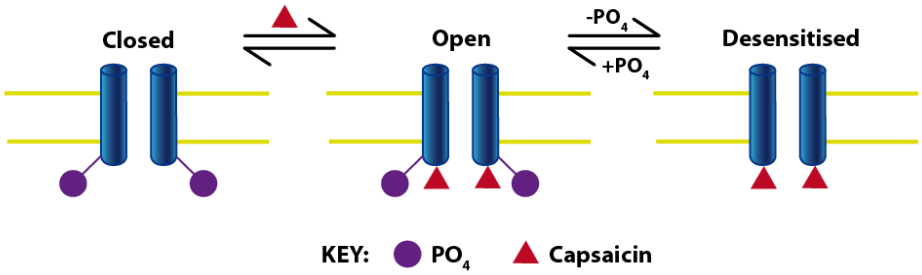

Figure 7: TRPV1 structure, binding sites and key state modulation.

Adapted from: Nagy et al, Eur. J. Pharmacol 500: 351-369 (2004), Garcia-Sanz et al, J.Neurosci. 24: 5307-5314. (2004) & Suh et al, Curr. Phar. Design 11: 2687-2698 (2005).

TRPV1 is modulated through regulation of key intracellular pathways which modulate protein phosphorylation, including PKC, PKA, CaMKII, and ERK1/2 (Zhang et al., 2011). Intracellular PIP_2 binds to TRPV1, inhibiting its activation, which can be overcome by either PLC activation, releasing PIP_2, or by binding of PIP_2 by Pirt (Kim et al., 2008). Calcium pathways regulate TRPV1 desensitisation, with dephosphorylation by the calcium-dependent phosphatase calcineurin and binding

of the calcium-binding protein calmodulin both acting to increase TRPV1 inhibition (Rosenbaum and Simon, 2007, Docherty et al., 1996).

TRPV1 may also be sensitised by a variety of extracellular inflammatory mediators, via modulation of key intracellular pathways (see figure 8). These lower the thermal activation threshold to below body temperature and thereby have the potential to generate spontaneous pain. ATP modulates TRPV1 activity both directly and indirectly. Indirect modulation is mediated through extracellular ATP binding to the metabotropic (G-protein coupled) P2Y1 receptor, activating PLC cleavage of PIP_2 into IP_3 and DAG, which activates PKC. Activated PKC reduces the thermal activation threshold from around 42°C to 35°C (Tominaga et al., 2001). Intracellular ATP also sensitises TRPV1 directly through binding to one of the ankyrin domains (Lishko et al., 2007). Once activated, an influx of calcium and magnesium ions release ATP from its binding site and free the channel to interact with Ca-Calmodulin, which desensitises TRPV1 (Lishko et al., 2007). Extracellular bradykinin modulates TRPV1 through the same intracellular pathway, acting via its receptor, BK2 (Sugiura et al., 2002). Histamine induces inward calcium channels through binding to the G protein-coupled H1 receptor, and activation of TRPV1 via PLA_2-arachidonic acid-eicosanoid pathways (Shin et al., 2002, Shim et al., 2007). $TRPV1^{-/-}$ mice do not exhibit histamine-induced scratching, while serotonin-induced scratching is preserved (Shim et al., 2007).

As well as the TRPV1 channel characteristics, the numbers of TRPV1 receptors can also be a key modulator of TRPV1 currents in the longer term, thereby modulating signalling intensity. This is executed by altering membrane trafficking, whereby

TRPV1 is translocated to the cell surface by exocytosis in v-SNARE associated vesicles. The SNARE protein partners snapin and synaptogamin IX facilitate neuronal exocytosis in a Ca^{2+}-dependent manner. This process is induced by PKC and is inhibited by botulinum toxin A (Planells-Cases and Ferrer-Montiel, 2007). Thus, agents which can activate TRPV1 through phosphorylation of the channel by PKC also increase membrane translocation of the channel, further increasing their overall excitatory effect of the cell. Figure 7 summarises TRPV1 structure and binding sites of key modulatory molecules, as well as a summary of channel kinetics. Figure 8 illustrates key modulatory pathways of TRPV1 activation.

Cutaneous non-neuronal TRPV1 expression

In addition to neuronal expression of TRPV1 as discussed above, TRPV1 is expressed by other cutaneous cells, which may have implications for neuroimmune communication and co-regulation. TRPV1 protein (immunohistochemistry) and mRNA (PCR) have been detected in normal human epidermal keratinocytes (NHK) and immortalised keratinocyte cell lines (HaCaT) (Ständer et al., 2004, Southall et al., 2003). Functional studies exposing cultured keratinocytes to capsaicin have described calcium influx, elevation of proinflammatory mediators (COX-2, IL-8, PGE_2, ATP), keratinocyte proliferation and increased expression of heat shock protein, MMP-1 (also evoked by heat) (Southall et al., 2003, Li et al., 2007, Denda et al., 2010) possibly suggesting TRPV1 activity. These effects were inhibited by prior application of the TRPV1 antagonist, capsazepine, or in TRPV1 knockout cell lines supporting this assertion. A recent study using TRPV1 reporter mice to examine TRPV1 expression did not report keratinocyte TRPV1 expression. However the

authors do not specifically comment on their observations in the skin and thus it is not clear whether TRPV1 was or was not seen (Cavanaugh et al., 2011).

The evidence concerning TRPV1 expression in Langerhans' cells is difficult to interpret. Some authors report increased TRPV1 mRNA expression when cultured monocyte-derived dendritic cells (mDC) cells mature into functional dendritic cells. These cells have corresponding functional TRPV1 responses. In mature mDC, capsaicin inhibits a number of immune responses, including cytokine-induced differentiation, phagocytosis, activation and pro-inflammatory cytokine secretion (Toth et al., 2009) implying receptor presence. Conversely, a study of bone-marrow derived dendritic cells (BM-DC) did not find TRPV1 mRNA or evidence of capsaicin-induced calcium currents (O'Connell et al., 2005). No studies exist reporting on the effect of TRPV1 agonists on native Langerhans' cells. The data derived from studies of cultured dendritic cells may not accurately predict Langerhans' cell responses *in vivo*, as there has been recent debate concerning their origins. Many studies are conducted on dendritic cells cultured from monocyte or bone marrow-derived precursors, previously thought to be the source of Langerhans' cells, however recent evidence suggests that Langerhans' cells may actually originate primarily from yolk sac precursors (Chorro and Geissmann, 2010).

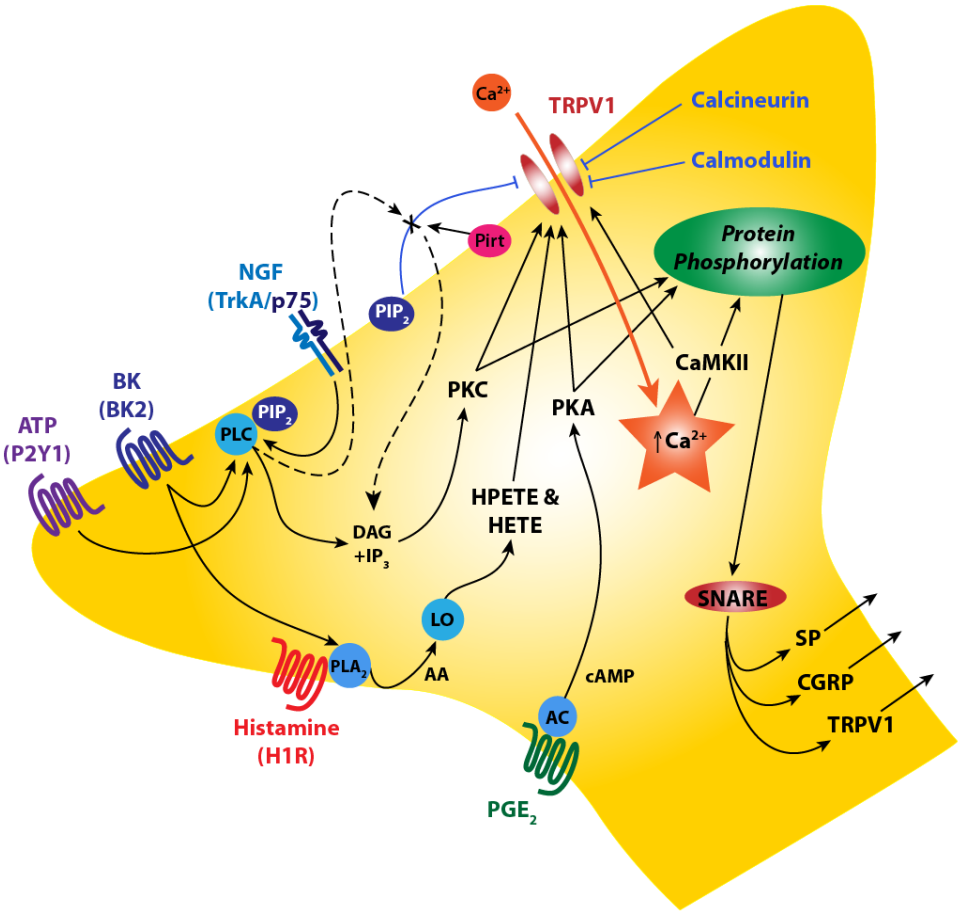

KEY:

AA	arachidonic acid
AC	adenylate cyclase
ATP	adenosine triphosphate
BK	bradykinin
CaMKII	calcium calmodulin-dependant protein kinase II
CGRP	calcitonin gene-related peptide
DAG	diacylglycerol
HPETE/ HETE	eicosanoids
LO	lipoxygenase
NGF	nerve growth factor
PGE_2	prostaglandin E2
PIP_2	phosphatidylinositol 4,5-bisphosphonate
Pirt	phosphoinositide interacting regulator of TRP
PKA	protein kinase A
PKC	protein kinase C
PLA_2	phospholipase A_2
PLC	phospholipase C
SNARE	soluble NSF attachment protein receptor
SP	substance P
TRPV1	transient receptor potential vanolloid receptor 1

Figure 8: Key mechanisms in TRPV1 activation
Derived from Nagy 2004, Planells-Cases & Ferrer-Montiel 2005 & Zhang et al. 2011

Evidence for cytokine dysfunction in painful human neuropathies

Some recent studies have found imbalance in immune tone to be a common factor in several neuropathic pain states, with pain linked to increased proinflammatory cytokines and diminished pain to anti-inflammatory cytokine levels. For example, serum from patients with complex regional pain syndrome showed an increase in pro-inflammatory (TNF-α, IL-2) and decrease in anti-inflammatory (IL-4, IL-8, Il-10) cytokines (Üçeyler et al., 2007a). Another study of normal subjects, and those with painful versus painless neuropathies, found an increase in TNF-α and IL-2 in the serum of subjects with painful neuropathy, and an increase in IL-10 in those with painless neuropathy. These findings were independent of whether the underlying pathology was inflammatory or not (Üçeyler et al., 2007c). The findings in this latter paper may not be completely valid, as diabetic neuropathy was included in the 'noninflammatory' subgroup, and diabetic neuropathy is known to be associated with activation of inflammatory pathways (Vincent et al., 2011). Elevated cutaneous mRNA levels of inflammatory cytokine have been reported in patients with small fibre neuropathy (SFN), with IL-6 and IL-8 elevated in painful idiopathic SFN. In a subset of subjects with a length dependent idiopathic SFN (proximal intraepidermal nerve fibre density (IENFD)/distal IENFD > 5), distal levels of TNF-α, IL-8, IL-1β and IL-6 were much greater than in the proximal skin of the same individual (Üçeyler et al., 2010).

Whilst these findings are of interest, it remains unclear whether the immune changes are causal in pain pathogenesis, due to a common underlying inflammatory pathology, or a response to nerve damage. The potential modulatory role of immune changes in the skin neighbouring the terminal receptive field of cutaneous

nociceptors in the generation of neuropathic pain is explored further in Chapter 5 of this thesis. The following section summarises some of the key features of the cytokines studied, focussing on their potential role in pain and neurocutaneous interactions. Figure 9 shows a summary of key pathways of T cell differentiation, effector molecules and immunological functions. Figure 10 summarises some of the key cutaneous neuroimmune interactions that may be relevant factors in possible mechanisms of initiation and maintenance of neuropathic pain.

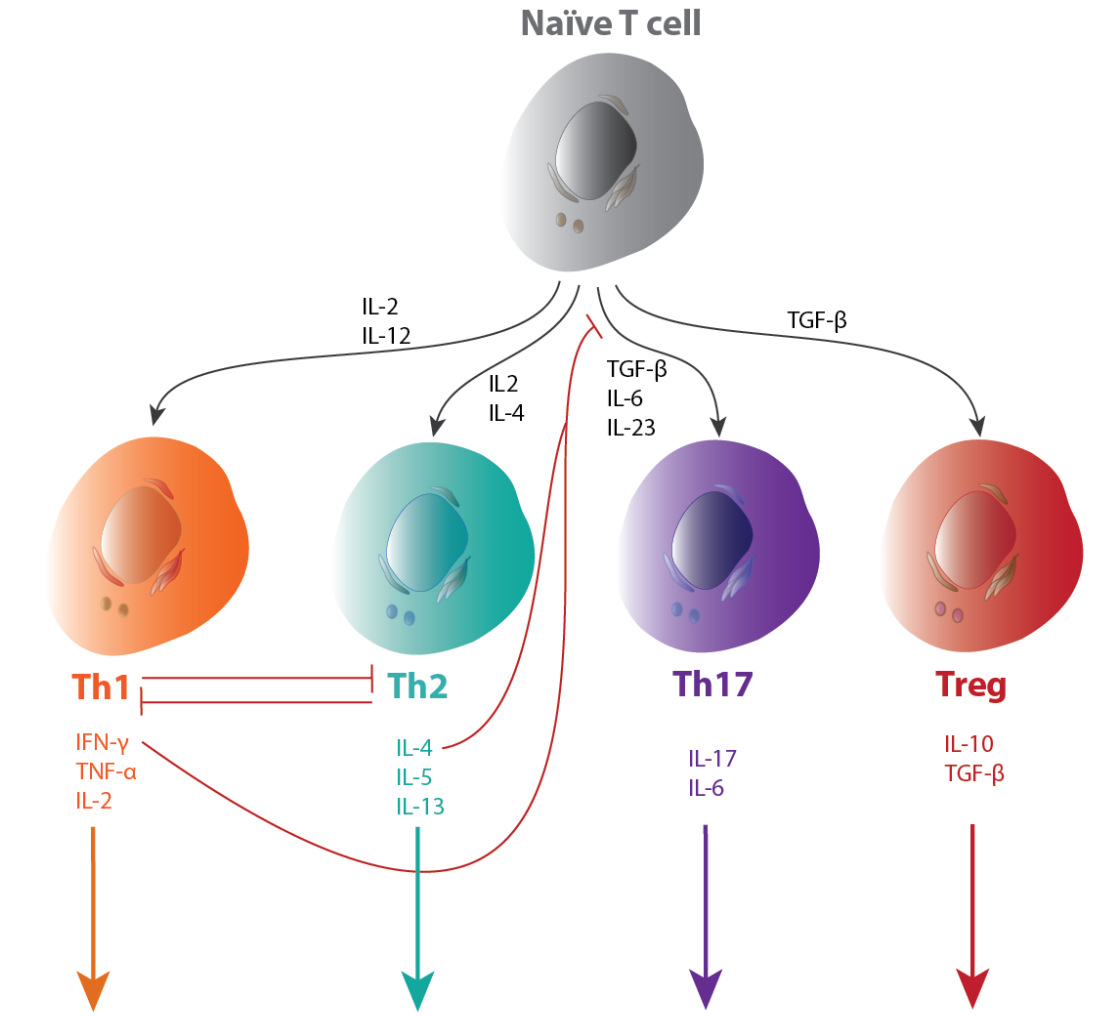

Notes: All are T4+ lymphocytes
IL-1 excess or IL-1Ra deficiency enhances Th1 and Th17 responses
Th - T-helper cell; IL - interleukin; TGF - transforming growth factor; IFN - interferon

Figure 9: Key pathways of lymphocyte differentiation, effector molecules and function

Cytokines implicated in modulation of neuropathic pain:

IL-1β

Interleukin 1β (IL-1β) is a key pluripotent pro-inflammatory cytokine produced by macrophages, monocytes, dendritic cells, natural killer cells, microglia and Schwann cells (Thacker et al., 2007, Kiguchi et al., 2010, Dinarello, 2009). IL-1β increases synthesis of inflammatory mediators, including COX-2, phospholipase A, inducible nitric oxide synthetase (iNOS), adhesion molecules, chemokines and angiogenic factor (Dinarello, 2009). These increase PGE2, NO, IL-6, immune cell recruitment, vasodilatation, angiogenesis and pain sensitivity, and act systemically to produce fever and hypotension. IL-1β acts as a growth factor for B cell production, a costimulator of T-cells, and a key initiator of Th17 responses (Dinarello, 2009).

IL-1β mRNA is rapidly upregulated in the DRG following chronic constriction injury (CCI) of the sciatic nerve (Üçeyler et al., 2007d) and Schwann cells also produce IL-1β in response to nerve injury, augmenting myelin phagocytosis by macrophages (Shamash et al., 2002). Intraneural, intraplantar or systemic IL-1β induces thermal hyperalgesia and mechanical allodynia (Zelenka et al., 2005, Follenfant et al., 1989, Fukuoka et al., 1994, Ferreira et al., 1988). Blockade of IL-1β signalling reduces pain behaviour and DRG spontaneous activity following nerve injury (Wolf et al., 2006). IL-1β also potentiates TRPV1 activation in a heterologous expression system and induces CGRP release by sensory ganglion cells (Camprubí-Robles et al., 2009, Neeb et al., 2011, Hou et al., 2003).

TNF-α

TNF-α is a complex cytokine that can exist as a free soluble or membrane-bound form. It is secreted by monocytes, macrophages, mast cells, fibroblasts, smooth muscle cells, endothelial cells, keratinocytes, T-cells and NK cells (Bos, 2004). Schwann cells also secrete TNF-α through activation of the NF-κB pathway in response to injury or inflammation (Qin et al., 2012). This Schwann cell cytokine response initiates an early immune response to injury, which is then augmented by recruited immune cells, particularly macrophages (Shamash et al., 2002). TNF-α can exert both pro- and anti-inflammatory actions, as well as acting as a growth factor. TNF-α synthesis is primarily regulated by IFN-γ, but modulated by TGF-β, IL-6, PGE_2 and vitamin D_3. TNF-α can also be stimulated by IL-1, substance P, and bradykinin and can act in an autocrine fashion to further increase its own release (Bos, 2004). TNF-α promotes fever, cachexia, macrophage and neutrophil chemotaxis, phagocytosis and cytotoxicity, and is an important regulator of Langerhans cell maturation (Bos, 2004).

Intraneural or subcutaneous injection of TNF-α evokes hyperalgesia and allodynia and increases ectopic firing of nociceptors, which is blocked by a TNF-receptor antagonist (Sorkin and Doom, 2000, Wagner and Myers, 1996, Sorkin et al., 1997). Pretreatment with the TNF-α antagonist etanercept prevented development of allodynia in a rat spinal nerve ligation model of neuropathic pain (Schafers et al., 2003). TRPV1 is sensitised by TNF-α via a PKC-dependent mechanism (Russell et al., 2009). Tetrodotoxin-resistant voltage-gated sodium channels (TTX-R) in sensory neurons exhibit increased currents after exposure to TNF-α, contributing to

nociceptor sensitisation and pain behaviours (Czeschik et al., 2008, Jin and Gereau, 2006).

IL-6

Interleukin 6 is an early pro-inflammatory cytokine generated primarily by monocytes, but also by bone marrow cells, fibroblasts, endothelial cells, lymphocytes, Langerhans' cells and keratinocytes (Bos, 2004, Gallucci et al., 2000). It is important for regulation of B-, T- and NK- cell function, and hepatocyte generation of acute phase proteins. IL-6 also acts as an amplifier of the immune response, released in response to IL-1 and TNF-α stimulation. Several autoimmune diseases such as systemic lupus erythematosus, systemic scleroderma and pemphigus vulgaris are associated with elevated levels of IL-6 (Bos, 2004).

The effect of IL-6 on sensory neurons is complex, and appears to depend on the site of administration as well as other soluble factors present. Skin perfused (by microdialysis) with IL-6 in conjunction with the soluble IL-6 receptor (sIL-6R) released more CGRP in response to heat than control or solely IL-6 perfused skin (Opree and Kress, 2000). Neuronal firing rate in response to stimulation of the receptive field in a skin-nerve preparation increased with low dose of IL-6, but decreased with higher doses, or a combination of IL-6 and sIL-6R (Flatters et al., 2004). Heat hyperalgesia has been reported after intrathecal injection of IL-6 (Oka et al., 1995, Flatters et al., 2004), and an IL-6 knockout mouse exhibits delayed onset of mechanical allodynia following spinal nerve ligation compared to wild-type (Ramer et al., 1998).

IL-10

IL-10 is an immunosuppressive cytokine primarily synthesised by monocytes, but also by Th1 and Th2 T-cells, cytotoxic T-cells, mast cells, B lymphocytes and keratinocytes. IL-10 has a number of actions, acting to reduce synthesis of inflammatory cytokines (including IFNγ, IL-1β, IL-6, IL-8, and TNFα), mast cell chemotaxis and inhibition of antigen presentation by dendritic cells (Bos, 2004, Pietrzak et al., 2009). IL-10 increases IgG production by B cells. The net effect of IL-10 is to suppress cellular and allergic immune responses, whilst increasing humoral and cytotoxic ones (Bos, 2004).

IL-10 mRNA is rapidly upregulated in the DRG following CCI (Sommer and Schäfers, 2004, Üçeyler et al., 2007d). Intraplantar IL-10 reduces hyperalgesia evoked by intraplantar carrageenan or inflammatory cytokine injection, and from nerve injury (when administered at the site of injury) (Poole et al., 1995, Wagner et al., 1998). Intrathecal IL-10 reverses neuropathic pain associated with the chronic constriction and paclitaxel-induced neuropathic pain models in rodents (Milligan et al., 2006, Ledeboer et al., 2007).

IFN-Ɣ

IFN-γ is a key regulator of tissue inflammation and immune response, released primarily by Th1 cells. IFN-γ promotes the release of pro-inflammatory cytokines in the skin, including IP-10, IL-1, IL-6, IL-8, TNF-α and CCL5/RANTES (Bos, 2004). IFN-γ also facilitates antigen presentation, induces Th1 differentiation, increases NK cell and macrophage activity and leucocyte migration. IFN-γ has been implicated in autoimmune disease such as systemic lupus erythematosus (Bos, 2004). IFN-γ has

also been found to upregulate keratinocyte Th1 chemokines whilst downregulating Langerhans' cell Th2 chemokines, suggesting it may act as a regulator of immune tone in the skin (Mori et al., 2008).

IL-17 and Th17 cells

Th17 cells are a subset of effector T-cells, important in clearance of pathogens resistant to initial Th1 and Th2 responses, particularly fungal pathogens. They are also in pathogenesis of autoimmune diseases, where they act to create persistent inflammation (Peck and Mellins, 2009). Cytokines produced by Th17 cells (IL-17, IL-21, IL-22, GM-CSF, G-CSF, IL-6 and TNF-α) are potent inducers of tissue inflammation. Th17 cells differentiate in response to TGF-β and IL-6 / IL-21 co-stimulation. IL-17 is a proinflammatory cytokine, which acts to increase release of the inflammatory cytokines (TNF-α, IL-1β, IL-6), chemokines, and metalloproteinases, and is a potent neutrophil chemoattractant (Korn et al., 2009).

Neural IL-17 increases within 8 days of nerve injury (Noma et al., 2011). IL-17 sensitises nociceptors, with intraplantar or intraneural injection of IL-17 resulting in increased thermal hyperalgesia and mechanical allodynia. IL-17 null mice exhibit reduced allodynia and thermal hyperalgesia in response to partial sciatic nerve ligation than their wild type counterparts (Kim and Moalem-Taylor, 2011).

MCP-1

Monocyte chemoattractant protein (MCP-1, also known as CCL2) is a member of the CC family of chemokines and is a powerful chemoattractant for monocytes, memory T-cells and dendritic cells. It is primarily produced by monocytes and

macrophages, but also by epithelial, endothelial and smooth muscle cells, fibroblasts, astrocytes and microglia. Synthesis and release of MCP-1 is stimulated by IL-1β, TNF-α and endotoxin and regulated by IFN-γ, IL-4, IL-10 and IL-13. Keratinocytes and fibroblasts produce MCP-1 in response to IFN-γ and TNF-α respectively, promoting increased recruitment of dendritic (Langerhans') cells (Giustizieri et al., 2001, Nakamura et al., 1995, Ouwehand et al., 2010). MCP-1 is an important chemokine in the early stages of cutaneous wound healing, and in some inflammatory skin conditions (Gillitzer and Goebeler, 2001, Bos, 2004).

Hyperalgesia is reported in MCP-1 overexpressing mice (White et al., 2009). MCP-1 induces elevation of intracellular calcium and CGRP release via PLC/PKC pathways in cultured DRG neurons, and evokes thermal and mechanical hyperalgesia when injected into the plantar skin of mice (Qin et al., 2005). Focal demyelination increases expression of MCP-1, RANTES and IP-10, as well as their receptors, on sensory neurons that also exhibit transient elevation of intracellular calcium in response to MCP-1. Hyperalgesia following nerve injury may be reversed by the administration of a MCP-1 receptor antagonist (Bhangoo et al., 2007).

IP-10

IFN-induced protein of 10 kDa (IP-10, also known as CXCL10) is a chemokine of the CXC family, which binds to the G-protein coupled receptors CXCR3 and CCR3. CCR3 is highly expressed on Th2 cells and cytotoxic T-cells, whilst Th1 cells express CXCR3. Other cells expressing CXCR3 include B cells, natural killer cells, dendritic cells and macrophages. Stimulation of CXCR3 promotes chemotaxis of cells bearing CXCR3 (Bos, 2004, Liu et al., 2011). IFN-γ stimulates IP-10 release from leukocytes,

neutrophils, eosinophils, monocytes, epithelial and endothelial cells. A positive feedback loop exists, as IP-10 recruits IFN-γ producing Th1 cells, which then acts to further promote IP-10 release (Liu et al., 2011). IP-10, with MCP-1 and IL-8 are the most abundant chemokines produced by keratinocytes in response to activation by inflammatory cytokines. In particular, IFN-γ, with or without TNF-α, promotes production of IP-10 and MCP-1 in both keratinocytes and dendritic cells (Liu et al., 2011, Bos, 2004).

RANTES

Regulated (increased) upon activation, expressed by normal T-cells and secreted (RANTES, also known as CCL5) is a chemokine which binds to the receptor CCR5. RANTES is produced by platelets, macrophages, eosinophils, fibroblasts, endothelial cells, keratinocytes and Langerhans' cells (Levy, 2009, Fujita et al., 2004, Sanmiguel et al., 2009). RANTES acts to recruit T-cells, dendritic cells, eosinophils, natural killer cells, mast cells and basophils to the site of inflammation, and to induce migration of activated Langerhans' cells from the epidermis, as well as activating macrophages. RANTES has been linked with several inflammatory diseases (arthritis, atopic dermatitis, colitis), atherosclerosis and development of breast and prostate cancer (Levy, 2009). Schwann-cell derived RANTES is a mediator of HIV-neurotoxicity through activation of an autocrine TNF-α release and binding pathway through TNFR1 in DRG cells (Keswani et al., 2003). RANTES and its receptor are also upregulated in sensory neurons following focal demyelination, but there are no reports of the effects of direct application of RANTES to nerves (Bhangoo et al., 2007).

NGF-β

Nerve growth factor (NGF) is a neurotrophic factor important for developmental survival and appropriate target-tissue innervation of trkA positive nociceptors (Albers et al., 1994, Diamond et al., 1992, Goodness et al., 1997). The TrkA-NGF responsive population of nociceptors has extensive overlap with the CGRP/SP positive and TRPV1 positive population, whilst the IB4 population loses TrkA sensitivity in later development (Averill et al., 1995, Bennett et al., 1996, Bennett, 2001). In the adult, target production of NGF is an important regulator of sprouting and reinnervation of target tissue (Pertens et al., 1999).

Systemic administration of NGF results in thermal hyperalgesia, as does local inflammation-induced elevation in NGF (Lewin et al., 1994). NGF application to murine cultured DRG neurons also increases response to noxious heat, in both the IB4-positive and IB4-negative populations (Stucky and Lewin, 1999). A monoclonal antibody against NGF, tanezumab, has recently been developed and shown some benefit in osteoarthritic pain, although some concerns have been raised about side effects (Lane et al., 2010).

NGF enhances TRPV1 currents (Shu and Mendell, 1999, Zhu et al., 2004) through phosphorylation, increased expression and membrane insertion (Xue et al., 2007, Zhu and Oxford, 2011, Zhang et al., 2005). NGF also sensitises nociceptors through activation of neutrophils, stimulating their production of leukotriene B4 which activates TRPV1 (Bennett et al., 1998, Vigna et al., 2011); and through degranulation of mast cells, inducing the release of various sensitising mediators including bradykinin, histamine and 5-hydroxytryptamine (Lewin et al., 1994,

Štempelj and Ferjan, 2005). NGF stimulates cytokine release from dendritic cells, depending on existing skin conditions (IL-6 in allergic subjects, IL-10 in healthy controls) (Noga et al., 2007). NGF increases DRG synthesis of CGRP and SP (Lindsay and Harmar, 1989, Park et al., 2010), and increases evoked release of CGRP from peripheral terminals (Bowles et al., 2006). NGF induces keratinocyte proliferation (Pincelli et al., 1994), and keratinocyte NGF overexpression induces epidermal hyperinnervation (Albers et al., 1994).

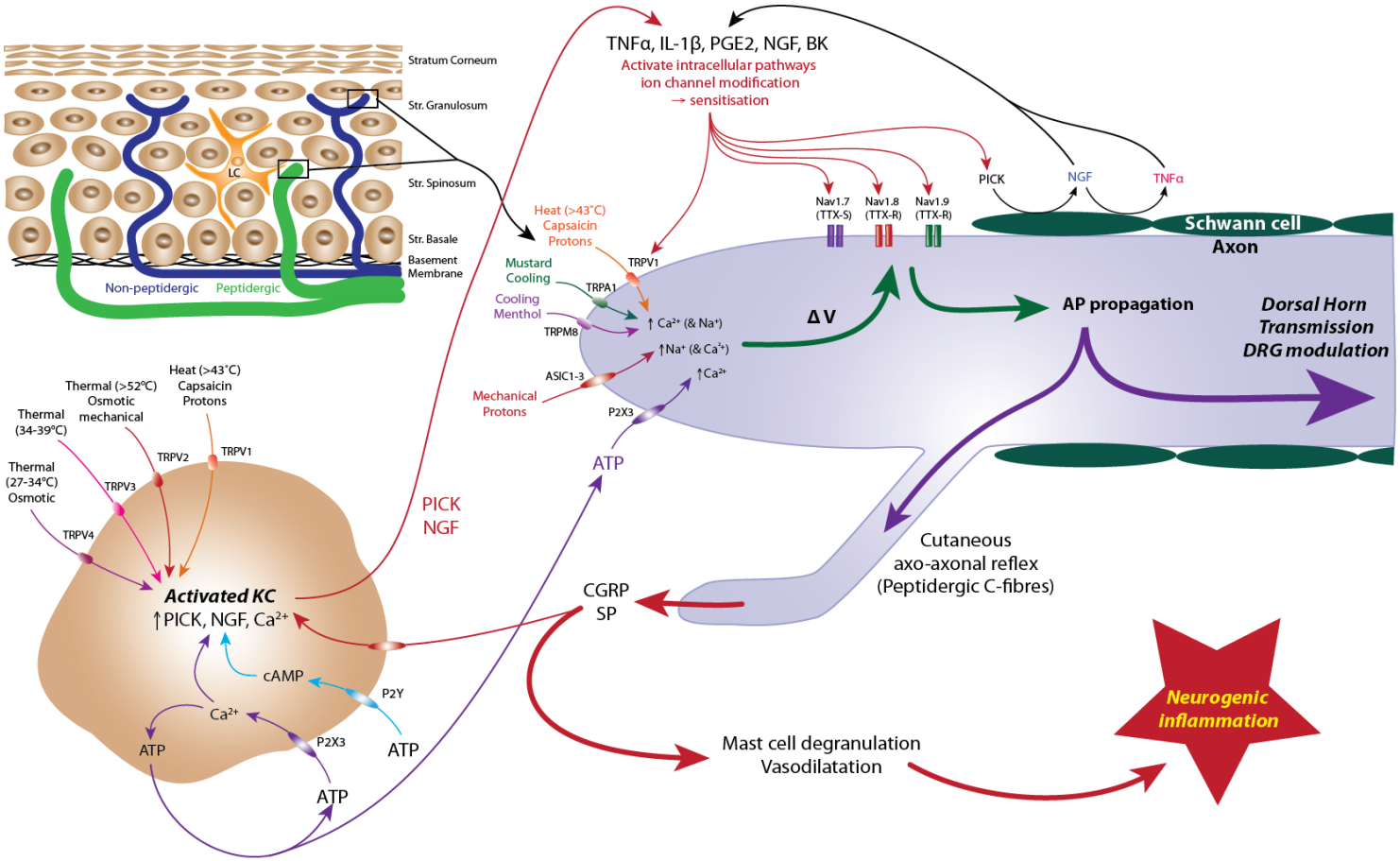

Figure 10: Summary of some of the key neuro-immune interactions in the skin which may be relevant in neuropathic pain.
IL: interleukin; TNFa: tumour necrosis factor alpha; TRPV: transient receptor potential vanilloid receptor; TRPA1: transient receptor potential ankyrin type 1; TRM8: transient receptor potential subfamily M type 8; TTX-S: tetrodotoxin sensitive; TTX-R: tetrodotoxin resistant; Nav: voltage-gated sodium channel; NGF: nerve growth factor; P2X3: P2X purinergic receptor type 3; ATP: adenosine triphosphate; CGRP: calcitonin gene-related peptide; SP: substance P; ASIC-3: acid-sensing ion channel type 3; PICK: pro-inflammatory cytokines (particularly TNF-α, IL-1β, IFN-γ, IL-6); AP: action potential

Cellular Components of the Cutaneous Immune System

In addition to the potential effect of the cytokines discussed above, the skin contains a complex array of immune cells to maintain integrity and respond to threats, which may also play a role in modulation of pain perception, as they comprise the cellular environment in which nerve endings exist. In the epidermis, the primary immune cell is the epidermal dendritic, or Langerhans' cell, however the keratinocytes also have immune functions, and sparse T cells are present (Torvin Möller et al., 2009, Shipton, 2013, Metz and Maurer, 2009). In the deeper dermis, there are two populations of dendritic cells, Langerin positive and negative, as well as T- cells (most are memory T-cells), mast cells and macrophages. Additional cells are recruited to the dermis in inflammatory states, including granulocytes, monocytes, additional dendritic cells, and T-cells (Shipton, 2013).

Langerhans cells

Close contacts have been observed between Langerhans' cells and intraepidermal nerve fibres (Hosoi et al., 1993, Gaudillere et al., 1996). In addition there is considerable overlap in the signalling molecules to which both cell types are responsive, making them of interest in understanding potential neuroimmune interactions in neuropathic pain associated with neuropathy. A recent study also found that targeted depletion in Langerhans' cells in mice reduced cutaneous innervation, as well as inducing mechanical (but not thermal) hyperalgesia (Doss and Smith, 2014). Conversely, denervation has been associated with increased Langerhans' cell numbers (Hsieh et al., 1996,

Lauria et al., 2005). This provides further support to the presence of a degree of interdependence and influence between nerve cells and Langerhans' cells.

Langerhans' cells are a subset of dendritic cells (DCs), which form one of the key groups of cellular elements in the skin immune system. These cells are spread throughout the epidermis and dermis and form a continuous network of professional antigen presenting cells (APC). They are located in the epidermis, primarily in the suprabasal region and form a regular, near-interconnected network throughout the epidermis with their protrusions. Langerhans cells make up between 3-5% of the nucleated cells of the human epidermis (Merad, Ginhoux, & Collin 2008). Their function and cell marker expression profile varies, with the two major groups being the epidermally situated Langerhans cells, and the deeper dermal dendritic cells, with further subtypes existing in inflammatory skin pathology. Langerhans cells express CD1a, which may also be seen in a small number (~10%) of dermal dendritic cells, thought to be largely migrating Langerhans cells (Shipton, 2013). Dendritic cells can initiate an adaptive immune response through their ability to stimulate naive T-cells, generating specific immune responses. They also participate in the innate immune response through the release of pro-inflammatory or modulatory cytokines. Langerhans cells also play an important role in the maintenance of tolerance and induction of regulatory T-cells (Lutz and Kurts, 2009, Merad et al., 2008).

They originate from a population of radioresistant haematopoetic precursor cells resident in the skin from embryonic development, although they may also

derive from circulating cells in certain inflammatory skin diseases (Shipton, 2013, Merad et al., 2008). The Langerhans cell is an immature dendritic cell, which undergoes phenotypic and functional differentiation (maturation) upon exposure to antigen, and it is in the mature state that it initiates a T-cell response. There is a continuous low level of Langerhans cell migration to draining lymph nodes, which is thought to play a role in immune tolerance. This migration is increased on exposure to antigen, a process that is regulated, in part, by TNF-α and IL-1β (Shipton, 2013). They express a variety of surface markers, which vary over the lifetime of the cell dependent upon its maturational state. These include CD45, MHC class II, CD1a, CD11c, CCR6, Langerin and CD205 (Teunissen, 2004). They contain a characteristic, but poorly understood intracellular organelle, the Birbeck granule, thought to play a role in endocytosis and specific to epidermally located Langerhans cells (Merad, Ginhoux, & Collin 2008;Teunissen 2004).

Modulation of Langerhans cell responses:

Langerhans cells have the capacity to modulate the local immune milieu via their ability to express either a Th1 or Th2 cytokine profile. Immature dendritic cells may express a tolerogenic profile, while mature dendritic cells produce either Th1 polarizing cytokines (IL-1β, IL-12, IL-18 and TNF-α) or Th2 polarising cytokines (IL-10 and CCL 17) (Toebak et al., 2008). A variety of compounds act on Langerhans cells to modulate their functional interactions with T-cells to drive either a Th1 (T cells produce high levels of IFNγ) or Th2 dominant response (T cells produce high levels of IL-4). Compounds which act to promote an

inflammatory, cell-mediated immunity Th1 response include ATP, BK, SP, TRPV1 and IFN-γ. Substances which inhibit the Th1 and promote an anti-inflammatory, antibody-dominant Th2 response include histamine, CGRP, α-MSH, cAMP, Vitamin D and UVB irradiation (Teunissen, 2004). Please refer to Figure 11 for a summary of key factors and their proposed effect on Langerhans cells.

Pro-Th1 stimulating factors acting on Langerhans cells

Langerhans cells have also been shown to express functional P2X7, indicating the capacity to respond to ATP (Tran et al., 2010). ATP has been shown to promote IL-1β and TNF-α release by Langerhans cells (Ferrari et al., 2000, Pizzirani et al., 2007, Burnstock, 2012), and to increase their antigen presenting capacity, inducing contact hypersensitivity in mice (Boulais and Misery, 2008, Yamamoto et al., 1996). Damaged cells release a range of damage-associated molecular pattern molecules (DAMP), which drive inflammatory responses, one of which is ATP. It is proposed that activation of P2X7 by ATP may be one of the mediators of the pro-inflammatory Langerhans cell response to DAMPs (Fukuhara et al., 1975).

Substance P also has immunomodulatory effects. The high-affinity neurokinin-1 receptor NK1R is expressed on murine CD11c positive skin Langerhans and dermal dendritic cells. Stimulation of NK1R increases nuclear translocation of NF-κB and pushes the LC to generate an immunostimulatory, Th1 response (Mathers et al., 2007).

In addition to its role in cutaneous sensory transduction, the TRPV1 receptor may be present on Langerhans cells. There is one positive (Bodo et al., 2004)

and one negative (Ständer et al., 2004) report of TRPV1 expression in *in situ* Langerhans cells. Blood derived dendritic cells express functional TRPV1, and in culture, incubation with capsaicin did not induce cell death, but did inhibit differentiation, maturation and phagocytosis, as well as shifting the cytokine profile of these cells to an anti-inflammatory, rather than pro-inflammatory one (Toth et al., 2009).

Pro-Th2 stimulating factors acting on Langerhans cells

CGRP positive fibres are often observed in close apposition to the cell body of Langerhans cells in the epidermis (Hosoi et al. 1993). Recent murine in vitro studies of the effect of CGRP stimulation on the behaviour of Langerhans cells support the idea that CGRP contacts may regulate immune functioning of these cells. Ding et al found that exposure of Langerhans cells to CGRP increased their ability to present antigen to Th2 cells, whilst decreasing their ability to present antigen to Th1 cells. They also found that CGRP inhibited Langerhans cell production of Th1 chemokines CXCL9 and CXCL10 in response to IFN-gamma stimulation (Ding et al. 2008). Overall, this suggests that CGRP positive nerve contacts with Langerhans cells may act to suppress Th1 inflammatory immune processes in the normal, resting epidermis, and that loss of these contacts may result in an increase in Th2, inflammatory behaviour of Langerhans cells.

Increased intracellular levels of cAMP in Langerhans cells are the result of the action of a number of effector molecules, including catecholamines, CGRP, VIP and histamine (Shepherd et al., 2005). Raised levels of cAMP act to inhibit

activation of the NFκB pathway, pushing the cell towards a Th2 response (Peters et al. 2006).

The active metabolite of vitamin D is 1,25-dihydroxyvitamin D_3 (VD_3), which acts via its nuclear receptor (VDR). Vitamin D_3 is produced in the skin following exposure to sunlight, then metabolised in the kidney to 1,25-dihydroxyvitamin-D_3. Keratinocytes and melanocytes are also able to produce 1,25 $(OH)_2D_3$ following UVB exposure (Gorman et al., 2010a). The Vitamin D_3 receptor, VDR is expressed in immune cells, including dendritic cells, mast cells and T-cells. Topical 1,25$(OH)_2D_3$ suppresses dendritic cell maturation and Th1 cytokine expression. It also reduces dendritic cell arborisation and prompts migration to lymph nodes in murine skin, with induction of regulatory T-cells and reduced skin contact hypersensitivity responses (Gorman et al., 2010b).

Histamine acts via H_4 receptors in LC to downregulate CCL-2 expression in isolated cultured Langerhans cells, and increases *in vivo* migration of Langerhans cells from the epidermis (Gschwandtner et al., 2010). Degranulating mast cells *in vitro* polarise dendritic cell response to Th2 rather than Th1 (Mazzoni et al., 2006). The effect of histamine stimulation on other skin cells, particularly mast cells and the release of mediators which in turn may alter Langerhans cell behaviour must be taken into account when considering the effect of histamine stimulation on intact skin.

Hydrocortisone and dexamethasone also suppress dendritic cell maturation and Th1 cytokine expression. Glucocorticoids induce apoptosis in immature dendritic cells, but suppress activation of dendritic cells after antigen uptake

through reduction of MHCII, co-stimulatory molecule and cytokine expression. Glucocorticoids inhibit DC migration and induce a tolerogenic phenotype, with increased phagocytic activity and IL-10 expression (Baschant and Tuckermann, 2010).

Ultraviolet B radiation induces a number of immune changes in the skin, with effects on Langerhans cells, keratinocytes and melanocytes. UVB irradiation induces apoptosis and reduction in number of Langerhans cells in murine skin, and upregulates keratinocyte production of RANKL, which induces Langerhans expression of IL-10 through binding to RANK expressed on their surface. UVB-induced cutaneous immunosuppression does not occur in Langerhan cell-depleted mice, nor in the case of blockade of RANK, OX-40 ligand or IL-10 (Yoshiki et al., 2010).

Other modulatory influences of Langerhans cell maturation

The neurotrophins NGF and BDNF have been reported to effect changes in cytokine secretion from dendritic cells, acting via RhoA and RacA GTPases. However the net balance between pro- and anti-inflammatory cytokines appears to be dependent upon underlying skin pathology (Noga et al. 2007).

Non-neural adrenergic signalling also modulates dendritic cell immune responses. Beta-adrenergic signalling impairs the ability of Langerghans cells to present antigen in vitro, as well as downregulating cytokine production via the induction of cAMP which inhibits NFκB (Goyarts et al., 2008). Norepinepherine also reduces TNF alpha and increases Langerhans cell migration (Goyarts et al., 2008).

Adenosine may be released by a variety of cells and modulates dendritic cell function through interaction with adenosine receptors on dendritic cells. Adenosine promotes chemotaxis of immature dendritic cells and inhibits IL-12 production in mature dendritic cells.

TNF-α induces dose-dependent migration of human Langerhans cells from the epidermis (Cumberbatch et al., 1999). Thalidomide inhibits TNF-α production by Langerhans cells as well as their capacity to present antigen to Th1 clones (Deng et al., 2003).

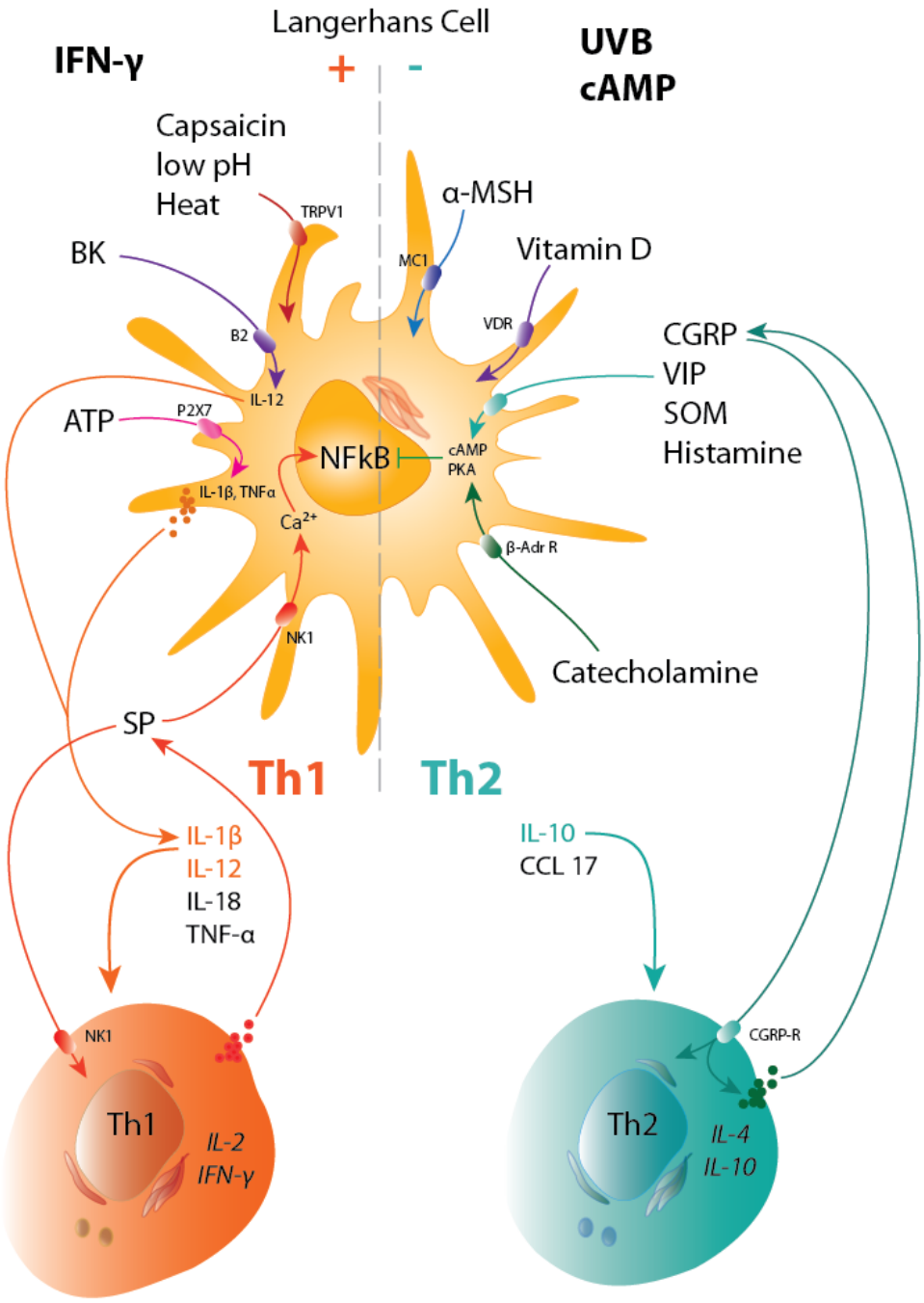

Figure 11: Proposed key immunomodulatory effects on Langerhans cells.

Langerhans cell interaction with sensory nerves

1. Effect of denervation

There are varying reports of the effect of denervation on Langerhans cells. One recent study found an increase in Langerhans cells in the denervated skin, but not neighbouring skin or the spared nerve injury model in rats (Dauch et al., 2013). However, Langerhans cells were identified using PGP 9.5, rather than a specific Langerhans cell stain. It is known that a variable proportion of Langerhans cells express PGP 9.5, and that this number increases after nerve injury (Hsieh et al., 1996), so this may simply reflect a functional change in immunoreactivity, rather than a true change in cell numbers. Similar findings and limitations are presented in a study of chemotherapy-induced neuropathy in rats (Siau et al., 2006). Increased Langerhans cells, identified by S-100, were seen in the skin of a group of 5 patients with complex regional pain syndrome, with the greatest numbers seen in the patient with the lowest innervation density (Saporta, 2014). Another study, using the Langerhans cell specific CD1a marker, found no change in Langerhans cell numbers in patients with post herpetic neuralgia, despite marked denervation (Oaklander et al., 2003). Langerhans cells were found to be increased in the cornea in early diabetic corneal neuropathy (Tavakoli et al., 2011). Taken together, these studies may suggest that Langerhans cells are increased early in neuropathy, but decrease later. This is reflected by Tavakoli's findings that the Langerhans cell numbers, whilst higher in diabetic neuropathy patients than in controls, were relatively lower in more severe neuropathy. More recently, increased numbers of

Langerhans cells have been observed in small fibre neuropathy, but no correlation with pain assessed by VAS score was identified (Casanova-Molla et al., 2012). The increase in Langerhans cells was particularly marked in a diabetic subgroup, who also showed a more profound loss of IENFD.

Possible effect of Langerhans cells and neuropathic pain

A recent study in a diabetic mouse model found an increase in epidermal and subepidermal Langerhans cell numbers during the period of mechanical allodynia. This change was proposed to be mediated by epidermal nerve fibre derived NGF-TrkA signaling to epidermal Langerhans cells, and from TNF-α positive subepidermal fibres to subepidermal immature Langerhans cells. The increase was abolished with an intrathecal p38-MAPK inhibitor, which also reduced mechanical allodynia and TNF-α expression in subepidermal fibres. No changes were seen in the non-diabetic control mice (Bertelsen et al., 2013). These findings, in conjunction with the anatomical studies above, support a role for Langerhans cell modulation of neuropathic pain, although the pathways require further study.

Objectives of this study

Neuroimmune interactions in the skin are an area of interest in particular considering the possibility of identifying new therapeutic targets for neuropathic pain which could be modulated topically, potentially with less systemic side effects than many currently used agents. Cutaneous nerves also offer a potentially more accessible window on neurobiology of neuropathy and neuropathic pain in human subjects. If results from animal models can be reliably explored using skin biopsies, either of glabrous or hairy skin, rather than sural nerve biopsies, it would allow far easier exploration of pathogenic mechanisms, natural history of disease and possible responses to therapies.

1. c-Jun expression in demyelinating neuropathies.

   This section of the thesis aims to determine whether:

   A. Schwann cell c-Jun upregulation demonstrated in animal models of neuropathy is also seen in human disease, using a cohort of patients with both axonal and demyelinating neuropathies, with the latter split between genetic and inflammatory forms; and

   B. Whether it is possible to use glabrous skin biopsy to examine these same pathways in dermal myelinated nerve fibres.

2. Dermal microdialysis evaluation of the immune effect of acute nociceptor activation.

   This section of the thesis aims to determine:

A. Whether acute nociceptor activation by the application of topical capsaicin is sufficient to induce an acute inflammatory response in the absence of nerve damage; and
B. To establish the ELISA cytokine assay in dermal microdialysis fluid in our laboratory, prior to the last section of this project

3. Small fibre function, immune changes and pain in Anderson-Fabry disease.

   This section of the thesis aims to determine whether pain in a single neuropathy type (Anderson-Fabry disease) is determined by the presence of a pro-inflammatory cytokine profile in the skin, or is associated with alteration in Langerhans' cell density.

Chapter 3: c-Jun expression in human neuropathies: using skin nerves to study pathologic mechanisms.

Abstract:

Introduction:

Cutaneous nerves have potential to provide an accessible window on pathogenic mechanisms in human neuropathies. Animal research and cell models continue to identify new pathways involved in neuropathies, as well as potential ways of modifying those pathways for therapeutic gain. A key limit to the translation of these findings into human disease is the ability to demonstrate that the mechanisms identified in these models exist and behave in similar ways in human nerves. Studying human nerves has traditionally been limited to sural nerve biopsy, which is both invasive, and limited to examination at a single time point, thus precluding studies of pathological evolution and of any therapeutic response. The development of skin biopsy demonstrating cutaneous nerves in the study of neuropathy over the last ten to fifteen years offers a new alternative to study pathogenic mechanisms and their response to modulation in human subjects, with minimal patient discomfort and potential for longitudinal studies.

Hypothesis and aims:

I postulated that c-Jun may be upregulated in human neuropathies, either as an aetiological factor, or as a modulator of outcome, and that these changes could be observed in both sural and cutaneous nerve samples. This aim of this study was to demonstrate that skin biopsy could be used to establish whether recently identified changes in transcription factor signalling pathways in demyelinating neuropathies

could be shown to have altered function in human dermal nerve fibres, and how these changes correlated with disease states.

Methods:

This pilot study used semi-quantitative immunohistochemical techniques to assess c-Jun in human neuropathies, by comparing human sural nerve samples taken from normal controls and from patients with variety of neuropathies, both axonal and demyelinating. The data from these human nerve samples were then compared with the same immunohistochemical techniques applied to cutaneous nerves in glabrous skin biopsies taken from normal controls and patients with the same diseases as the nerve samples.

Subjects:

Nerve tissue was obtained, after prospective or retrospective informed consent, from 28 patients with a variety of axonal and demyelinating neuropathies (diagnosis based on neurophysiology) and from 2 normal controls (normal control nerve tissue is very difficult to obtain). Skin biopsy tissue was obtained, after informed consent, from 4 normal subjects (normal was defined by the absence of any symptoms related to neuropathy), 5 patients with chronic inflammatory demyelinating polyneuropathy, 3 patients with genetically confirmed CMT1A and one patient with Guillain-Barré syndrome.

Results:

c-Jun immunoreactivity was identified in diseased, but not healthy nerve tissue in both the sural nerve and glabrous skin samples. c-Jun-IR was upregulated in the Schwann cell nuclei of axonal neuropathies. Upregulation was more varied in

demyelinating neuropathies, with Schwann cell nuclei, and axons both exhibiting immunoreactivity.

Conclusion:

c-Jun immunoreactivity is increased in diseased, but not healthy nerves, and this can be demonstrated in both sural nerve tissue and in myelinated nerve fibres in glabrous skin.

Note: This section of the thesis has been published: Hutton, E.J. et al (2011) c-Jun expression in human neuropathies: a pilot study. Journal of the Peripheral Nervous System, 16(4):295-303.

Background:

Schwann cell dedifferentiation following nerve injury is important to permit neural survival and axonal regrowth. Animal studies have shown that the transcription factor c-Jun is upregulated in Schwann cells of injured and pathological nerves where it acts as an important regulator of Schwann cell plasticity, promoting dedifferentiation and demyelination. This pilot immunohistochemical study investigates whether c-Jun is upregulated in nerves available from skin and nerve biopsies in human neuropathies. We examined c-Jun expression in normal and diseased human nerves, as well as in dermal myelinated nerve fibres. Our findings show that although as predicted c-Jun is rarely expressed in normal nerves, it is expressed in Schwann cell nuclei of pathological nerves as predicted by animal studies. Pathological dermal myelinated nerve fibres also show clear nuclear c-Jun expression. Further studies of c-Jun expression will help clarify its role in human neuropathies.

Neuropathies may be divided into two subgroups: those that primarily affect the myelin sheath (demyelinating neuropathies) and those that primarily affect the axon (axonal neuropathies), and may be genetic or acquired. Charcot-Marie-Tooth disease (CMT) is the most frequent inherited neuropathy in humans affecting 1 in 2,500 of the population and can be primarily demyelinating (CMT1) or axonal (CMT2). To date there are over 40 causative genes associated with CMT(Jerath and Shy, 2015). Therapies are currently limited for many neuropathies, especially the genetic neuropathies where there are no effective treatments. Better

understanding of human Schwann cell biology may identify new therapeutic targets.

c-Jun was initially shown to be a key transcription factor in the governance of Schwann cell phenotype in a study of its expression in cultured Schwann cells, as well as in rat sciatic nerve crush and transection models (Macedo et al., 2012). Shy et al demonstrated that increased c-Jun expression was seen in nonmyelinating and denervated Schwann cells, but not in myelinating Schwann cells (Shy et al., 1996). Recent animal studies have further defined pathways in the developmental regulation of myelination, as well as dedifferentiation of Schwann cells following nerve injury (Jessen and Mirsky, 2008). Myelinating Schwann cells dedifferentiate when they are removed from axonal contact in injured nerves or in culture. Dedifferentiated cells can remyelinate under appropriate conditions (Parkinson et al., 2008). Regulatory factors control the phenotypic switch in myelinating Schwann cells between myelination and dedifferentiation / demyelination. Positive regulators which drive Schwann cells towards myelination include (among others) the transcription factors Krox-20, Sox-10 and NF-κB and the cytoplasmic messenger cAMP whilst negative regulators include c-Jun, Notch, Sox-2 and the trophic factor NT3 (Jessen and Mirsky, 2008).

c-Jun is a basic leucine zipper protein which forms homo- or heterodimers with Fos, Jun and ATF proteins to form the AP-1 complex (Jochum et al., 2001). AP-1 modulates a variety of processes, including cell differentiation, proliferation, apoptosis and oncogenic transformation. AP-1 activity is induced by growth factors, cytokines and extracellular stresses and is modulated by other transcriptional

regulators, as well as by upstream kinases. One effect of AP-1 induction is further upregulation of c-Jun (O'Reilly et al., 2011). While the action of c-Jun in the AP-1 complex is regulated through phosphorylation by Jun-NH_2-terminal kinase (JNK), other actions of c-Jun, particularly its role in myelin regulation, are independent of its phosphorylation status (Parkinson et al., 2008).

Following nerve injury in rodents, c-Jun, phospho-c-Jun, JNK 1 & 2 and phospho-JNK 1 & 2 are all rapidly upregulated, particularly phospho-JNK 1 & 2 (Parkinson et al., 2008). Myelin degeneration following nerve injury in a Schwann cell specific *c-Jun* knockout mouse is delayed, and myelin phagocytosis impaired, as was expression of other markers of Schwann cell dedifferentiation including L1, N-cadherin and $p75^{NTR}$ (Arthur-Farraj et al., 2007, Jessen and Mirsky, 2008, Parkinson et al., 2008). Regeneration and functional recovery was also impaired in these mice. Activation of the p38 MAPK pathway also appears to be important, with p38 MAPK increasing c-Jun levels, inducing myelin breakdown and change to an immature Schwann cell phenotype (Pereira et al., 2013). Schwann cell c-Jun expression also appears to modulate neuronal survival through upregulation of growth factors such as artemin and GDNF (De Francesco et al., 2013).

Activation on JNK is modulated by two primary pathways, which may be modulated by several factors. Activation of MAP kinases (MAPK) by molecules such as TGF-β, TNF-α and ligation of the TCR phosphorylates and activates JNK, Conversely, activation of MAP kinase phopshpholipases (MKP) by molecules such as TNF-α dephosphorylates and suppresses JNK activity (Kamata et al., 2004). TNF-α has a complex modulatory effect on JNK, which is regulated by the balance of several

intracellular mechanisms. Apoptosis is augmented by NF-κB, concomitant activation of TNFR2 and prolonged, high concentration exposure to TNF-α, all of which act to potentiate JNK activation. Conversely, activation of the IKK-NF-κB pathway or low level, transient exposure to TNF-α act as a negative regulator of apoptosis. Overall, prolonged and robust JNK activation promotes apoptosis, whilst transient activation promotes cellular proliferation (Kamata et al., 2004). Figure 1 below summarises some of the key components of the c-Jun pathway and possible outcomes of its activation.

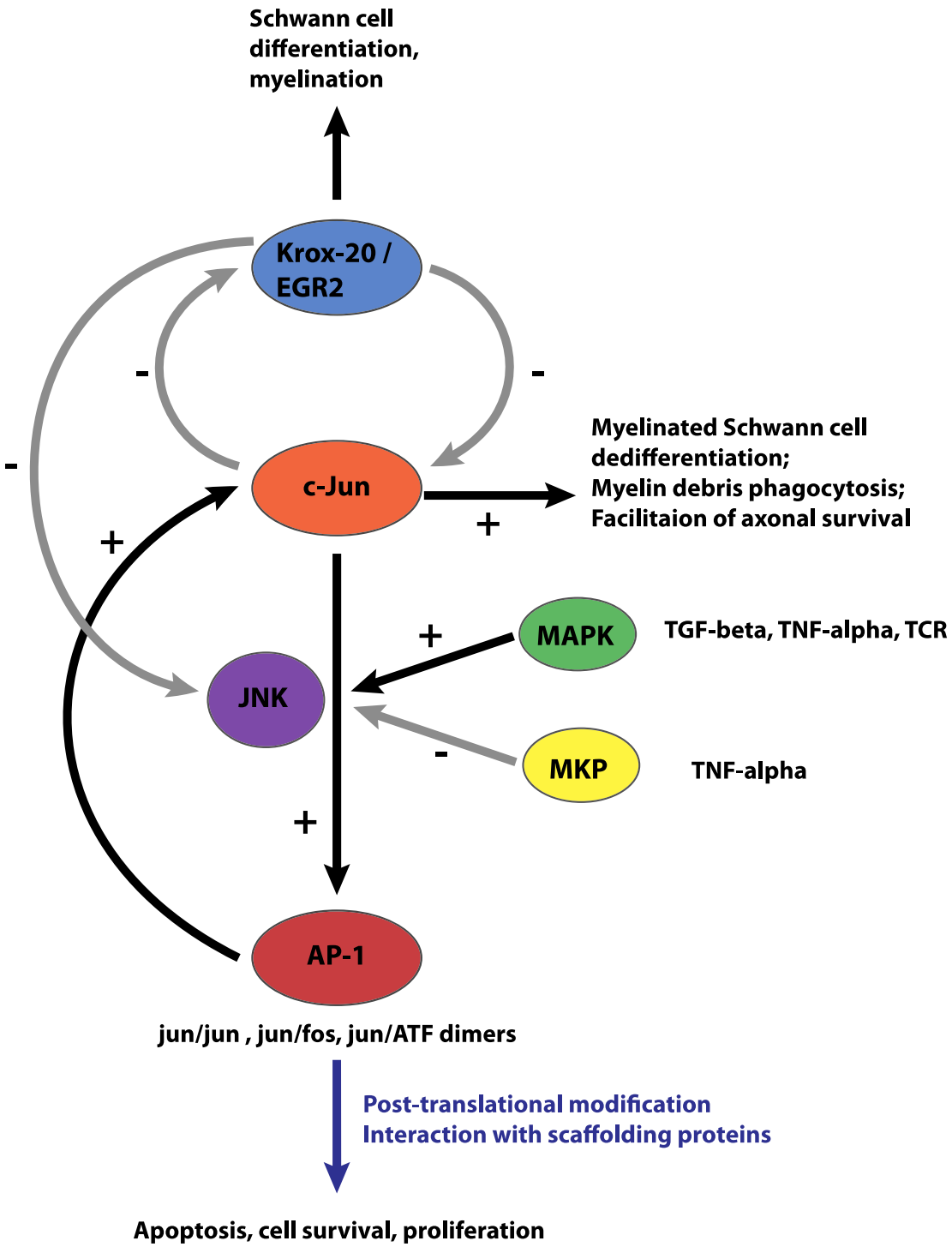

Figure 1: Key components of the c-Jun pathway

Materials and Methods:

Subjects:

Ethical approval for this project was obtained from the Joint National Hospital for Neurology and Neurosurgery and Institute of Neurology Research Ethics Committee.

Consent was obtained from 28 patients either prior to routine nerve biopsy for diagnostic purposes or retrospectively (see table 1 for subject details). Nerve biopsies were taken according to standard clinical procedures at the National Hospital for Neurology and Neurosurgery, with all biopsies being from the sural nerve apart from 2 patients (dorsal ulnar nerve in cases 13 and 14). Although the availability of normal nerve biopsy tissue is limited, 2 archival nerves were identified and used in this study (cases 29 and 30). Case 29 was taken from a 20 month-old male with a suspected mitochondrial disease, and was pathologically normal for age. Case 30 was taken from a 53 year-old female with neuropathic pain in the legs and normal neurophysiological studies. Her nerve was reported as 'within normal limits' but did have some epineurial perivascular T-lymphocytes.

For the skin biopsies, informed consent was obtained from 9 patients with neuropathies and 4 normal controls (see table 2 for subject details). Subjects were defined as 'normal' on the basis of an absence of any symptoms of neuropathy, however they were not examined and did not undergo neurophysiology. A 3-mm punch biopsy was taken from the glabrous skin at the lateral border of the non-dominant index finger of each subject after anaesthesia with 2% intradermal lignocaine. The skin biopsies were performed according to the techniques described

by McCarthy et al, but without adrenaline in the local anaesthetic due to the end circulation in the fingers (McCarthy et al., 1995).

Nerve and dermal myelinated nerve biopsies for this study were from patients with a variety of diagnoses including axonal neuropathies (vasculitic neuropathy, sensorimotor axonal neuropathy, idiopathic axonal neuropathy, motor neuron disease, carcinomatous radiculopathy, preganglionic sensory neuropathy), inherited demyelinating neuropathies (CMT1A), acquired inflammatory demyelinating neuropathies (GBS, CIDP) and a group with mixed axonal and demyelinating neuropathies (CMT-X, POEMS, amyloid neuropathy). The diagnoses of CIDP, GBS and POEMS syndrome were made using established criteria (Hadden et al., 2006, Hughes and Cornblath, 2005, Lunn and Willison, 2009). The cases of CMT1A and CMTX1 all had a genetically confirmed diagnosis.

Methods:

1. Tissue collection:

Nerve tissue was obtained from spare tissue sections remaining after diagnostic nerve biopsies had been performed.

Skin biopsies were taken from the lateral palmar surface of the second finger of the non-dominant hand in patients and normal controls after informed consent had been obtained. The area was cleaned with Chorhexidine Acetate 0.015% + Cetrimide 0.15% (Travasept 100), and the skin anaesthetised with a bleb of 2% lignocaine introduced with a 27G syringe, taking care not to introduce the needle directly into the planned biopsy site. A 3 mm punch biopsy was then taken from the lateral palmar aspect of the forefinger and the core carefully removed with fine-

toothed forceps. Tissue was placed immediately in 10% neutral buffered formaldehyde and pressure applied to the biopsy site to achieve homeostasis. A steristrip and waterproof dressing was then applied.

2. Nerve tissue processing:

Tissue was immediately immersed in 3% glutaraldehyde in 0.05M/Sodium cacodylate buffer, pH 7.4 for 5 minutes, followed by immersion in 10% neutral buffered formalin (Sigma-Aldrich, UK) for 24 hours at room temperature and paraffin embedding. Four micron sections were cut for immunohistochemistry.

3. Skin tissue processing:

Tissue was fixed in 10% neutral buffered formalin (Sigma-Aldrich, UK) overnight, prior to embedding in paraffin and sectioning at 4µm.

4. Immunohistochemistry Methods:

Sections for Myelin Basic Protein (MBP) were processed using standard protocols on a Leica Bond Max Immunostainer, using 1:1000 mouse anti-mammal MBP (Convance, California, SMI-94). For the other antibodies, sections were rehydrated to water through successive xylene and alcohol baths. Sections were then blocked with 0.9% hydrogen peroxide in water to quench endogenous peroxidase activity, followed by 4 x 5 minute washes in PBS. For c-Jun and p-JNK staining, sections were treated with a citrate antigen unmasking step prior to the PBS washes, by incubating in a microwave for 20 minutes in 700mL of water containing 7mL antigen unmasking solution (Vector Laboratories, UK), followed by another 4 x 5 minute PBS washes.

Sections were then incubated for 1 hour with 2.5% horse serum (Vector Laboratories, UK) in PBS (with 0.1% Tween to improve permeabilisation). Protein gene product 9.5 (PGP 9.5) sections had 5% powdered non-fat milk added to the blocker. Sections were incubated in primary antibody diluted in 2.5% horse serum / PBS overnight at 4°C. Antibodies used were 1:1000 rabbit anti-PGP 9.5 (Ultraclone Ltd, Isle of Wight), 1:50 rabbit anti-human c-Jun (Santa Cruz Biotechnology Ltd, USA sc-1694) and 1:50 mouse anti-human p-JNK (Santa Cruz Biotechnology Ltd., USA, sc-6254). Following 4 x 5 minute PBS washes, sections were incubated with appropriate biotinylated secondary antibodies (Vector Laboratories, UK) for 1 hour at room temperature, then washed with PBS 4 x 5 minutes, before antigen visualisation using the VECTASTAIN® Elite ABC kit and 3,3' Diaminobenzidine (DAB) with haematoxylin counterstaining. Glioblastoma tissue was used as a positive control for c-Jun staining.

Protein gene product 9.5 (PGP 9.5) is an ubiquitin C-terminal hydroxylase expressed by all neurons of the peripheral nervous system, and is an established marker for dermal and intraepidermal nerve fibres (Lauria, 2005).

Analysis

1. Nerve Analysis:

Slides were examined and photographed using a Zeiss Axioscope 2 microscope and imaging system. The images were analysed and location and intensity of c-Jun immunoreactivity (IR) recorded for each subject, after coding the sections to allow for blinded analysis. Immunoreactivity was graded as follows: 0 – absent; 1 – faint staining; 2 – moderate staining; 3 – intense staining.

MBP staining was graded as follows: 0 – no positive myelinated fibres; 1 – occasional positive myelinated fibres; 2 – moderate numbers of myelinated fibres; 3 – full complement of myelinated fibres.

Assessment of inflammation and numbers of inflammatory cells was made on the existing diagnostic sections stained for CD4+ T-cells, CD8+ T-cells and CD68+ macrophages. Grading of inflammatory cell numbers was taken from the diagnostic reports issued by the reporting Neuropathologist.

2. Skin Analysis:

Sections were photographed and immunostaining intensity graded, after coding the sections to allow for blinded analysis. Dermal nerve c-Jun intensity was graded as follows: 0 – no intraneural staining; 1 – faint nuclear IR in some nerves; 2 – definite IR in a few nuclei within the dermal nerve; 3 – strong IR in several nuclei within the dermal nerve. Dermal MBP was graded in comparison to the pattern and intensity of staining observed in dermal nerves taken from normal controls. Grading was as follows: 0 – no IR; 1 – some faint IR; 2 – definite, but reduced IR either due to reduced numbers of positive fibres or by thinned myelin; 3 – full, 'normal' MBP IR. PGP 9.5 IR was graded in comparison to the pattern and intensity of staining observed in dermal nerves taken from normal controls. Grading was as follows: 0 – no IR; 1 – some faint IR; 2 – definite, but reduced IR, either due to reduced numbers of positive fibres or reduced intensity of staining; 3 – full, 'normal' PGP 9.5-IR.

An epidermal thickness was recorded for each subject, defined as the maximal width of the cellular epidermis, and as measured between the basement membrane and the junction of the stratum lucidem and stratum granulosum (where nuclei are

lost from the keratinocytes). Meissner's corpuscles were defined morphologically as dermal papillae containing PGP 9.5 positive fibres. The maximal width of these structures was recorded for each subject.

Slides were imaged using a Zeiss Axioscope 2 microscope and imaging system using automatic exposure correction. Composite micrographs were compiled using Adobe® Photoshop® CS4. The original micrographs were corrected for brightness and contrast and sharpened, then resized to create the composite figure.

3. Statistical Analysis:

Graphs and statistical analysis were undertaken using SPSS Statistics 17. Kendall's tau-c coefficient was used to evaluate the strength of associations between ordinal data sets. Skin morphology data was analysed using an unpaired t-test.

Materials:

3% glutaraldehyde solution in 0.05M Cacodylate buffer:

- Solution A: Cacodylate Stock (0.2M): 42.8g sodium cacodylate in 1L distilled water
- Solution B: 25% glutaradhyde in water (Sigma Aldrich)

50mL Solution A plus 24mL of Solution B plus 2.7 mL of 0.2M hydrochloric acid, made up to 200mL with distilled water, pH 7.4.

8% Paraformaldehyde stock

- Heat 80mL distilled water to 55°C
- Add 3-4 drops of 5M NaOH
- Add 8 grams paraformaldehyde and stir continuously
- When clear, vacuum filter
- Top off to 100mL and store at 4°C for up to 1 month.

Phosphate Buffered Saline (5X concentrate stock solution)

- 40g NaCl
- 1g KCl
- 5.75g $Na_2HPO_4.7H_2O$
- 1g KH_2PO_4
- Made up to 1L with distilled water, pH 7.4 (corrected with HCl / NaOH)

Results:

The clinical and pathological details of the subjects studied are given in Table 1.

1. Nerve biopsy tissue:

c-Jun immunoreactivity in nerve biopsy tissue:

c-Jun was not seen in normal nerve biopsy specimens (please refer to Figure 1 (A)). Figure 4 illustrates the dominant patterns of c-Jun-IR in each neuropathy subtype.

Axonal Neuropathies:

A variety of axonal neuropathy pathologies were studied, including vasculitic neuropathy, idiopathic axonal neuropathy, motor neuron disease, carcinomatous radiculopathy and preganglionic sensory neuropathy. c-Jun immunoreactivity (c-Jun-IR) was upregulated in the majority (86%) of axonal neuropathies examined. c-Jun-IR was localised to the Schwann cell nuclei in 42% of positive cases (Figure 1B) and to axonal cytoplasm in 50%, with faint myelin staining seen in the remaining case. At high magnification in both longitudinal and transverse sections, the identified nuclei were characteristic of Schwann cells, with elongated nuclear structures closely apposed to the nerve fibre they myelinate and orientated longitudinally to the nerve fibre (Castaneda et al., 2008). Immunoreactivity was also seen in axonal cytoplasm in this group (in 43% of the c-Jun positive axonal neuropathy cases), however the significance of this is unclear. There was no specific subtype of axonal pathology associated with either axonal or Schwann cell nuclear

staining in the axonal neuropathy group, although there were only small numbers of different types of axonal neuropathy studied (please refer to Table 1).

Table 1: Nerve Biopsy Data.

Macrophage activity/density: scant +; moderate ++; frequent +++. T-cell activity: scant +; moderate ++; frequent+++. Axonal loss: none 0; mild +; moderate ++; severe +++.

Abbreviations: DM-demyelination; SM-sensorimotor; NP-neuropathy; CIDP-chronic inflammatory demyelinating polyradiculoneuropathy; GBS-Guillain-Barré syndrome; SFN-small fibre neuropathy; POEMS-polyneuropathy with organomegaly, endocrinopathy, M-protein and skin changes; TTR-transthyretin; CMT-X-Charcot-Marie-Tooth, X-linked; CMT1A – Charcot-Marie-Tooth type 1A; EMG-electromyography; SC-Schwann cell; Mϕ -macrophages; OB-onion bulbs.

Case	**Age**	**Diagnosis**	**Neurophysiology**	**Pathology**			
				Mϕ	T-cells	Axonal loss	Myelin
1	47	Vasculitic NP	Axonal	+++	+++	++	No DM
2	71	Vasculitic NP	Axonal	++	+++	+	No DM
3	74	SM NP, ?inflammatory	Axonal	++	+	++ - +++	No DM
4	74	Idiopathic axonal NP	Axonal	++	0	++	No DM
5	74	MND (LMN) with sensory involvement	Axonal	+	0	+	No DM
6	56	Idiopathic axonal NP, ?inflammatory	Axonal	++	0	++ - +++	No DM
7	60	Axonal NP, impaired glucose tolerance	Axonal	+	+	+	DM
8	82	SM NP	Axonal	++	+	+++	No DM
9	73	Idiopathic axonal NP	Axonal	+	+	+	No DM
10	61	Axonal NP (Sjogrens)	Axonal	+	0	++ - +++	No DM
11	50	SM NP	Axonal	+	0	++ - +++	No DM
12	46	Acute SFN, Inflammatory	Axonal	+++	+	++ - +++	No DM
13	42	Preganglioinic Sensory NP	Axonal	+	0	++	No DM
14	73	Carcinomatous radiculopathy	Axonal	+++	0	+	No DM
15	40	POEMS	Mixed	++	0	++	No DM
16	41	POEMS	Mixed	+++	+	++	No DM

Table 1 continued:

Case	Age	Diagnosis	Neurophysiology	Pathology			
				Mϕ	T-cells	Axonal loss	Myelin
17	67	Amyloid neuropathy (TTR)	Mixed	++	0	+++	No DM
18	74	CIDP	Mixed	0	++	+++	De- & re-myelination
19	68	CIDP	Demyelinating	+	+	+	De- & re-myelination
20	73	CIDP	Demyelinating	+	0	+	Frequent demyelination
21	58	CIDP	Mixed	+++	++	+	De- & re-myelination
22	33	GBS	Inexcitable nerves.	++	+	++ - +++	DM, Mϕ associated DM
23	22	CMT-X (Connexin-32)	Mixed	0	0	++	DM, OB
24	60	CMT1A	Demyelinating	+	+	++ - +++	DM, OB
25	42	CMT1A	Not available	0	0	+++	OB
26	41	CMT1A	Not available	0	0	+++	OB
27	27	CMT1A	Demyelinating	+	+	++	OB
28	55	CMT1A	Not available	0	0	++	OB
29	20 mth	Normal	Not available	0	0	0	No DM
30	53	Normal	Normal	+	+	0	No DM

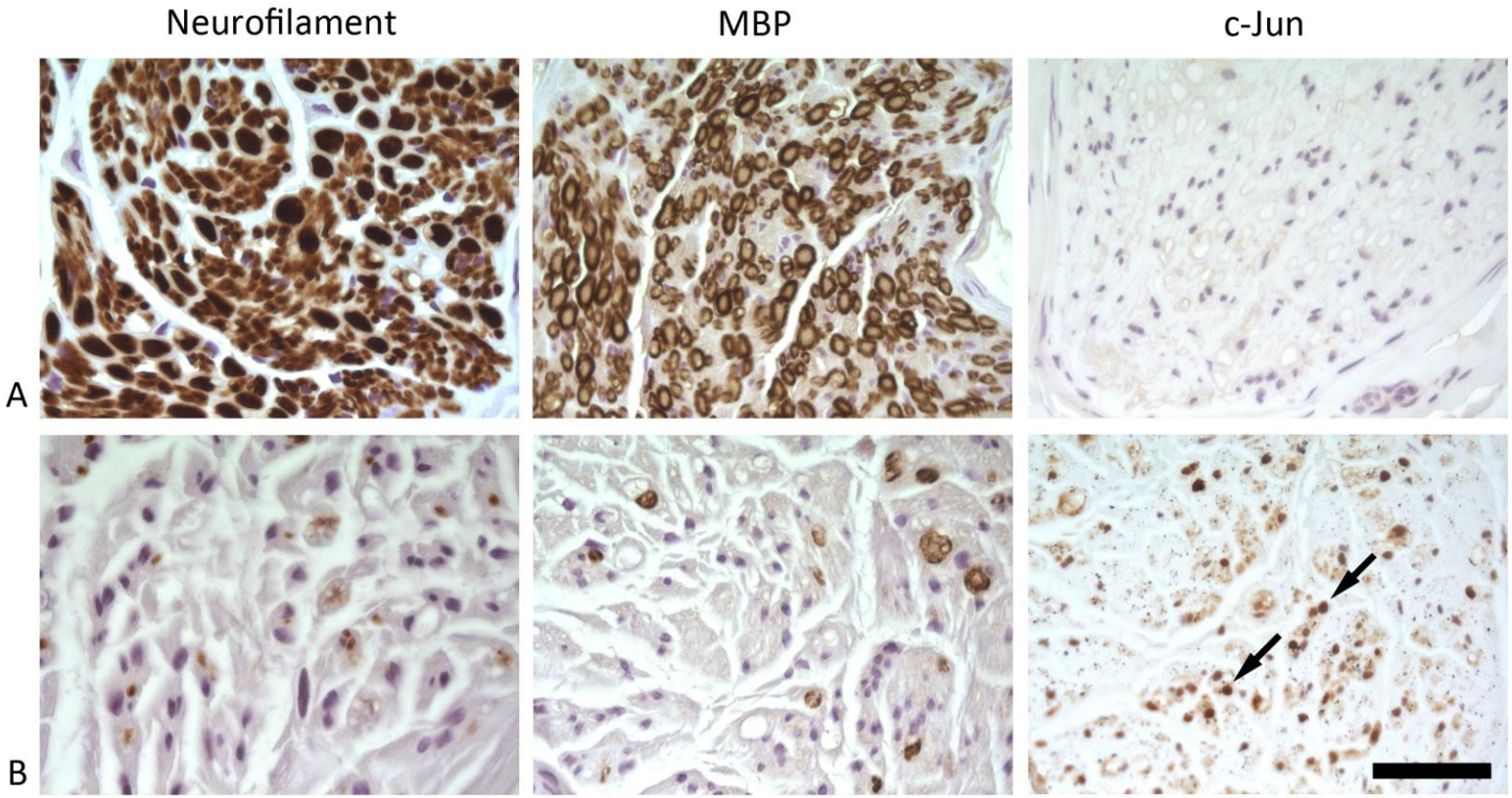

Figure 2a: Upregulation of c-Jun in axonal neuropathy

A: normal nerve (20 months old) - note absence of c-Jun-IR in the normal nerve;

B: axonal neuropathy - note the clear increase in c-Jun-IR in the Schwann cell nuclei (arrows).

Scale bar = 40 micron

Charcot-Marie-Tooth type 1A:

In the CMT1A patients Schwann cell nuclear c-Jun immunopositivity was seen in half of the cases studied. c-Jun IR in the CMT-1A nerves was less intense than in the acquired neuropathies, perhaps reflecting a more chronic disease process with slower, more protracted biologic mechanisms (Figure 2B(C))). Figure 3 shows the cellular localisation (by morphology) of c-Jun in the different demyelinating neuropathies studied.

Acquired demyelinating neuropathies:

In the five cases of acquired demyelinating neuropathies, clear nuclear c-Jun-IR was seen in only one case of CIDP. c-Jun-IR was, however, seen in myelin sheaths in several subjects with CIDP and GBS (Figure 2B(A) and 2B(B)); the significance of this is unclear, and animal data is not available for comparison. Further evaluation of this group is needed, however was beyond the scope of this pilot study.

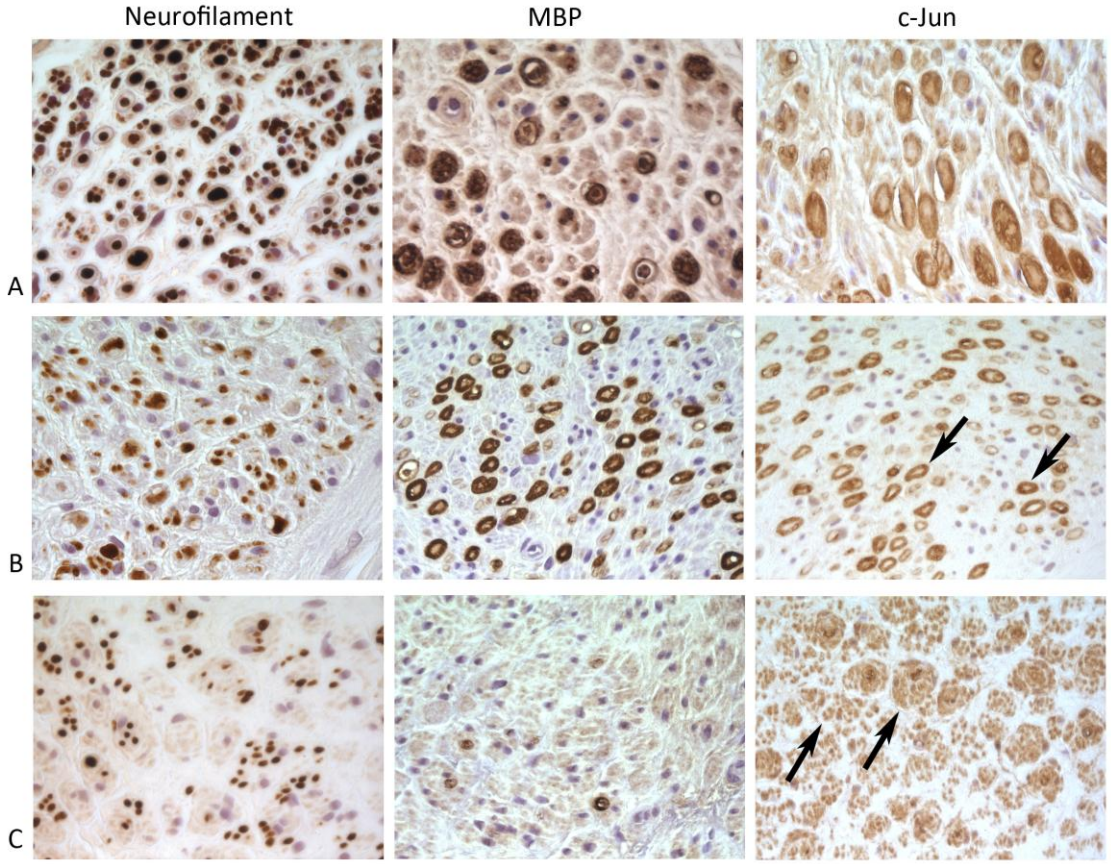

Figure 2B: Upregulation of c-Jun (nerve) in other human neuropathies
A: chronic inflammatory demyelinating polyradiculoneuropathy (arrows indicating myelin-based c-Jun-IR); B: Guillain-Barré syndrome (arrows indicating myelin-based c-Jun-IR); C: Charcot-Marie Tooth disease type 1A (arrows indicating c-Jun-IR (larger axons and Remak axons). Scale bar = 40 micron

p-JNK-IR in nerve biopsy tissue:

p-JNK activity was less clearly defined, but tended to occur primarily in a distribution and morphology consistent with cytoplasmic macrophage and fibroblast immunoreactivity (figure 3). The intensity of p-JNK-IR also correlated most strongly with macrophage activity in the biopsy (Kendall's tau-c 0.367, p=0.005). The nerve from the subject with CIDP (figure 3(C)) shows the clearest example of a macrophage-like morphology.

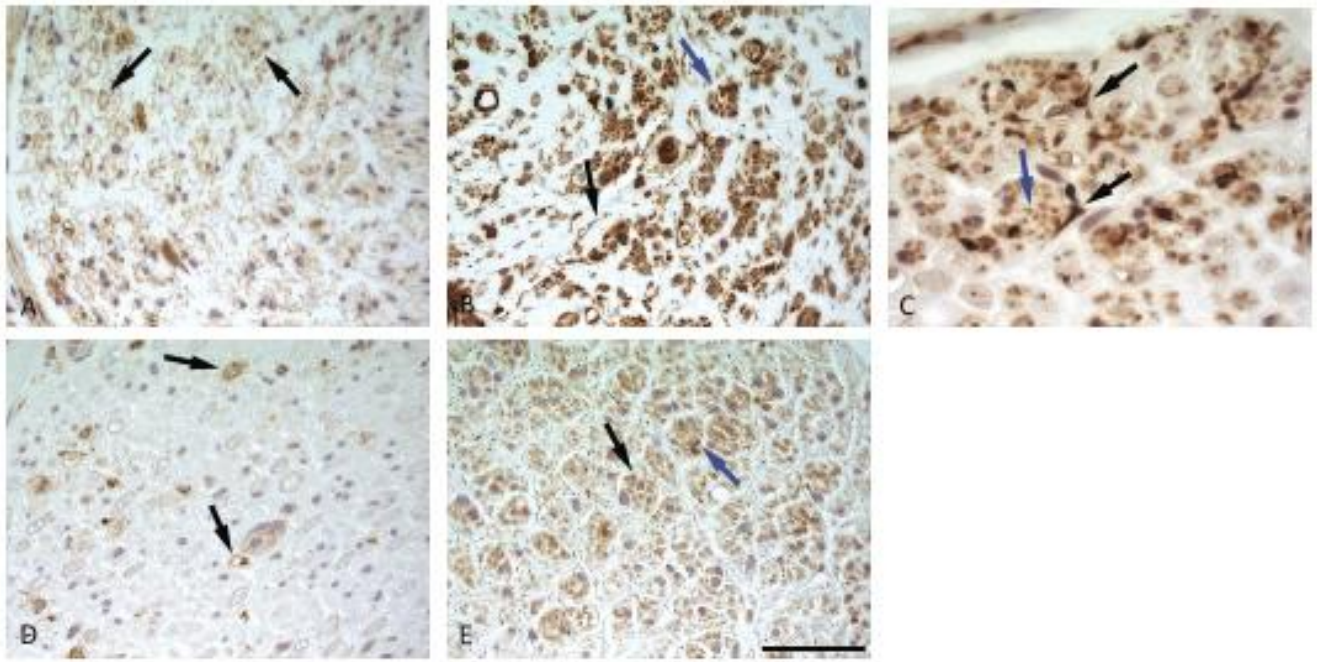

Figure 3: p-JNK-IR

A: Normal nerve - 20 months old (arrows show scattered p-JNK-IR in fibroblasts and myelin/Schwann cells);
B: axonal neuropathy (black arrow: fibroblast; blue arrow: axons);
C: chronic inflammatory demyelinating polyradiculoneuropathy (black arrow: macrophage; blue arrow: axons);
D: Guillain-Barre syndrome (arrows: macrophages); E: Charcot-Marie-Tooth Type 1A (black arrow: axon; blue arrow: macrophage).
Scale bar = 40 micron

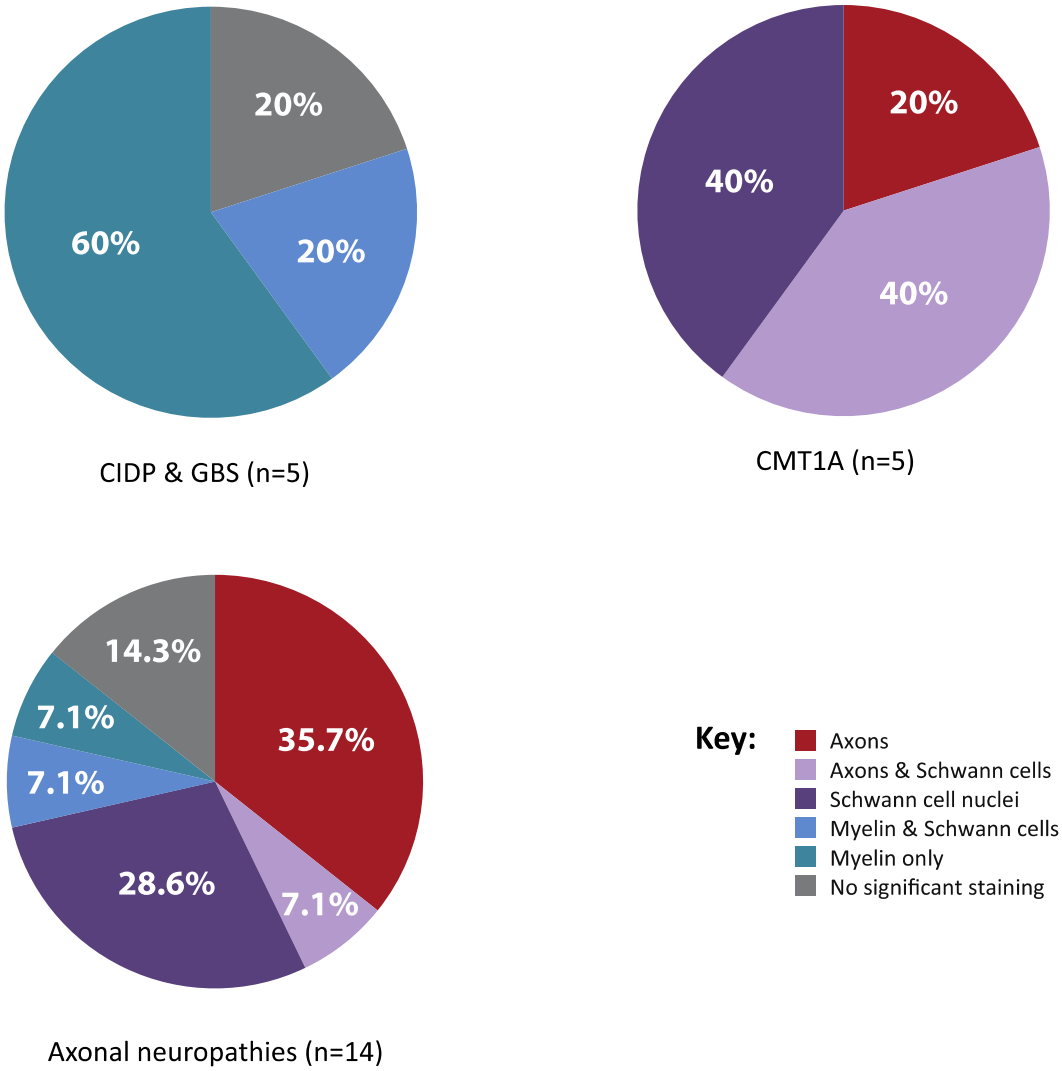

Figure 4: Main patterns of c-Jun immunoreactivity in different neuropathy subtypes
Patients with CMT-X, POEMS and amyloid neuropathy excluded.

Skin biopsy tissue:

Skin Morphology:

All subjects tolerated the skin biopsy well, with no complications reported. The details of the subjects studied are given in Table 2.

Several changes in skin morphology were observed in the patients with chronic neuropathies. These included reduced epidermal thickness (mean difference 49.3 μm (95% CI: 10.5 – 88.12, p=0.017), which has been previously observed in patients with neuropathies (Atherton et al., 2007). Reductions in the width and numbers of Meissner's corpuscles were also observed in the subjects with CMT1A, CIDP and GBS in comparison to normal controls (see Figure 5B-D, mean difference in width between neuropathy subjects and controls 17.6 μm (95% CI: 6.4 – 28.8, p=0.005)). Figure 5a, panel A shows a section of typical skin demonstrating the epidermal thickness, a healthy Meissner's corpuscle and the location of the dermal nerve bundles. Meissner's corpuscles have been previously reported to decrease in density with increasing age (Bolton, Winkelmann, & Dyck 1966), as well as in neuropathies (Dickens, Mulker, & Winkelmann 1963;Dyck, Winkelmann, & Bolton 1966). In our study the correlation between age and numbers of Meissner's corpuscles was not significant (Kendall's tau-c -0.28, p=0.2), however the numbers are too small to analyse the effect of age in subgroups divided by diagnosis.

Table 2: Skin biopsy data

c-Jun intensity: 0 no intraneural staining; + faint nuclear c-Jun-IR in some nerves; ++ definite c-Jun-IR in a few intraneural nuclei; +++ strong c-Jun-IR in several intraneural nuclei. PGP 9.5 intensity (compared to pattern and intensity seen in normal dermal nerves): 0 no PGP 9.5-IR; + some faint PGP 9.5-IR; ++ definite, but reduced PGP 9.5-IR (reduction in density or intensity of positive fibres); +++ full pattern of PGP 9.5-IR. MBP intensity (compared to normal dermal myelinated nerve bundles): 0 no MBP-IR; + some faint MBP-IR; ++ definite, but reduced MBP-IR (reduced numbers of positive fibres or reduced intensity (myelin thinning); +++ full, normal-equivalent MBP-IR. Abbreviations: CIDP-chronic inflammatory demyelinating polyradiculoneuropathy; GBS-Guillain-Barré syndrome; CMT1A-Charcot-Marie-Tooth type 1A.

Case	Age	Diagnosis	c-Jun Intensity	PGP 9.5 Intensity	MBP Intensity	Epidermal Thickness (μm)	Meissner's Corpuscle width (μm)
1	36	Normal	0	+++	+++	230	64
2	48	Normal	0	+++	++	290	38
3	46	Normal	0	+	+	300	47
4	28	Normal	++	+++	+++	212	28
5	63	CIDP	++	+	++	187	25
6	67	CIDP	+++	+	++	190	26
7	77	CIDP	++	+	0	191	30
8	51	CIDP	+++	++	++	228	26
9	68	CIDP	+++	++	++	196	26
10	74	CMT1A	+	+	++	211	20
11	34	CMT1A	+++	++	++	219	29
12	47	CMT1A	+++	++	+	203	27
13	26	GBS	++	++	++	253	31

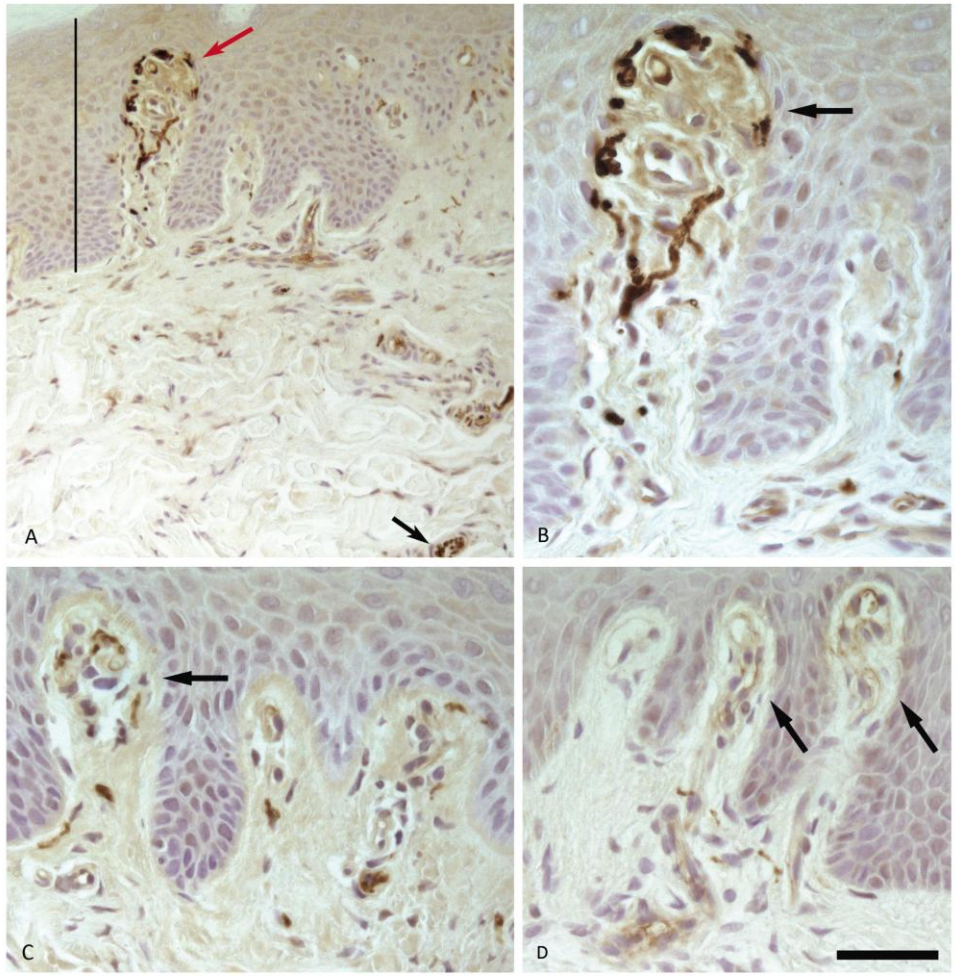

Figure 5: Skin Morphology (PGP 9.5)
Figure A shows normal skin morphology. The red arrow indicates a healthy, 'full' Meissner's corpuscle. The black arrow indicates the size and location of a typical dermal nerve. The black line indicates the cellular epidermis, which was the region measured in each subject to the maximum epidermal thickness. Figure B shows a high power photomicrograph of a normal Meissner's corpuscle (arrow). Figure C shows a partially atrophic Meissner's corpuscle from a subject with CMT1A (arrow), while figure D shows atrophic Meissner's corpuscles from a subject with CIDP (arrows).
Scale bar = 40 micron.(20 micron in Panel B, 80 micron in Panel A)

Skin innervation and c-Jun-IR:

c-Jun-IR was absent in 75% of the control nerves (Figure 6A), whilst moderate immunoreactivity was seen in one subject. Markers of dermal innervation density (PGP 9.5) and of myelinated fibres (MBP) were reduced in the pathological subjects compared with the controls (Figure 6). c-Jun-IR was increased in all 9 of the pathological biopsy specimens (Figure 6B-D).

Characteristic dermal nerve staining patterns in each of the diagnostic subgroups examined are shown in Figure 6. As expected, PGP 9.5 and MBP staining was reduced, although not completely absent in the dermal nerves of subjects with GBS, CIDP and CMT1A compared with the normal subjects. c-Jun-IR was absent within the nerve in the normal subjects, but normal staining of endothelial cells was seen. In the subjects with neuropathies, increased c-Jun-IR was clearly seen in nuclei within the dermal nerve. On the basis of morphology these are likely to be Schwann cell nuclei, with the most intense c-Jun staining of individual Schwann cell nuclei seen in the subject with GBS (figure 6C). Figure 7 highlights the differences in innervation density, myelination and c-Jun-IR between the demyelinating neuropathy subtypes studied.

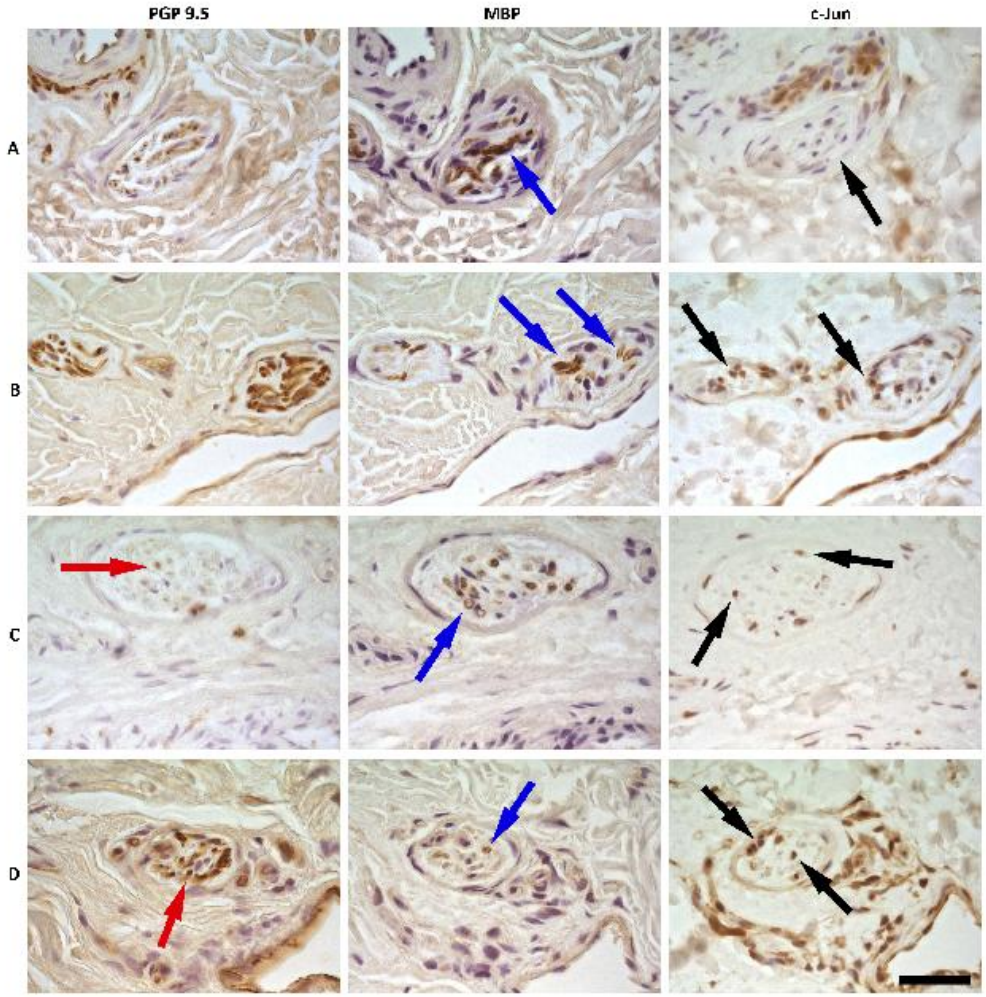

Figure 6: Skin Immunohistochemistry

A: normal skin, showing dermal nerve containing a number of myelinated fibres (blue arrow) but no c-Jun-IR within the nerve (black arrow);

B: chronic inflammatory demyelinating polyradiculoneuropathy, showing good numbers of PGP 9.5 positive fibres, indicating relative axonal preservation, but reduced MBP staining, and particularly thinned myelin (blue arrows). C-Jun-IR is seen in nuclei within the nerve, morphologically corresponding to schwann cell nuclei (black arrows);

C: Guillain-Barré syndrome, showing reduced numbers of PGP 9.5 fibres (red arrow), reduced numbers and thinning of the myelin sheath (blue arrow), and c-Jun positive Schwann cell nuclei (black arrows);

D: Charcot-Marie-Tooth disease type 1A, showing relative axonal preservation within the dermal nerve (PGP 9.5, red arrow), but loss of myelin (blue arrow), and c-Jun positive Schwann cell nuclei.

Adjacent sections are shown in each series.
Scale bar = 40 micron

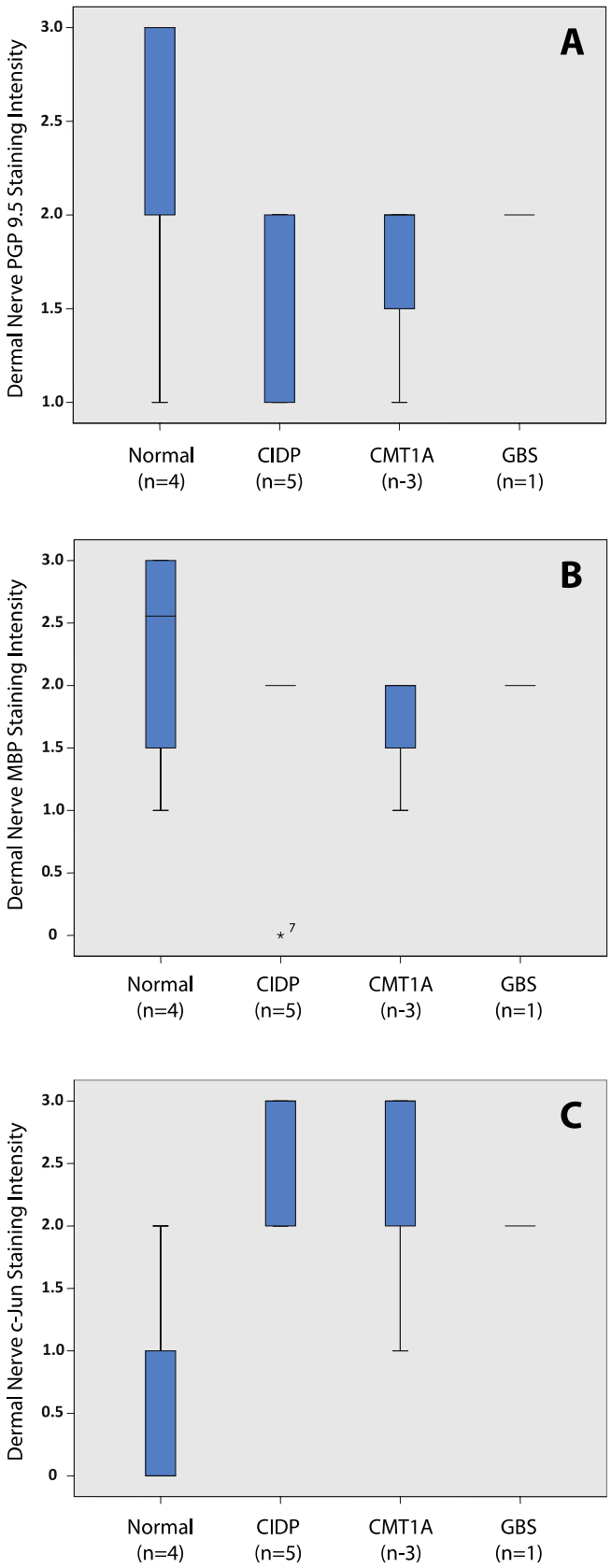

Figure 7: Skin Immunohistochemistry.
Data shown as median (central line), interquartile range (box), range (bars). Immunohistochemical intensity ratings given in the text.

A: Trend to reduced intensity of dermal nerve PGP 9.5-IR in demyelinating neuropathies, compared with healthy nerves (NS, p=0.23, ANOVA);

B: Trend to reduced MBP-IR in dermal nerves in demyelinating neuropathies (NS, p=0.70, ANOVA);

C: increased c-Jun in demyelinating neuropathies compared to healthy controls ($p<0.05$, ANOVA).

Discussion:

This small pilot study of c-Jun immunoreactivity demonstrates that c-Jun is expressed in pathological, but not in normal nerves, both in nerve biopsy specimens and in dermal nerve bundles. Faint c-Jun-IR was detected in one normal myelinated dermal nerve specimen, however the significance of this is unclear given that 'normality' was based on history, and not neurophysiologically confirmed. Of note, this subject also had the thinnest epidermis and narrowest Meissner's corpuscles of the normal volunteers. A detailed history was not taken from normal controls, just a screening one to exclude neuropathy symptoms. In addition, it is not known whether factors such as minor trauma (which may not exhibit any obvious signs) may have any effect on distal innervation.

Axonal neuropathies show upregulation of c-Jun in Schwann cell nuclei, but also in axonal profiles

Axonal neuropathies are probably the closest human correlate to animal models using nerve transaction as a model for a neuropathy. We found c-Jun-IR was markedly upregulated in human axonal neuropathies. Schwann cell nuclear c-Jun-IR in this group mimics the findings of upregulation of c-Jun expression following nerve transection observed in animal studies of (Arthur-Farraj et al., 2007, Jessen and Mirsky, 2008, Macedo et al., 2012). Immunoreactivity was also seen in some of the remaining axons in this group. The significance of this is uncertain, but may perhaps reflect an alternate role for c-Jun, such as activation of apoptotic pathways after a failure of regeneration. c-Jun regulation is complex, and modulated by several phosphorylation pathways, including JNK 1-3, ERK 1 and 2 and p38 MAPK. Each of these pathways has its own activating factors, such as loss

of trophic factor signalling (e.g. NGF), excitotoxicity, hypoxic / ischaemic insult and inflammation (Raivich, 2008). Whilst brief activation is associated with repair and regeneration, prolonged activation and / or high levels of c-Jun are thought to be linked to activation of apoptotic pathways (Raivich, 2008, Ferraris et al., 2012). It is tempting to speculate that the variation is pathological localisation noted in this study may reflect nerves at different stages of disease, differing severity of the initial insult, or other factors such as stronger concurrent inflammation or ischemia.

c-Jun is upregulated in Schwan cell nuclei in demyelinating neuropathies, with additional expression in axons in the more chronic, less inflammatory CMT1a, and in myelin in the more acute, inflammatory CIDP and GBS

c-Jun was also clearly upregulated in the nuclei of Schwann cells in demyelinating diseases, judging from our observations on nerves and skin biopsies tissue. This was seen in a number of different demyelinating pathologies including CMT1A, CIDP and GBS. Observations on nerve biopsies confirmed c-Jun upregulation in about 50% of CMT1A nerves. Of note, the positive Schwann cell nuclei in the CMT-1A group were seen in the younger two subjects, which is in keeping with the idea the Schwann cell nuclear upregulation is c-Jun occurs earlier in the neuropathy in an attempt to promote repair, and that this response is lost later in the disease, with axonal and fibroblast expression correlating with a later phase of cell death.

c-Jun biology is complex, which is aptly demonstrated by a recent study examining the response of an isolated Schwann cell c-Jun knockout mouse to nerve injury (Arthur-Farraj et al., 2012). This showed marked alteration in the nerve expression of over 172 molecules, including growth factors, adhesion molecules, growth-

associated proteins and transcription factors (Arthur-Farraj et al., 2012). The expression of c-Jun itself is regulated by many factors, including the AP-1 transcription complex, of which c-Jun is often one of the dimerising components. AP-1 is regulated by several signals, including the MAPK pathways (Erk1/2, JNK and p38). Inflammatory mediators, particularly TNF-α, are dose-dependent modulators of the activity of JNK and p38 MAPK, and through them of AP-1. Inflammation may therefore contribute to further upregulation of c-Jun beyond that induced by nerve injury (Kamata et al., 2004, Myers et al., 2003). Given that both c-Jun and TNF-α can promote repair at transient, lower levels, and apoptosis and more sustained, higher levels, this balance may have a role in shifting between repair and apoptosis. This may be particularly relevant in understanding the differences in the cellular distribution of expression of c-Jun in the more acute, inflammatory demyelinating neuropathies (CIDP and GBS) in comparison to the more protracted, less inflammatory course of CMT1A.

It would be interesting to conduct a larger study to explore further whether there are age- or duration-related changes in c-Jun-IR in the demyelinating neuropathies. One may hypothesise an evolution of the primary pathology in CMT1A from a demyelinating, Schwann cell dominated process in which ongoing attempts at regeneration are made, to a later phase of more prominent secondary axonal loss. Likewise, correlation with duration of disease and vigour of immune response in CIDP and GBS may help us better understand the unexpected myelin-based upregulation of c-Jun seen in this group. Longitudinal dermal nerve biopsy may be of help in such studies, given its relatively non-invasive nature compared with traditional sural nerve biopsy.

p-JNK-IR appears to be independent of c-Jun-IR in human neuropathies.

Whilst p-JNK immunoreactivity was commonly observed in the nerves of both neuropathy patients and normal controls, and the distribution was more variable, with most prominent expression in macrophages and fibroblasts. This would suggest that nerve damage and the type of that damage is less of a determinant of p-JNK expression than it is on c-Jun expression. The independence of p-JNK and c-Jun immunoreactivity, and its distribution primarily in macrophages and fibroblasts suggests that p-JNK may be more responsive to 'housekeeping' activities of the nerve. The lack of dependence of c-Jun-IR on p-JNK levels in in keeping with the findings of animal studies, which show that the activation of c-Jun following nerve injury is independent of phosphorylation by JNK (Parkinson et al., 2008). As TNF-α also promotes JNK activation (Kamata et al., 2004), this may explain the more defined macrophage p-JNK-IR seen in the inflammatory demyelinating neuropathies (GBS and CIDP) compared to the other patient groups.

Dermal myelinated nerve fibres were useful for studying c-Jun expression in human neuropathies. In dermal myelinated nerves from patients with demyelinating neuropathies, c-Jun-IR was seen in Schwann cell nuclei. c-Jun-IR is largely absent from dermal nerves in healthy controls. Epidermal nerves have previously been described to show frequent degenerating and regenerating axons, thought to be attributable to continuous nerve fibre remodelling in response to injuries induced by minor daily skin trauma (Arthur and Shelley, 1959). Such remodelling could involve dermal nerve plasticity and prompt local cycles of demyelination and remyelination in response. This process may explain

the moderate c-Jun-IR seen in one of our normal controls, although no obvious trauma was observed. A recent study of dermal innervation in CMT, whilst showing reduced innervation density of Meissner's corpuscles and intrapapillary myelinated fibres in CMT1A compared to normal controls, did demonstrate some overlap in innervation density between the patient group (n=10) and the normal controls (n=45), but did not discuss factors in the normal group which may be linked to denser of lesser innervation density (Manganelli et al., 2015). The numbers in our cohort were small, and larger normal numbers of normal subjects would be helpful to explore the range of normal variation in both morphology and c-Jun expression in this relatively new technique.

Limitations and further directions

There are several difficulties encountered in translating findings from experimental models of neuropathy to human studies. By their nature, animal and cell models allow for a monogenic population (or controlled alteration of an isolated gene), with homogenicity of age, sex, time of nerve injury and severity of the injury. In contrast, studies of human neuropathology, even in a single pathology, will have variation in disease duration and severity. There are then the added factors of variability in host response, including age, comorbidities, and genetics, which may influence factors such as the immune and inflammatory response to nerve damage.

The complexity of c-Jun biology, with multiple factors that can modify both its expression, and shift the net effect between proliferation / repair and apoptosis, make it difficult to conduct a patient-based study. In addition to the subjects

being enrolled at varying points in the time-course of their neuropathy, they will exhibit wide inter-individual variability in factors modulating these pathways, such as immune function, the net effect of which means that they may have varying degrees of activation of these competing pathways.

Despite the above concerns, there were clear differences seen in glabrous skin myelinated nerve fibres between the neuropathy patients and normal controls. The relatively non-invasive nature of the technique, coupled with ability to examine 5 five micron wax-embedded sections which are considerably easier to process in a conventional neuropathology laboratory than the protracted, technically more demanding floating 50 micron sections used to determine intraepidermal nerve fibre density make glabrous skin biopsy a potentially useful tool in understanding neuropathology in human neuropathies. This technique would also lend itself to following a patient cohort over time, allowing better understanding of the evolution of neuropathy, and its response to treatment.

Conclusions:

c-Jun immunoreactivity is increased in diseased, but not healthy nerves, and may be semi-quantitatively studied in both nerve biopsies and dermal nerves in glabrous skin biopsies. Findings in human neuropathy mimic those reported in animal models, suggesting that c-Jun activation plays a similar role in human Schwann cell biology, inducing dedifferentiation and demyelination in response to loss of axonal integrity. The additional c-Jun-IR seen in axons and myelin requires further study, in order to determine the role other factors, such as immune activation and apoptosis play in the evolution of human neuropathies. A similar

study undertaken in a larger cohort, with staining for other markers such as TNF-α, AP-1 and markers of apoptosis would help to clarify this. Longitudinal evaluation of glabrous skin evolution, particularly in CMT1A could help define whether the dominant role of c-Jun does indeed shift over time from one of Schwann cell proliferation and promotion of repair to one of apoptosis and axonal loss. This small pilot study confirms the utility of skin nerve examination in the study of pathogenic mechanisms in human neuropathies.

Chapter 4: Use of dermal microdialysis to determine the immune effect of acute nociceptor activation

Abstract

Introduction:

Recent studies suggest changes in the local immune profile of the skin (with a higher level of pro-inflammatory and a lower level of anti-inflammatory cytokines) may be a relevant aetiological factor in development and maintenance of neuropathic pain. However it remains unclear whether these changes are a response to nerve damage, nociceptor activity or a reflection of the underlying pathology in painful neuropathy.

Hypothesis:

I proposed that neurogenic inflammation induced by acute activation of nociceptors by topical application of capsaicin would not be sufficient stimulus to induce any immediate changes in immune profile in the innervated skin. This was important to determine prior to the next phase of my project, which examines whether ongoing, proinflammatory immune activation is a necessary addition to nerve damage in the development of neuropathic pain in Anderson-Fabry neuropathy.

Methods:

A dermal microdialysis catheter was inserted in the bilateral volar forearms of healthy subjects and a one-hour baseline collection of dermal microdialysis fluid was made. Topical capsaicin (1% in methylcellulose gel) was then applied to the forearm in a methylcellulose gel matrix, and three further hourly aliquots of dermal microdialysis fluid were collected and cytokine levels analysed using a multiplex ELISA assay. The nine cytokines assayed were selected according to those pro- and

anti-inflammatory cytokines postulated to modulate pain behaviour and nociceptor activity. Neurogenic activation in the capsaicin treated skin was confirmed by laser Doppler imaging measurement of the flare response.

Subjects:

Ten healthy volunteers were recruited and the study performed over a single 4-hour collection period. All subjects were studied starting at 9am to eliminate any diurnal variation in skin cytokine levels. The contralateral, untreated arm of each subject acted as his or her own control.

Results:

No significant difference for any of the cytokines measured was observed between the capsaicin-treated and control arms at any timepoint during the study. Neither was there any correlation observed between cytokine levels and pain scores or flare response. MCP-1 and IL-6 increased over the duration of the study in both treated and untreated arms.

Conclusion:

Capsaicin-evoked neurogenic inflammation was not sufficient to alter cytokine profile. Progressive elevation in MCP-1 and IL-6 was observed, and is likely to indicate a response to tissue damage from the introduction of the microdialysis catheter.

Background

Neuroimmune interactions in the skin are an area of interest for pain and neuroscience research because of developments in detection of low level analytes now allows the exploration of possible new therapeutic targets for neuropathic pain. Local agents might be applied topically, with fewer systemic side effects than many currently used agents. In order to pursue this line of enquiry, we first need to understand the bidirectional effects of nerve-immune interaction in the skin, and how resident skin cells may modulate these. Some of the possible key mechanisms in understanding these links are summarised in figure 10 in the background chapter.

1. Effects of nociceptor activation:

   Direct TRPV1 activation induces a local inflammatory cytokine and NGF release from keratinocytes. However, neuropeptide release in response to nociceptor activation induces a much larger number of cascades, including mast cell degranulation, keratinocyte activation and Langerhans' cell modulation, potentially far more effective inflammatory mechanisms. Mast cell degranulation and keratinocyte activation increase levels of the inflammatory mediators IL-1β, TNF-α, IL-8, NGF, ATP and histamine, whilst the effect of Langerhan's cell modulation may depend on the relative levels of CGRP and SP release. ATP release may also induce local calcium signalling through keratinocyte purinergic receptors, potentially augmenting the response (Koizumi et al., 2004).

Neuropeptides may also increase local synthesis of chemotactic cytokines, such as MCP-1, IP-10, IL-17 and TNF-α, augmenting an initial inflammatory immune response.

2. Effects of immune mediators on nociceptors:

   A number of cytokines are known to modulate nociceptor excitability and pain behaviours. Inflammatory cytokines such as IL-1β, TNF-α, IL-6, IL-17, MCP-1 and NGFβ are known to sensitise nociceptors directly. IFN-γ may be considered an indirect sensitiser, as although there are no reports of direct effects, it is a key initiator of inflammatory immune response, and increases the levels of the other cytokine molecules. IL-10 is an anti-inflammatory cytokine known to have algesic effects. Other chemotactic cytokines may indirectly augment sensitisation through recruitment of cells to the skin that release inflammatory, sensitising mediators, augmenting an initial response.

In neuropathy, it may be that an initial inflammatory response driven by nociceptor damage or increased firing generates local inflammatory changes in the skin. In subjects with persistent neuropathic pain, it may be that either their initial inflammatory response is stronger, the counter-regulatory anti-inflammatory resolution phase weaker, or the tendency to establish persistent inflammation through a shift to Th17 activity may be stronger. There are two aspects of this question that need to be resolved:

1. Does acute activation of nociceptors alone induce inflammatory changes in the skin (addressed below); and

2. Is there a difference in immune profile in subjects with chronic neuropathic pain than those purely with neuropathy, where the damage to the nerves is similar and from the same cause? (addressed in next section of thesis)

This study sought to determine whether acute activation of cutaneous nociceptors by topical capsaicin would alter the skin's immune profile. The aim of this section of the project was three-fold. Firstly, I wished to establish a new low volume and highly sensitive analytical system or dermal microdialysis. Next I wished to establish that dermal microdialysis in normal controls was able to detect the cytokines of interest, and to establish the operating range of the assay. Lastly, I wished to determine whether acute activation of nociceptors altered the levels of cutaneous cytokines, as this has not previously been established.

Background to Methods:

1. Dermal Microdialysis

Dermal microdialysis is an *in vivo* sampling technique used to measure hydrophilic molecules in the dermal extracellular fluid. The technique utilises a hollow, fluid-containing semiporous membrane, which permits the diffusion of molecules of a certain size, limited by the membrane pores, along a concentration gradient (Ungerstedt, 1984). Microdialysis can be used to either extract compounds of interest from the skin, or to introduce bioactive agents into the skin, as the direction of flux depends on the relative concentration gradient of the substance between the tissue and the dialysate. It may also be used in combination to study real-time effects of an agent on its surrounding tissue. Early studies used membranes with small pores, which limited the diffusion of proteins. The

introduction of larger pore (3000kDa) membranes in the 1990s enabled the study of bioactive proteins such as cytokines and growth factors (Schmelz et al., 1997, Schmelz et al., 1999). Combined with refinement of the multiplex ELISA technique with better dynamic range, it is now possible to measure very low concentrations of cytokines and growth factors in the skin in very small volumes of dialysate.

The extraction efficiency, or relative recovery of molecules from the surrounding tissue by microdialysis, is complex and influenced by a number of factors. These include perfusion flow rate and duration, membrane surface area, molecular size and hydrophilicity of the analyte, matrix properties of the surrounding media (e.g. viscosity) and temperature. Larger protein molecules have a diffusion coefficient around an order of magnitude lower than that for neurotransmitters such as dopamine, with extraction efficiency of 1-5% for proteins 10kDa or larger across a 100kDa membrane perfused at 0.5-1 µL/min (Ao and Stenken, 2006). In addition to reduced recovery due to their increased size, proteins may be adsorbed onto the microdialysis membrane (Schnetz and Fartasch, 2001). The relative recovery of a solute is given by the concentration in the dialysate divided by the concentration in the tissue, and is proportional to the flow rate. For example the relative recovery of glucose is nearly 100% at flow rates of 1 µL/min, but drops logarithmically to around 20% at 15 µL/min (Petersen et al., 1992). Total protein extraction also falls over time, with initial yields of 0.6 mg/mL in the first 20 minutes of dialysis to 0.2 mg/mL 100 minutes later (perfusion with Ringer's lactate at 4 µL/min) (Schmelz et al., 1997). A microdialysis study using a concentric microdialysis catheter found recovery rates: ~20% for IL-1β, 12-18% for IL-5, IL-6, IFN-γ and ~5% for IL-2, IL-4 and TNF-α (Sjögren and Anderson, 2009). This variability indicates that the technique is

most useful for establishing relative changes, rather than absolute tissue concentrations.

Another key variable in the technique is the depth of catheter insertion. The depth of catheter insertion measured by ultrasound, ranges from 0.4 – 1mm (Groth and Serup, 1998, Fartasch et al., 1997). As epidermal thickness ranges from approximately 70 μm in the arm to around 370 μm in the fingertip, this places the catheter within the dermis (Whitton and Everall, 1973). Microdialysis insertion produces a degree of local skin trauma, neural activation and immune reaction to the presence of a foreign body. Neurogenic activation induces a cutaneous flare response, which has been assessed by laser Doppler imaging. Initially distributed along the intradermal length of the catheter, it becomes more intense at the points of entry and exit from the skin. The increased blood flow begins to resolve by 15 minutes after insertion and returns to resting levels by 60 minutes (Anderson et al., 1994, Schmelz et al., 1997). An earlier study found longer lasting changes in blood flow (90-120 minutes), however this study used a larger cannula (21G) through which the microdialysis membrane was threaded, making direct comparison difficult (Groth and Serup, 1998). The magnitude, but not recovery duration, is reduced with the prior administration of local anaesthetic (Groth and Serup, 1998). Cytokine levels are elevated by catheter insertion, with elevation of IL-6, IL-8, TNF-α and IL-1β returning to baseline over 24 hours (Averbeck et al., 2006). Another group found levels of IL-1β, IL-6 and IL-8 were detectable after one hour, peaked at 5-8 hours and returned to baseline by 24 hours after catheter insertion (Sjögren and Anderson, 2009).

Responsiveness of the technique to topical agents has been previously demonstrated for examination of total protein content, with a 300% increase in protein extravasation in the area of histamine-induced wheal, but no change in the area of histamine-induced flare. In contrast, capsaicin did not induce any plasma extravasation either at the site of stimulation or in the region of the flare response. The histamine flare area also exhibited elevation of CGRP, but not SP (Schmelz et al., 1997).

2. Laser Doppler Imaging measurement of Flare

Laser Doppler Imaging is a method of measuring relative changes in capillary flow in the upper layers of the skin, developed in the 1990's (Essex and Byrne, 1991). The technique uses a narrow beam single wavelength laser (633nm, 1mm diameter beam) shone in a raster pattern over a region of skin (approximately $10cm^2$ in our study). The beam passes into the upper layers of the skin, to a depth of approximately 1 mm, and is reflected off moving blood cells in capillary beds. The moving cells induce a frequency shift in the reflected beam, which is received by photodiodes. The magnitude of the shift correlates with the blood volume and velocity. The imaging device builds up a 256 x 256 pixel image of the scanned region, in which each pixel is a point measurement of flux, thereby building a 2 dimensional map of relative blood flow in the skin. As absolute velocities cannot be calculated, the relative changes in flux are reported as arbitrary flux units (Essex and Byrne, 1991, Moor Instruments, 2012). The equipment is regularly calibrated against the Brownian motion detected in a vial of polystyrene microspheres (Moor Instruments, 2012). A series of scans can be taken over the same region, with

subtraction of a resting baseline scan possible to distinguish changes in perfusion from baseline blood flow. Neurogenic inflammation induced by activation of C-mechano-insensitive, heat-insensitive (CM_iH_i) and C-mechano- and heat-sensitive (CMH) fibres releases neuropeptides within the receptive fields of these neurons, inducing vasodilatation and increased perfusion of capillary beds, allowing Laser Doppler Imaging to map the extent of the induced flare response. This method thus provides one method to investigate functional integrity of C-fibres in the skin.

3. Multiplex enzyme-linked immunoabsorbant assay (ELISA)

Cytokine production is tightly regulated, and cytokines are usually only detectable in body fluids in the context of an immune response, and then at low levels (picomole per litre) (Ao and Stenken, 2006). As cytokines tend to work in groups of molecules with related effects, a panel of cytokines and chemokines was selected for this study, which included key components of inflammatory and counter-regulatory anti-inflammatory cytokine and chemokine networks, as well as those implicated in modulation of nociceptor function and neuropathic pain states. A variety of analytical techniques are available to detect and quantitate cytokine production, including PCR (for mRNA), radio-immunolinked assays (RIA) and enzyme-linked immunoabsorbent assays (ELISA) (for protein). Some cytokines, such as IL-1β undergo considerable regulation between mRNA synthesis and protein release. As it is the secreted proteins that are biologically active, these were felt to be the more pertinent focus for this study. Multiplex ELISA was therefore selected due to the need to balance a sensitive and specific assay with the ability to detect multiple analytes within a small sample volume.

Multiplex ELISA techniques have developed to capture and quantitate a variety of analytes simultaneously within a small sample volume. A set of microspheres (beads of 5-7µm diameter) is labelled with a primary fluorophore at specific concentrations. The intensity of the fluorophore detected gives the bead a unique 'address'. Each bead with the same concentration of fluorophore (address) is coated with an antibody specific to a single cytokine analyte. The set of beads coated with the individual antibodies are mixed to produce a set of beads that bind the range of cytokines of interest. These are incubated with the sample, then with a second detection antibody that binds to the cytokines. The intensity of the second antibody allows detection of the amount of bound cytokine attached to each bead subset by flow cytometry. The final concentration of each analyte is obtained by plotting internal bead density (denoting each cytokine) against the concentration of the detection antibody fluorophore to obtain the concentration of each cytokine in the sample. One hundred beads are sampled for each address and the intensities of the second fluorophore averaged to produce the final value used to calculate the concentration. Figure 1 summarises the multiplex ELISA method (Ao and Stenken, 2006). Multiplex bead-based assays have been found to have good correlation (R=0.9-1.0) with single analyte, solid-state single ELISA methods (Elshal and McCoy, 2006).

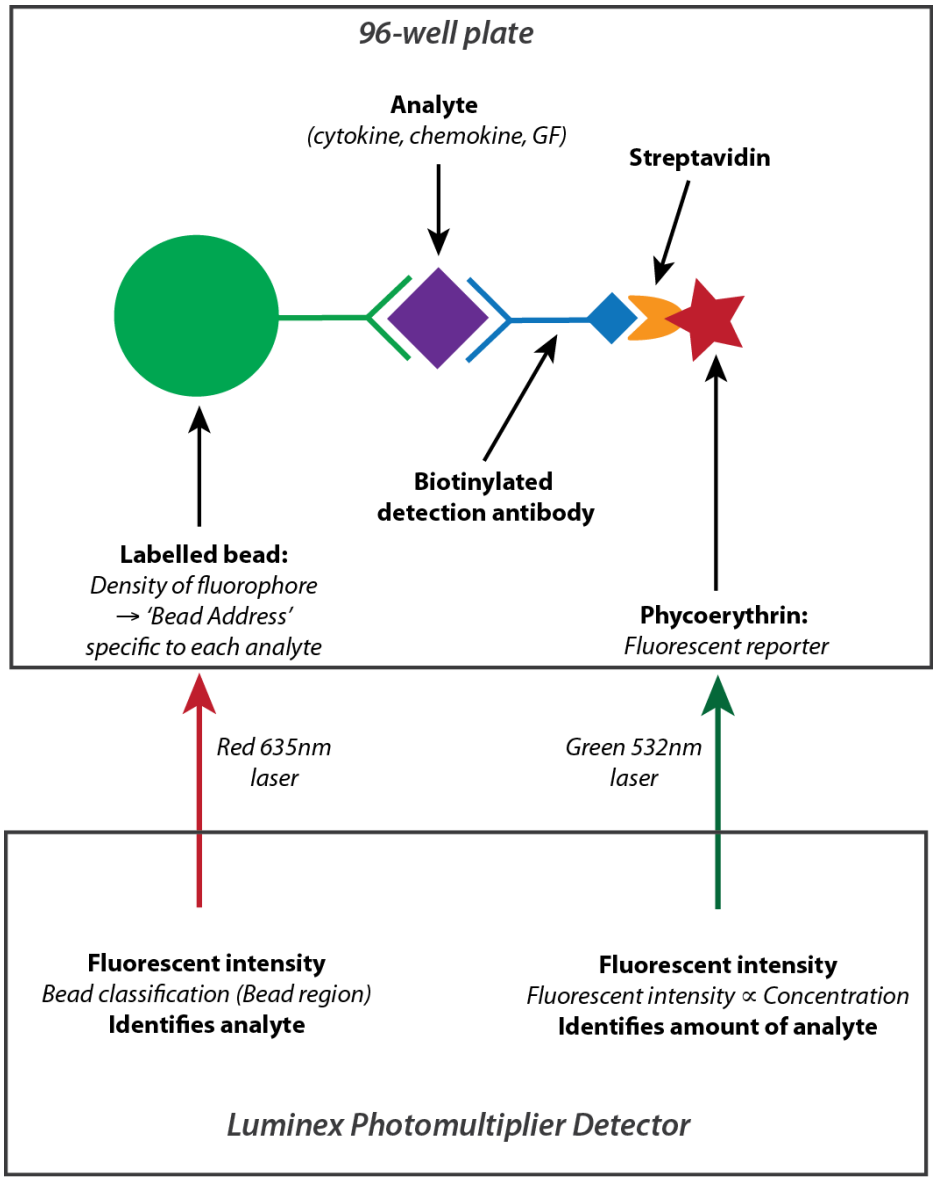

Figure 1: Summary of multiplex ELISA method

The data obtained in immunoassays is not linearly distributed, so a straight line-of-best fit is inappropriate (Findlay et al., 2000). Whilst logarithmic plots improve the fit, the data is usually also not symmetrically distributed, meaning that the upper and lower asymptotes do not mirror each other. In order to incorporate this, and thereby reduce error from lack-of-fit, modelling of calibration curves for this technique have been progressively refined, resulting in the 5PL (five-parameter

logistic) curve-fitting method used in this study (Gottschalk and Dunn, 2005, Findlay and Dillard, 2007).

Modelling of the calibration is derived from the equation below (Findlay and Dillard, 2007), with the points illustrated on one of the calibration graphs from the study - a 10-point calibration curve for IL-6:

$$y = d + \frac{a - d}{\left(1 + \left(\frac{x}{c}\right)^{b}\right)^{g}}$$

Where:

y = assay signal
x = analyte concentration
a = estimated response as concentration approaches zero (lower asymptote)
b = slope factor of linear section of curve
c = mid-range concentration / point of inflection / C_{50}
d = estimated response as concentration approaches infinity (upper asymptote)
g = the degree of asymmetry of the curve around the C_{50}. If m = 1, there is perfect symmetry to the curve.

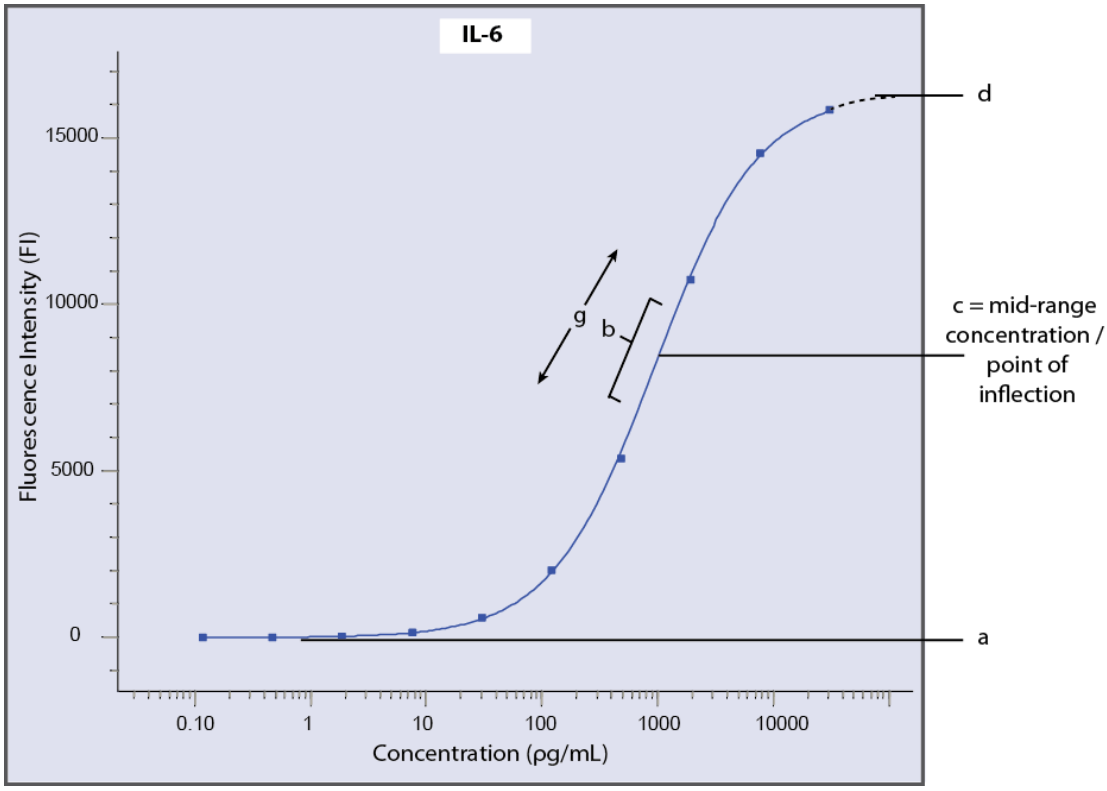

Methods

1. Dermal Microdialysis Method

Microdialysis catheters were kindly supplied by the laboratory of Professor Martin Schmelz, Department of Anesthesiology, Mannheim, University of Heidelberg, Germany. These are 0.4mm diameter microdialysis membranes with a pore cutoff for proteins above 3000kDa (cytokines are 8-80kDa (Ao and Stenken, 2006)). The membrane is attached to a 26G introducing needle at one end and a length of Tygon tubing at the other, which connects to a 27G needle attached to a saline-filled syringe. The microdialysis catheter is perfused at a rate of 0.2 mL per hour (3.3 µL/min), regulated by a syringe pump.

All subjects were pretreated by the application of 5% EMLA local anaesthetic cream (2.5% lidocaine / 2.5% prilocaine eutectic mixture) for 45-75 minutes (until analgesia to pinprick was obtained). The microdialysis catheter was primed with saline, and the 26G introducing needle held with a needle holder and inserted at a 30° angle to the skin surface, then flattened off immediately on piercing the skin. The needle was advanced parallel to the skin surface, as superficially as possible without breaking the skin surface. The needle was advanced for 1.5cm, then pushed through the skin surface and the microdialysis membrane gently drawn through, keeping straight alignment with the intracutaneous path. Once the membrane was drawn through to within 2 mm of the joint with the Tygon tubing, the needle was cut off, leaving a 3 cm distal length of membrane. The proximal Tygon tubing was connected to the syringe pump, and flushed to remove any air. A 1.5 mL Eppendorf tube containing 30 µL of Roche complete protease inhibitor was taped below the

cut end of the tubing to collect the fluid, and microdialysis commenced at a flow rate of 0.2 mL/hr (3.3 µL/min). Please see below for justification of inclusion of protease inhibitor based on the preliminary experiments.

Despite the changes in cytokine yield over time discussed above, there is a precedent for the use of a 1 hour stabilisation period prior to stimulation experiments, using the same technique and catheters which this project employed & utilised in this study of the effect of topical capsaicin on cutaneous cytokine production (Schmelz et al., 2003). Figure 2 illustrates the microdialysis method.

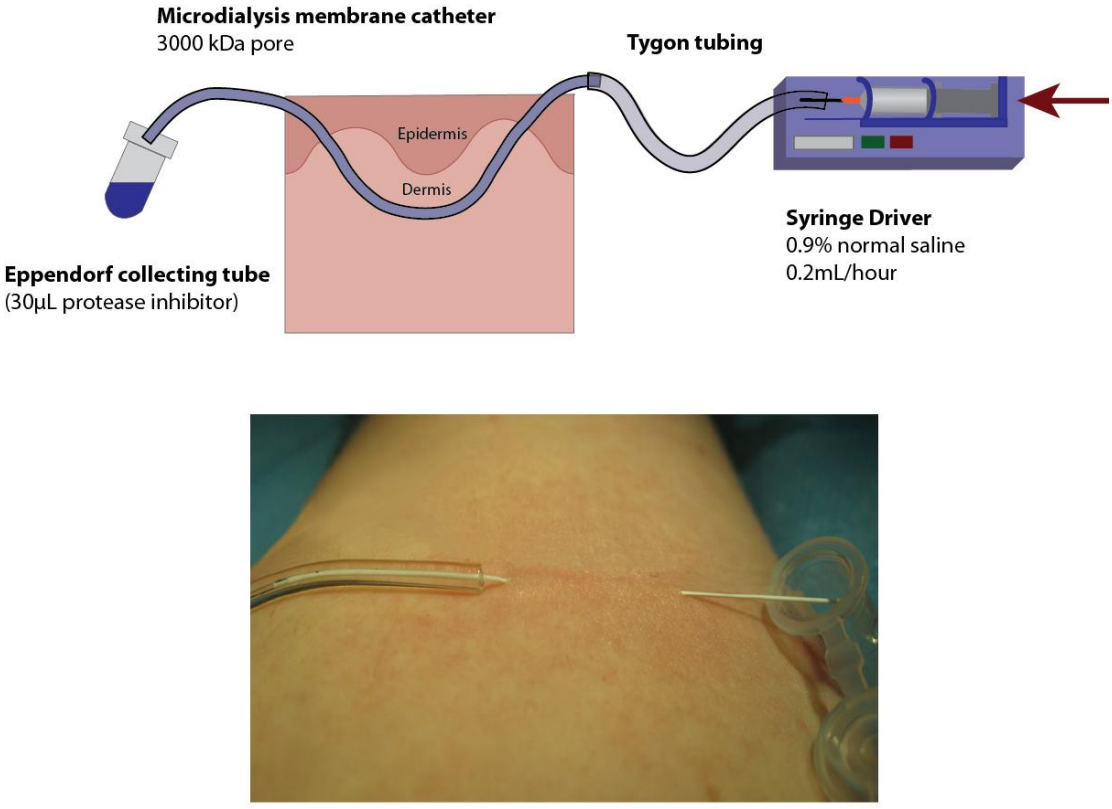

Figure 2: Dermal microdialysis method

2. ELISA Method

Note: All reagents and buffers were equilibrated to room temperature prior to use. Each wash was performed using 100 µL of wash buffer per well, then vacuum filtering the plate and returning it to the plate holder. After each wash on the vacuum manifold, blot the base of the plate on clean paper towel. The plate was kept on the plate holder at all other times to prevent contamination. The vacuum manifold was calibrated using a flat-bottomed 96 well plate. The pressure was set at -1 to -3 mmHg, such that 100 µL liquid was extracted over 3-4 seconds to clear the well.

The standards were prepared for a 10-point calibration curve using the low PMT (RP1) settings. Standards were prepared according to the company instruction for a mixed assay, using Cytokine Group I Human Cytokine Standard (IL-1β, IL-6, IL-10, IL-17, TNF-α, IFN-γ, IP-10, MCP-1 and RANTES) and Group II Human Cytokine Standard (NGFβ). Each vial of lyophilised standard was reconstituted using 250 µL of standard diluent, vortexed for 3 seconds, then incubated on ice for 30 minutes. After incubation, 64 µL of each reconstituted standard was added to a vial containing 72 µL of standard diluent to make the S1 standard, which was vortexed for 3 seconds. Sequential 1:4 serial dilutions were prepared to make standards S2-S10. The standard diluent constituted the blank for the assay. The samples for the assay were thawed and kept on ice until just prior to use. Microdialysis samples were used undiluted.

The coupled beads were prepared by adding 4,600 µL of assay buffer to a 6 mL vial. Coupled beads were vortexed for 30 seconds, then 575 µL of each of the coupled

beads (for Human Cytokine Group I and Group II) were added to the 6 mL vial, which was vortexed for 3 seconds. The prepared beads were wrapped in aluminium foil and equilibrated at room temperature for 20 minutes prior to use. Just prior to adding the beads to the assay well, they were vortexed for 30 seconds.

The plate was pre-wetted by adding 100 µL of assay buffer per well, then vacuum filtering and blotting the base of the plate on paper towel. 50 µL of coupled beads were added per well, and then two washes were performed. Fifty microlitres of each of the standards and samples were added to the appropriate wells according to original assay plan, with each sample or standard run in duplicate. Each vial was vortexed for three seconds immediately prior to adding to the plate. The plate was then covered with sealing tape, wrapped in foil and incubated at room temperature for 30 minutes on the shaker (1,100 rpm for 30 seconds, then 300rpm).

The detection antibodies were prepared by vortexing for 15-20 seconds, followed by a 30 second spin. Three hundred microlitres of each detection antibody was then added to a 6 mL vial containing 2,400 µL of detection antibody diluent, which was vortexed for three seconds immediately prior to use.

The plate was removed from the shaker and three washes performed. Twenty-five microlitres of detection antibody were added to each well, and the plate then covered with sealing tape, wrapped in foil and incubated at room temperature for 30 minutes on the shaker (1,100 rpm for 30 seconds, then 300rpm).

The streptavidin-PE 100x was vortexed for 20 seconds, and then spun for 30 seconds. Sixty microlitres of streptavidin-PE 100x was added to a 6 mL vial

containing 5,940 µL of assay buffer, vortexed for 3 seconds and protected from light until use.

The plate was removed from the shaker and washed 3 times, then 50 µL of streptavidin-PE was added per well (after a 3 second vortex). The plate was covered with sealing tape, wrapped in foil and incubated at room temperature for 10 minutes (with shaking at 1,100 rpm for 30 seconds, then 300rpm). After incubation, the plate was removed from the shaker and 3 washes performed. The beads were then resuspended using 125 µL of assay buffer per well.

The Luminex reader was switched on and allowed to stabilise for at least 30 minutes prior to use. The reader was calibrated, after confirming that the CAL1 and CAL2 settings were the same as those printed on the bottle of Bio-Plex calibration beads. The low PMT (RP1) target value was used. The plate protocol and the analyte details (bead regions and predicted concentrations for dilution curves) were entered. The data acquisition settings were confirmed as follows: 50 beads per region, bead map set to 100 region, sample size set to 50 µL, and DD gates set to 5,000 (low) and 25,000 (high). The plate was shaken for 30 seconds at 1,100 rpm immediately prior to being placed in the reader and the analysis run was commenced.

The reliable limit of the standard curve was determined by the region for which the observed / predicted concentrations x 100% fell in the 70 – 130% range. The level of fluorescence detected for the lowest point of the curve was also checked against the level recorded for the blank, and if the fluorescence for the lowest point of the curve within the 70-130% range fell beneath that of the blank, the next highest

point in the curve was selected as the lower limit of reliable quantification. The singular results for each pair of samples were compared, and if one sample was clearly greatly divergent across analytes, it was removed from the assay, and that point considered only from the reliable single sample point. This occurred very rarely.

Validation of ELISA

The reliability of an immunoassay is determined by a number of measures. The 2 key measures are precision (SD/mean x 100%) and accuracy (Observed/Expected concentration x 100%). FDA guidelines for immunoassay evaluation published in 2000 set a recommended acceptable level for accuracy of 75-125% but comment that this could be expanded, and indeed common practice is to accept the reliable region of the calibration curve as that in which accuracy is between 70-130%, which has been used in this study (Findlay et al., 2000, Urbanowska et al., 2006).

The limit of blank (LOB) is the lowest limit at which an assay can reliably determine the difference between the presence and absence of an analyte, but not necessarily be able to reliably quantitate the amount of the analyte present. It is calculated using at least 20 repeated blank samples by the following:

$$LOB = mean_{blank} + 1.645(SD_{blank})$$

This gives a LOB at which 95% of blanks will be true blanks, but will include some samples that are not true blanks. This means that the false positive (Type I error) and false negative (Type II error) rates are 5% at the LOB (Armbruster and Pry, 2008). The limit of quantification (LOQ) is the level at which concentration, not just

presence, of the analyte may be reliably determined. It may be calculated based on the LOB by the following equation:

$$LOQ = mean_{blank} + 2(SD_{blank})$$

Alternately, LOQ may be determined by repeated analysis of samples containing a known, low concentration of the analyte in order to empirically determine the level at which the signal : noise ratio permits accurate quantification. This method uses the formula:

$$LOQ = mean_{blank} + 1.645(SD_{low\ concentration\ sample})$$

The information on the assay limits provided by BioRad on the Precision Pro assay used for this study are presented below (Table 1) (Bio-Rad, 2012). They are based on an 8-point calibration curve, rather than the 10-point curve this study used to try to optimise the sensitivity of the assay for low concentrations. Using a 10-point calibration curve, I obtained lower reliable values for all cytokines (except NGF-β) than the published data provided by the company using an 8-point curve. The range between our lower limit of quantification (LLOQ) and that published by the company, should however, be interpreted with caution, as it is likely to be less robust. Precision of the assay is robust for all cytokines in our laboratory.

Table 1: Company published dynamic range					
	Working Range		Sensitivity	Precision	
	Lower Limit / LLOQ (ρg/mL)	Upper Limit / ULOQ (ρg/mL)	Limit of detection (LOB) (ρg/mL)	%CV (Intra-assay)	%CV (Inter-assay)
IL-1β	3.2	3261.0	0.6	6	8
IL-6	2.3	18880.0	2.6	7	11
IL-10	2.2	8840.0	0.3	5	6
IL-17	4.9	12235.0	3.3	8	6
IFN-γ	92.8	52719.0	6.4	15	9
IP-10	18.8	26867.0	6.1	11	9
MCP-1	2.1	1820.0	1.1	9	7
RANTES	2.2	8617.0	1.8	9	6
TNF-α	5.8	95484.0	6.0	8	6
NGF-β	1.0	4247.0	0.2	4	7

Table 2 presents the ranges of the assay which were within the acceptable ranges for precision and accuracy based on the analysis of 3 x 10-point standard curves run in our laboratory, with each curve run in duplicate.

Table 2: Overall assay dynamic range in our laboratory				
	Working Range		Precision	
	Lower Limit (ρg/mL)	Upper Limit (ρg/mL)	%CV (mean intra-run precision, working range)	%CV (mean inter-run precision, working range)
IL-1β	0.1	2903.7	5.6	11.3
IL-6	1.6	23944.5	5.9	17.8
IL-10	0.4	1793.3	3.9	10.6
IL-17	1.6	23612.8	14.4	6.5
IFN-γ	32.8	26525.0	6.2	9.9
IP-10	11.7	36114.9	12.3	14.2
MCP-1	1.5	1578.7	5.9	16.7
RANTES	6.2	5386.9	6.3	18.3
TNF-α	0.3	24177.7	8.6	7.5
NGF-β	1.1	13256.0	6.6	11.1

Table 3 presents the values this study obtained for cutaneous cytokines using dermal microdialysis in the forearms of 10 healthy controls (5 male). Data is from 20 forearms (2 per subject, collected simultaneously) over 1 hour at a flow rate of 0.2 mL/hr. Values that are below our established LLOQ are highlighted in grey, and thus effectively not detectable (ND). Those that are between our LLOQ and that of the company are highlighted in pale blue, and must be interpreted with caution.

Table 3: Normal control dermal microdialysis cytokine levels.

	Mean (pg/mL)	SD	RSD (%)	Median (pg/mL)	Lower 95% CI (pg/mL)	Upper 95% CI (pg/mL)	Skewness
IL-1β	0.5	0.7	135	0.4	0.0	1.0	2.11
IL-6	5.9	6.1	103	3.2	1.6	10.3	1.02
IL-10	1.0 (ND)	1.0	100	1.0 (ND)	0.3 (ND)	1.6	0.52
IL-17	13.6	11.8	87	12.6	5.1	22.0	1.13
IFN-γ	15118.7	6808.5	45	17164.4	10248.2	19989.2	-0.93
IP-10	650.9	286.3	44	614.4	446.0	855.7	0.34
MCP-1	63.2	174.9	277	8.5	-61.9 (ND)	188.3	3.16
RANTES	54.8	45.5	83	37.9	-23.5 (ND)	259.7	0.87
TNF-α	5.0	3.6	71	5.2	2.5	7.6	0.38
NGF-β	6.2	7.9	128	5.4	0.5 (ND)	11.9	1.92

Key to Table 3: ND: effectively not detected as outside real detection limits; SD: standard deviation. Relative standard deviation (RSD) is a measure of variability, calculated by SD/mean x 100%. Skewness indicates deviation from the normal distribution (skew = 0). Positive skew indicates a distribution with a right-sided tail and negative skew indicates a left-sided tail. All cytokines assayed are not normally distributed, with most demonstrated a right-sided tail to their distribution.

Effect of protease inhibitor on cytokine yields

The effect of protease inhibitor on microdialysis cytokine yields was assessed by a preliminary experiment using single subject. Both arms were prepared as above, with microdialysis catheters inserted in the mid-volar forearm bilaterally. A simultaneous 2-hour collection from each arm was obtained using a flow rate of 0.2 mL/hr. One collection vial contained 30 µL of Roche Complete Protease Inhibitor. The protease inhibitor was prepared by dissolving the tablet to make a x7 stock solution as per the company instructions, then taking an aliquot estimated to provide the appropriate final concentration based on the estimated microdialysis volume. The results of this experiment are presented in the graphs in figure 3, which shows the effect of protease inhibitor (purple) on cytokine yield compared to that in the untreated simultaneous collection in the contralateral arm (blue). The top graph presents data for all the cytokines tested, the second graph presents an expansion of the axis to better illustrate the effect on cytokines with low concentrations. Low concentration cytokines are presented in the second graph with an expanded y-axis for clarity. Use of protease inhibitor increased recovery of all cytokines, with particularly dramatic effects on IFN-γ and IL-17.

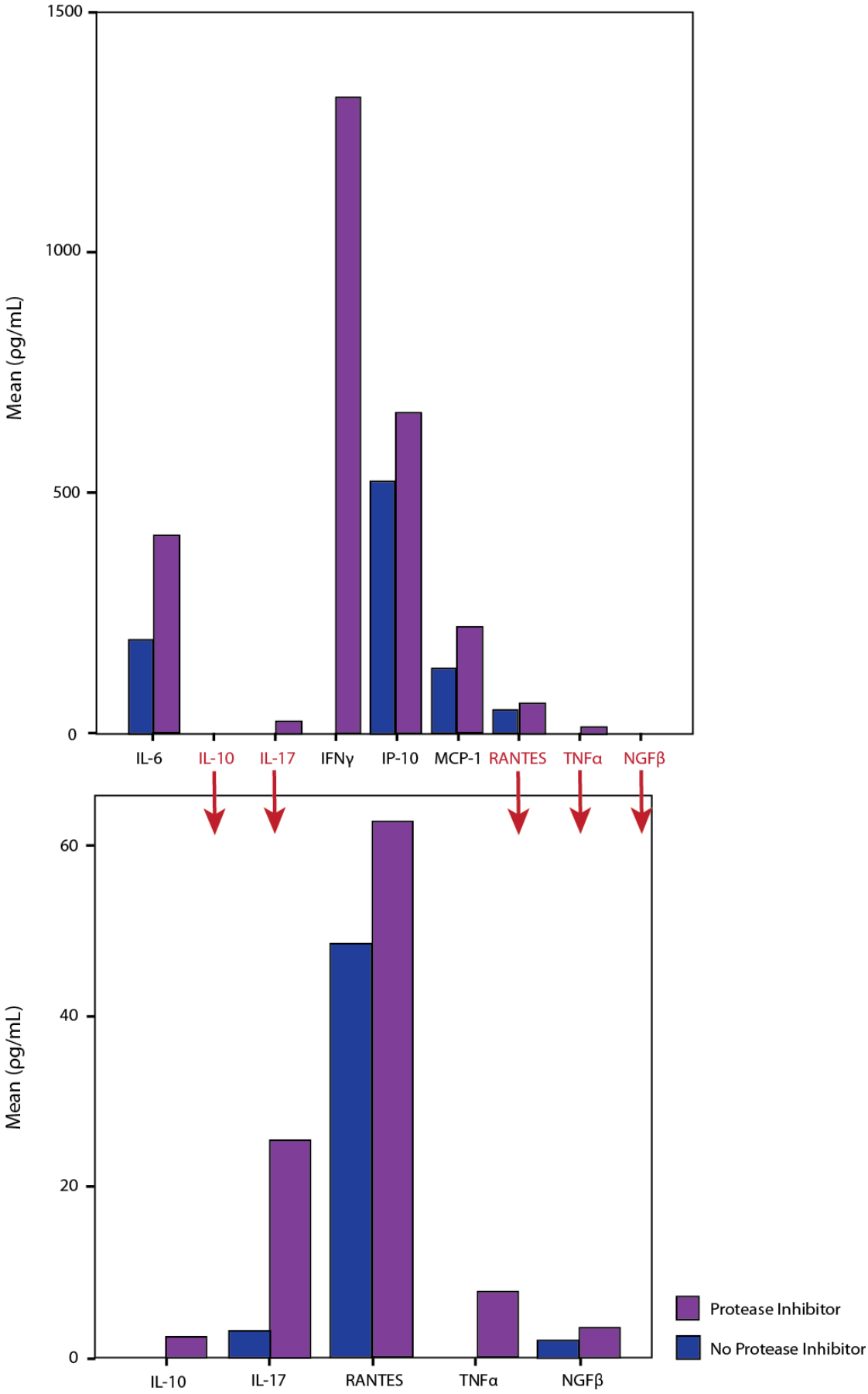

Figure 3: Effect of protease inhibitor on analyte recovery

Subjects:

Ethical permission to conduct the study was obtained from the Great Ormond Street and Institute of Child Health Research Ethics Committee (REC) (now London – Bloomsbury REC). Ten healthy normal volunteers (5 male, 24-49 years) were recruited. Subjects were excluded if they had any pre-existing dermatological or neurological disease, or were on any regular medication (other than the oral contraceptive). Subjects were asked to avoid heavy exercise for 3 days prior to the study, not to eat in the hour prior to the study, and to consume no alcohol for the day prior to the study, in order to minimize sources of potential variability in cytokine levels.

Experimental design:

The study was commenced at 9am for all subjects to minimize diurnal variation in cytokine levels. Subjects were seated comfortably in a room maintained at a comfortable ambient temperature (21-23°C) with their arms supported by pillows. EMLA cream was applied to the midpoint of each volar forearm for 45 – 90 minutes (until pinprick sensation was dulled). Skin was cleansed with chlorhexidine, then a single microdialysis catheter (0.4 mm diameter, 3000kDa cutoff) was inserted in each volar under sterile conditions (method detailed below). Hourly aliquots of microdialysis fluid were collected in separate protease inhibitor-containing Eppendorf tubes from each arm over a 4-hour period, with each aliquot placed on dry ice immediately after removal from the patient. Fluid volume collected in each Eppendorf tube was recorded by weight (post – pre collection weight). After one hour, the area over the left microdialysis catheter was covered with 1% topical

capsaicin gel, applied over a 0.79cm^2 area directly over the catheter. The area of gel in contact with the skin was controlled using a 1cm internal diameter ring of Comfeel® (Coloplast) adherent to the skin, and contained within a 1cm internal diameter lidded O-ring held to the Comfeel ring using a steristrip. The control arm was covered with the same mechanism, but using plain KY® Jelly. Capsaicin gel was prepared using 50 mg of capsaicin powder (Sigma Aldrich, M2028) dissolved in 0.5 mL 100% ethanol then mixed with 4.5 mL KY® Jelly to make a final 1% w/v capsaicin gel. The gel remained *in situ* for the remaining 3 hours of the protocol. Vials were stored on dry ice at the end of each 1 hour collection and then transferred to an -80°C freezer until analysis by multiplex ELISA.

Time and peak intensity of pain / itch was recorded using a 0-10 numerical rating scale. Residual flare at the end of the 3 hours of capsaicin stimulation was recorded over the treated and control arms using Laser Doppler Imaging as a surrogate marker of nociceptor activation.

Summary of Protocol:

	Right arm	Left arm (control)
Start	**Microdialysis catheter inserted under EMLA analgesia.**	**Microdialysis catheter inserted under EMLA analgesia.**
0-60 min	Collect first hour fluid (Baseline).	Collect first hour fluid (Baseline).
60 min	**Application of 1% topical capsaicin**	**Application of KY jelly (control)**
60-120 min	Collect first stimulated hour fluid	Collect first stimulated hour fluid
120-180 min	Collect second stimulated hour fluid.	Collect second stimulated hour fluid.
180-240 min	Collect third stimulated hour fluid.	Collect third stimulated hour fluid.
240 min	Remove capsaicin and dialysis catheter.	Remove KY Jelly and dialysis catheter.
240 min	LDI Flare	LDI Flare

Note: all microdialysis collections taken over 1 hour with a flow rate of 0.2 mL/hr into a collection vial containing 30 µL of Roche complete protease inhibitor.

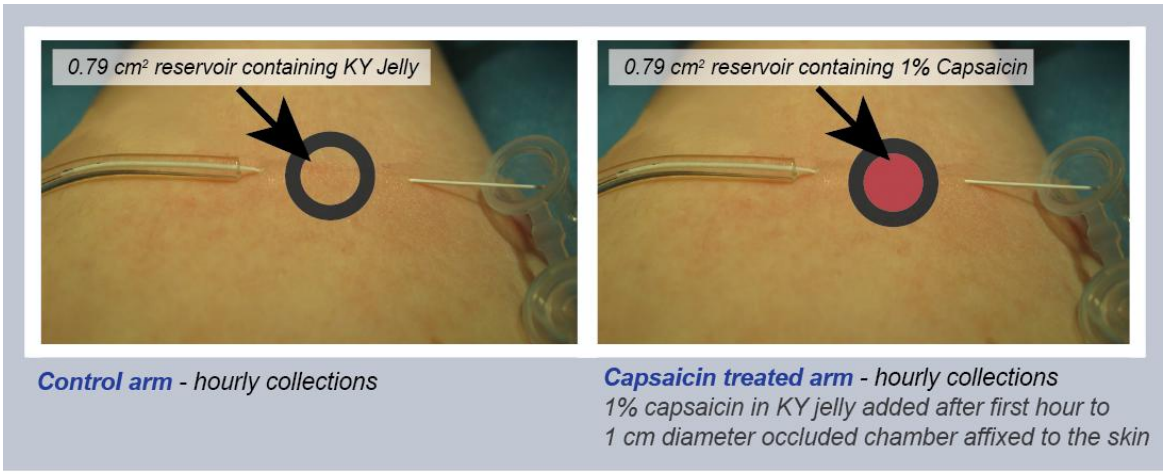

Photograph showing experimental design

Cytokine data collection:

IL-17, IFN-γ and IP-10 were robustly quantifiable in all subjects. IL-1β concentrations are all within the range of reliable detection, but uncertain concentration, as are most subjects TNF-α and some subjects with low levels of IL-6. Nearly all levels of IL-10 fell in the undetectable range, as did some subjects with the lowest levels of MCP-1 and RANTES.

In the following experiments, individual assay results were included or excluded from analysis dependent on whether they were within the accuracy range for the standard curve run with the assay. If below the accuracy range for the curve run simultaneously with the assay, they were allocated a value of 0.

Analysis:

Samples were analysed using Bio-Rad Bio-Plex Precision Pro™ multiplex ELISA as described in the Methods section. Changes in cytokine levels in the treated and non-treated arms were evaluated using two-way repeated measures ANOVA (timepoint and treatment) with Bonferroni correction for repeated measures (time) to evaluate whether there were significant changes between the treated and untreated groups at any timepoint, as well as whether there were changes over time. All samples were corrected for volume of collection prior to analysis. Significance was assumed at 0.05 and analysis was performed using SPSS 20.0. Data are presented as mean ± SD unless otherwise noted.

Results:

The peak VAS score was recorded at 49 ± 25 minutes, with an intensity of 2.4 ± 0.8 on a 0-10 scale. Subjects reported the sensation uniformly as a burning / stinging pain. Doppler flare response in the treated arm was 8.6 ± 3.7 cm with an intensity of 38.5 ± 12 units. Flare in the control arm was 1.2 ± 0.9 cm. Please see Table 4 for details of capsaicin response and flare characteristics. Microdialysis fluid collected per hour was 174 ± 3 µL. Figure 15 shows some typical flare recordings and the experimental setup for the treated and untreated limbs.

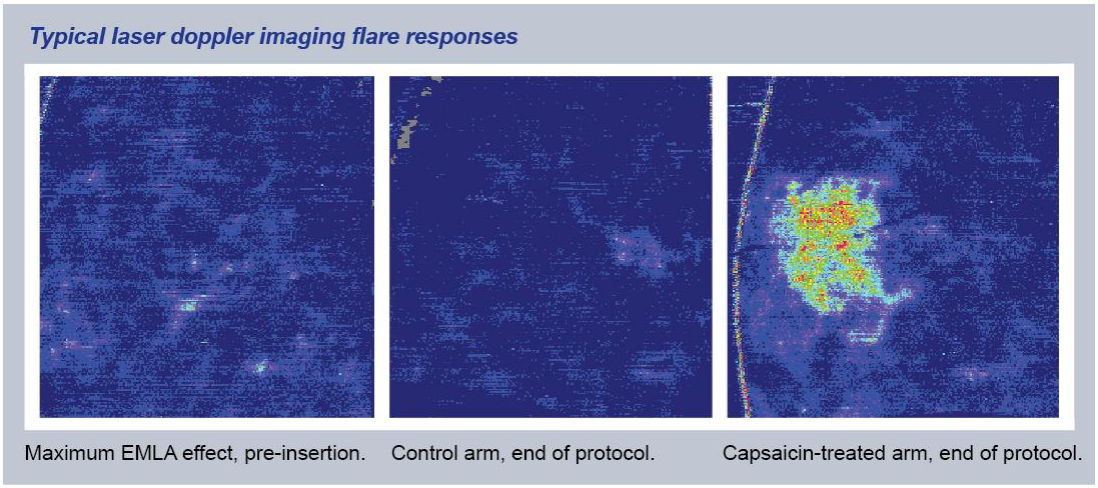

Typical laser Doppler flare response

Cytokine values for IL-1β, IL-10, IL-17, TNF-α and NGF-β remained below the LLOQ throughout the study. Results for IP-10, MCP-1, RANTES, IL-6 and IFN-γ were all above the LLOQ and are presented in the graphs below. Significance calculated using two-way ANOVA with Bonferroni correction for repeated measures. The limits of detection for the assay based on the concurrently run standard curves are shown in Table 5.

Table 4: Subject demographics, pain response and flare characteristics.												
	Subject 1	Subject 2	Subject 3	Subject 4	Subject 5	Subject 6	Subject 7	Subject 8	Subject 9	Subject 10	Mean	SD
Gender	M	F	F	F	F	M	M	M	M	F	-	-
Age	34	36	49	39	30	30	31	25	24	29	**32.7**	**7.3**
Time to onset of capsaicin effect (mins)	10	15	10	15	15	20	10	10	5	20	**13**	**4.8**
Time to peak capsaicin effect (mins)	60	60	90	70	60	60	30	20	10	30	**49**	**25.1**
Max. VAS	3	3	1	2	3	3	3	1	2	3	**2.4**	**0.8**
Max. Flare Intensity (Capsaicin arm) (units)	48.2	43.1	19.9	27.3	29	31.4	46.9	58.8	41.6	39.1	**38.5**	**11.7**
Max. Flare Area (Capsaicin arm) (cm^2)	15.7	7.8	3.3	6.2	8.4	6.5	12.2	4.6	9.8	11.0	**8.6**	**3.7**
Max. Flare Area (Control arm) (cm^2)	2.7	0.5	0	1.0	2.1	1.6	0.8	2	0.6	0.5	**1.2**	**0.9**

Table 5: Cytokine limits of detection for capsaicin study assay (ρg/mL)										
	IL-1β	TNF-α	IL-6	IL-10	IL-17	IFN-γ	MCP-1	IP-10	RANTES	NGFβ
Lower limit of detection	0.11	0.24	0.14	0.11	1.57	6.18	0.27	35	6	1.13
Upper limit of detection	416	4609	24834	2191	22584	29444	1919	30565	1928	5581

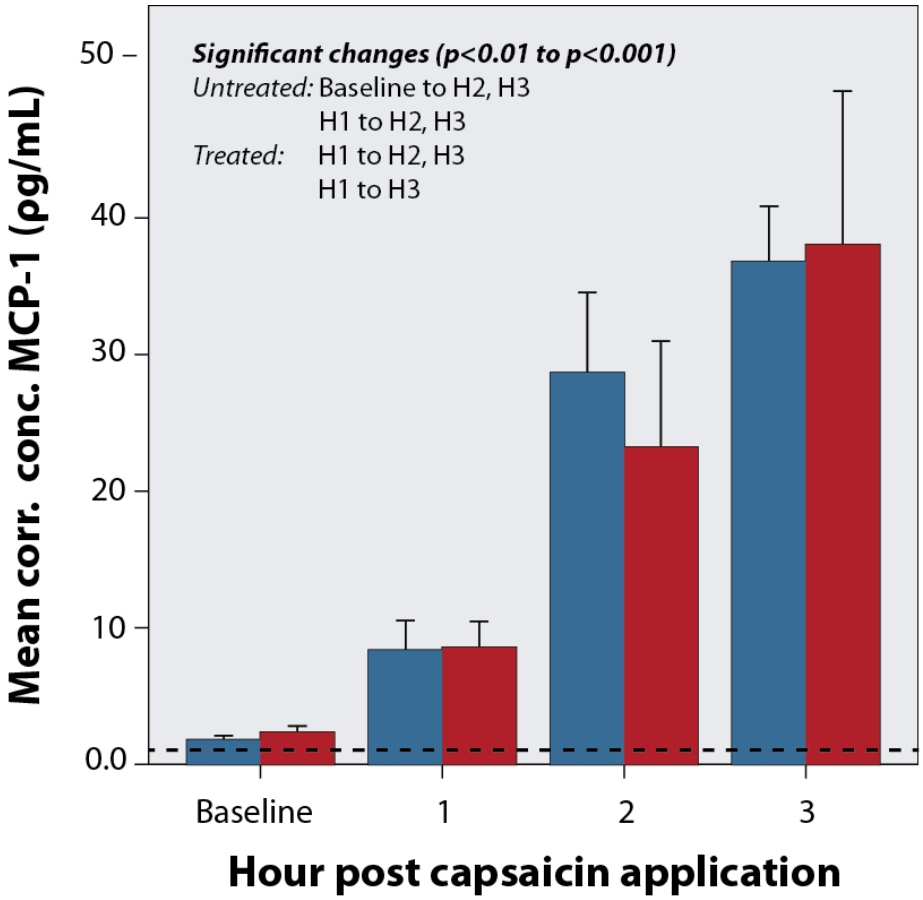
Significant changes (p<0.01 to p<0.001)
Untreated: Baseline to H2, H3
H1 to H2, H3
Treated: H1 to H2, H3
H1 to H3
Mean corr. conc. MCP-1 (pg/mL)
50
40
30
20
10
0.0
Baseline
1
2
3
Hour post capsaicin application

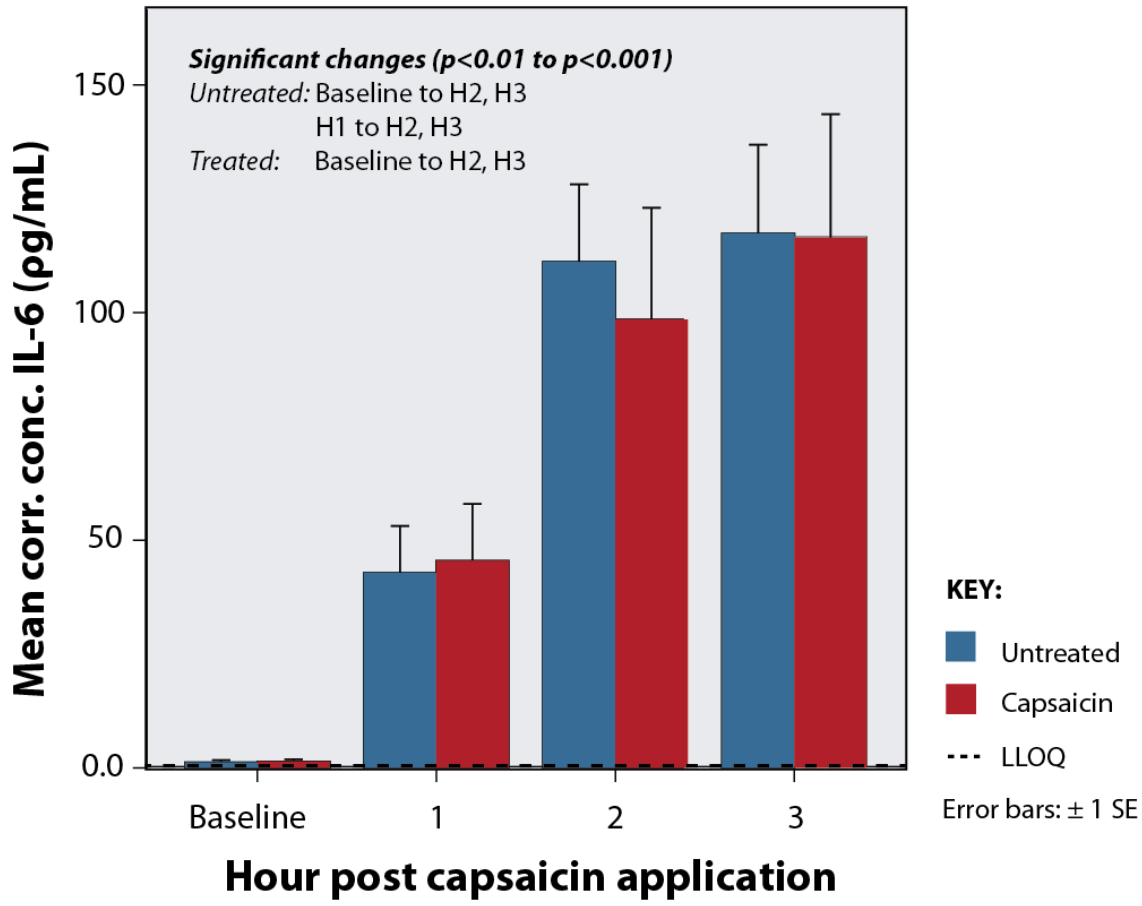
Significant changes (p<0.01 to p<0.001)
Untreated: Baseline to H2, H3
H1 to H2, H3
Treated: Baseline to H2, H3
Mean corr. conc. IL-6 (pg/mL)
150
100
50
0.0
Baseline
1
2
3
Hour post capsaicin application
KEY:
Untreated
Capsaicin
LLOQ
Error bars: ± 1 SE

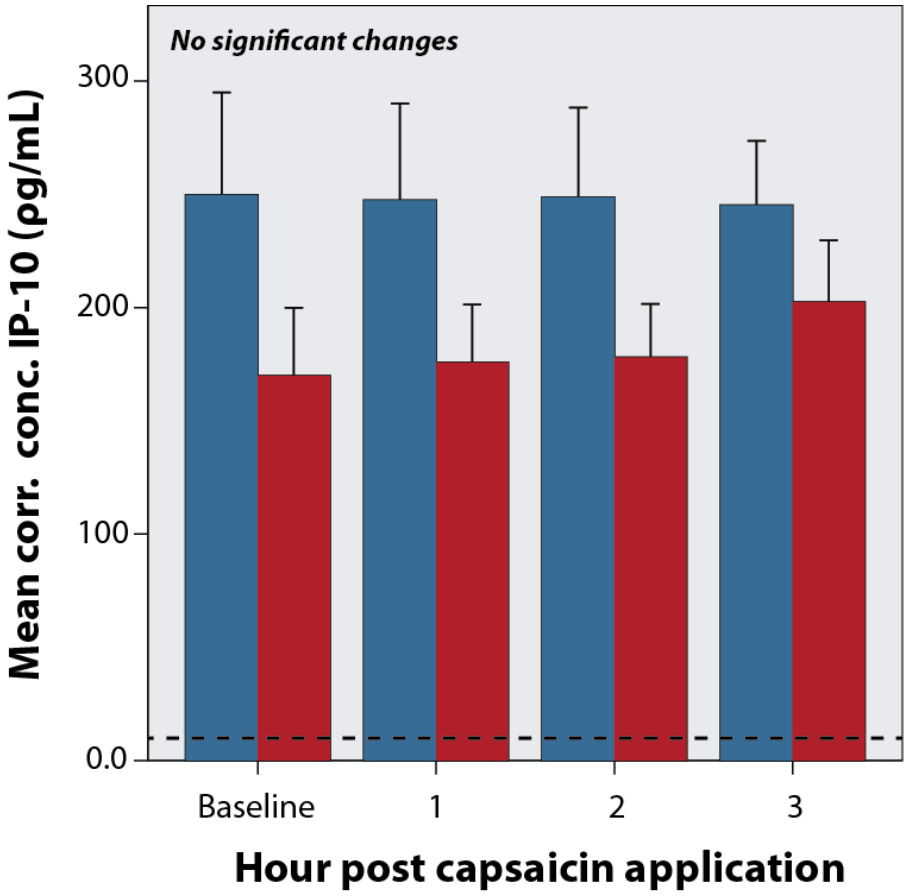
No significant changes
Mean corr. conc. IP-10 (pg/mL)
300
200
100
0.0
Baseline
1
2
3
Hour post capsaicin application

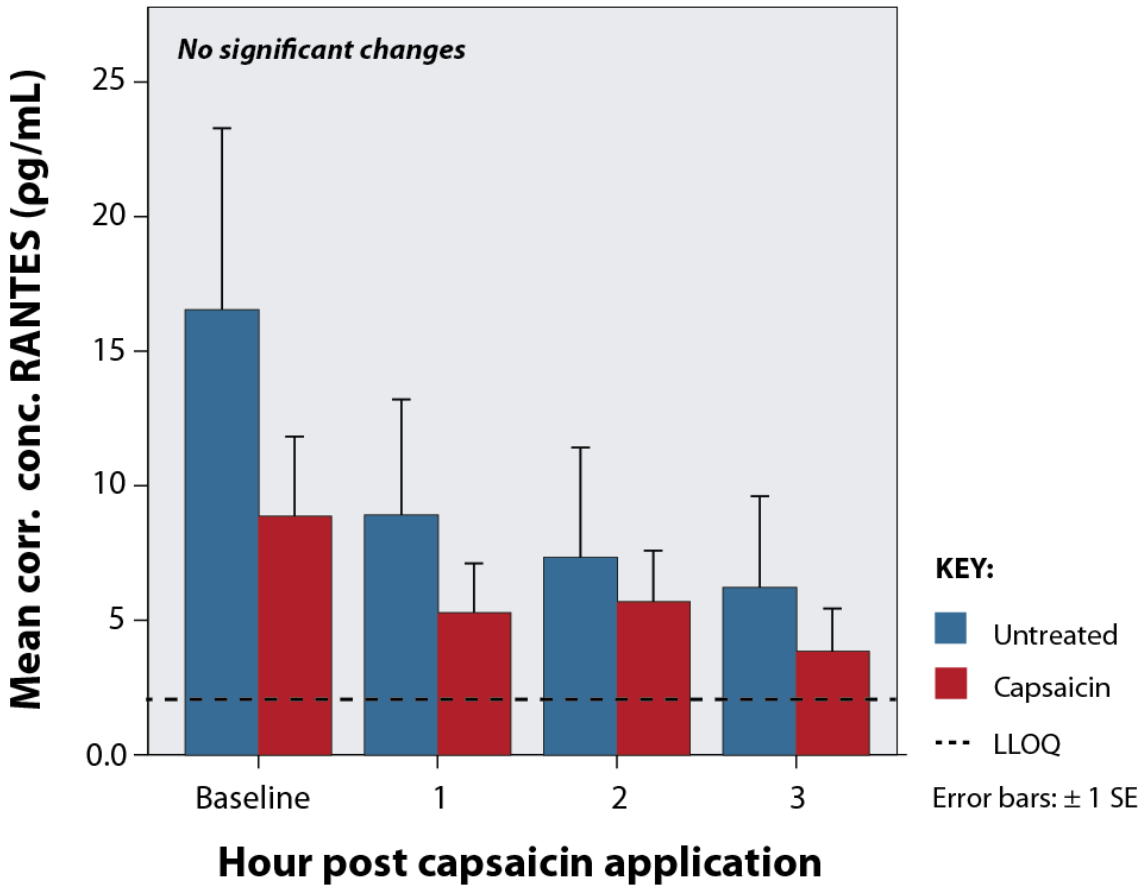
No significant changes
Mean corr. conc. RANTES (pg/mL)
25
20
15
10
5
0.0
Baseline
1
2
3
Hour post capsaicin application
KEY:
Untreated
Capsaicin
LLOQ
Error bars: ± 1 SE

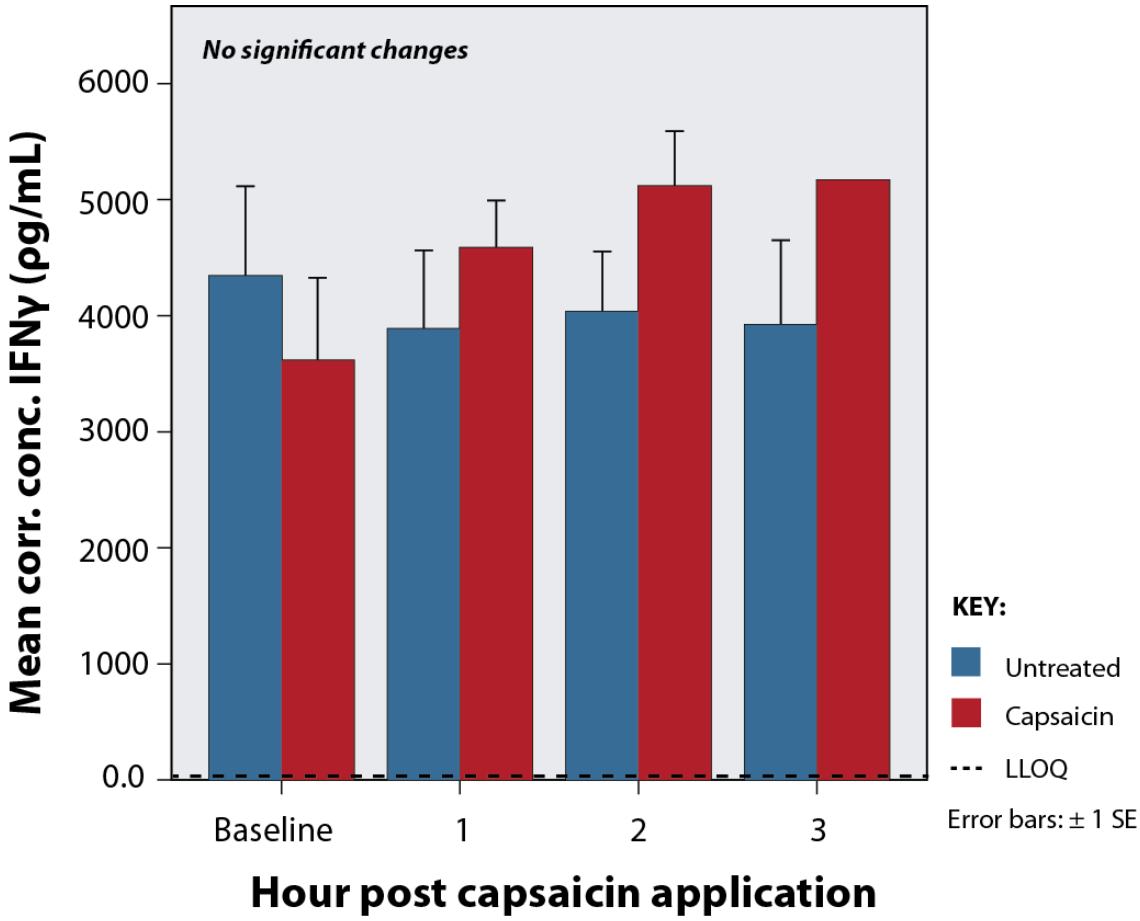

No significant changes (at $p<0.05$ or below) between the treated and untreated limb at a single timepoint were observed for any cytokines. Significant changes (at $p<0.01$ to $p<0.001$ level) were only seen over time for MCP-1 and IL-6. No significant correlations were seen between pain scores, time to peak onset of pain or flare response in the treated limb at the conclusion of the study and cytokine levels.

Discussion:

The effect of acute nociceptor activation on nine cytokines thought to be of key interest in skin immune regulation and genesis of pain, as well as NGF-β were assessed by dermal microdialysis and multiplex ELISA at hourly intervals in 10 subjects who each acted as their own control. The only significant changes in cytokine levels seen were increases over time in MCP-1 and IL-6, which is not unexpected, as inflammatory cytokines which are known to increase following insertional trauma (Averbeck et al., 2006, Sjögren and Anderson, 2009). No changes were seen between the treated and untreated arms in any of the cytokines measured at any time point. The presence of a capsaicin-induced flare remaining in the treated, but not in the untreated arm after 3 hours suggests nociceptors were activated appropriately by the topical capsaicin, although the low VAS score suggests that nociceptors were relatively mildly activated.

These findings indicate that acute activation of the capsaicin-sensitive polymodal nociceptors that mediate flare response and neurogenic inflammation is insufficient to evoke acute changes in key cutaneous cytokines. This suggests that the inflammatory changes observed in patients with painful small fibre neuropathy are not mediated purely by nociceptor activation, but either require additional stimulus, or a longer duration of activation to evolve.

Acute nociceptor activation may induce inflammatory changes in the skin that this study did not detect in its 3-hour examination, perhaps through initiation of cellular changes in cells such as Langerhans' cells and keratinocytes. SP, and particularly CGRP, have been found to regulate immune tone in Langerhans'

cells through regulation of NF-κB activation. Modulation of cellular machinery, production and secretion of effector cytokines and chemokines may take longer than the 3-hour window of this study. Similarly, recruitment of other immune cells such as macrophages and lymphocytes would take longer than processes dependent on immediate cytokine release. Other possible explanations for the lack of inflammatory change include the need for a more intense stimulus (only low-levels of pain were induced); the combination of neuropeptide release and activation of cellular stress and injury pathways relating to the underlying pathology of the neuropathy; or changes in skin biology (particularly that of keratinocytes and Langerhans' cells) induced by loss of nerve fibre contact.

A further consideration is that the peptidergic population represents only around 15% of epidermal fibres (Wallengren and Sundler, 2004, Chao et al., 2007). Other fibre types, such as the IB4 / P2X3 positive population may be of interest in this context, as P2X3 mediated ATP signalling has been implicated in pain, and ATP activates a number of inflammatory pathways in the skin. P2X3 knockout mice have normal acute nociceptive responses, but less increase in pain behaviour with chronic, but not acute, inflammation models. Of note, the knockout mice also do not exhibit any change in response to capsaicin (Souslova et al., 2000). P2X3 antagonist or antisense treatments have also been found to reduce hyperalgesia in models of neuropathic and inflammatory pain, but not response to acute pain (Jarvis et al., 2002, Barclay et al., 2002, Honore et al., 2002). It is interesting that selective depletion of IB4 neurons in the rat sciatic nerve results in severe tissue ulceration without changes in nociception (Vulchanova et al., 2001), while neonatal capsaicin reduces peptidergic

innervation in rats, with no histological epidermal changes (Martínez-Martínez et al., 2011). Additionally, capsaicin is used topically to reduce peptidergic innervation therapeutically for human pain without causing damage to skin integrity (Anand and Bley, 2011). It is tempting to speculate that the relative loss of peptidergic and non-peptidergic fibres may be an important factor in skin inflammation. Inflammatory mediators could then sensitise remaining nociceptors.

To answer these questions, an extended study with stronger nociceptor activation would be ideal. However it is difficult for subjects to remain immobile for prolonged periods, making such an examination by microdialysis difficult.

Conclusion and future work:

This study shows that chemical activation of the TRPV1+ve subpopulation of nociceptors does not alter the levels of key pro- or anti-inflammatory cytokines in the skin acutely (within hours). This suggests that changes in cytokine levels associated with neuropathic pain either require a longer period of activation, or that immune changes in the skin in the context of neuropathy are dependent on a combination of nociceptor activation and nerve damage, or perhaps are dependent on the subtypes of fibres involved. A third possibility is simply that certain neuropathy pathologies both induce pain and induce cytokine changes, with immune changes being dependent on the nerve pathology rather than a causal agent in the development of pain.

To further address this issue, the final part of my study examines a population of patients with a single neuropathy subtype, Anderson-Fabry disease, which is

frequently, but not invariably, associated with neuropathic pain, as well as a group of normal controls. These subjects will undergo a detailed clinical and neurophysiological characterisation of their neuropathy (including IENFD), evaluation of their pain levels, and a detailed cutaneous immune profile using dermal microdialysis and assessment of Langerhans' cell density on skin biopsy. By correlating the levels of pain with the immune profiles in these subjects, and comparing them with healthy controls, I hope to establish which immune changes occur in painless neuropathy compared to those that occur in neuropathy with pain. The fact that they all have the same, non-immune mediated neuropathology should limit confounding effects of variable neuropathology in evaluating immune changes.

Chapter 5: Small fibre function, immune changes and pain in Anderson-Fabry neuropathy

Abstract

Introduction:

Several studies have linked pain in neuropathy with systemic or local immune changes, but have included a variety of pathologies, leading to conflicting results. I sought to identify whether inflammatory changes in skin cytokines or intrinsic immune cells corresponded with the painfulness of neuropathy in a single neuropathy subtype, Anderson-Fabry disease with a high incidence of neuropathic pain. By comparing the presence or absence of pain with a variety of neurophysiological, histological and immunological measures, I hoped to obtain a clearer understanding of the role of inflammation in the painfulness of a neuropathy.

Hypothesis:

I postulated that Anderson-Fabry patients with a painful neuropathy would exhibit a higher level of proinflammatory cytokines and / or lower levels of anti-inflammatory cytokines in the skin than those with a painless neuropathy. A secondary aim was to explore whether changes in Langerhans cell density or morphology correlated with the painfulness of the neuropathy.

Methods:

Detailed neurophysiology, including quantitative sensory testing, pain and mood questionnaires, dermal microdialysis collection of interstitial fluid for

multiplex ELISA analysis of cytokines and skin biopsy at the proximal and distal leg for intraepidermal nerve fibre density (IENFD) and Langerhans cell numbers and morphology were performed at a single visit on each subject. Blood samples were also taken to exclude other causes for neuropathy and to measure systemic cytokine levels. Cytokines included IL-1β, IL-6, IL-10, IL-17, TNF-α, IP-10, MCP-1, RANTES and the growth factor NGF-β.

Subjects:

Fourteen patients with Anderson-Fabry disease (age 47 ± 12.7y, 5 men) with varying amounts of neuropathic pain and 14 healthy volunteers (age 33 ± 10.1y, 7 men) were studied. Seven of the Anderson-Fabry patients had significant pain on a composite VAS score.

Results:

IENFD displayed a proximal-distal gradient in all Anderson-Fabry subjects, and was significantly lower than control subjects at both sites in Anderson-Fabry. Proximal and distal IENFD correlated with the sum of the three pain-defining VAS scores, and proximal IENFD with current VAS score. Quantitative sensory testing showed significant differences in several modalities between patients and controls in the lower limb, but only in warm detection threshold in the upper limb. Only upper limb paroxysmal heat sensation correlated with the presence of pain. Several pain measures correlated with proximal MCP-1 and proximal IL-6, as well as serum TNF-α and RANTES. Linear density of Langerhans cells was significantly reduced at the calf in Anderson-Fabry patients compared to controls ($p=0.035$) with a non-significant trend to reduced density at the

thigh. Langerhans cells were also morphologically abnormal in the Anderson-Fabry patients.

Conclusion:

Anderson-Fabry patients have a small fibre neuropathy confirmed on morphological and functional studies. Whilst overall cytokine levels between groups did not show marked differences, some interesting correlations between pain scores and inflammatory cytokine levels were observed. The altered density and morphology of Langerhans cells in Anderson-Fabry patients warrants more detailed study.

Background: Anderson-Fabry disease

Anderson-Fabry disease is an X-linked lysosomal storage disease characterized by a mutation on the GLA gene causing deficiency of the enzyme α-galactosidase A and leading to accumulation of the glycosphingolipid enzyme substrate, globotriaosylceramide (Gb3, or GL-3) in various tissues (Biegstraaten et al., 2012, Zarate and Hopkin, 2008). Symptom onset is usually in childhood in men, with a more severe phenotype, but later in affected female heterozygotes, who exhibit milder symptoms. Life expectancy in untreated Anderson-Fabry disease is reduced by 20 years in men and 15 years in women (Zarate and Hopkin, 2008). Enzyme deficiency (less than 5-10% residual activity) leads to deposition of glycosphingolipids (globotriaosylceramide and galactosylceramide) in tissues and cells leading to organ dysfunction and clinical expression of the disease. Organ damage is mediated by impaired tissue perfusion and diffusion due to glycosphingolipid deposition in the vascular endothelium, particularly in the kidneys, heart, skin and nervous system, but fibrosis and inflammation may also be involved, as well as deposition in other cell types such as renal podocytes (Zarate and Hopkin, 2008).

Symptoms worsen with age. Some patients may have disease activity focused on one organ system more than others. The clinical picture has not been found to correlate closely with the genotype, and considerable variation in age of onset, severity and pattern of organ involvement is seen within single families. Renal dysfunction is more frequent and severe in men, but both women and

men can develop cardiac and cerebrovascular disease. The spectrum of organ involvement and subsequent disease may include:

- Neurological: neuropathic pain, MRI white/grey matter and posterior circulation lesions, TIA, stroke, hearing impairment
- Gastrointestinal: gastrointestinal symptoms,
- Skin and eyes: hypohidrosis, skin angiokeratomas, corneal opacities,
- Renal: proteinuria and hyperfiltration, end-stage renal disease,
- Cardiac: hypertrophic cardiomyopathy, left-ventricular hypertrophy, systolic and diastolic dysfunction, arrhythmia

The natural progression of Anderson-Fabry disease has been slowed by the introduction of enzyme replacement therapy (ERT) with alpha agalsidase (Fabrazyme®, Genzyme Corporation, Cambridge, MA, USA) or beta agalsidase (Replagal®, Shire Human Genetic Therapies, Boston, MA, USA). Clinical improvement across several organ systems has been shown in treatment trials, including renal and cardiac function, thermal detection thresholds, evoked sweating and reduction in pain severity (Schiffmann et al., 2003, Wilcox et al., 2008). Despite functional improvements in small fibre function, no increase in intraepidermal nerve fibre density at the lower lateral thigh was found after 18 months of ERT, suggesting any improvement in neuropathic pain and sensation with ERT may be mediated by metabolic and functional changes, rather than nerve fibre regeneration (Schiffmann et al., 2006).

Small fibre neuropathy in Anderson-Fabry disease

Small fibre neuropathy manifests through the involvement of both sensory and autonomic small fibre populations. Pain is often one of the earliest manifestations of Anderson-Fabry disease, starting in childhood and contributing significantly to morbidity throughout life. There are two primary types of pain experienced in Anderson-Fabry disease: chronic pain and Fabry crisis pain. Symptoms typically begin in the hands and feet with chronic burning and shooting pains and dysaesthesias, thermal sensory loss (particularly cold perception) and paraesthesias. Symptoms of autonomic involvement include hypohidrosis, impaired pupillary constriction, saliva and tear production and gastrointestinal dysmotility (Burlina et al., 2011). The median age of onset at 9 years in males and 16 years in females (Wilcox et al., 2008). Early in the disease course, males experience more severe pain, although this tends to equalize later in life (Wilcox et al., 2008).

Provoked crises of extreme pain may be precipitated by a number of stimuli. Crises occur more frequently in early life, tending to decrease in frequency with age. They may be precipitated by a number of triggers including heat, stress, common illnesses, fatigue and exercise. These episodes of pain typically start in the hands and feet and radiate proximally.

Proposed pathophysiology of sensory dysfunction in Anderson-Fabry disease:

Sensory dysfunction in Anderson-Fabry disease is thought to be due primarily to impairment of peripheral neuronal function secondary to Gb3 accumulation in blood vessels, neurons, Schwann cells and skin cells surrounding cutaneous

sensory receptors. These factors are thought to combine to impair key neuronal functions, with clinical effect mediated through a combination of axonal hyperexcitability, ectopic spontaneous firing and central sensitisation (Burlina et al., 2011).

Deposition of Gb3 in vascular smooth muscle and endothelial cells of epineurial and endoneurial blood vessels results in ischaemic damage to nerve fibres due to reduced blood flow and associated thrombotic complications. Accumulation of Gb3 within dorsal root ganglion cells is also reported (Kaye et al., 1988). They are thought to be particularly vulnerable due to the fenestrated epithelium of their supplying blood vessels. Length-dependent loss of small myelinated and unmyelinated fibers has been demonstrated in sural nerve biopsies and through intraepidermal nerve fiber analysis (Scott et al., 1999). Ultrastructural studies confirm degeneration of dermal axons, with remaining axons showing swollen segments filled with inclusions, presumably of lipid, and loss of intracellular organelles (Cable et al., 1982b, Vital et al., 1984). Pain and paraesthesias are attributed to a combination of poor perfusion of peripheral nerves, and / or glycosphingolipid accumulation in axons and dorsal root ganglia cells, leading to atrophy of small fibres (Zarate and Hopkin, 2008).

Neurophysiology and histology of neuropathy in Anderson-Fabry:

Nerve conduction studies in Anderson-Fabry patients find that large fibre function is largely normal in patients who do not have concomitant renal impairment, but a higher than expected incidence of carpal tunnel syndrome (around 25% of patients) is noted in several studies (Luciano et al., 2002,

Laaksonen et al., 2008). When large fibre nerve involvement occurs, amplitude is more affected than velocity, suggesting an axonal neuropathy (Lakomá et al., 2014). Alterations in ion channel function and excitability of sensory nerves have been linked to Anderson-Fabry disease, and may contribute to pain. The mechanism underlying these changes in some cases may be elevated levels of glycolipid directly (Choi et al., 2015), whilst in others the cause is not as clearly defined (Geevasinga et al., 2012). Nerve excitability testing in Fabry patients has revealed lower thresholds and increased hyperpolarizing current/threshold gradients in Fabry patients compared with controls, suggestive of upregulation of inward rectifying currents in Fabry disease. 'Fanning-in' of threshold electrotonus, suggestive of membrane depolarization, has been demonstrated in large myelinated fibres in Fabry's disease (Tan et al., 2005). Sensory axons have also been found to have a reduced threshold and increased hyperpolarizing current/threshold gradient (I/V), suggestive of changes in ion channels involved in the inward rectifying current, I_h (Matafora et al., 2015, Tan et al., 2005, Geevasinga et al., 2012). These changes correlated with disease severity and pain scores (Geevasinga et al., 2012). Unlike in motor axons, sensory axons did not demonstrate membrane depolarization, suggesting that ischaemia, previously postulated as the cause of altered Fabry neuron neurophysiology in motor axons (Tan et al., 2005), is unlikely to be the sole explanation of altered function.

In a DRG cell culture model, application of clinically relevant concentrations of lyso-Gb3 resulted in increased calcium influx in capsaicin-sensitive peptidergic DRG neurons, which were predominantly IB4 negative. This was mediated by

increased voltage-activated Ca^{2+} currents (Choi et al., 2015). Thus, the improvement in pain with enzyme replacement therapy (Schiffmann et al., 2001) may be at least partially mediated by the effect of lowering levels of Gb3 on ion channel function.

Length-dependent loss of intraepidermal nerve fibre density, altered thermal and vibration perception, and reduced autonomic innervation of cutaneous structures have been found in some asymptomatic women in addition to affected patients with Anderson-Fabry (Mauhin et al., 2015, De Francesco et al.). This suggests that small fibre neuropathy may be an early manifestation of the disease, evident on testing prior to the development of clinical symptoms or involvement of other organ systems. Structural loss of small fibres has been reported in nearly all males and up to 50% of women with Anderson-Fabry's disease (Geevasinga et al., 2012).

Methods

Power calculations for planning of study cohort size:

A number of power calculations were performed prior to the study, based on reported cytokine values in serum and interstitial fluid. These were based to determine the number of subjects needed in the Anderson-Fabry patients groups with and without pain which would be required to yield 80% power (alpha = 0.05, two-tailed) for the study to be able to reject the null hypothesis of zero correlation between pain and variation in cytokine levels.

Based on a 50% higher level of pro-inflammatory cytokines in the subgroup of Anderson-Fabry patients with significant pain, this returned an estimated required subgroup sample size of 28 per group. Based on a 100% higher level of proinflammatory cytokines in the subgroup of Anderson-Fabry patients with significant pain, this returned an estimated subgroup sample size of 12 per group.

Inclusion and exclusion criteria and baseline screening tests:

Subjects were recruited from the Metabolic Clinic at the National Hospital for Neurology and Neurosurgery (Queens Square) and from the Lysosomal Storage Disorders Unit at the Royal Free Hospital. Potential subjects were identified by the treating clinicians (Dr. Robin Lachman, Prof. Atul Mehta and Dr. Derralynn Hughes) and sent information about the study and a form to return if they were interested in being contacted to discuss the study further. Clinicians did not send letters to patients known to have significant co-morbidities (please refer to

exclusion criteria). Patients interested in participating then returned a response form and were followed up by telephone. If no exclusion criteria were identified and they remained willing to participate, they were recruited into the study. The combined group of Anderson-Fabry patients being treated at the two sites was estimated to be around 400. Clinicians sent letters of invitation to patients without significant comorbidities, but unfortunately a record of the number of letters sent out was not kept. Of the patients that were returned the form and were contacted by phone, the majority agreed to take part in the study, with only a few declining due largely to difficulties in spending an entire day in testing.

Normal controls were drawn from volunteers responding to a university-wide email to all staff and students. Respondents were selected to try to maintain as closely as possible an age and gender matched population for comparison with the Anderson-Fabry patients.

Each subject was studied over a single day. Inclusion criteria for all subjects included: Age 18-75 years; ability to undergo the testing in the study protocol; and signed informed consent. For the Anderson-Fabry patients inclusion criteria also included: Clinical diagnosis of Anderson-Fabry disease, confirmed by low alpha-Gal A activity in leukocytes or plasma, or of glycolipid deposits on skin biopsy, or by genetic testing. Exclusion criteria for all participants included: intercurrent illness; immunodeficiency (HIV, lymphoma, malignancy, immunosuppressive therapy (greater than 7.5mg prednisolone/day, TNF-alpha inhibitors, chemotherapy)); diabetes: significant peripheral vascular disease:

significant renal failure (GFR <60mL/min): substance abuse or psychiatric illness; pregnancy; neurological disorder: connective tissue disease and insufficient command of English for informed consent to be obtained.

After obtaining written informed consent and screening for inclusion and exclusion criteria, each subject underwent an initial assessment, to evaluate suitability for inclusion in the study and to exclude other causes of neuropathy. This included medical and medication history and baseline blood tests (Urea, electrolytes, creatinine, liver function tests, vitamin B12, folate, homocysteine, calcium, magnesium, fasting blood glucose level, thyroid function, full blood count, erythrocyte sedimentation rate, C-reactive protein, serum protein electrophoresis and immunofixation and autoantibodies (ANA, ENA, dsDNA, RF). If the patient had not been tested for hepatitis B, C and HIV in the last 6 months, this was also performed, if appropriate after appropriate counselling as per routine clinical practice.

Scores and Scales

A number of scores and scales were assessed to determine pain intensity, profile and the possible coexistence of anxiety and depression, as these are known to alter cytokine profiles. Scales included the following:

1. Visual Analogue Pain Scale (VAS): Pain intensity was evaluated using visual analogue scales to assess limb pain at different time points. The study protocol did not specifically record the pain distribution of the patients involved, however the descriptions given were primarily that of the distribution seen in a length-dependent neuropathy. The Neuropathic Pain

Symptom Inventory (see below) was included to try to obtain a more detailed characterisation of the patient's pain, particularly the neuropathic features. Participants were asked to place a mark on a linear scale for their current level of pain, worst pain in the last month, least pain in the last month, average pain in the last month and inconvenience due to pain (how much pain interfered with their daily life). For each parameter, a mark was made on a 10-cm long line, scoring 0 cm = no pain, and 10 cm = the most intense pain one can imagine. The distance in cm is measured from the start of the scale to the patient's mark, and provides the score. A subject was classified as having significant pain if their rating fell ≥ 3 cm for 2 out of 3 of the following: pain at time of assessment, average pain in the last 4 weeks, and inconvenience due to pain. This method has been utilised by other authors for similar studies (Üçeyler et al., 2007b). Please refer to appendix for study VAS forms.

2. Neuropathic Pain Symptom Inventory (NPSI): Spontaneous *versus* evoked pain was characterised using the Neuropathic Pain Symptom Inventory (NPSI) (Bouhassira et al., 2004). The NPSI was developed to characterise clinical subgroups of patients with neuropathic pain, as patients with different patterns of neuropathic pain, for example variable levels of spontaneous versus evoked pain, may reflect differences in underlying pathologic mechanisms and responsiveness to treatment. It is a reliable psychometric tool for evaluation of the different dimensions of neuropathic pain syndromes. It uses 12 questions with graded responses (0-10) which

produces a summary showing the degree of burning and deep spontaneous pains, paroxysmal pain, evoked pain and paraesthesia / dysaesthesia experienced by the subject. Please refer to appendix for study NPSI form.

3. Hospital Anxiety and Depression Scale (HADS); this scale was developed in 1983 (Zigmond and Snaith, 1983) to screen hospital patients for significant levels of anxiety and depression. It is a 14-question scale, with seven questions, each scoring zero to three, pertaining to depression and seven to anxiety. These result in a score out of 21 for each, with scores over 8 correlating with significant mood disturbance. Please refer to appendix for study HADS form.

Histamine Flare

Histamine flare response was evaluated on the mid anterolateral shin and mid volar forearm of the non-dominant limb in each subject. In each study, a baseline skin perfusion scan was performed using laser Doppler imaging (LDI2-IR, Moor Instruments, UK). One percent histamine in a methylcellulose gel matrix (see below) was then iontophoresed into the skin for 1 minute using 250 μAmp passed through an iontophoresis chamber of 22mm diameter (MIC2 Iontophoresis controller with ION6 chamber, Moor Instruments, UK).

Further laser Doppler scans were taken at 3, 9 and 15 minutes after baseline. Prior to analysis, baseline blood flow was digitally subtracted from the subsequent images. The maximum flare area and intensity were calculated using digital imaging software (ImageJ). This was done by taking a ratio of the

outline of the flare image (traced manually to include all points above background signal) to the total imaged area and multiplying this result to the total imaged area (recorded by the laser Doppler software). The included area included the area covered by the histamine reservoir in all calculations.

Method for Histamine Gel (1% histamine in 1.5% methylcellulose)

1. 1.5 % Methylcellulose Gel (Sigma-Aldrich, UK, 4000cps):

1. 1.5 grams of methylcellulose was dispersed slowly (usually over 20-30 minutes) in 50 ml of boiling water and mixed well;
2. When dispersed, 50 ml ice cold water was added and the beaker immersed in a larger container of crushed ice;
3. The mixture was stirred continuously until clear (generally 10-15 minutes).

2. 1% Histamine Gel (makes 50mls):

1. 0.5 grams of histamine dihydrochloride powder (Sigma-Aldrich, UK) was added to 1mL deionized water and agitated to disperse;
2. One mL of histamine solution was combined with 49ml (49.735g) of methylcellulose gel at room temperature and mixed using a plastic stirring rod;
3. The gel was allowed to settle overnight, then refrigerated until required.

Quantitative Sensory Testing

Quantitative sensory testing was performed according to the standardised protocol developed by the German Research Network on Neuropathic Pain (DFNS) (Rolke et al., 2006). Thermal thresholds (cold and warm detection thresholds, heat pain and cold pain thresholds) were tested using the method of limits on the non-dominant dorsal radial hand and dorsum of foot. Patients were asked to respond to changes in warming and cooling by pressing a button at the first detection of a temperature change. There were four trials for warming and four for cooling. Paradoxical heat sensation was tested using thermal sensory limits and alternating hot and cold stimuli. Subjects were asked to press a button as soon as they detected a change in temperature, and to state whether the change was towards warm or cool. Warm and cool sensations were presented three times each. Paradoxical heating sensations to cool stimuli were noted. Mechanical detection thresholds were measured using the method of limits and a standardised set of von Frey hairs, which exert graded forces on the skin. Five threshold measurements were made, and the geometric mean of these used as the final result. Mechanical pain thresholds were determined using a set of weighted pinprick of graded stimulus intensity, with the first percept of sharpness defining the response. Five threshold measurements were made, and a geometric mean of these used as the final result. Mechanical pain sensitivity was assessed using the graded intensity pinprick stimuli, with subjects asked to rate each stimulus from 0 to 100 (“no pain” to “most intense pain imaginable”) to obtain a stimulus response curve to detect pinprick hyperalgesia. Dynamic mechanical allodynia was assessed as part of this test,

using three light tactile stimuli as moving innocuous stimuli at standardised force (e.g. cotton wisp, brush, cotton wool tip), applied over a 2cm length of skin. Wind-up ratio (WUR) was measured as the intensity of a single pinprick stimulus intensity (rated 0-100) and an estimated mean rating of 0-100 for a series of 10 repeated stimuli of the same intensity given at 1 second intervals. These were repeated 5 times, and the WUR taken as the ratio of the mean rating of the five series divided by the mean rating of the five single stimuli. Vibration detection threshold (VDT) was measured as a disappearance threshold performed using a graded (0-8) Rydel-Seiffer 64 Hz tuning fork placed over a bony prominence (ulnar styloid or medial malleolus). The VDT is the mean of three readings of the point on the scale at which the subject can no longer feel vibration. The pressure pain threshold (PPT) is performed over a muscle (thenar eminence, instep) using a pressure gauge with a $1cm^2$ probe that exerts a force up to $20kg/cm^2$ (corresponding to ~2000kPa). The PPT was determined by the mean of the threshold from 3 series of ascending stimulus intensities (slowly increasing ramps of 50kPa/s (~$0.5kg/cm^2s$).

Neurophysiology

Three motor nerves (median, ulnar, and peroneal nerves) and four sensory nerves (ulnar, median, radial and sural nerves) were examined. The following parameters were assessed: motor conduction velocity (MCV), distal motor latencies (DML), compound muscle action potential (CMAP) amplitudes, sensory conduction velocity (SCV), and sensory action potential (SAP) amplitude. All

nerve conduction studies will be performed on the non-dominant upper and lower limb.

Surface electrodes were used for bipolar stimulation, with the following stimulation sites for motor studies: median nerve (stimulation at elbow and wrist); ulnar nerve (stimulation above and below the elbow, and at wrist); and peroneal (stimulation at head of the fibula and dorsum of the ankle). A pair of surface electrodes with belly-tendon arrangement was used to record the compound motor action potentials (CMAPs) from abductor pollicis brevis, abductor digiti minimi, extensor digitorum brevis (EBD).

Distal latency was measured from the stimulus artefact to the onset of negative response. Proximal and distal CMAP amplitude was measured from peak to peak and from the baseline to the negative peak. The motor terminal latency index (TLI) was calculated for all subjects according to the formula: distal conduction distance (mm) / (CV (ms^{-1}) x DML (ms)). The values in normal controls in our cohort were consistent with those of healthy controls reported by other authors (Trojaborg et al., 1995).

Sensory conduction velocity was measured using surface electrodes and orthodromic technique along the ulnar nerve from the fifth finger to the wrist and the median nerve from the second finger to the wrist. Radial sensory studies were performed antidromically, stimulating over the radial border of the forearm and recording from the anatomical snuff box. Sural sensory studies were also performed antidromically, recording from the lateral ankle and stimulating from the posterior calf. SCV was measured between the onset and

peak latency, and SAP amplitudes were measured between the negative and positive peaks.

Foot and hand skin temperature were controlled to 32-34^0 C and recorded; when necessary limbs were warmed by immersion in warm water until a temperature of at least 32 degrees Celsius was reached.

Cytokine Analysis of Dermal Microdialysis Fluid

Dermal microdialysis and analysis by multiplex ELISA were carried out as described in the previous chapter. Dialysis catheters were inserted over the proximal thigh and distal calf, within 10cm of the site from which biopsies were taken. Dialysate was collected over 1 hour with the subject supine.

Histology: IENFD, Langerhan's cells

Punch skin biopsies for intraepidermal nerve fibre density and Langerhan's cell quantification were taken from the non-dominant limb, 10 cm proximal to the lateral malleolus and 20 cm distal to the anterior superior iliac spine, according to the method described by the Johns Hopkins group (McCarthy et al., 1995, McArthur et al., 1998).

Sterile technique was used. The skin was cleaned with chlorhexidine acetate 0.015% + cetrimide 0.15% (Travasept 100). Half to one millilitre of 2% Xylocaine was then infiltrated to raise a small bleb, and allowed to take effect. Analgesia at the margins of the anaesthetised area was confirmed, taking care to leave the biopsy site free from all needle intrusion. A 3mm punch biopsy was then taken (Stiefel 3mm disposable biopsy punch), and carefully removed using fine-

toothed forceps, taking care not to exert any compressive or stretching force on the tissue. The biopsy was immediately placed in chilled 2% PLP fixative and stored at 4°C for 22 hours. Pressure was exerted over the biopsy site to achieve haemostasis, and then the site was covered with a steristrip and waterproof dressing. The subject was instructed to leave the dressing intact for 24 hours, and then change it daily until no longer oozing and scabbed over.

Following immersion fixation, the biopsy was washed in 3x20 minute washes of 0.1M Sorrenson's phosphate buffer, then immersed in cryoprotectant at 4°C overnight. Tissue at this stage was stored for no more than 1 week before further processing. Tissue was embedded in OCT mounting medium and then 50µm thickness sections were cut on a freezing microtome. Each section was placed in TBS-filled compartments of a 96-well plate, with two sections per well. Tissue sections were taken such that for each antibody, tissue from a range of sites within the biopsy was examined. The initial few sections from each side of the block were discarded.

Two 10-minute TBS washes were performed, by aspirating the fluid using a 200µL pipette, then refilling the wells. Sections were then incubated with blocker for 4 hours on a shaker table at room temperature, followed by incubation with the primary antibody for 36 hours at 4°C on a shaker table. PGP 9.5 (rabbit) (Chemicon) was used at 1:1250, CD1a (mouse) Dako, Clone 010) was used at 1:50. Sections were then rinsed in 3 x 15-minute TBS washes and then incubated with the biotinylated secondary antibody (Vector) at 1:500 for 1 hour at room temperature. After 2 x 15-minute TBS washes, the sections were

incubated in 30% methanol in PBS with 1 % hydrogen peroxide to quench endogenous peroxidase for 30 minutes, then washed in PBS 2 x 10-minutes.

Sections were then incubated in avidin-biotin complex (Vectastain Elite ABC kit, Vector Laboratories, UK) for 1 hour at room temperature. After 2 x 15-minute washes in PBS, sections were incubated in SG substrate (Vector Laboratories, UK), 3 drops in 5mL PBS with 3 drops hydrogen peroxide to visualise antibody binding. After a further 2 x 15 minute PBS washes, sections were mounted on microscope slides and air-dried. Slides were then washed in tap water for 1 minute, then dipped in 0.5% eosin for 4 seconds, dehydrated through graded alcohol and histoclear baths, then coverslipped with DPX.

Results

Demographics

Fourteen normal controls (7 male, age range 23 – 61 years (mean 33 years)) and fourteen patients (5 males, with age range 27 – 69 years (mean 47 years)) were recruited. Table 1 shows the demographic characteristics of the normal volunteers and Table 2 that of the Anderson-Fabry group.

Table 1: Demographic characteristics of normal control group

Normal Controls - Demographic Characteristics						
Case No.	Age	Gender	HAD - A	HAD -D	Smoker: Pack-Years	BMI
1	33	M	1	1	0	24.9
2	61	F	3	1	0	25.9
3	33	M	5	1	1	21.5
4	35	M	5	0	0	21.4
5	47	F	3	0	2	29.9
6	30	M	6	2	7	22.8
7	30	F	6	0	3	20.1
8	35	M	4	2	4	27.3
9	31	M	5	2	2	21.7
10	30	F	2	0	0	21.6
11	25	F	9	0	0	26.3
12	23	M	5	2	0	23.5
13	25	F	9	0	0	27.4
14	24	F	2	1	0	282

Notes on Table 1: None of the normal subjects had significant pain or were taking pain medications. HAD – A: Hospital Anxiety and Depression Scale (Anxiety component); HAD – D: Hospital Anxiety and Depression Scale (Depression component); BMI: Body Mass Index.

Table 2: Demographic and pain characteristics of Anderson-Fabry patient group

Anderson-Fabry patients - Demographic Characteristics										
Case No.	Age	Gender	Pain	Trophic Changes: Hair, skin, nails	Loss of sweating	HAD - A	HAD - D	Pain Medication	Smoker: Pack-Years	BMI
1	45	M	N	Y	Y	5	0	N	0	25.4
2	51	F	N	N	N	1	1	N	0	21.2
3	28	M	Y	Y	Y	18	10	N	15	20.8
4	37	F	Y	Y	N	3	4	N	0	22.8
5	61	M	Y	Y	Y	13	9	Y	38	19.3
6	39	F	N	N	N	7	1	N	0	32.6
7	53	F	Y	Y	Y	14	6	Y	0	29.3
8	27	F	N	N	Y	3	1	N	0	18.2
9	56	F	N	N	N	6	5	N	10	25.0
10	36	M	N	N	Y	3	0	N	0	20.8
11	59	F	Y	Y	Y	8	2	N	0	19.5
12	55	M	Y	N	N	5	4	N	0	19.7
13	42	F	Y	N	N	15	8	Y	5	21.8
14	69	F	Y	Y	N	7	8	Y	15	28.5

Notes on Table 2: Pain is defined as a VAS score of >3/10 on two or more of the following: Current pain, Average pain over the last month, and Inconvenience due to pain. HAD – A: Hospital Anxiety and Depression Scale (Anxiety component); HAD – D: Hospital Anxiety and Depression Scale (Depression component); BMI: Body Mass Index.

Blood tests

A number of blood tests were conducted on participants, including fasting blood glucose level, full blood count, erythrocyte sedimentation rate, C-reactive protein, liver function, urea, creatinine, calcium, magnesium, Vitamin D, Vitamin B12, folate, homocysteine, thyroid function tests, serum protein electrophoresis, ANA, ANCA, RF, Hepatitis B and C serology, HIV. There were no significant differences found between normal volunteers and Anderson-Fabry

patients, other than a slightly higher Hb level in normal controls (mean difference ± SEM, 1.1 ± 0.4 g/dL, p=0.014), and a slightly higher WCC in Anderson-Fabry patients (1.5 ± 0.5 $x10^9$/L, p=0.004).

Pain Scores

Normal controls had occasional positive VAS ratings over the last month due to injuries or headaches (Average pain over last month: VAS mean 0.1, S.D. 0.3; Worst pain in last month VAS mean 1.3, S.D. 1.5). None had any current pain, and none of the normal controls had ratings above 0 on any aspect of the Neuropathic Pain Symptom Inventory (NPSI). The ratings given by the Anderson-Fabry group are presented in Table 3 below. The total NPSI is scored out of 100, with each sub-component scored out of 10. Overall, Anderson-Fabry subjects scored more highly on the superficial spontaneous and paraesthesia subscores, with lowest ratings on the evoked pain score.

The VAS scores have a maximum value of 10. The sum of three VAS scores is the total of the three scores used to divide the Anderson-Fabry patients into those with significant levels of pain, and those without significant pain. These three scores include current pain, average pain over the last month, and inconvenience due to pain. When used to define the presence or absence of pain as a binary function, pain was defined as a score of greater than or equal to 3/10 in two of these three parameters.

Table 3: Pain scale ratings in Anderson-Fabry patients

Anderson-Fabry patients - Pain Scores												
Case No.	NPSI: Total	NPSI: Sup. Spont	NPSI: Deep Spont	NPSI: Parox. Pain	NPSI: Evoked	NPSI: Paraesth	VAS: Sum of 3 measures	VAS: Current	VAS: Av. Last month	VAS: Worst last month	VAS: Least last month	VAS: Inconven-ience
1	0	0	0	0	0	0	0	0	0	0	0	0
2	4	0	0	0	0	2	0	0	0	0	0	0
3	51	10	2	8	0	10	18	1	7	9	1	10
4	30	4	2	2	6	0	11	2	4	6	1	5
5	69	7	4	10	6	8	24	7	7	10	7	10
6	9	2	0	0	0	3	3	2	1	3	0	0
7	70	9	5	9	6	8	23	5	9	10	2	9
8	9	1	0.5	0.5	1	2	3	0	1	1	1	2
9	0	0	0	0	0	0	3	0	1	3	0	2
10	12	0	6	0	0	0	0	0	0	2	0	0
11	34	5	2	4.5	0.67	7	12	2	4	6	1	6
12	12	4	1.5	0.5	0	2	7	0	3	4	0	4
13	3	0	0	0	0	1.5	8	0	3	7	0	5
14	16	6	1.5	0	1	2	9	0	5	7	2	4
Mean	**22.8**	**3.4**	**1.8**	**2.5**	**1.5**	**3.3**	**8.6**	**1.4**	**3.2**	**4.9**	**1.1**	**4.1**
S.D.	**24.5**	**3.6**	**2.0**	**3.8**	**2.5**	**3.5**	**8.2**	**2.2**	**2.9**	**3.5**	**1.9**	**3.7**

Notes on Table 3: VAS Sum of 3 measures includes Current pain, Average pain over the last month, and Inconvenience due to pain.

Mood

Table 1 and 2 include the results of the Hospital Anxiety and Depression score ratings in the normal and patient groups. The scale rates symptoms as normal if they fall between 0-7, borderline if they fall between 8-10 and abnormal if they are ≥ 11. In the normal population, two subjects had borderline ratings for anxiety, with no abnormal ratings for either anxiety or depression. In the Anderson-Fabry group, four patients had abnormal anxiety ratings, with one in the borderline range. Four patients had borderline depression ratings, but none were in the abnormal range.

Strong (R>0.7, Pearson correlation) correlations were seen between HAD anxiety and depression ratings and intensity of chronic pain, particularly with VAS ratings for average pain over the last month, worst pain over the last month and inconvenience due to pain. No significant correlation was found with the current VAS rating. Moderate correlations were seen with mood scores and NPSI ratings for superficial spontaneous and paraesthesias, but not with the overall NPSI score. These findings would indicate that the overall *intensity* of pain in Anderson-Fabry is more closely linked to mood disturbance than the *quality* of unpleasant sensation experienced.

Neurophysiology

Routine nerve conduction studies were conducted on all patients and normal controls and compared to departmental normative values. Skin temperature was above 31 °C in all subjects at the time of study.

A summary of the large fibre neurophysiological studies in normal controls and Anderson-Fabry patients is presented in Table 4 below. Intergroup differences were calculated using independent groups T-test. Anderson-Fabry patients had significantly lower motor and sensory amplitudes in the lower limbs compared with controls, supporting a degree of length-dependent axonal involvement. Differences in the upper limbs were of lower magnitude, with the main difference being slower ulnar conduction velocity. There were no significant differences seen in large fibre function between the group of Anderson-Fabry patients with significant levels of pain compared to those without pain (comparisons done using ANOVA with Bonferroni correction for multiple

comparisons). Figures 1 and 2 presented the neurophysiological data in graphical form.

Table 4: Neurophysiological results in normal controls and Anderson-Fabry patients.

Parameter	**Normal**	**Fabry**	Difference: p-value
	Mean ± SD	Mean ± SD	
Ulnar TLI	0.47 ± 0.05	0.46 ± 0.05	0.625
Ulnar Distal CMAP	9.5 ± 1.9	9.1 ± 0.5	0.511
Ulnar CV (motor)	**61.3 ± 4.8**	**56.7 ± 6.8**	**0.050**
Median TLI	0.37 ± 0.05	0.35 ± 0.05	0.275
Median Distal CMAP	**10.9 ± 6.8**	**8.5 ± 2.1**	**0.006**
Median CV (motor)	55.2 ± 4.0	52.1 ± 4.9	0.088
Peroneal TLI	0.33 ± 0.07	0.35 ± 0.08	0.541
Peroneal Distal CMAP	**5.5 ± 2.2**	**3.5 ± 2.5**	**0.032**
Peroneal CV	51.4 ± 6.7	47.2 ± 4.9	0.068
Tibial TLI	0.47 ± 0.10	0.41 ± 0.11	0.159
Tibial Distal CMAP	14.0 ± 5.4	11.8 ± 6.3	0.341
Tibial CV	48.1 ± 3.2	45.2 ± 6.2	0.153
Median SAP amplitude	16.7 ± 4.7	14.8 ± 8.7	0.469
Median CV (sensory)	59.4 ± 2.9	54.6 ± 10.5	0.113
Ulnar SAP amplitude	10.9 ± 3.6	8.7 ± 4.2	0.160
Ulnar CV (sensory)	**59.9 ± 3.8**	**53.1 ± 8.8**	**0.014**
Radial SAP amplitude	29.9 ± 10.9	30.6 ± 17.4	0.900
Radial CV	60.4 ± 6.1	58.4 ± 7.7	0.460
Sural SAP amplitude	**14.6 ± 5.8**	**9.8 ± 5.6**	**0.031**
Sural CV	46.3 ± 4.8	43.4 ± 13.7	0.458

Notes on Table 4: TLI = terminal latency index; CMAP = compound motor action potential amplitude (mV); SAP – sensory amplitude (μV); CV = conduction velocity (ms^{-1}). Parameters that showed a significant difference between normal controls and patients are presented in bold. The TLI is presented instead of the distal motor latency to allow comparison between groups, as a fixed stimulating – recording electrode distance was not used.

Figure 1: Nerve conduction velocity in Anderson-Fabry Patients v Healthy Volunteers

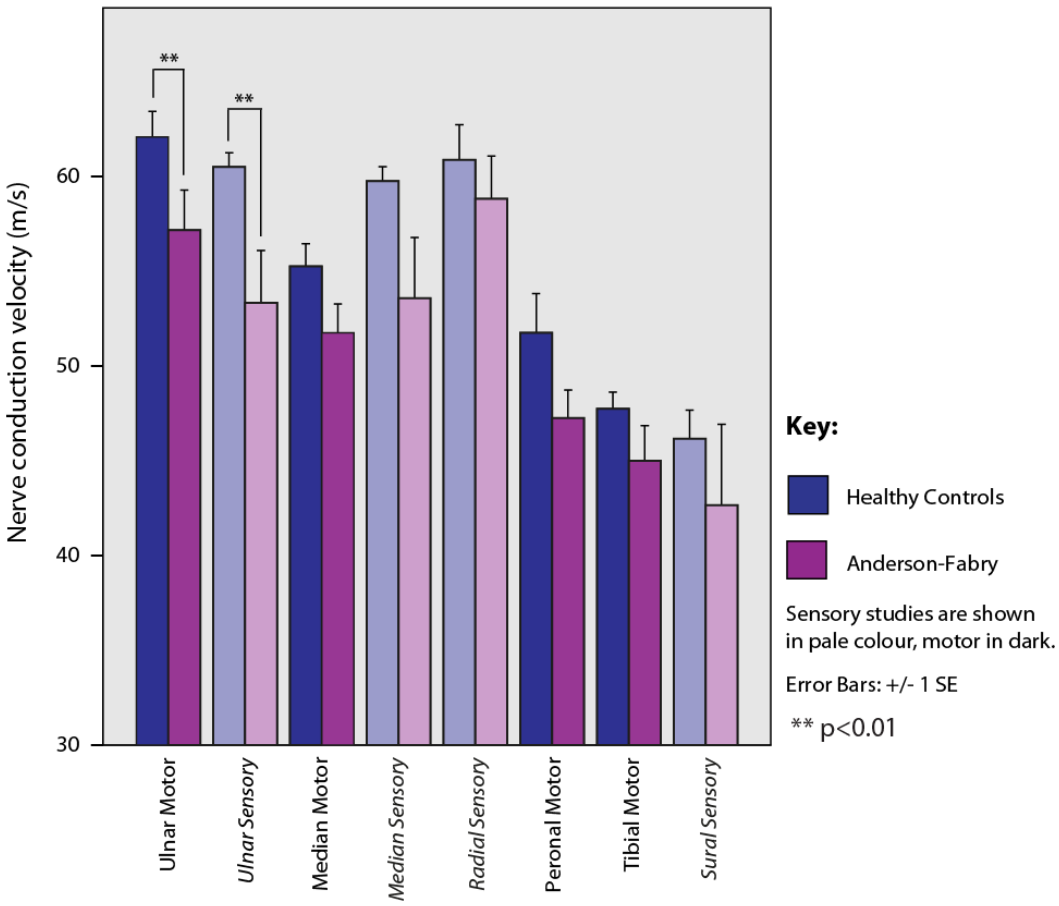

Figure 2: Distal CMAP / SAP amplitude in Anderson-Fabry Patients v Healthy Volunteers

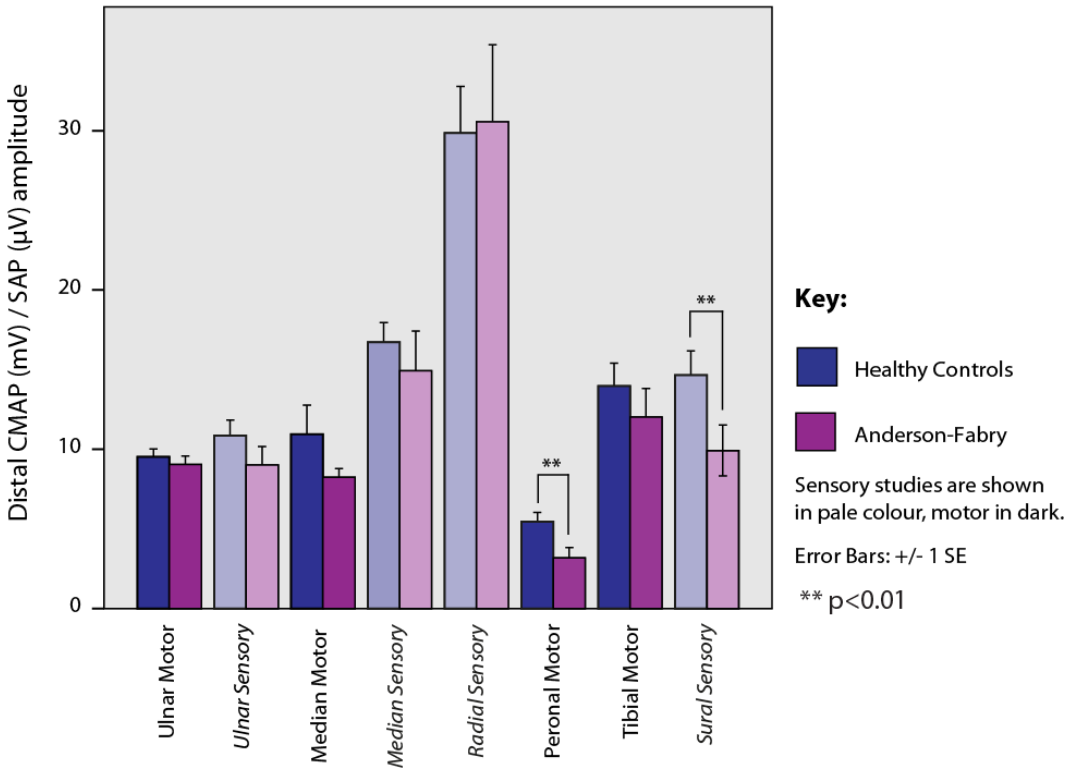

Histamine-induced flare

Histamine iontophoresis was used to induce a neurogenic flare response in the leg (anterior shin) and forearm (mid-volar surface) in all subjects. Figure 3 illustrates a comparison of the flux recording from a control and a subject with Anderson-Fabry.

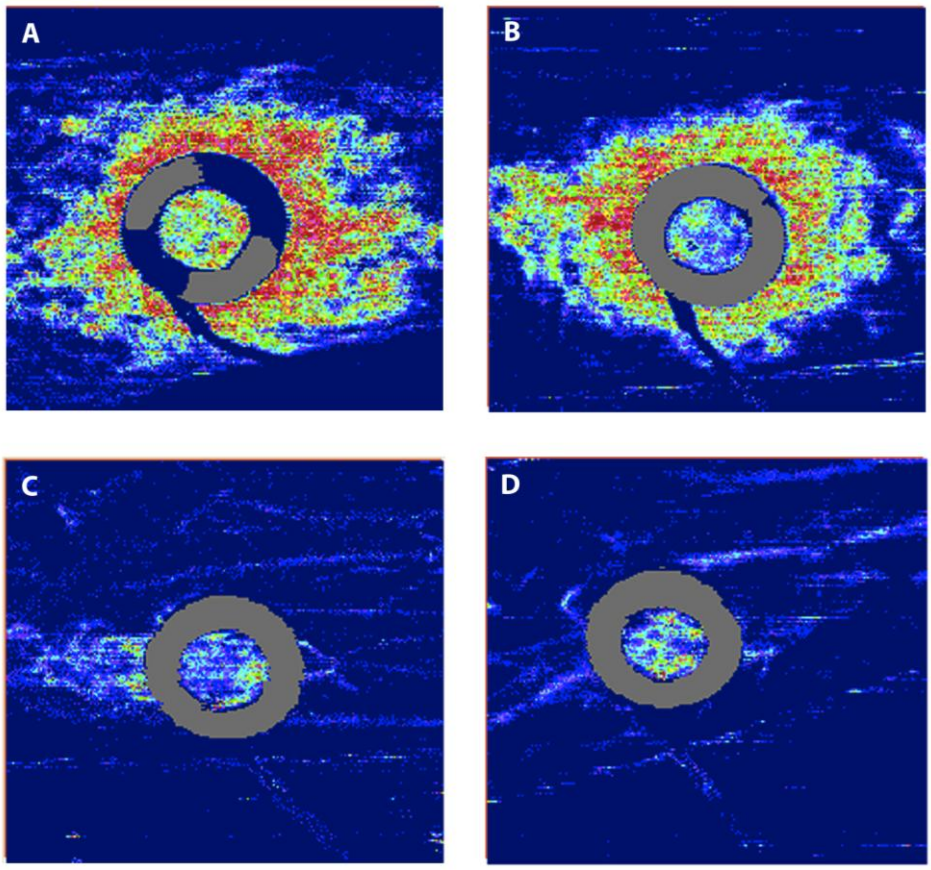

Figure 3: Examples of Histamine-induced Flare responses in Normal Controls (A, B) and Anderson-Fabry patients (C, D).
These images show flux recordings obtained following histamin-iontophoresis induced neurogenic flare in the dorsal forearm. Higher degrees of flux, indicating greater changes in blood flow are shown by warmer colours. The central ring is the border of the iontophoresis chamber. Note the central region of direct histamine action of blood vessels, causing dilatation and increased flux.The surrounding area indicates the extent and intensity of the neurogenic flare. Note the much larger extent and intensity of the flare response in the normal controls compared to the patients.
All images are from the volar forearm and are taken 9 minutes after the start of stimulation.

Flare responses were larger in intensity and area in normal subjects than in patients with Anderson-Fabry. These differences only reached significance in the upper limb studies.

Table 5 and Figure 4 present the data for flare area, intensity and VAS score recorded for the maximal itch / prickling caused by the histamine in Anderson-Fabry patients and normal controls. Differences between groups were compared using independent t-tests. Flare responses and differences between groups were most marked in the upper limb, which may partially reflect less effective penetrance of iontophoresed histamine in the thicker skin of the leg compared to the volar forearm.

As skin thickness and innervation may be affected by age and gender, linear regression analysis was carried out to determine the relative contribution of Anderson-Fabry, gender and age to the histamine flare response. In the upper limb, the strongest contributor to flare area, intensity and lowered VAS response was the presence of Anderson-Fabry, with age and gender not significant. In the lower limb, none of the parameters (age, Anderson-Fabry, gender) were significant in determining flare area or VAS, while male gender predicted a reduction in flare intensity, again perhaps related to thicker skin in men.

Table 5: Histamine flare results

Histamine Flare	Normal	Anderson-Fabry	Between group difference
Parameter	Mean ± SD	Mean ± SD	p-value (Indep t-test)
Arm: Flare Area (cm^2)	**48 ± 9**	**36 ± 2**	**0.005**
Arm: Flare Intensity (flux units)	**135 ± 33**	**63 ± 30**	**0.000**
Arm: Flare itch (VAS)	5 ± 2	3 ± 2	0.104
Leg: Flare Area (cm^2)	35 ± 11	31 ± 15	0.459
Leg: Flare Intensity (flux units)	71 ± 33	49 ± 28	0.076
Arm: Flare itch (VAS)	4 ± 2	4 ± 2	0.652

Figure 4: Histamine flare responses in Anderson-Fabry patients and controls

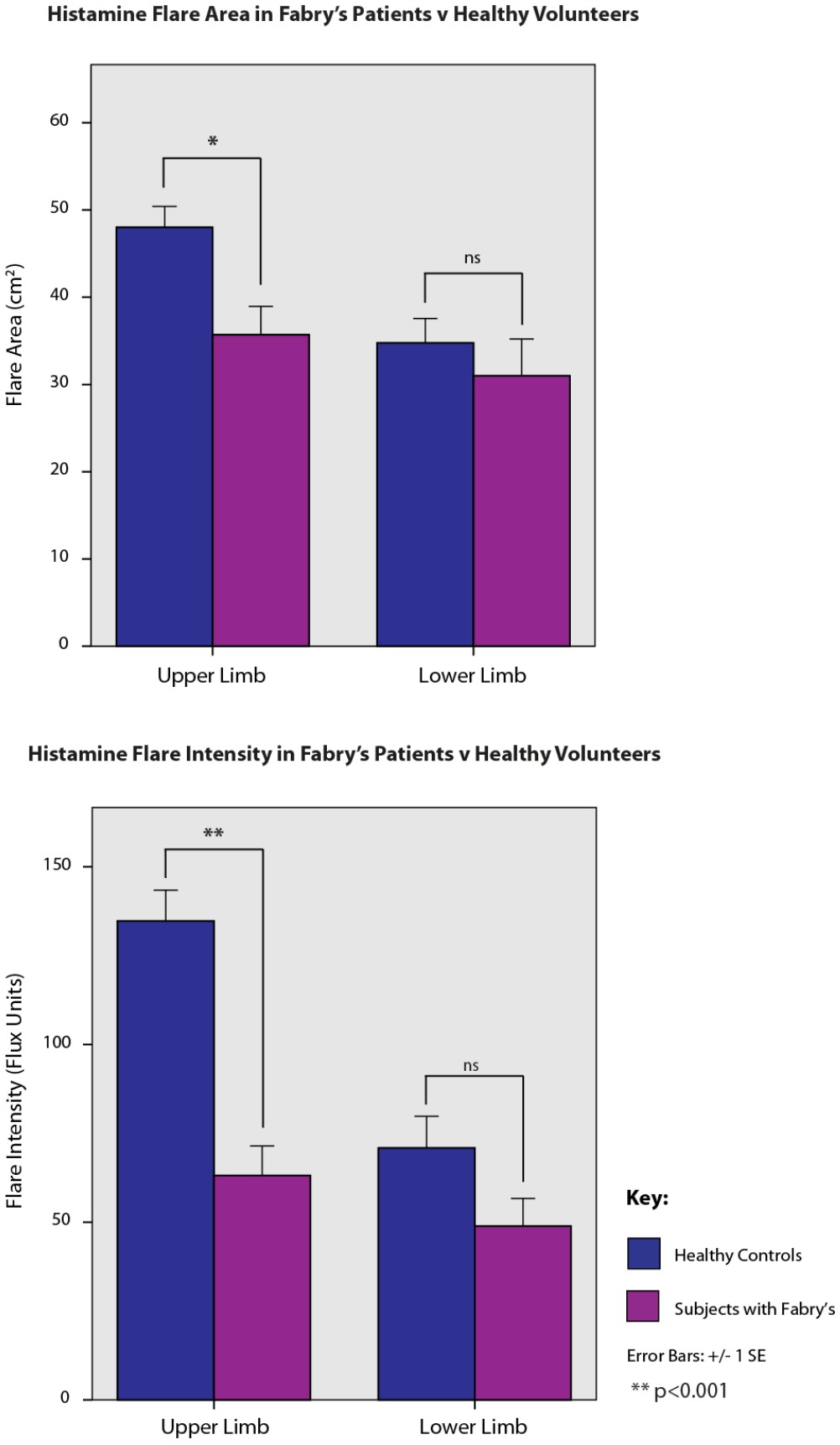

Quantitative sensory testing

The results of quantitative sensory testing are presented in Table 6. Temperature detection and pain thresholds are in degree centigrade. A baseline of 32°C is used for these tests, so a detection threshold is more sensitive the closer to 32°C it falls. In contrast, if a pain threshold lies closer to 32°C than in the normal population, it indicates thermal hyperalgesia. Figure 5 summarises the thermal threshold results for normal controls and Anderson-Fabry patients in the hand and the foot. Note the reduced sensitivity to thermal stimuli at both sites in the patient group, more marked at the foot than in the hand, in keeping with a length dependent process. There is reduced sensitivity to heat pain in the patient group overall, but a tendency towards cold hyperalgesia compared with the healthy control group. The statistical comparisons between groups are presented in Table 6. Significant differences were found in the cold and warm detection thresholds at both sites, and in the heat pain threshold in the foot. The thermal sensory limens indicates sensitivity to a continually changing temperature, and was also significantly increased in Anderson-Fabry patients at both sites, providing further functional evidence of a small fibre neuropathy affecting temperature perception in this group. There was also greater abnormal paradoxical heat perception with cool stimulation to the foot in the Anderson-Fabry group compared with control. This is thought to reflect block or loss of thinly myelinated Aδ afferents (Campero and Bostock, 2010).

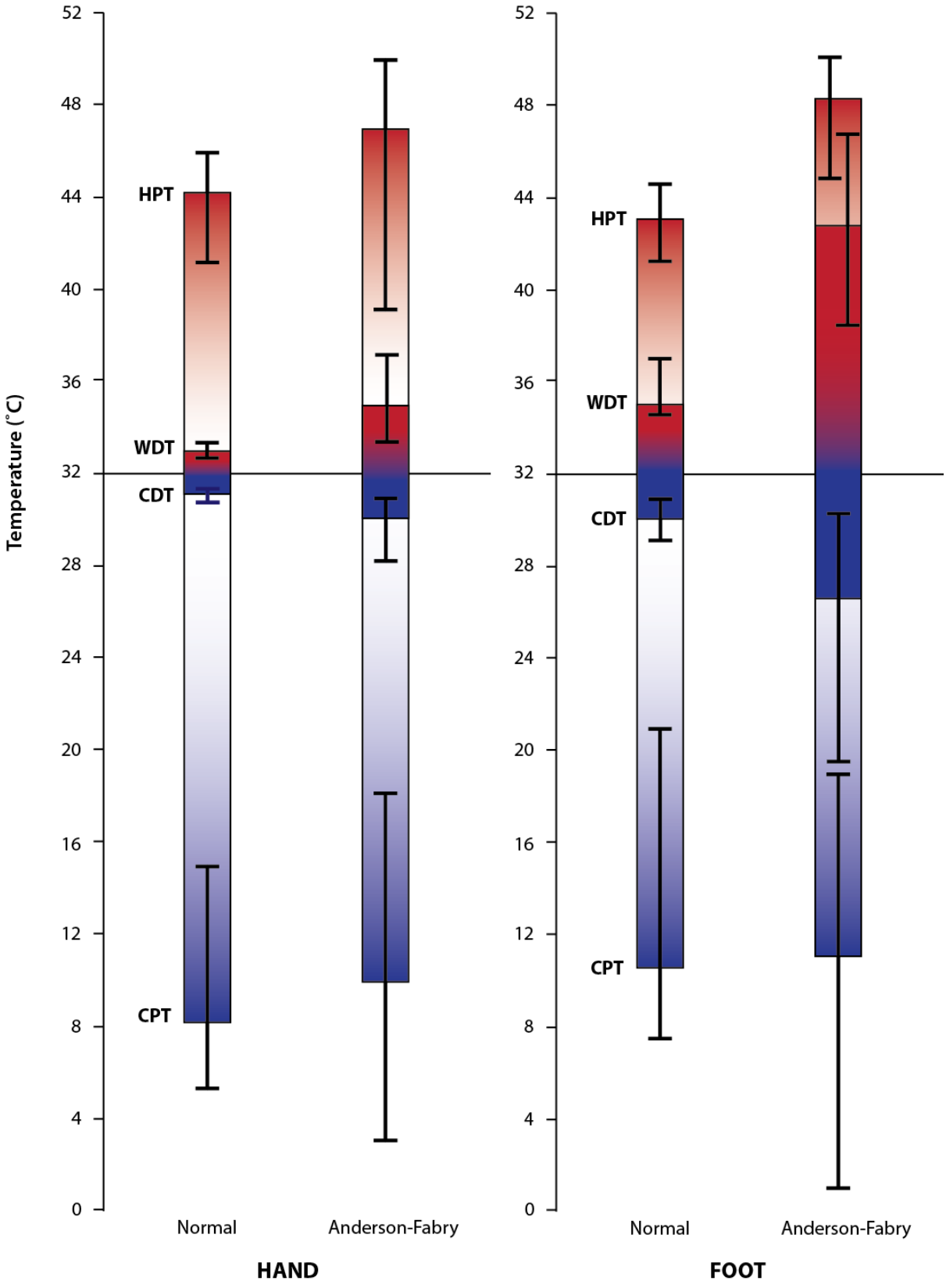

Figure 5: Thermal thresholds in normal controls and Anderson-Fabry patients.
The ends of the bars indicate the median value for detection and pain thresholds, and whiskers indicate the 25-75% range for each parameter. CPT = cold pain threshold; CDT = cold detection threshold; WDT = warm detection threshold; HPT = heat pain threshold. Baseline = 32°C.

Several parameters within the QST group of tests are known to have a skewed distribution (Rolke et al., 2006), whilst others are normally distributed. To correctly assess the significance of the variation in parameters between Anderson-Fabry patients and healthy controls, the Kolmogorov–Smirnov test was applied to each test within each population group to test for the normality of its distribution. Data found to be normally distributed are presented as mean and standard deviation, with comparison between groups made using the independent groups t-test. Data found not to adhere to a normal distribution are presented as median and interquartile range, and differences between groups compared using a Mann-Whitney U-test. Table 6 presents a summary of the overall QST data and highlights parameters that were significantly different in between normal and patients. Thermal thresholds and thermal pain sensitivity in Anderson-Fabry patients differed from controls at both sites tested, while vibration detection threshold and mechanical detection threshold, assessing larger myelinated fibre function (Aβ) was only significantly different at the foot. These findings support a length-dependent neuropathy, and suggest the neuropathy in Anderson-Fabry may affect smaller unmyelinated fibres earlier than larger, myelinated ones.

A second analysis comparing the three subgroups (comprising: normal controls, Anderson-Fabry (no pain) and Anderson-Fabry (with pain)) was conducted using ANOVA with Bonferroni correction for multiple comparisons. This showed significant differences between normal and Anderson-Fabry (with pain) for the parameters in the table below, but not between normal and Anderson-Fabry (no pain) or between the subgroups of Anderson-Fabry with and without pain.

This suggests that although overall, Anderson-Fabry patients differ from controls in these parameters, the bulk of the effect is mediated by the subgroup with pain, suggesting that these patients have a more severe small fibre neuropathy. The only exception to the above was that a significant difference was found between normal and the painless subgroup of Anderson-Fabry patients in the warm detection threshold in the foot ($p=0.003$), and in paradoxical heat sensation in the hand in painful Anderson-Fabry patients compared with controls, which was not seen in the pooled comparison ($p=0.008$).

Table 6: Summary of quantitative sensory testing results

Hand - Quantitative Sensory Testing results				
Normal v Fabry	Normal controls Mean ± SD or Median (IQR)	Anderson-Fabry Mean ± SD or Median (IQR)	Mean difference in Anderson-Fabry	p-value
Cold Detection Threshold	**31.2 (31.0, 31.4)**	**30.3 (28.4, 31.0)**	**-4.8**	**0.001**
Warm Detection threshold	**33.3 (32.9, 33.5)**	**35.1 (33.3, 37.2)**	**3.5**	**0.003**
Thermal Sensory Limens	**5.0 ± 2.5**	**10.8 ± 6.4**	**5.8**	**0.006**
Paradoxical Heat Sensation	0.0 (0.0, 0.0)	0.0 (0.0, 1.0)	0.2	0.352
Cold Pain Threshold	10.7 ± 8.2	10.9 ± 9.1	0.2	0.947
Heat Pain threshold	43.3 ± 3.1	44.6 ± 5.6	1.3	0.452
Mechanical Detection Threshold	2.0 (1.0, 3.3)	1.4 (1.1, 3.1)	4.1	0.804
Mechanical Pain Threshold	169.5 ± 108.3	147.4 ± 122.5	-22.1	0.617
Mechanical Pain Sensitivity	3.7 ± 5.6	3.3 ± 5.0	-0.4	0.826
Mechanical Allodynia	0.0 (0.0, 0.5)	0.0 (0.0, 0.1)	-0.3	1.000
Wind-up Ratio	1.5 (1.3, 1.9)	1.5 (1.3, 2.9)	0.1	0.804

Foot - Quantitative Sensory Testing results				
Normal v Fabry	Normal controls Mean (SD) or Median (IQR)	Anderson-Fabry Mean (SD) or Median (IQR)	Mean difference in Anderson-Fabry	p-value
Cold Detection Threshold	**30.0 (29.0, 30.9)**	**23.6 (19.4, 30.3)**	**-6.3**	**0.016**
Warm Detection threshold	**36.0 ± 2.4**	**42.2 ± 4.6**	**6.2**	**0.000**
Thermal Sensory Limens	**9.3 ± 4.7**	**22.0 ± 11.1**	**12.7**	**0.001**
Paradoxical Heat Sensation	**0.0 (0.0, 1.0)**	**1.1 (0.0, 2.0)**	**0.7**	**0.044**
Cold Pain Threshold	12.1 ± 7.6	10.4 ± 8.8	-1.7	0.596
Heat Pain threshold	**43.0 ± 2.3**	**46.4 ± 4.7**	**3.3**	**0.024**
Mechanical Detection Threshold	**4.0 (1.5, 5.8)**	**116.2 (4.4, 22.8)**	**11.9**	**0.021**
Mechanical Pain Threshold	110.5 ± 76.7	102.0 ± 63.2	-8.5	0.751
Mechanical Pain Sensitivity	1.4 (0.3, 2.9)	1.8 (0.6, 4.8)	0.1	0.603
Mechanical Allodynia	0.0 (0.0, 1.0)	0.0 (0.0, 0.3)	-0.3	0.734
Wind-up Ratio	2.1 ± 0.8	2.3 ± 0.9	0.2	0.631
Vibration Detection Threshold	**7.5 ± 0.5**	**6.8 ± 1.1**	**-0.8**	**0.027**

Notes on Table 6: Normally distributed parameters are presented as mean ± SD and are compared using independent-groups T-test. Non-normally distributed parameters (highlighted in red) are presented as median (interquartile range) and are compared using the Mann-Whitney U-test. Parameters that are significantly different between normal controls and Anderson-Fabry patients

are highlighted in bold. The mean difference is the amount by which Anderson-Fabry patients differ compared with normal controls.

Abbreviations: CDT – cold detection threshold; WDT – warm detection threshold; TSL – thermal sensory limens; PHS – paradoxical heat sensation; CPT – cold pain threshold; HPT – heat pain threshold; MDT – mechanical detection threshold; MPT – mechanical pain threshold; MPS – mechanical pain sensitivity; ALL – dynamic mechanical allodynia; WUR – wind-up ratio; VDT – vibration detection threshold; and PPT – pressure pain threshold.

Normalisation of QST data.

As the normal range for quantitative sensory testing parameters is known to vary with age and gender, it is useful to normalize the raw data to facilitate group comparisons of the type and degree of dysfunction, despite differences in the normal ranges within the groups dependent on age and gender. It also enables graphical representation of the group data, with the range -1.96 to +1.96 incorporating data falling within 95% confidence interval for age (ie: ± 2 S.D. when converted to a normalized scale). Values above the grey zone in the graphs below indicate gain of function (hyperalgesia and allodynia), while those below the grey zone represent loss of function (hypoaesthesia).

The raw data is initially converted to a z-score using published normative values for age and gender (Rolke et al., 2006) by the following equation:

$$Z - score = \frac{Value\ (subject) - Mean\ value\ (normal\ population)}{S.D.\ (normal\ population}$$

I used the published normative data (Rolke et al., 2006) rather than that obtained in our group, as subdividing 14 normal subjects by age and gender would render the groups too small for valid statistical data to be obtained. For certain parameters (WDT, TSL, CPT, HPT, MDT, MPT and PPT), the polarity of the Z-score was then reversed, to enable consistent graphical representation of gain or loss of function.

Figures 6A and 6B show the comparison of QST profile between the controls and Anderson-Fabry patients, in the hand (6A) and the foot (6B). The main deficits in the Anderson-Fabry patients are seen in warm and cold detection thresholds (and the associated thermal sensory limens) and in mechanical detection threshold, indicating loss of function in C, Aδ and Aβ fibre types. No significant gain of function was noted (for example, thermal or mechanical hyperalgesia), although more paradoxical heat sensation was seen in patients than controls, thought to correlate with dysfunction or loss of thinly myelinated Aδ cold afferents. Although the z-scores do not fall outside the normal range in these graphs, there was a statistically significant difference in vibration detection threshold at the foot in the patient group compared with controls, again supporting a length-dependent neuropathy. Men are more severely affected than women, particularly in measures of loss of function (Figure 7A and 7B).

Figure 6A: Mean normalised quantitative sensory testing results (Hand)

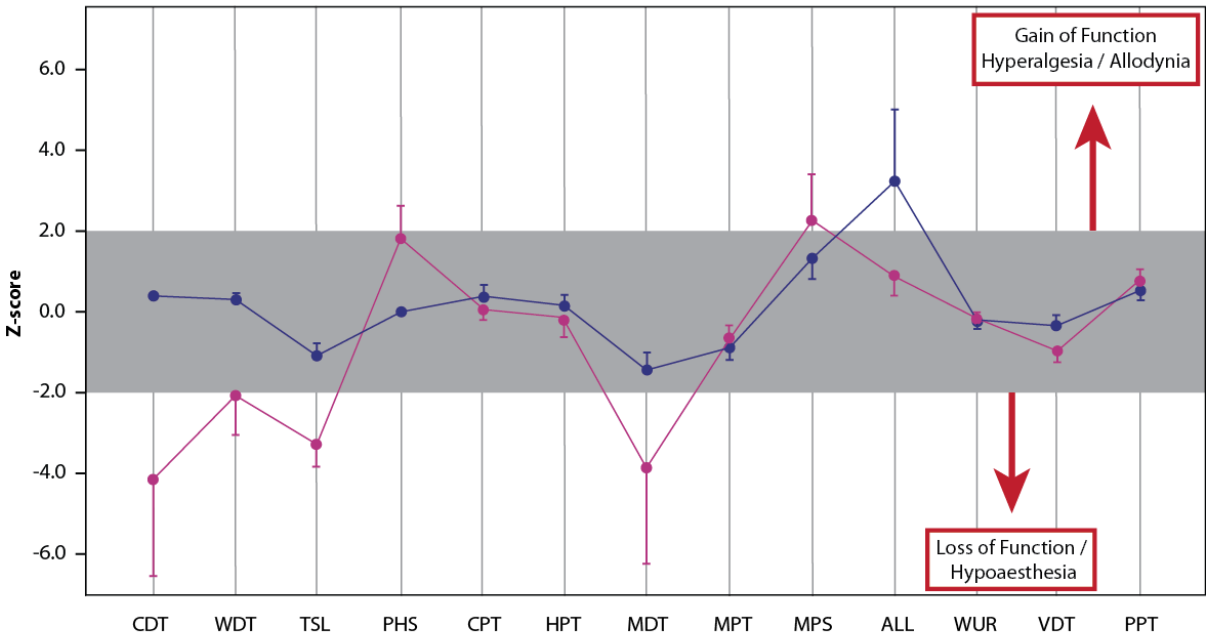

Figure 6B: Mean normalised quantitative sensory testing results (Foot)

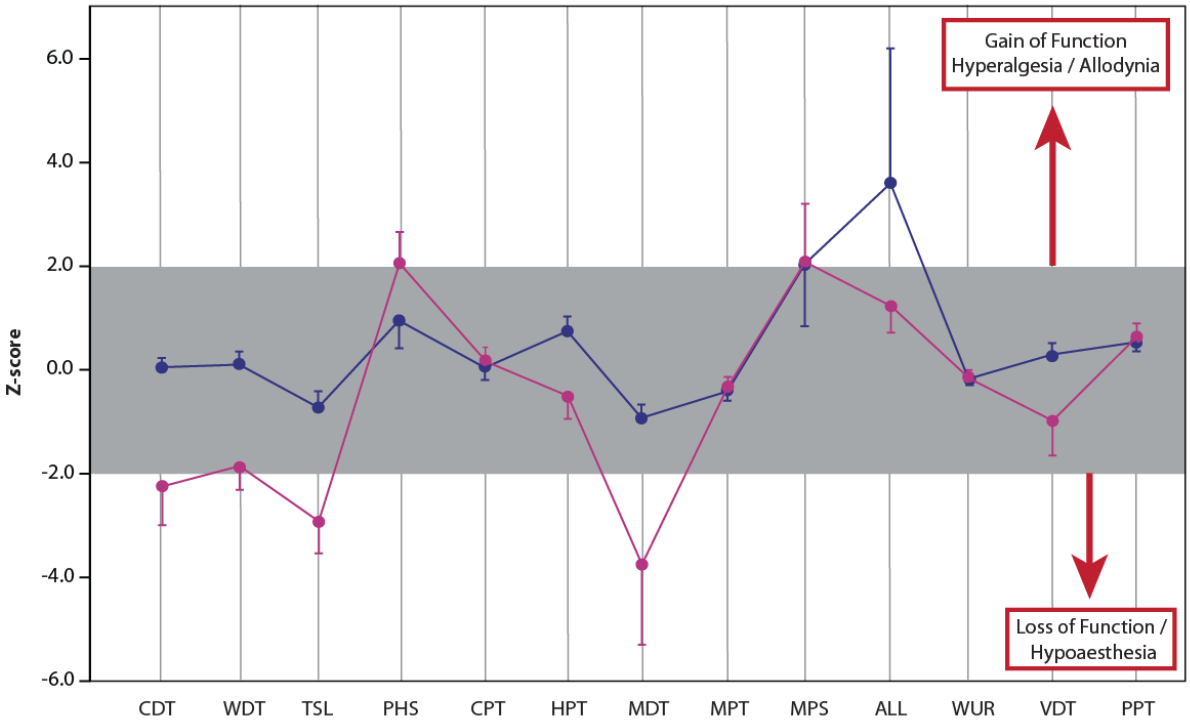

Figure 6: Mean normalised values for QST parameters in Anderson-Fabry patients (pink) and healthy controls (blue).

CDT: cold detection threshold, WDT: warm detection threshold, TSL: thermal sensory limens, PHS: paradoxical heat sensation, CPT: cold pain threshold, HPT: heat pain threshold, MDT: mechanical detection threshold, MPT: mechanical pain threshold, MPS: mechanical pain sensitivity, ALL: dynamic mechanical allodynia, WUR: wind-up ratio, VDT: vibration detection threshold, PPT: pressure pain threshold.

The grey zone represents the 95% confidence interval for the normal population based on published data (Rolke et al, 2006).

Error bars = 1 S.E.

Figure 7A: Mean normalised QST results in Anderson-Fabry by gender (Hand)

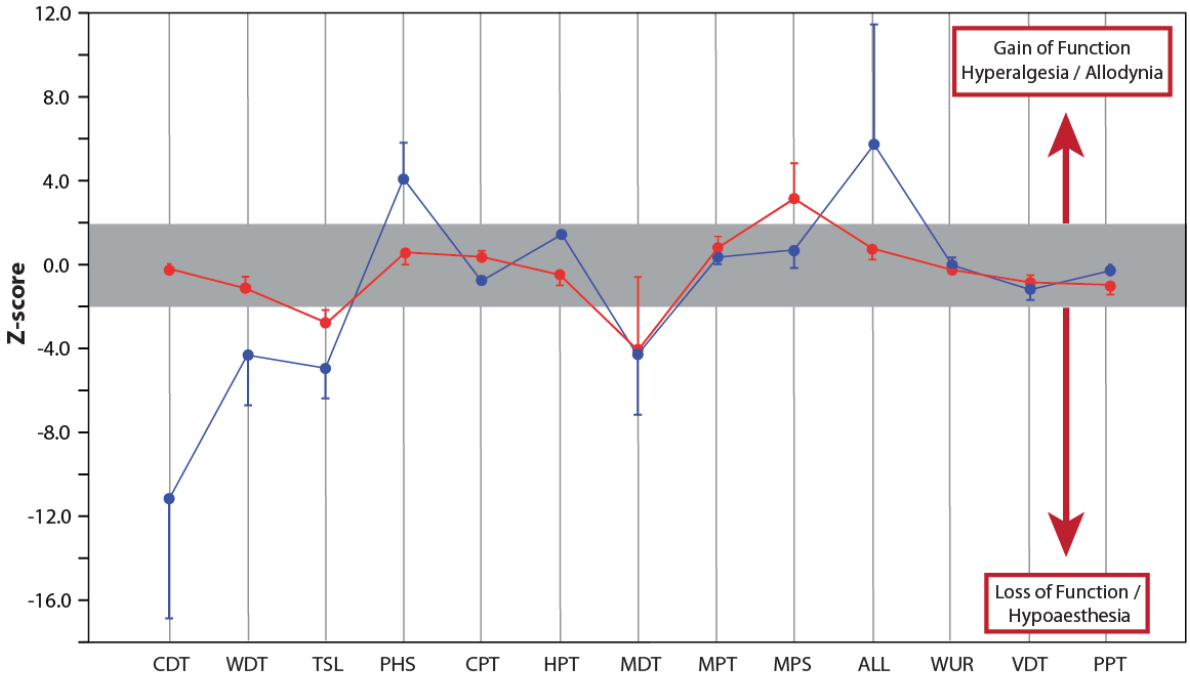

Figure 7B: Mean normalised QST results in Anderson-Fabry by gender (Foot)

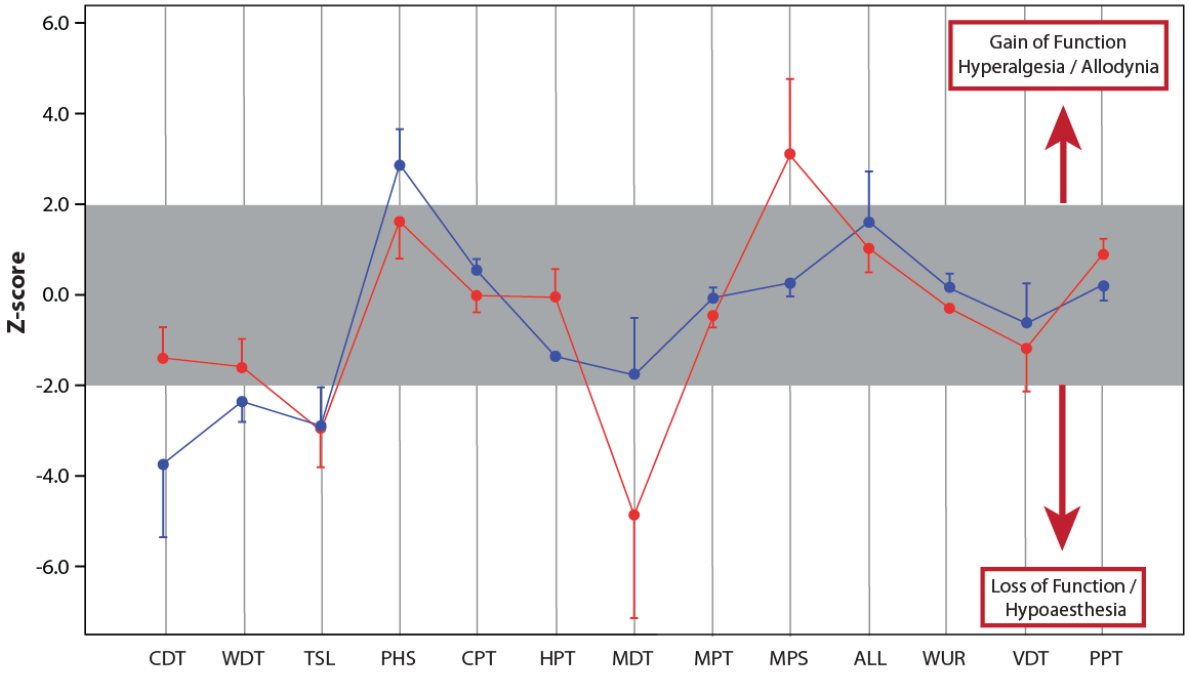

Figure 7: Mean normalised (z-scores) values for QST parameters in Anderson-Fabry patients by gender: women (red), men (blue).
CDT: cold detection threshold, WDT: warm detection threshold, TSL: thermal sensory limens, PHS: paradoxical heat sensation, CPT: cold pain threshold, HPT: heat pain threshold, MDT: mechanical detection threshold, MPT: mechanical pain threshold, MPS: mechanical pain sensitivity, ALL: dynamic mechanical allodynia, WUR: wind-up ratio, VDT: vibration detection threshold, PPT: pressure pain threshold.
The grey zone represents the 95% confidence interval for the normal population based on published data (Rolke et al, 2006).
Error bars = 1 S.E.

Patients with significant levels of pain in Anderson-Fabry also have more severe small fibre dysfunction. Figure 8A and 8B illustrate the relative differences in QST profile between the normal and two subgroups of Anderson-Fabry patients subdivided by the presence of significant pain. Those patients with significant pain tend to have a more severe neuropathy. This particularly severely affects cold and mechanical detection thresholds, suggesting more severe or earlier involvement of myelinated compared to unmyelinated afferents. Those with pain also exhibit increased mechanical pain sensitivity and increased paradoxical heat sensation, also consistent with loss of small myelinated fibres. Mechanical pain sensitivity is a stimulus-response measure, whereby elevation indicates a greater degree of pain experienced for a particular stimulus.

In summary, several significant differences were found in Anderson-Fabry patients compared to our control population: in both the hand and foot, cold and warm detection thresholds, as well as the thermal sensory limens were increased. In addition, in the foot, mechanical detection threshold, vibration detection threshold and heat pain threshold were increased in the patient group. No significant differences were seen between patients and controls in parameters evaluating hyperalgesia or central sensitisation (mechanical pain sensitivity, dynamic mechanical allodynia or wind-up ratio). These findings are consistent with a length-dependent small fibre neuropathy, with greater effect on small myelinated (Aδ and Aβ) fibres, but also involving unmyelinated C-fibres. The subgroup analyses suggest that the subgroup of Anderson-Fabry patients with significant pain tend to have more severe small fibre dysfunction

than those without pain, but one that is characterized more by loss than gain of sensory function.

Figure 8A: Mean normalised QST results by subgroup (Hand)

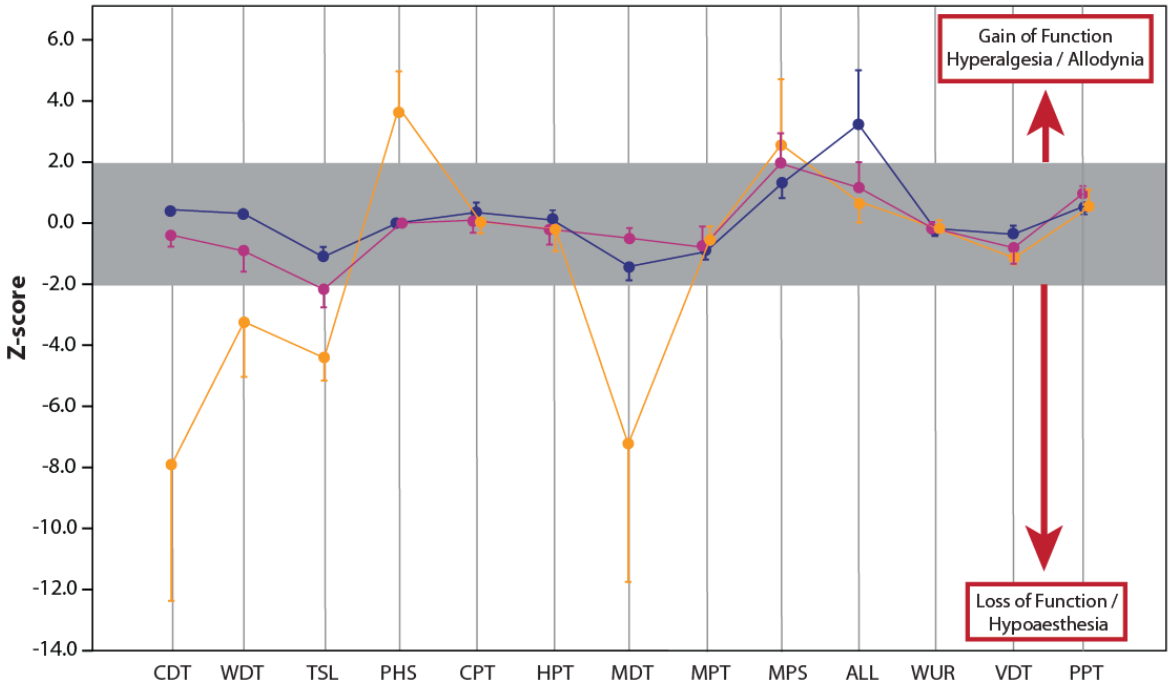

Figure 8B: Mean normalised QST results by subgroup (Foot)

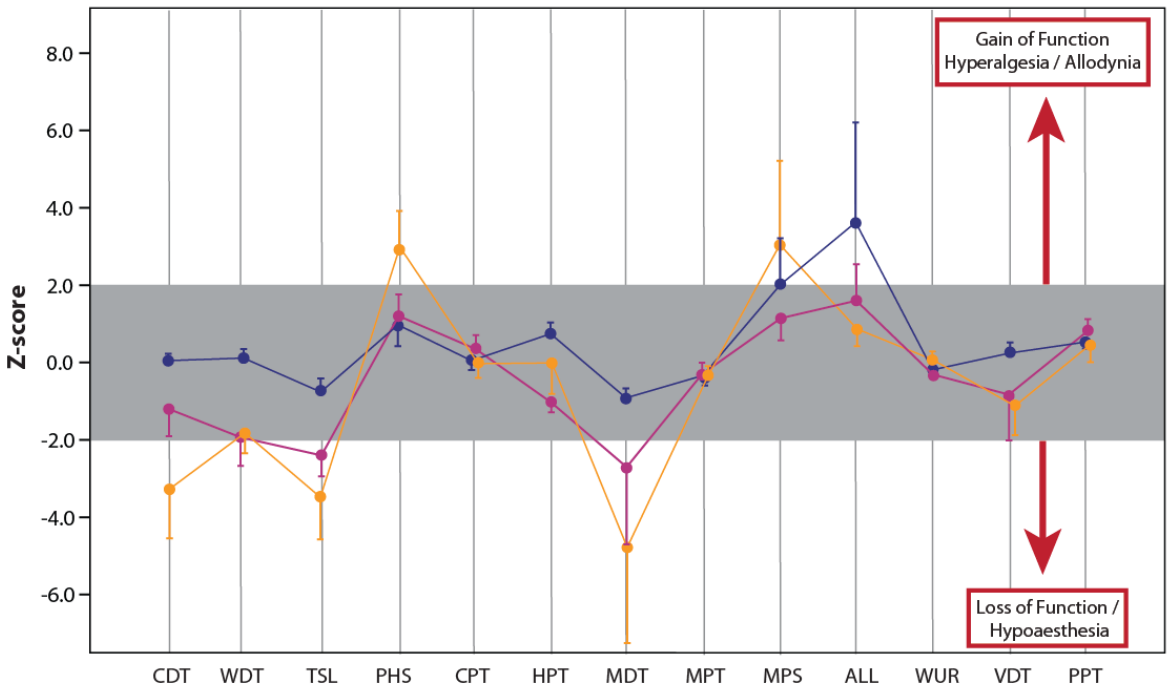

Figure 8: Mean normalised (z-scores) values for QST parameters in Anderson-Fabry patients without pain (pink), Anderson-Fabry patients with pain (yellow) and healthy controls (blue).
CDT: cold detection threshold, WDT: warm detection threshold, TSL: thermal sensory limens, PHS: paradoxical heat sensation, CPT: cold pain threshold, HPT: heat pain threshold, MDT: mechanical detection threshold, MPT: mechanical pain threshold, MPS: mechanical pain sensitivity, ALL: dynamic mechanical allodynia, WUR: wind-up ratio, VDT: vibration detection threshold, PPT: pressure pain threshold.
The grey zone represents the 95% confidence interval for the normal population based on published data (Rolke et al, 2006).
Error bars = 1 S.E.

Immune profile

Cytokine concentrations at the three sites studied (proximal and distal leg and serum) were compared between subgroups: Normal controls, Anderson-Fabry patients without significant pain and Anderson-Fabry patients with significant pain. Full data are available for all subjects with the exception of the proximal thigh site in one normal control, due to collection difficulties. Volumes of microdialysis fluid from each site were: 176 ± 40 µL at the proximal thigh and 175 ± 72 µL at the distal calf (mean ± SD), giving a mean flow rate of 2.9 µL / min. There was no significant difference in the volume of fluid collected between healthy volunteers and patients, nor between the two patient subgroups. When both normal and patient groups were divided into equal subgroups according to the volume of dialysate collected (larger volume *versus* lesser volume), no significant differences were found in any of the cytokines measured dependent upon the volume.

Statistical comparisons were made between subgroups (normal, Anderson-Fabry (no pain) and Anderson-Fabry (with pain) using a one-way ANOVA with Bonferroni correction for multiple comparisons. Comparisons between the total normal and Anderson-Fabry groups were made using independent t-tests. Significant differences within each site between groups are shown in Figures 9A – 9I below. Comparisons were not made between sites within groups as the research question is the association between cytokines and the presence of neuropathy and the presence of neuropathic pain, rather than the difference between sites in an individual. β-NGF remained undetectable at all sites in all

subjects, so was excluded from further analysis. The only statistically significant differences between the subgroups were found for:

- IFN-γ measured at the proximal thigh, which was higher in pain-free Anderson-Fabry than in either Anderson-Fabry patients with significant pain or normal controls, and
- IL-1β at the distal calf between healthy volunteers and the total Anderson-Fabry group.

Across all groups, cytokines were distributed variably across compartments. IL-1β and IFN-γ were found at lower concentrations in the serum than in tissue, whilst IL-6, IL-10, and particularly MCP-1, IP-10 and RANTES are higher in serum. IL-17 is fairly constant across compartments. This variability in relative concentration would argue against a simple equilibration of cytokine levels between serum and tissue compartments.

Figure 9A: IL-1β across sites and subject groups

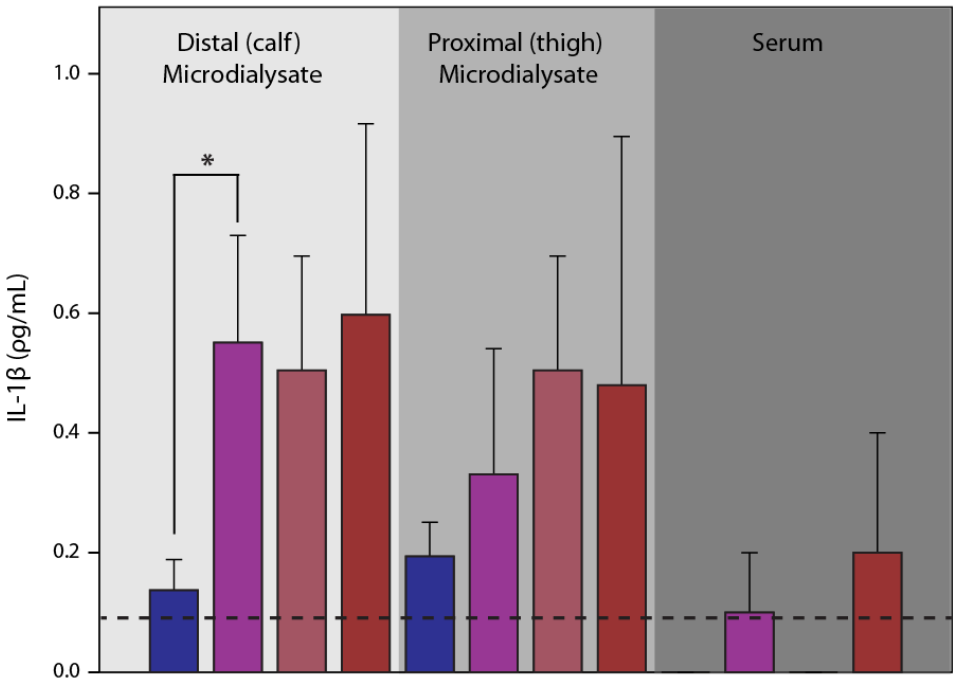

Figure 9B: IL-6 across sites and subject groups

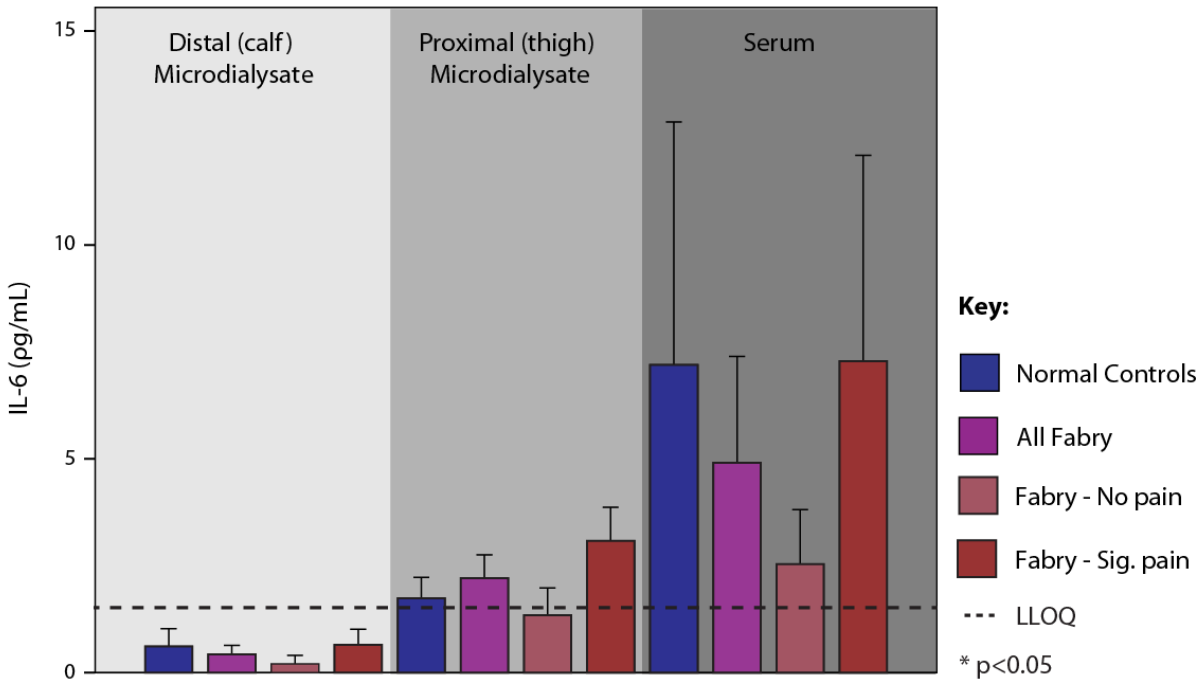

Figure 9C: IL-10 across sites and subject groups

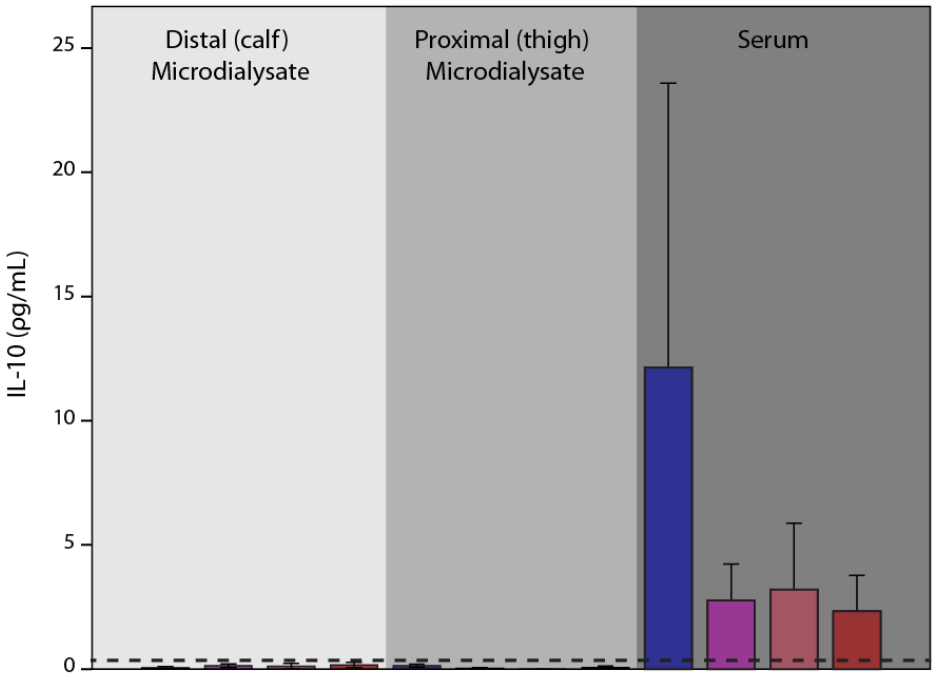

Figure 9D: IL-17 across sites and subject groups

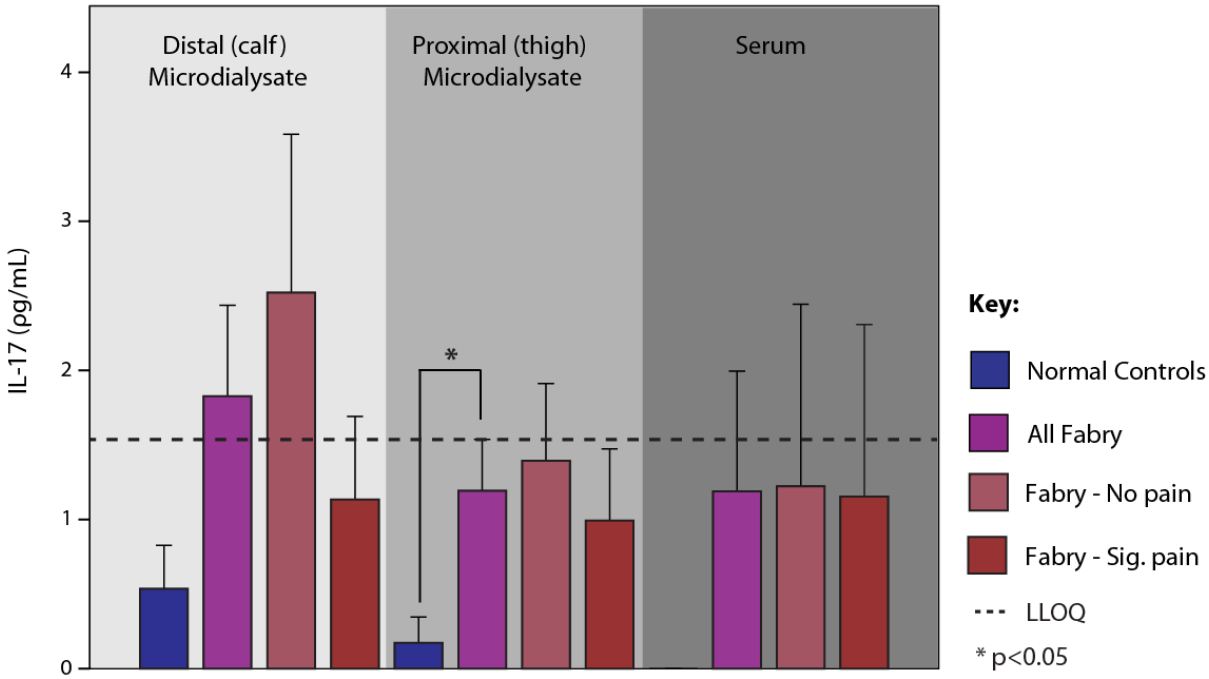

Figure 9E: TNF-α across sites and subject groups

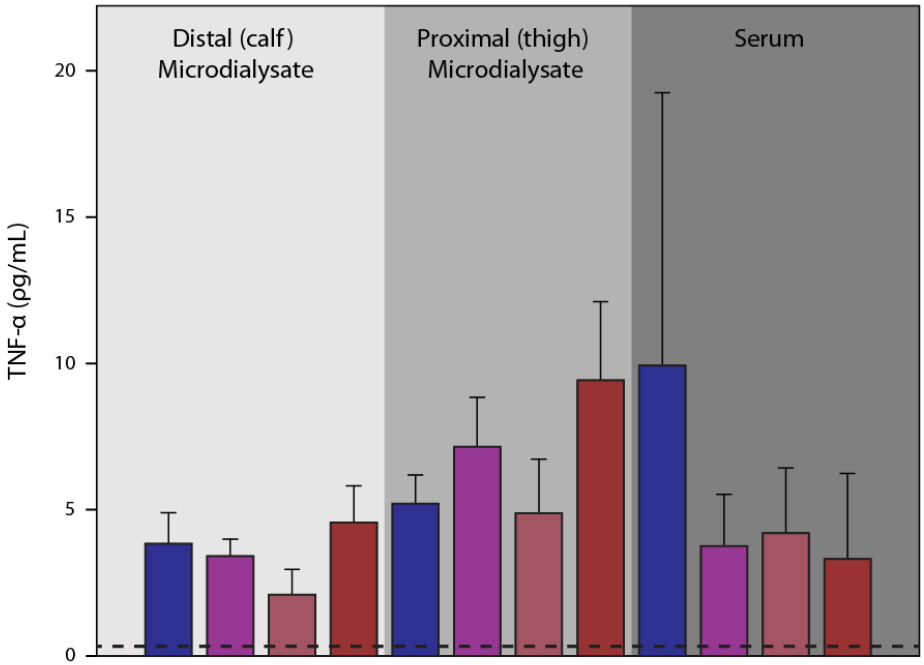

Figure 9F: IFN-γ across sites and subject groups

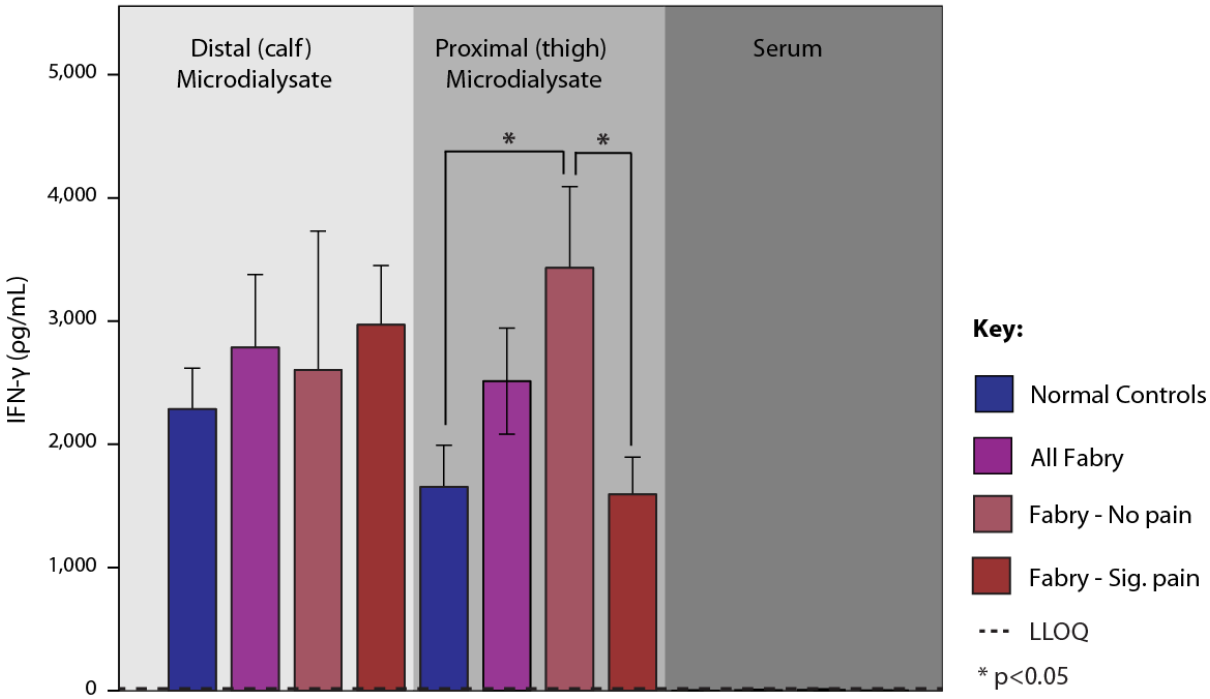

Figure 9G: MCP-1 across sites and subject groups

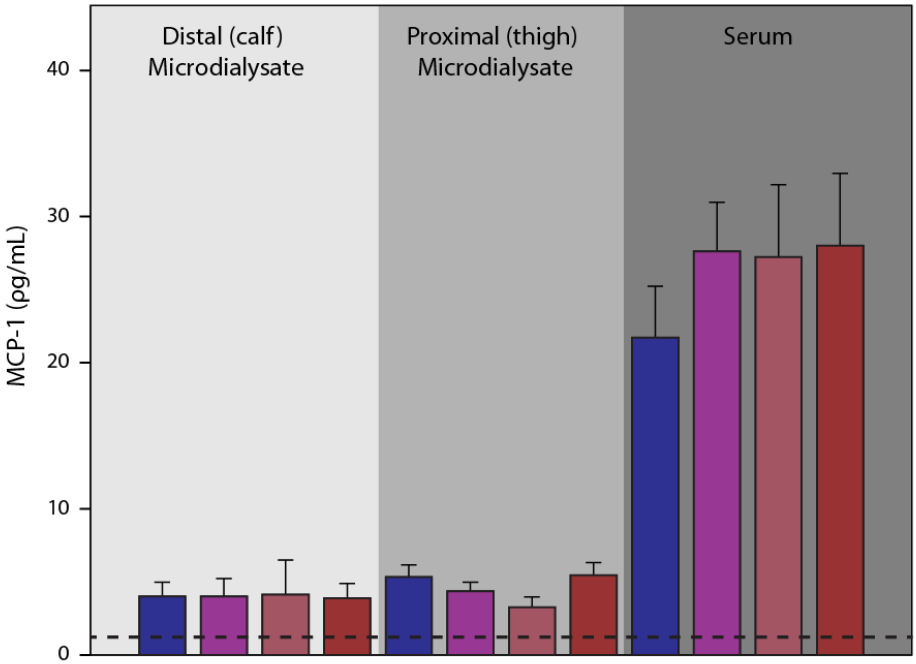

Figure 9H: IP-10 across sites and subject groups

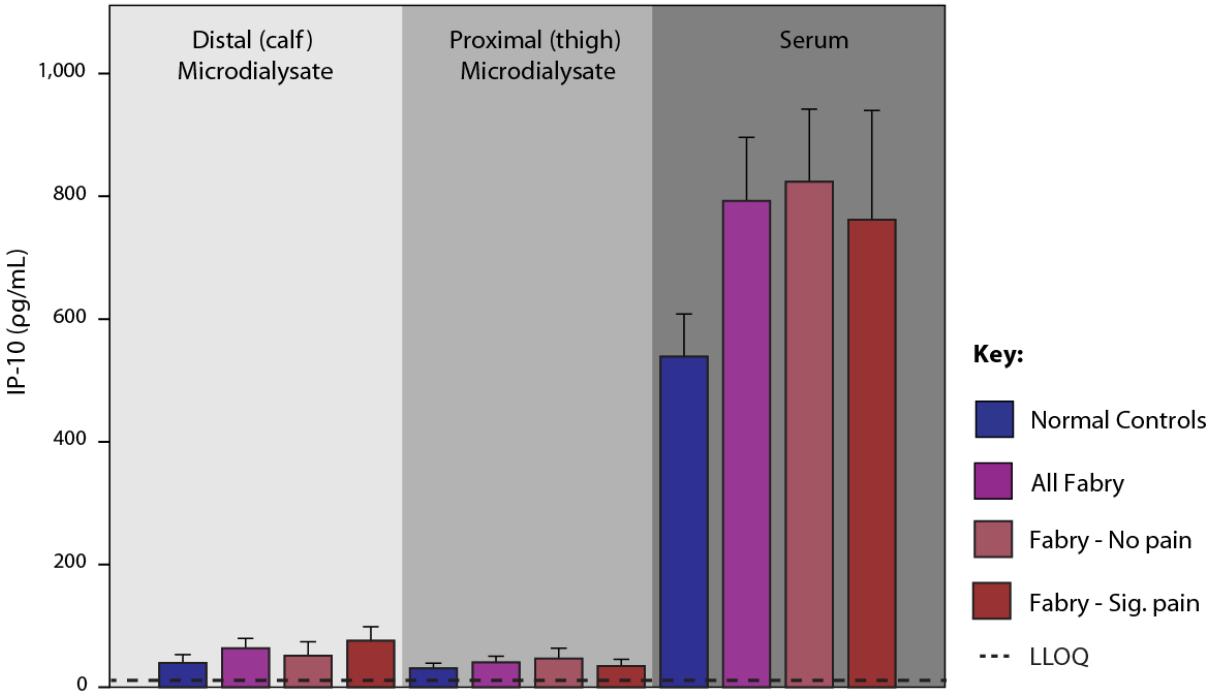

Figure 9I: RANTES across sites and subject groups

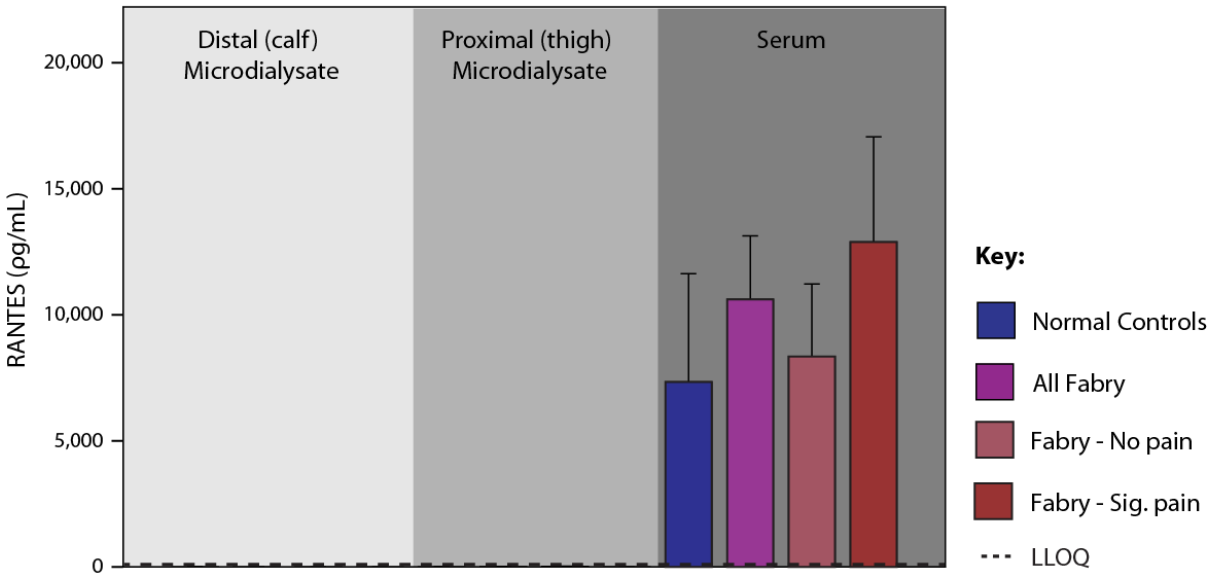

The only significant differences seen between groups were in distal IL-1β and proximal IFN-γ. Distal IL-1β was higher in Anderson-Fabry patients than in controls, but not different in the presence of pain. Proximal IFN-γ was higher in painless Anderson-Fabry patients than those with pain, but this association was not seen distally or in the serum.

In addition to the significant differences presented above, some other cytokines showed a trend to a difference between subgroups ($0.1>p>0.05$). These included distal and proximal IL17, which tended to be lower in normal controls than the painless Anderson-Fabry group, as well as lower levels of distal IL17 in normal controls compared to the total Anderson-Fabry group. Serum IP-10 also showed a trend to lower levels in serum in normal controls compared to the Anderson-Fabry group. Overall, the differences in cytokine levels detected in between group comparisons were mostly linked to the presence of neuropathy,

rather than with the presence of pain, with the only cytokine difference in the painful neuropathy group being lower levels of IFN-γ in microdialysis fluid from the thigh.

Continuous cytokine – pain comparisons: correlations

Although some significant differences between groups defined on the presence or absence of pain as a categorical variable, correlations were found between some cytokines (particularly IL-6 and MCP-1) and continuous pain measures. Pearson's bivariate correlation was used to analyse normally distributed variables, and Spearman's test for those pairs in which one or both pairs were not normally distributed. The cytokine – continuous pain measure correlations with a significant level of correlation are presented in Table 7 below.

Table 7: Significant correlations found between key continuous measures of pain and cytokines (Note: only those which showed a significant correlation are presented)

Correlation between cytokines and pain measures - NPSI			
Cytokine	Correlation coefficient	p-value	Statistical method
Proximal IL-6	0.694	**0.006**	Pearson
Proximal MCP-1	0.653	**0.011**	Pearson
Serum IL-6	0.544	**0.044**	Pearson
Serum RANTES	0.615	**0.019**	Pearson

Correlation between cytokines and pain measures - Current VAS			
Cytokine	Correlation coefficient	p-value	Statistical method
Proximal IL-6	0.659	**0.010**	Pearson
Proximal MCP-1	0.728	**0.003**	Pearson
Serum TNF-α	0.590	**0.026**	Pearson
Serum IL-6	0.783	**0.001**	Pearson

Correlation between cytokines and pain measures - Total VAS			
Cytokine	Correlation coefficient	p-value	Statistical method
Proximal IL-6	0.639	**0.014**	Pearson
Serum IL-6	0.588	**0.027**	Pearson
Serum RANTES	0.550	**0.041**	Pearson

Mood and cytokines:

As cytokine levels have been reported to be affected by mood, and vice versa (Raedler, 2011), all subjects were requested to complete the Hospital Anxiety and Depression Score screening tool for anxiety and depression. A correlation analysis was conducted in both the normal and patient groups between the HAD-A and HAD-D scores and measured cytokine levels. The only significant correlation found was in the normal group, with a moderate correlation between serum IP-10 and the HAD-Anxiety score, with an R value of -0.539,

p=0.047. Therefore it is unlikely that intercurrent mood disturbance had any significant influence on the study results.

Histology

Intraepidermal nerve fibre density (IENFD)

Intraepidermal nerve fibre density was calculated at each biopsy site from the average of four random sections. Intraepidermal fibres were counted according to the rules defined by McCarthy et al (McCarthy et al., 1995), which are summarized in Figure 10. The number of fibres was divided by the epidermal length (in mm) to obtain a linear density of epidermal nerve fibres in each section. An average of the 4 sections counted was then recorded as the intraepidermal nerve fibre density at that site in each subject. Slides were coded to ensure blinded analysis. Some examples of typical epidermal nerve fibres seen in normal controls and Anderson-Fabry subjects are illustrated in figure 11.

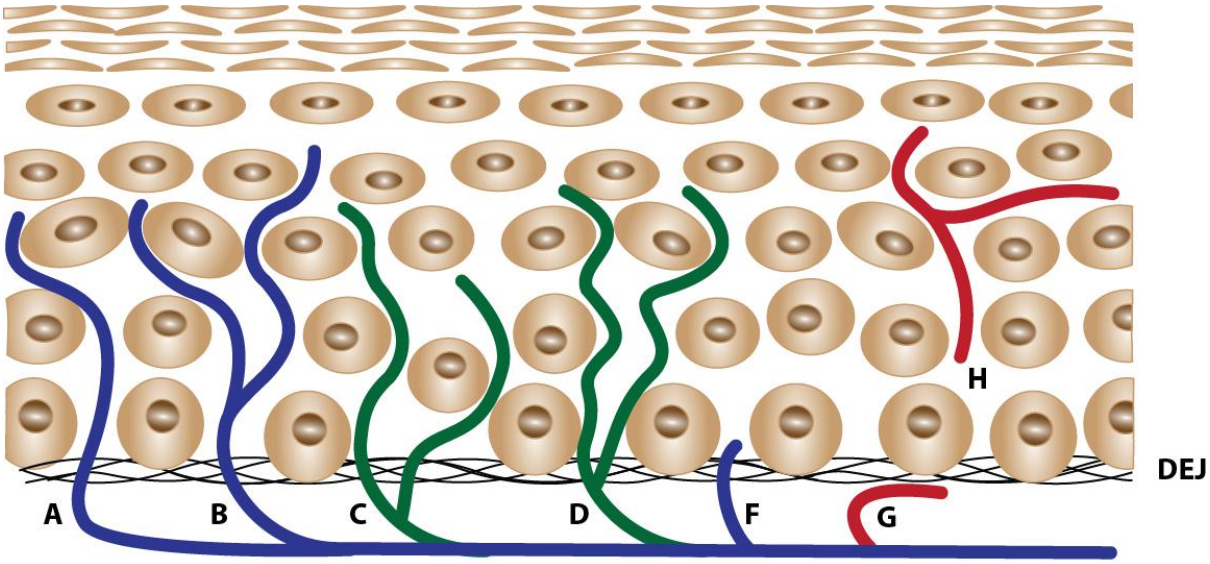

Figure 10: Rules for counting intraepidermal nerve fibres.
Fibres are counted as they cross the dermal-epidermal junction (**DEJ**).
A: Single fibre crossing DEJ = 1, **B:** Single fibre branching immediately after crossing DEJ = 1, **C:** Fibre branching immediately prior to crossing DEJ = 2, **D:** Fibre branching as it passes through the DEJ = 2, **F:** Fibre terminating immediately after crossing DEJ = 1, **G:** Fibre approaching, but not crossing the DEJ = 0, **H:** Fibre seen within the epidermis, but not crossing the DEJ = 0.

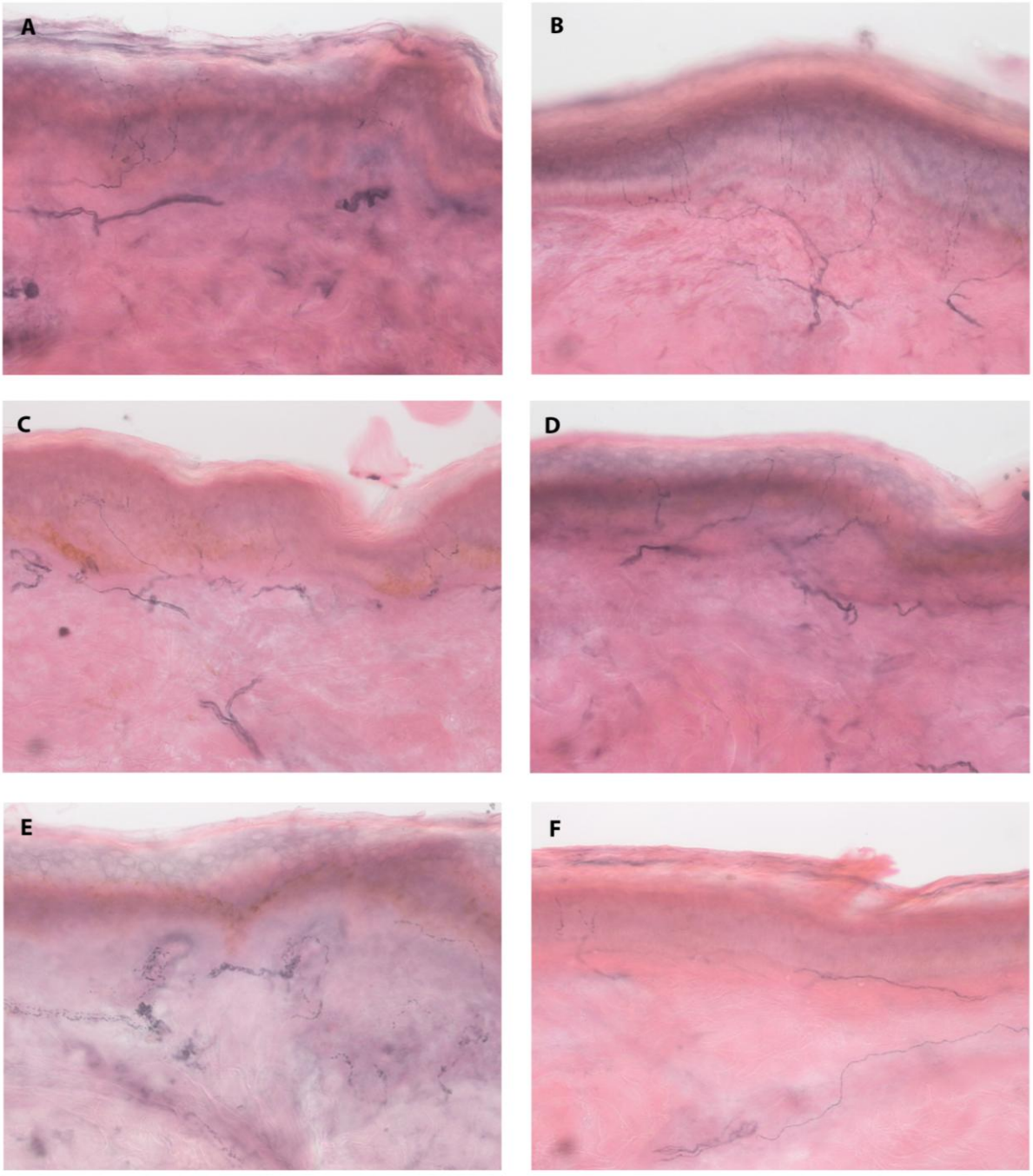

Figure 11: Epidermal nerve fibres in normal controls and Anderson-Fabry patients.

A, B: Normal control (#8, thigh and calf respectively), **C:** Normal control (#4, thigh), **D:** Normal control (#9, calf), **E:** Severely affected Anderson-Fabry patient (#5; thigh), **F:** Moderately affected Anderson-Fabry patient (#1, calf).

In addition to diminished intraepidermal nerve fibre density, reduced autonomic innervation density of dermal organs such as sweat glands and arrector pilae muscles was also prominent in the Anderson-Fabry patients. These changes were not quantitated, but correlated with the severity of small fibre neuropathy seen in IENFD and quantitative sensory testing. Figures 12 and 13 illustrate the loss of innervation in these structures in the Anderson-Fabry patients.

Abnormal morphology of nerve fibres was also observed in the Anderson-Fabry group, with dilatation of subepidermal nerve fibres within dermal nerves, beading of smaller dermal nerve fibres, and prominent large varicosities, particularly around the hair follicle. These large varicosities differ from the small varicosities that are occasionally seen in intraepidermal nerve fibres in both healthy controls and patient groups. The larger varicosities in the Anderson-Fabry group are 2-3 times larger, and sometimes appear to contain intra-axonal inclusions. Some examples of these morphological features are shown in figure 14.

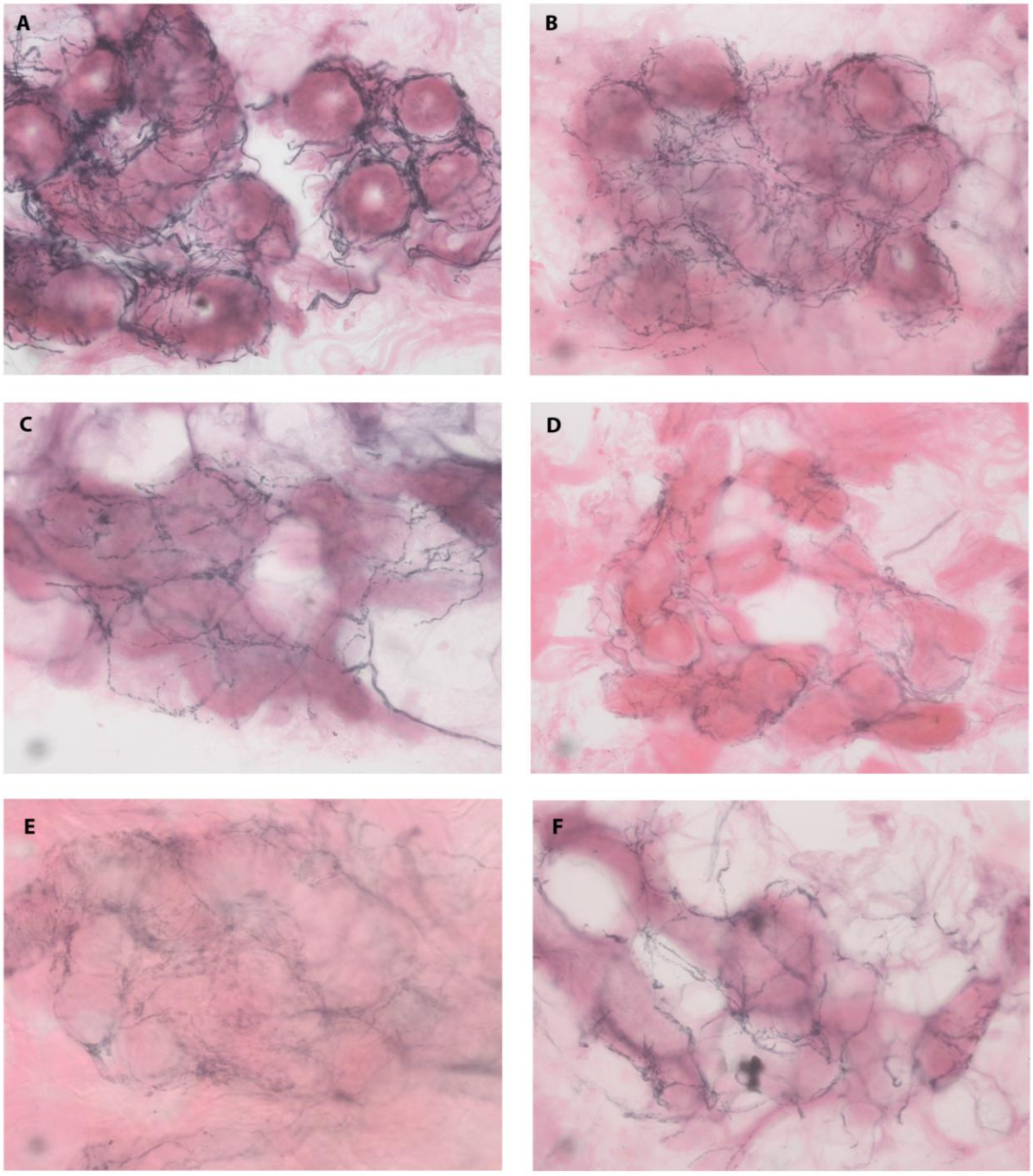

PGP 9.5, eosin counterstain

50 micron

Figure 12: Innervation of sweat glands in normal controls and Anderson-Fabry patients.

A, B: Normal controls (#8 and #3), **C-F:** Anderson-Fabry patients, (C: #7; D: #11; E: #12; F: #13). Note the dense innervation of sweat glands in the normal controls compared to the paucity of innervation seen in the Anderson-Fabry patients.

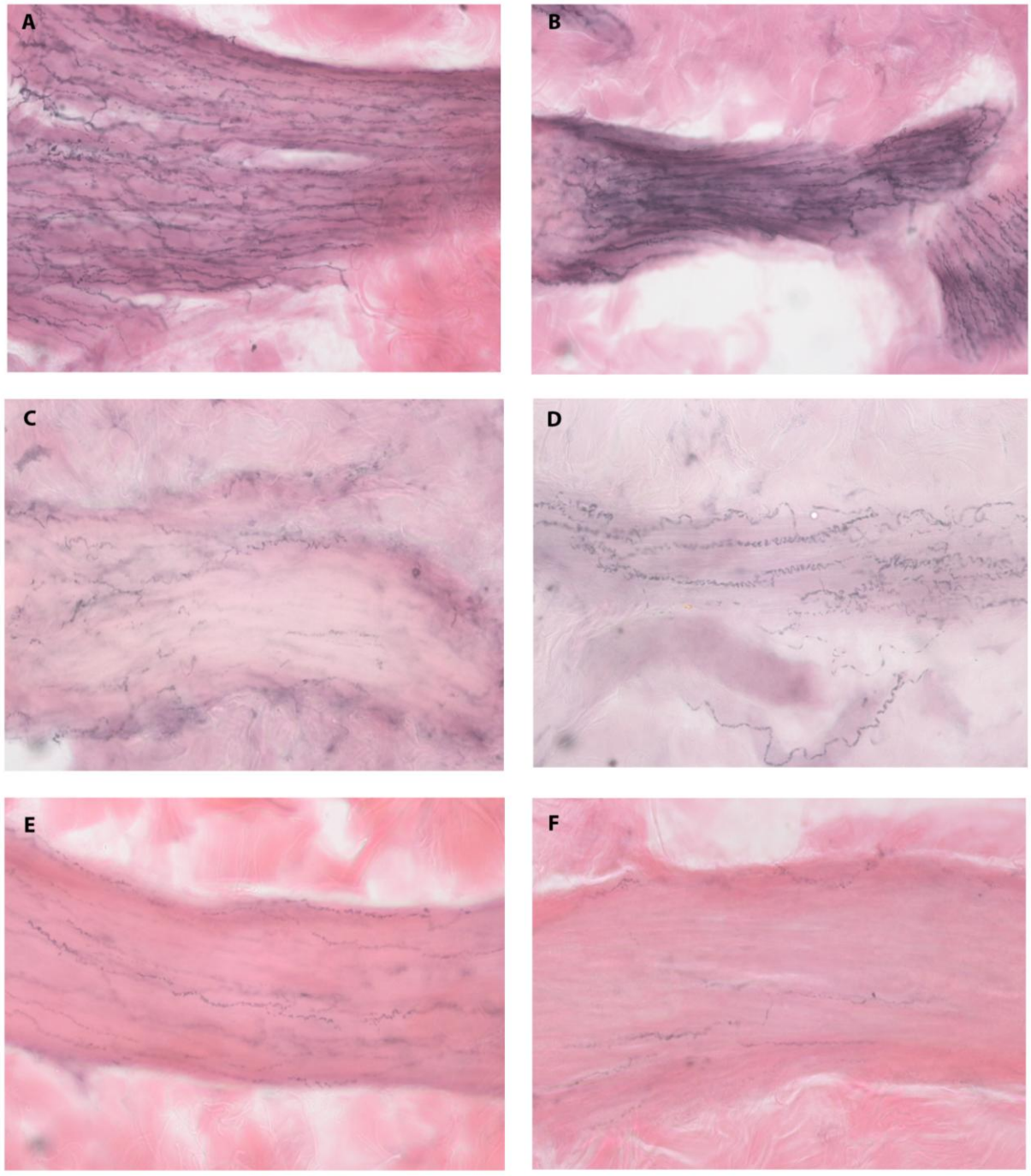

Figure 13: Innervation of arrector pilae muscle in normal controls and Anderson-Fabry patients.

A, B: Normal controls (#8 and #11), **C-F:** Anderson-Fabry patients (C: #5; D: #4; E: #1; F: #11). Note the richly innervated arrector pilae muscles in the normal controls and the sparse innervation seen in the Anderson-Fabry patients.

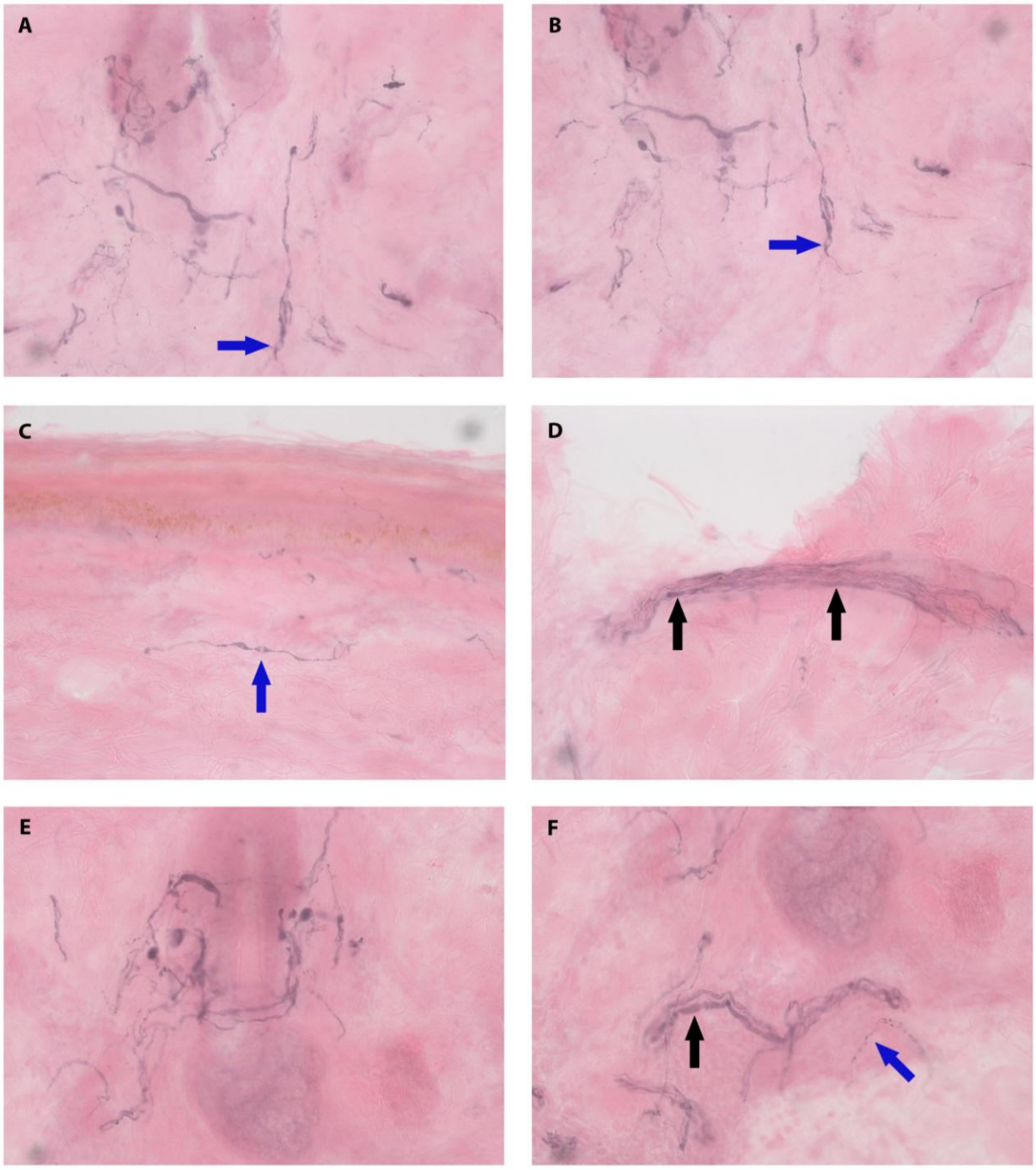

PGP 9.5, eosin counterstain

50 micron

Figure 14: Abnormal morphology in dermal and perifollicular nerve fibres in skin biopsies from Anderson-Fabry patients.

A-D: Anderson-Fabry patient #14 (A, B: abnormally dilated and varicose fibres in the piloneural complex of the hair follicle; C: abnormal varicosity of subepidermal nerve fibre. A possible inclusion within the nerve is seen in figures B and C (blue arrows); D: dilated nerve fibre within dermal nerve (black arrow).
E, F: Anderson-Fabry patient #13 (E: abnormal varicosities in perifollicular nerve fibres; E: abnormally dilated dermal nerve (black arrow) and beading of smaller dermal nerve fibre (blue arrow))

The mean linear density of intraepidermal nerve fibres at the proximal and distal leg in healthy controls and Anderson-Fabry patients is presented in Table 8, and shown graphically in Figure 15. While women and men in both groups show a significant difference in IENFD at both proximal and distal sites, the difference is greater in men, which is consistent with male Anderson-Fabry patients having a more significant neuropathy than females. There was no significant correlation between age and distal IENFD in either the Anderson-Fabry patients or the normal controls, although there was a trend to a negative correlation in the normal group (Pearson's correlation coefficient = -0.521, p=0.056). This was confirmed by linear regression, which showed the presence of Anderson-Fabry disease has a stronger effect on distal IENFD than age: R^2=0.664, distal IENFD = 18 - 0.134(Age, p=0.022) - 6.152(Fabry, p=0.000).

Table 8: IENFD in healthy controls and Anderson-Fabry patients

IENFD: Normal and patient groups				
Site (subgoup)	***Normal*** Mean (SD)	***Anderson-Fabry*** Mean (SD)	***Mean difference***	***p-value***
Proximal (all)	16.4 (4.9)	9.4 (5.1)	6.9	**0.001**
Proximal (women)	16.8 (6.6)	10.5 (4.7)	6.3	**0.043**
Proximal (men)	16.0 (3.0)	7.5 (5.8)	8.4	**0.008**
Distal (all)	13.6 (3.7)	5.6 (3.3)	8.0	**0.000**
Distal (women)	13.2 (4.9)	6.7 (2.2)	6.6	**0.012**
Distal (men)	14.0 (2.3)	3.6 (4.3)	10.4	**0.000**

Figure 15: IENFD in healthy controls and Anderson-Fabry patients

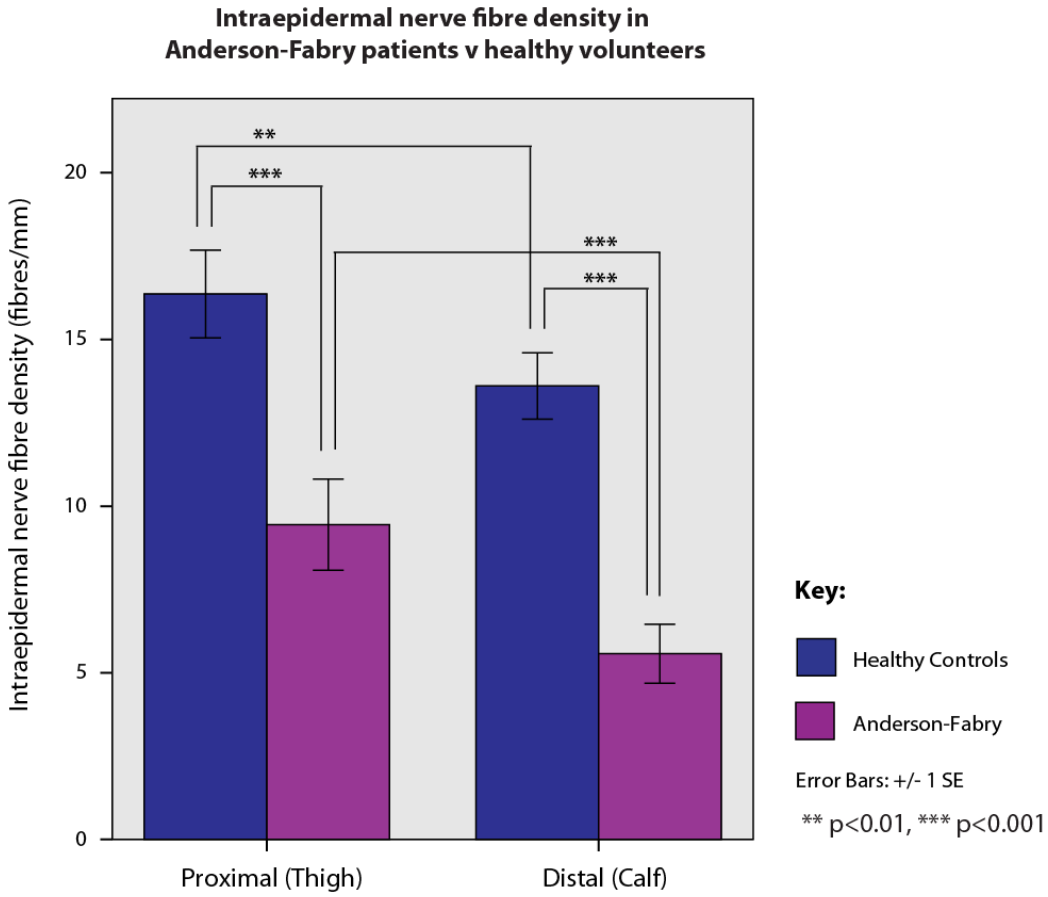

Differences in proximal and distal IENFD between subgroups of patients with and without pain are shown in Table 9, and graphically in Figure 16. The greatest difference between healthy controls and Anderson-Fabry patients in IENFD proximally is seen in subjects with pain, whilst distally, a significant difference was seen between healthy controls and both subgroups of Anderson-Fabry patients, although of a greater magnitude in the subgroup with pain. There was no significant difference between Anderson-Fabry patients with and without pain at either site.

Table 9: IENFD in healthy controls and Anderson-Fabry patients by subgroups

Proximal IENFD - Intergroup comparisons				
Group comparison	Mean difference	95% confidence interval	p-value	Statistical method
Normal - Fabry (All)	6.9	3.0, 10.8	**0.001**	Independent T-test
Normal - Fabry (no pain)	5.2	-0.7, 11.1	0.098	ANOVA (Bonferroni)
Normal - Fabry (with pain)	8.7	2.8, 14.5	**0.003**	ANOVA (Bonferroni)
Fabry (no pain) - Fabry (pain)	3.5	-3.3, 10.3	0.608	ANOVA (Bonferroni)

Distal IENFD - Intergroup comparisons				
Group comparison	Mean difference	95% confidence interval	p-value	Statistical method
Normal - Fabry (All)	8.03	1.33,5.30	**0.000**	Independent T-test
Normal - Fabry (no pain)	7.39	3.17, 11.62	**0.000**	ANOVA (Bonferroni)
Normal - Fabry (with pain)	8.68	4.45, 12.90	**0.000**	ANOVA (Bonferroni)
Fabry (no pain) - Fabry (pain)	1.28	-3.59, 6.16	1.000	ANOVA (Bonferroni)

Figure 16: IENFD in healthy controls and Anderson-Fabry patients with and without pain

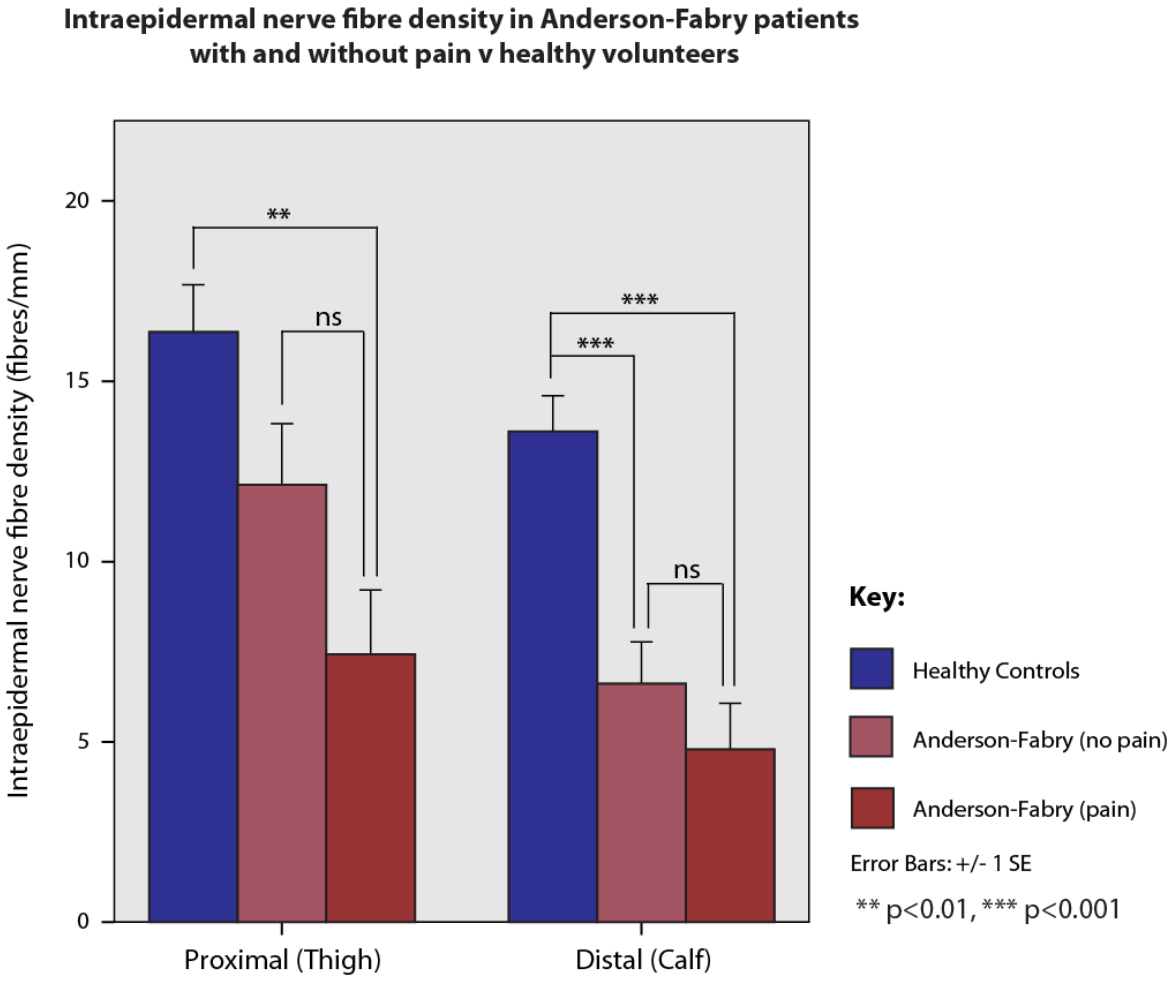

Note: Proximal - distal differences are significant within each subgroup, but are omitted for clarity. Normals <0.01, Anderson-Fabry (both) < 0.05

A significant proximal to distal gradient was seen in all groups of Anderson-Fabry patients, as well as in healthy controls (Table 10). The magnitude of the gradient was, however, greatest in the group of Anderson-Fabry patients without pain.

Table 10: Proximal-Distal gradient in IENFD in healthy controls and Anderson-Fabry patients by subgroups

Proximal - Distal IENFD - Paired T-Test		
Group comparison	Mean difference (SD)	p-value
Normals	2.8 (3.2)	**0.006**
Anderson-Fabry (All)	3.9 (3.5)	**0.001**
Fabry (no pain)	5.5 (4.0)	**0.020**
Fabry (with pain)	2.6 (2.6)	**0.049**

These data suggest that:

1. There is significant loss of IENFD proximally and distally in Anderson-Fabry patients compared with controls (Table 8);

2. Men have a more severe small fibre neuropathy than women (Table 8);

3. There is a similar magnitude of distal fibre loss in Anderson-Fabry patients with and without pain (Table 9);

4. There is a greater loss of proximal nerve fibres in Anderson-Fabry patients with pain than those without (Table 9 and 10).

In order to investigate the association of epidermal nerve fibre loss and functional characteristics, correlations were examined between proximal and distal IENFD and measures of pain intensity (VAS scores), pain quality (Neuropathic pain symptom inventory) and small fibre function (quantitative sensory testing). Correlations used were either bivariate Pearson (for normally distributed variables) or Spearman (for non-normally distributed variables).

Current VAS is VAS score at the time of investigation; sum of three key VAS scores is the sum of current VAS, VAS score for average pain over the last month and VAS score for inconvenience due to pain; total VAS score is as above with the addition of VAS score for worst pain in the last month and VAS score for least pain in the last month. The transformed z-scores were used for the quantitative sensory testing parameter comparisons, to correct for the variability in normal ranges due to gender and age. Tests returning significant correlations in each group are presented in Table 11. It is interesting to note that correlations relating to pain measures were only significant for measures of pain intensity, not of pain quality. Significant correlations with QST parameters were more frequently seen for those functions subserved by small myelinated fibres (cold detection, vibration detection and pressure pain threshold) rather than unmyelinated fibres (warm detection threshold). Also of note, correlations were more frequently significant with proximal IENFD, which is in keeping with the above finding that there is a greater loss of proximal than distal innervation in Anderson-Fabry patients with significant pain.

Table 11: Correlations between IENFD and measures of pain intensity, pain quality and functional loss.

Correlations of pain scores, QST parameters and IENFD in Anderson-Fabry patients		
Measure	Proximal IENFD (R, p-value)	Distal IENFD (R, p-value)
VAS scores		
Current VAS	-0.576, 0.031	ns
Sum of 3 key VAS scores	-0.562, 0.003	ns
Total VAS score	-0.591, 0.026	ns
Neuropathic Pain Symptom Inventory		
NPSI & subscales	ns	ns
Quantitative sensory testing: Hand		
Cold detection threshold	0.579, 0.030	
Warm detection threshold	0.659, 0.010	0.595, 0.025
Thermal Sensory Limens	0.676, 0.008	0.470, 0.090
Quantitative sensory testing: Foot		
Cold detection threshold	0.807, 0.000	ns
Vibration detection threshold	0.565, 0.035	ns
Pressure pain threshold	0.538, 0.047	ns

Langerhans cell density and morphology

Langerhans cell linear density was calculated at each biopsy site from the average of four random sections. Langerhans cells were counted according to predefined rules. A cell was counted only if a definite cell body with at least 2 processes emerging from it was seen. Isolated fragments of CD1a positive material not fulfilling these criteria were not counted. Also, only cell bodies above the dermal-epidermal junction were counted. Superficial dermal CD1a+ cells were considered to be part of the CD1a+ dermal dendritic cell population, not the epidermal Langerhans cell population. The number of cell bodies within the epidermis was divided by the length of the epidermis (in mm) to obtain a linear density. Four sections were counted in this way and averaged to obtain the Langerhans cell density at each site.

Some examples of typical Langerhans cell distribution and morphology in the skin of healthy controls and Anderson-Fabry patients are shown in figures 17 and 18. Note the densely stained, orderly rows of Langerhans cells in the normal controls, and the paler, smaller, less frequent and more disorderly arrangement of Langerhans cells in the Anderson-Fabry patients.

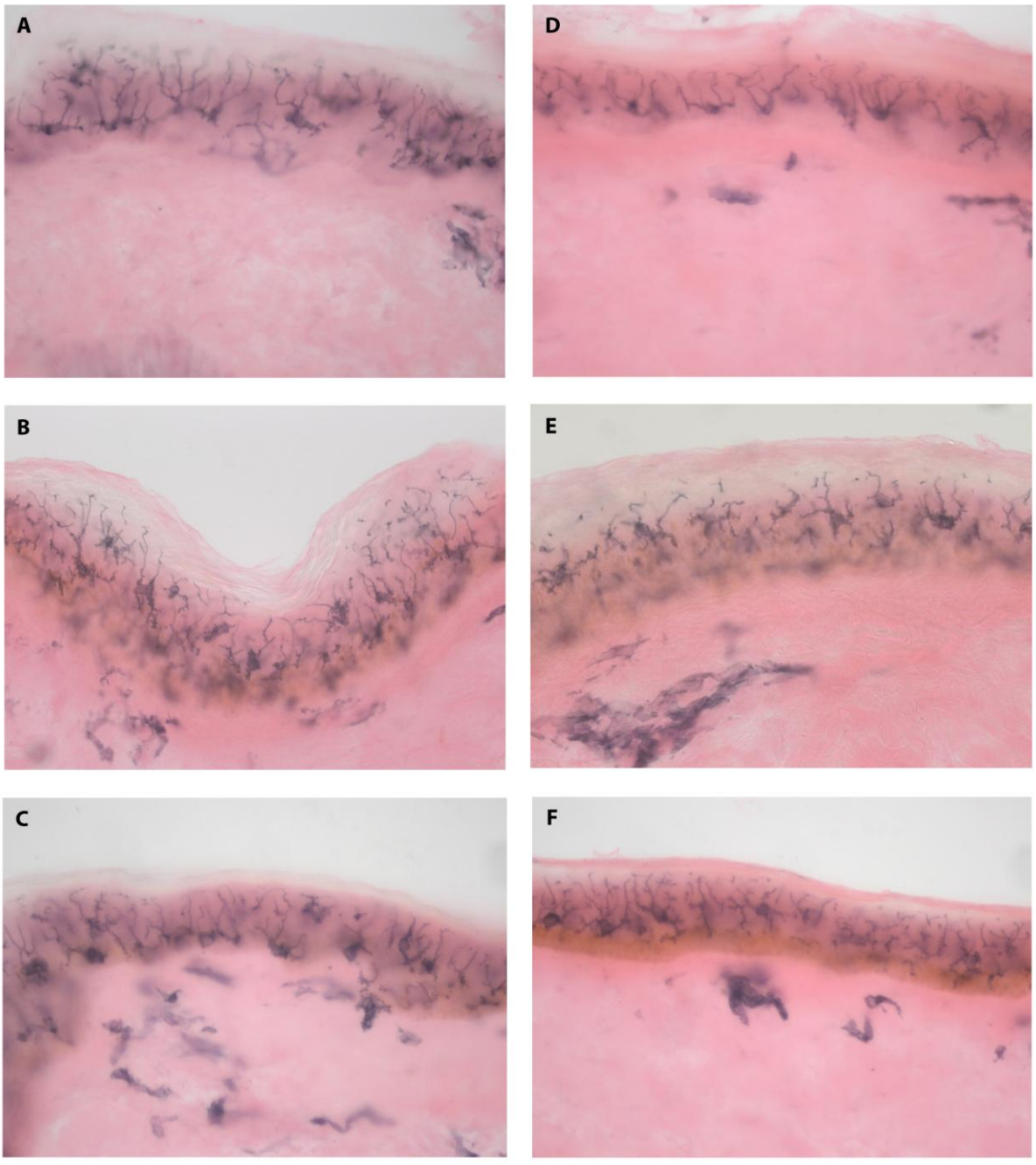

Figure 17: Langerhans cells in skin biopsies from normal control subjects: Thigh and Calf.

A, D: Normal #3, A-thigh, D-calf, **B, E:** Normal #7, B-thigh, E-calf, **C, F:** Normal #4, C-thigh, F-calf

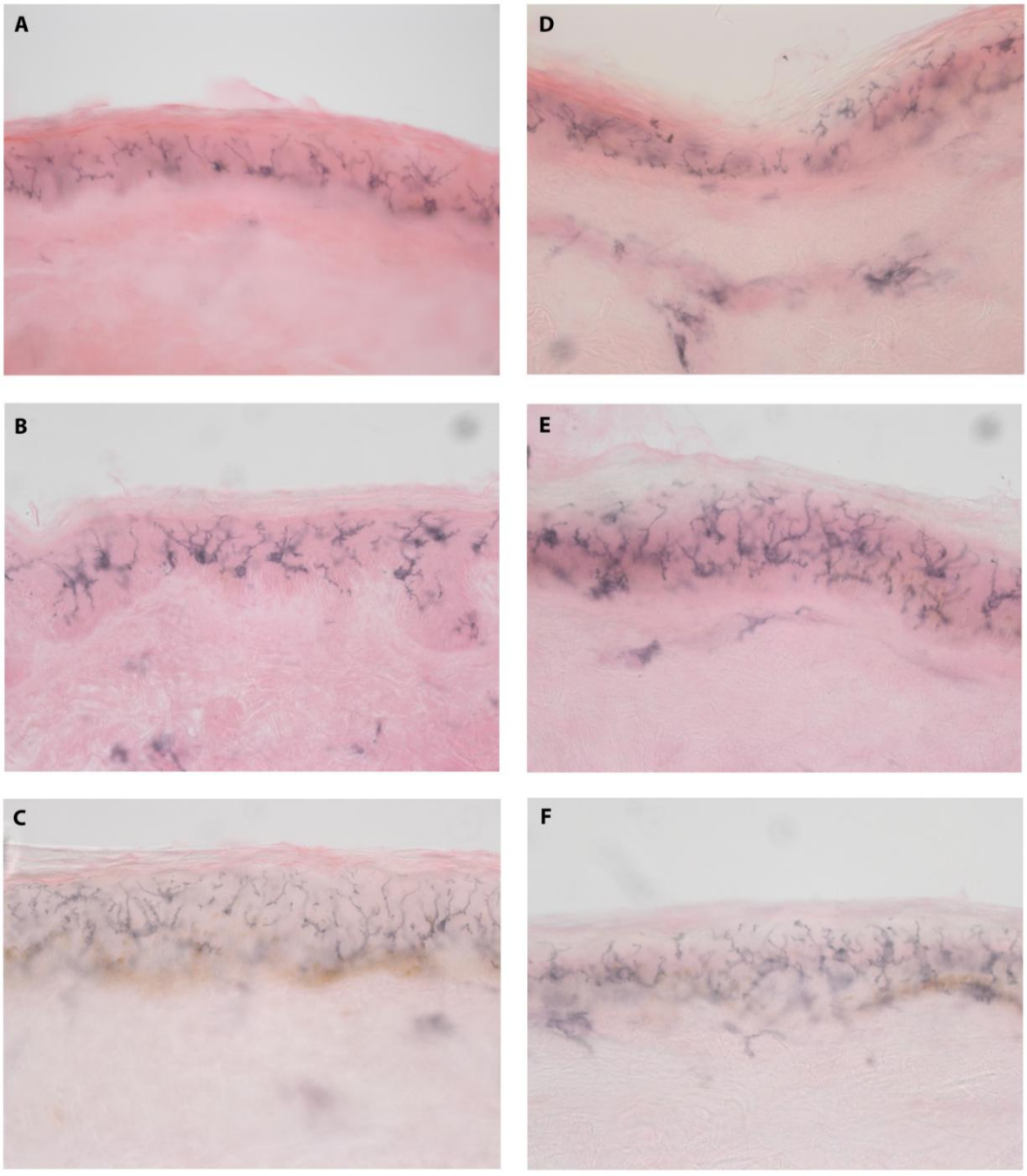

Figure 18: Langerhans cells in skin biopsies from Anderson-Fabry patients: Thigh and Calf.

A, D: Anderson-Fabry #4, A-thigh, D-calf, **B, E:** Anderson-Fabry #2, B-thigh, E-calf, **C, F:** Anderson-Fabry #5, C-thigh, F-calf

There was a significant reduction in Langerhans cells density at the calf in Anderson-Fabry patients, with a trend to reduction at the thigh. The reduction was greater in women than men at both sites (see Table 12). The difference was also greater between healthy controls and Anderson-Fabry patients without pain, than between controls and those with pain (Table 13). Also, while a proximal to distal gradient exists in all groups for Langerhans cell density, there is a greater distal reduction in Anderson-Fabry patients without pain than in those with pain (Table 14). Finally, although no significant differences were found in the between groups comparisons of proximal and distal IENFD: Langerhans cell ratio (using ANOVA with Bonferroni correction for multiple comparisons), in Anderson-Fabry patients with pain, compared to those without there was a trend towards a increase in the density of Langerhans cells at the calf relative to the IENFD. This is illustrated in Figures 19 A-C below.

Differences between groups, subgroups and biopsy sites were assessed using a combination of paired and independent T-tests and ANOVA with Bonferroni correction for multiple comparisons as appropriate.

Table 12: Langerhans cell linear density in normal and Anderson-Fabry patients

Langerhans cell density: Normal and patient groups				
Site (subgoup)	*Normal* Mean (SD)	*Anderson-Fabry* Mean (SD)	*Mean difference*	*p-value*
Proximal (all)	59.1 (14.7)	50.0 (13.3)	9.1	0.097
Proximal (women)	57.9 (15.8)	46.1 (12.1)	11.8	0.111
Proximal (men)	60.3 (14.7)	57.0 (13.6)	3.3	0.761
Distal (all)	53.1 (14.8)	41.9 (11.7)	11.3	**0.033**
Distal (women)	55.3 (17.2)	39.0 (9.3)	16.3	**0.029**
Distal (men)	51.0 (12.9)	47.1 (14.9)	4.1	0.620

Table 13: Langerhans cell linear density by site and subgroups

Proximal Langerhans cell density - Intergroup comparisons				
Group comparison	Mean difference	95% confidence interval	p-value	Statistical method
Normal - Fabry (All)	9.1	-1.8, 20.0	0.097	Independent T-test
Normal - Fabry (no pain)	11.8	-5.0, 28.5	0.254	ANOVA (Bonferroni)
Normal - Fabry (with pain)	6.5	-10.3, 23.3	0.998	ANOVA (Bonferroni)
Fabry (no pain) - Fabry (pain)	-5.3	-2.4, 14.1	1.000	ANOVA (Bonferroni)

Distal Langerhans cell density - Intergroup comparisons				
Group comparison	Mean difference	95% confidence interval	p-value	Statistical method
Normal - Fabry (All)	11.3	1.0, 21.6	**0.033**	Independent T-test
Normal - Fabry (no pain)	15.6	0.0, 31.2	**0.050**	ANOVA (Bonferroni)
Normal - Fabry (with pain)	7.0	-8.6, 22.6	0.787	ANOVA (Bonferroni)
Fabry (no pain) - Fabry (pain)	-8.6	-26.6, 9.4	0.689	ANOVA (Bonferroni)

Table 14: Proximal – Distal Langerhans cell linear density by group, site and gender

Proximal - Distal Langerhans cell density - Paired T-Test		
Group comparison	Mean difference (SD)	p-value
Normals	6.0 (6.7)	**0.005**
Anderson-Fabry (All)	8.1 (8.0)	**0.002**
Fabry (no pain)	9.6 (8.0	**0.032**
Fabry (with pain)	6.9 (8.3)	**0.049**

Figure 19A: Proximal Langerhans cell linear density compared to IENFD by subgroup.

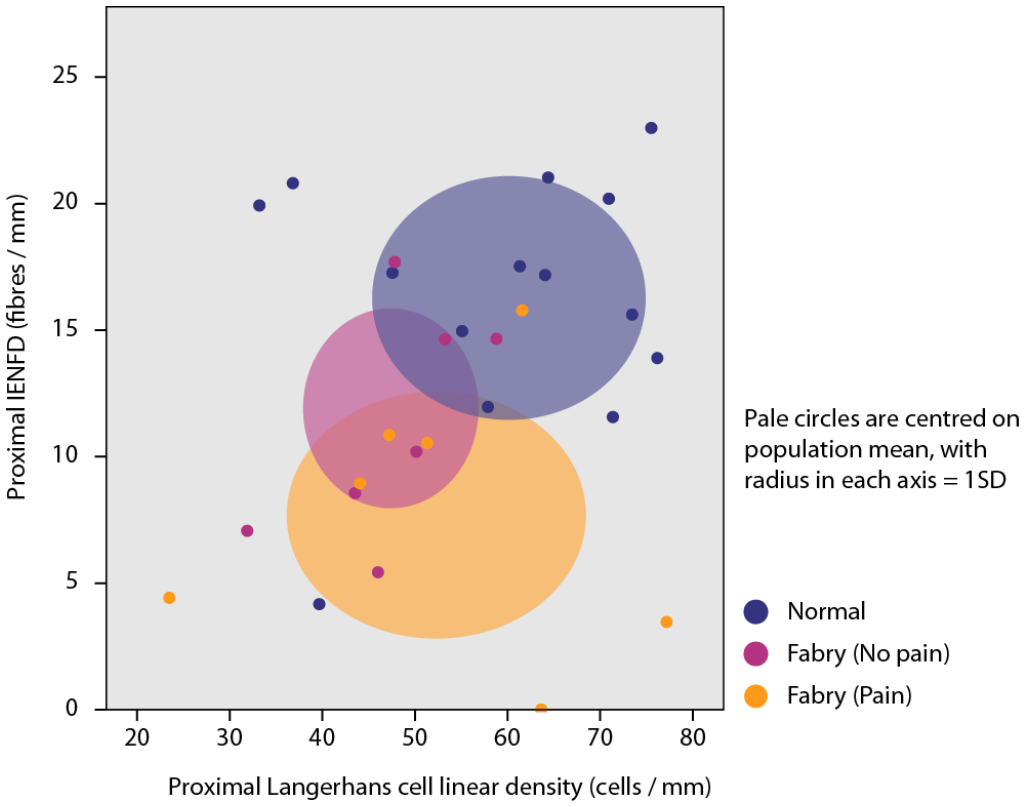

Figure 19B: Distal Langerhans cell linear density compared to IENFD by subgroup.

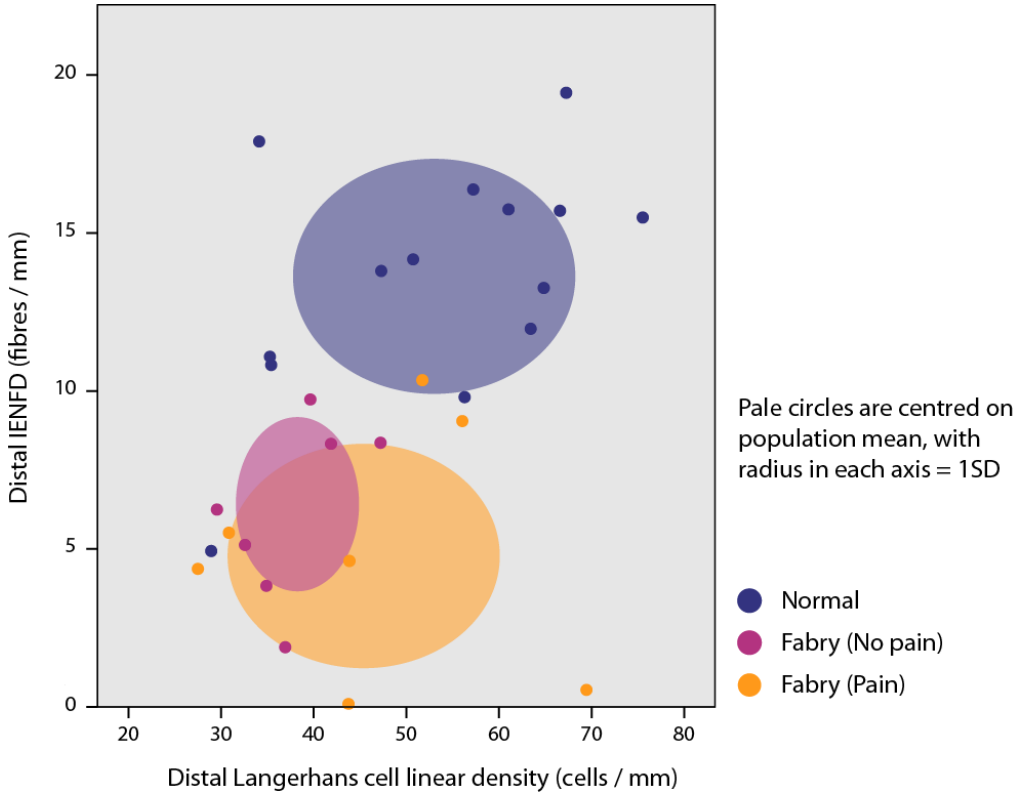

Figure 19C: Langerhans cell linear density compared to IENFD by subgroup.

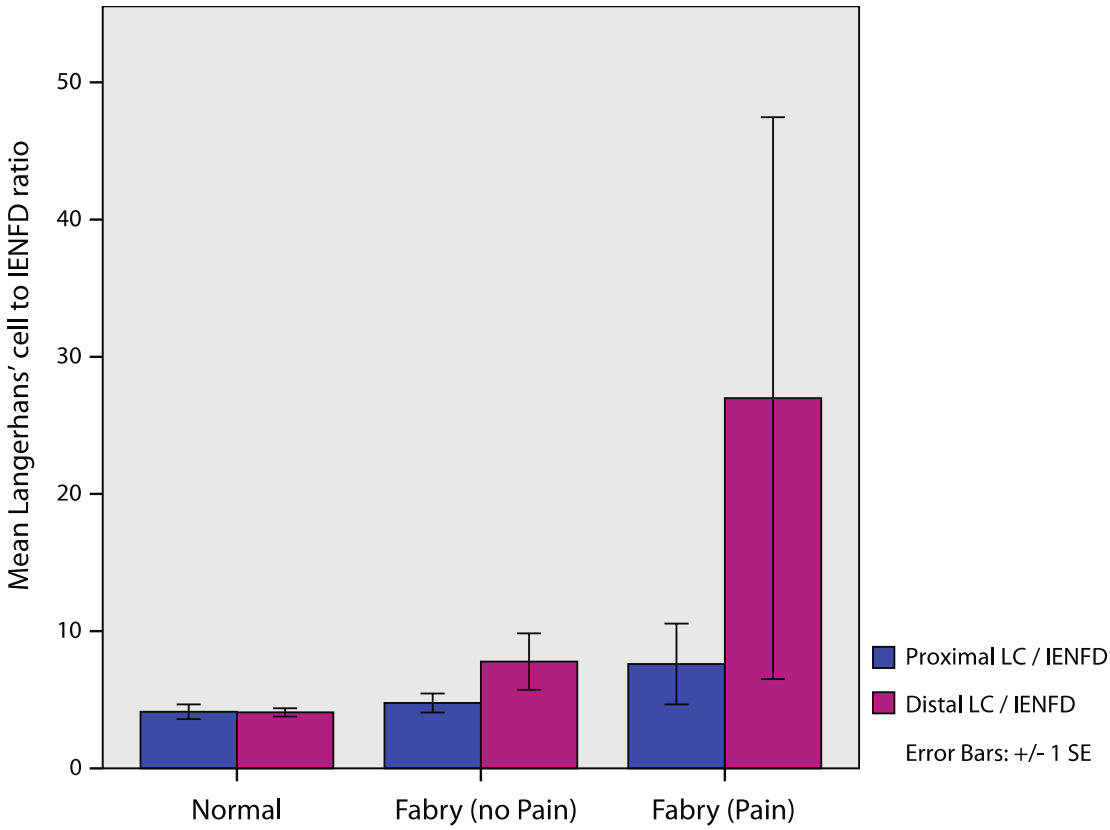

Langerhans Cell morphological changes in Anderson-Fabry disease

Morphological differences were noted in the Langerhans cells of Anderson-Fabry patients compared with those of healthy controls when visualized with the Langerhans cell antibody CD1a (see figures 17 and 18 for examples). Normally, Langerhans cells have densely stained, rounded to stellate cell bodies, forming 2 parallel layers in the epidermis. The deeper layer is often slightly elongated parallel to the dermal-epidermal junction, whilst the more superficial layer, located roughly in the centre of the thickness of the epidermis, are often more rounded and stellate in morphology. Several processes are seen emerging from each cell body, forming a dense surveillance network of fibres throughout the epidermis. Just deep to the dermal epidermal junction several larger CD1a+

cells are also often seen. If hair follicles or sweat gland ducts are present in the section, these are also densely lined with CD1a+ Langerhans cells.

In the Anderson-Fabry patients, Langerhans cell bodies were often smaller and more irregular in morphology, and less frequently seen organized into two well-ordered rows. The overall density of cell bodies along the epidermis was reduced, with lengths of epidermis in which no cell bodies were seen occurring frequently. Less frequent cells were seen lining hair follicles and sweat glands, and less subepidermal CD1a+ cells were seen. CD1a+ processes within the epidermis were still often frequent, but often appeared fragmented and disorganized.

These morphological differences were confirmed by examination of the Langerhans cells in 6 normal and 6 Anderson-Fabry patients by a second, blinded examiner (Dr Michael Lunn), who correctly identified all of the patients as being abnormal, and 5/6 of the normal controls as being normal. The slides were presented twice, with 100% concordance of the categorization by the blinded examiner between the 2 viewings.

Summary of Key Results:

- Neurophysiology:
    - Nerve conduction study parameters fell within normal limits for normal controls and Anderson-Fabry patients, although there was a slight reduction in lower limb sensory and motor amplitudes in patients compared to normal controls.
    - Histamine-induced flare responses were reduced in intensity and size in Anderson-Fabry patients compared to normal controls, although the difference was only statistically significant in the upper limb.
    - Quantitative sensory testing showed significant variation from normal control subjects in the Anderson-Fabry group, particularly in thermal detection thresholds at both the hand and the foot, with mechanical detection, vibration detection, heat pain and paradoxical heat sensation additionally involved in the lower limb. Compared with age and gender matched normative data, only cold and warm detection thresholds and mechanical detection thresholds fall outside of the normal range in Anderson-Fabry patients. Subgroup analysis found that men were affected more than women, and that Anderson-Fabry patients with pain had more abnormal results than those without pain.

- Immune Profile:
    - The only significant differences between normal controls, Anderson-Fabry patients with pain and Anderson-Fabry patients without pain were found in:
        - IFN-γ at the proximal thigh, which was elevated in pain-free Anderson-Fabry patients compared to those with pain and normal controls.
        - IL-1β at the distal calf, which was significantly higher in Anderson-Fabry patients than in normal controls, with no differences in the subgroups with and without pain
    - Trends to differences between groups ($0.1<p<0.05$) were seen in the following cytokines:
        - IL-17 (distal and proximal levels) tended to be higher in the painless Anderson-Fabry group compared to normal controls, with distal IL-17 also tending to be higher in the total Anderson-Fabry group than in normal controls.
        - Serum IP-10 tended to be higher in the Anderson-Fabry group than in normal controls.
    - Significant positive correlations were seen between several pain measures and several cytokines, including proximal thigh levels of IL-6 and MCP-1 and serum levels of TNF-α and RANTES.
- Histology
    - Intraepidermal nerve fibres:

        - Intraepidermal nerve fibre density was significantly reduced at both proximal and distal sites in Anderson-Fabry patients compared to controls, with men more severely affected.
        - There is a trend to more severe intraepidermal nerve fibre loss in Anderson-Fabry patients with pain, with a larger difference between the pain and no-pain groups seen at the proximal thigh than at the distal calf.
        - Pain scores had a significant negative correlation with proximal intraepidermal nerve fibre density.
        - The strongest correlations between intraepidermal nerve fibre density and QST parameters was seen at the proximal thigh, particularly with cold detection thresholds. In the lower limb, vibration detection and pressure pain thresholds also correlated with proximal intraepidermal nerve fibre density, whilst in the upper limb warm detection and thermal sensory limens correlated with proximal intraepidermal nerve fibre density.
    - Langerhans cells:
        - Langerhans cell density was significantly reduced at the calf in Anderson-Fabry patients, with a trend to reduction at the thigh. There was a trend to a larger reduction compared to normal control subjects in the patient subgroup without pain.

- As with intraepidermal nerve fibre density, there was a proximal to distal gradient in Langerhans cell density in both normal subjects and the patient cohort.
- The ratio of Langerhans cells to intraepidermal nerve fibre density was similar at both sites in normal controls, mildly increased distally in the pain-free Anderson-Fabry group, and markedly increased distally in the Anderson-Fabry subgroup with pain, although the result did not reach statistical significance.
- In Anderson-Fabry patients, Langerhans cells lost their usual two-layered arrangement in the epidermis, and developed morphological changes, including smaller, more irregular morphology of the cell body, with processes that were frequently fragmented and disorganized.

Neurophysiology:

Whilst there were some slight reductions in large fibre neurophysiology, particularly amplitude of responses compared with normal controls, the mean velocities and amplitudes in this cohort did not fall outside generally accepted normal ranges. The slight variation may in part reflect the slightly older age of the patients compared with controls, although Dütsch et al reported similar findings in Anderson-Fabry patients (Dütsch et al., 2002). There were significant differences in quantitative sensory testing, consistent with a length-dependent small fibre neuropathy, with greater effect on small myelinated (Aδ and Aβ) fibres, but also involving unmyelinated C-fibres. The quantitative sensory testing profile in Anderson-Fabry is characterized more by loss than gain of sensory function. The small fibre deficits were more profound in the male patients. A similar pattern of small fibre functional change was found in previous studies (Dütsch et al., 2002, Üçeyler et al., 2011, Biegstraaten et al., 2011).

The subgroup analyses suggest that in our Anderson-Fabry cohort, the subgroup with pain have more severe small fibre impairment. Previous studies reporting the correlation between severity of neuropathy and pain have yielded mixed results, but involved all female cohorts (Laaksonen et al., 2008, Torvin Möller et al., 2009). A recent study, which included male patients, also found no association between severity of neuropathy and pain. There are some factors to be considered in this paper, as two-thirds of the cohort were female, and in contrast to our study, demonstrated no QST abnormalities, whilst males had

abnormal cold detection threshold and thermal sensory limens. In addition, only one third were on enzyme replacement therapy. These factors suggest that overall the group had a milder phenotype than our cohort, which may affect the correlation of severity and pain (Biegstraaten et al., 2011).

The reductions in flare intensity and size in Anderson-Fabry patients were significant only in the upper, rather than lower limbs, in contrast to the other small fibre functional measures examined in this study. This may reflect relative sensitivity of the test at different sites, perhaps due to thicker skin in the lower limb blunting the iontophoresis of histamine.

Overall, the neurophysiological data support the findings of previous studies (Burlina et al., 2011, Lakomá et al., 2014, Mauhin et al., 2015, Biegstraaten et al., 2012). The correlation between severity of neuropathy and pain needs further refining. The difficulties arise in the phenotypic variability not just between hemizygotes and heterozygotes, but also within each group in terms of organ involvement and severity. There is also the question of enzyme replacement therapy and its potential impact, particularly on measures of function. Pain medication also will diminish the strength of any correlation with pain, but clearly cannot be withdrawn ethically. Larger cohort studies with planned stratification of these factors may help to clarify their potential impacts.

Cytokine Profile

IFNγ at the proximal thigh was significantly higher in pain-free Anderson-Fabry patients than in either the group with pain, or the normal controls. Distal calf IL-

1β was higher in Anderson-Fabry patients than normal controls, but showed no difference related to the presence of pain. IL-17 levels are difficult to interpret, as although they trended to be at higher levels in Anderson-Fabry patients, they were also around the lower limit of quantification for the assay. Despite the relative paucity of strong intergroup differences, there were significant correlations of moderate strength seen between proximal levels of IL-6 and MCP-1 and serum levels of TNF-α and RANTES. The association between proximal, rather than distal cytokine levels and pain is interesting, and may indicate a role for cytokines at a particular point in the evolution of painful neuropathy, as the distal site is more severely affected in terms of nerve fibre loss than the proximal one. Although there were correlations found between serum cytokine levels and measures of pain, which may indicate a link between a pro-inflammatory profile and pain, this must be considered in light of recent studies (see below) suggesting Anderson-Fabry disease may be linked to pro-inflammatory immune changes.

A recent study (Üçeyler et al., 2011) examined cytokine levels in Anderson-Fabry patients by skin mRNA, and found no differences in mRNA expression of TNF-α, IL-1β, IL-8, IL-10 or TGF-β1 between proximal and distal sites, or between patients and controls. Neither did they find an association with pain. Aside from the potential difference in cytokine levels measured by whole skin mRNA extraction compared to protein detection by ELISA in dermal microdialysis fluid, there are a number of other potential factors to consider in comparing their results to this study. These include the low proportion of patients on ERT at baseline (27%), a significant proportion with renal

impairment (50%), and less significant QST abnormalities in women than were found in our cohort.

Previous studies have found associations with inflammatory cytokines and pain, such as Üçeyler et al (2010) who found strong elevation in cutaneous mRNA expression for IL-6 and IL-8, and smaller elevation of TNFα and IL-1β in patients with painful small fibre neuropathy compared to healthy controls (Üçeyler et al., 2010). This is discordant to my findings in Anderson-Fabry patients, which may be due to a combination of methodological factors, included variable discordant profiles between dermal protein sampling by microdialysis compared to epidermal mRNA expression, as well as possible variations between gene expression and functional cytokine release. A key example of this is the regulation of the synthesis of mature IL-1β from pro-IL1β by inflammasome-regulated activation of caspase 1 (Guarda and So, 2010).

The lack of difference in serum cytokine levels in Anderson-Fabry patients is also contrary to previous findings of elevated proinflammatory cytokines (IL-2 and TNF-α) and reduced anti-inflammatory cytokines (IL-10, IL-4) in serum of patients with painful versus painless neuropathy (Üçeyler et al., 2007b). This may be an effect of the relatively small numbers studied, as there was considerable overlap in the levels found in individuals in the two groups in Üceyler's study.

Anderson-Fabry may impact on immune function

There have been a number of recent papers describing immune differences in immune function in Anderson-Fabry patients compared with healthy controls

that may impact on these results. These studies suggest that Anderson-Fabry disease may have a greater degree of disease and treatment related immune variance than was suspected when this study was originally conceived. These recent findings relate both to the disease process, and to treatment effects.

The first issue involves changes in innate immunity in Anderson-Fabry disease mediated by altered function of invariant natural killer cells (iNKT). Invariant natural killer (iNKT) cells are a subgroup of cytotoxic T-cells that have important roles in microbial infection, reducing autoimmune responses and tumour surveillance. Lysosomal activity is important in the regulation of activity of invariant natural killer (iNKT) cells, which recognize self and bacterial glycolipid antigens associated with MHC class I-like CD1d molecules (Pereira et al., 2013). It has been found that in Anderson-Fabry patients, increased levels of Gb3 acts on dendritic cells via toll-like receptor 4 to increase CD1d signaling via the T-cell receptor on invariant natural killer (iNKT) subsets, which in turn modulates peripheral blood mononuclear cell cytokine release via IFN-γ. The net effect is a shift to a more proinflammatory profile, with increased secretion of IL-1β, TNF-α and IL-6, and reduction in IL-4 (Mauhin et al., 2015, De Francesco et al., 2013).

The second recent finding that impacts on this study is that enzyme replacement therapy in Anderson-Fabry disease induces upregulation of transcription in components of several immune and inflammatory pathways, such as those involved in the molecular pathways for T-cell receptors, IL-2, IL-6 and innate and adaptive immunity (Ko et al., 2015). Increased serum levels of TNF-α and IL-6 have also been reported in Anderson-Fabry patients treated with

enzyme replacement therapy (Biancini et al., 2012). Whether these changes reflect a disease-induced derangement, or a response to a foreign product (enzyme replacement therapy), these findings may still be a serious confounder in this study.

These findings have important implications for this study, as any small shifts in immune function related to pain mechanisms may be swamped by fluctuations related to disease or treatment. This is of particular import given the small sample size.

Overall, the data suggests a link between inflammatory cytokines and pain in Anderson-Fabry neuropathy, but confirmation in a larger cohort would be desirable. Ideally, this would allow subgroup analysis of patients at different stages of the disease, and include groups receiving and not receiving enzyme replacement therapy. This would allow further exploration of the idea that inflammation may be important at particular stages in the development of neuropathy, as well as the effect of enzyme replacement therapy on Anderson-Fabry. There were no correlations with cytokine levels and HAD score in the patient cohort, indicating mood-induced cytokine variation is unlikely to be a significant confounder.

Histology:

1. Intraepidermal innervation.

Intraepidermal nerve fibre density was reduced overall in the patients compared with the controls, and exhibited a length-dependent gradient. Reduced autonomic innervation of arrector pilae muscles and sweat glands was

also observed in Anderson-Fabry patients. Sweat glands in Anderson-Fabry demonstrate atrophy and stromal inclusions (Fukuhara et al., 1975, Yamamoto et al., 1996), as well as reduced sympathetic skin response (Yamamoto et al., 1996). Reports of autonomic innervation of sweat glands are varied. One study reported no change in autonomic innervation of sweat glands in Anderson-Fabry disease, although the skin examined was taken from the proximal thigh, which may not be involved until later in the disease (Schiffmann and Scott, 2002). Coupled with a report of relatively uniform loss of sweat glands in Anderson-Fabry (Cable et al., 1982a), it has been proposed by some authors that loss of sweating is more closely linked to glandular dysfunction than to autonomic neuropathy (Schiffmann and Scott, 2002). A more recent paper did demonstrate a reduction in sweat gland innervation in Anderson-Fabry patients compared with controls (Liguori et al., 2010). My findings confirm that there is reduced cutaneous autonomic innervation in Anderson-Fabry disease, suggesting that reduced sweat production is likely due to a combination of reduced innervation and direct damage to sweat glands.

Proximal and distal IENFD inversely correlated with the sum of the three pain-defining VAS scores, and proximal IENFD with current VAS score. Reports of the association between IENFD and pain are varied, and most have small sample sizes. In a larger, mixed cohort, no association between intraepidermal nerve fibre density and pain was reported (Biegstraaten et al., 2012), however the neuropathy in this group appears to be milder (particularly in the female patients) than in my cohort, as there is less marked abnormality in quantitative sensory testing parameters. Two studies in female heterozygotes did find an

association between the severity of intraepidermal nerve fibre loss and pain scores (Torvin Möller et al., 2009, Laaksonen et al., 2008).

The effect of age of IENFD is hard to control in small studies, but may be a factor, as IENFD declines with age. The decline from the 3rd to the 7th decade at the ankle is from a median of 11.2 to 7.9 in women, and from 9.0 to 6.3 in men (Bakkers et al., 2009). This is a potential confounder given the Anderson-Fabry patients in this study were slightly older than the normal controls. However, in my cohort, the presence of Anderson-Fabry disease was a greater determinant of distal IENFD than age, although there was a trend to reduced distal IENFD in older subjects in the normal control group.

In addition to reduced innervation, there were frequent morphological abnormalities seen in Anderson-Fabry patients, including focal swellings, general dilatation and beading. These would warrant further study, to determine if they arise from mechanical obstruction due to G3b deposition, or to failure of axonal transport due to an energy deficit, such as mitochondrial failure. Recent work has suggested that mitochondrial loss and morphological change may predate degeneration of epidermal fibres in small fibre neuropathy (Choi et al., 2015). It would be useful to investigate these further with specific markers for mitochondria, lysosomes and G3b to determine their significance.

2. Langerhans' cells.

Linear density of Langerhans cells was significantly reduced at the calf in Anderson-Fabry patients compared to controls (p=0.035) with a non-significant trend to reduced density at the thigh. Langerhans cells were also

morphologically abnormal in the Anderson-Fabry patients. Of interest, there was a trend to higher numbers of Langerhans cells relative to remaining intraepidermal nerve fibres in Anderson-Fabry patients with pain compared to those without significant pain. This trend was present at both the proximal and distal sites, but separation was more pronounced distally. There is a slight increase in this ratio in the Anderson-Fabry patients compared with controls, but the increase in the ratio is far greater in those with pain. Whilst this may be partially explained by the trend to more severe neuropathy in those with pain, figures 19A and B indicate that this is not the only reason, as there are patients with elevated Langerhans cell numbers and relatively preserved IENFD in these plots. Langerhans cell changes in morphology and density would certainly bear further study in painful neuropathies, and the addition of markers of immune activation in Langerhans cells would be helpful to clarify the relevance of these preliminary findings.

A recent study in a diabetic mouse model found an increase in epidermal and subepidermal Langerhans' cells during the period in which the mice demonstrated allodynia, with Langerhans' cell numbers falling later in the disease course when the mice no longer demonstrated allodynia. This change was thought to be mediated by NGF-TrkA signaling to epidermal Langerhans cells, and from TNF-α positive subepidermal fibres to subepidermal immature Langerhans cells. The increase was abolished with an intrathecal p38 inhibitor, which also reduced mechanical allodynia and TNF-α expression in subepidermal fibres. This lead the authors to postulate a role for nerve-Langerhans' cell NGF signaling in the increase in Langerhans' cell numbers. No changes were seen in

the non-diabetic control mice (Dauch et al., 2013). Taken in conjunction with my findings of a trend to increased Langerhans cell numbers in subjects with pain, these findings support a role for Langerhans cell modulation of neuropathic pain, although the pathways require further study. It would be particularly interesting to determine whether Langerhans cells play a role in pain generation at particular points in the time course of neuropathy progression, as well as whether there are changes in markers of Langerhans cell activation, such as the shift to a more pro-inflammatory profile.

Limitations of the study:

Although every effort was made to match the patient and control groups, this was not completely possible, as the final Anderson-Fabry patient group did have a higher mean age than the controls, as well as a slight female preponderance. Unfortunately these factors could not be overcome, despite drawing the study population from two large metabolic units, and the normal controls from the University College London population. The normal controls were limited by the protocol requiring an entire day, which did restrict participation of those in full time employment, skewing the age demographic. This, combined with the small numbers in the study, means that the results must be interpreted with a degree of caution. The impact of analgesic use on the results also could not be controlled, and there were insufficient numbers to perform a reliable subgroup analysis to determine the effect this may have had on the results. It would also be interesting to compare patients receiving enzyme replacement therapy with treatment naïve subjects, but as all bar one subject was on treatment, this was not possible.

Conclusions

Anderson-Fabry patients have a small fibre neuropathy confirmed on morphological and functional studies, with a trend to a more severe neuropathy in those with pain. Cytokine profiles did not differ between patients and controls, with limited changes within the Anderson-Fabry population linked to pain, which were certainly insufficient to explain the painfulness of the neuropathy. The altered density and morphology of Langerhans cells in Anderson-Fabry patients is interesting, and warrants more detailed study, particularly with respect to the possible link between changes in Langerhans cells and the painfulness of the neuropathy. It would be useful to either study a larger patient cohort that could be stratified by disease stage, or to study a group of individuals at different time points to determine whether immune factors play a key role at particular points in the evolution of the neuropathy. It would appear that it may be more helpful to design a study correlating pain experience with morphological examination of nerve fibre and Langerhans cell density, as well as immunohistochemical evaluation of markers of Langerhans cell activation, as well as keratinocyte immune profile, as it appears that cell-cell interactions may be a more sensitive way of examining possible mechanisms than quantification of overall tissue cytokine levels. Finally, emerging data suggests that G3b levels may have a direct effect on immune function in addition to its effect on nerve function, which would need to be accounted for in any further study of immune factors in the painfulness of neuropathy in Anderson-Fabry disease.

Chapter 6: Conclusions

1. The skin can be used to study pathogenic mechanisms

The study of dermal nerve fibres in patients with neuropathy and healthy controls confirmed that they can be a useful tool in the study of pathogenic mechanisms of some diseases. The ability to identify changes in transcription factors and proteins at varying time-points in disease will be a useful tool for future use. There are, however, limitations inherent in the translation of animal research to human studies. These arise in part due to the fact that animal studies are done largely in a monogenic , gender- and age-controlled population, whilst human studies generally include individuals of variable ages, genders, and medical co-morbidities. They may also have neuropathies at varying stages of disease process, which as was explored in Chapter 3, may impact on the molecular neuropathology expressed. Some of these factors can be overcome by careful subject selection, others may be overcome through longitudinal studies, which certainly is something that dermal and epidermal nerve biopsy techniques allow. Indeed, better understanding of how molecular pathways may alter as a neuropathic disease (such as CMT1A) progresses may be helpful in identifying optimal windows in the disease to target with particular therapeutic strategies.

2. Acute activation of nociceptors is insufficient to provoke a specific inflammatory response within 3 hours.

Acute activation of TRPV1 nociceptors did not result in significant changes in cutaneous cytokine profile. This may indicate that the pro-inflammatory profile in painful neuropathy observed in some studies of painful human neuropathy is dependent upon other factors, such as cellular damage signals (DAMPs), immune cell recruitment or activation, or the subtypes of nerve fibres involved in the disease process (eg non-peptidergic versus peptidergic fibres). The relative role of peptidergic and non-peptidergic fibres need further exploration in human neuropathy, as although the majority of epidermal nerve fibres are non-peptidergic, they appear to have been the focus of less specific research, possibly in part due to greater difficulties in identifying this subgroup immunohistochemically due to cross-reactivity with markers such as IB4 with keratinocytes. Longer duration studies of the immune effect of nociceptor activation on immune profile would be of interest. These would allow exploration of whether a neurogenic stimulus without nerve damage would, over time, be sufficient to alter skin immune cell function (such as Langerhans' cells, keratinocyte activation and immune cell recruitment), and whether these changes altered perceived pain. Ideally a combination of assessment of soluble mediators and skin immunohistochemistry would help answer this question. The limitations would be on devising a model that would be tolerated by the research subjects.

My findings suggest that models of neuropathic pain which utilise application of topical agents or electrical currents, but do not induce nerve damage may not

accurately reflect the tissue responses, and pathogenic mechanisms in painful neuropathies. This reflects the ongoing difficulties in developing human neuropathic pain models (Schmelz, 2009).

3. Pain in Anderson-Fabry correlates with some pro-inflammatory cytokines, and may be associated with increased Langerhans cells relative to innervation density.

There was a trend towards a more severe neuropathy in patients with pain in Anderson-Fabry disease. Despite the lack of statistically significant differences in cytokine profile between the subgroups of Anderson-Fabry patients with and without pain, there were moderate correlations seen between measures of pain and levels of the pro-inflammatory cytokines IL-6, MCP-1, RANTES and TNF-α. IL-6, MCP-1 and RANTES. It is likely that the small sample size may have been a factor in the lack of statistically significant outcomes, particularly given the range of ages and severity of denervation seen. The fact that the correlation analysis does consistently link inflammatory cytokines with pain, rather than a mix of pro- and anti-inflammatory cytokines as may be expected in a truly chance finding also suggests there may be a true link.

The most interesting aspect of this part of the study was the clear trend to increased numbers of Langerhans cells relative to nerve fibres in patients with pain. As Langerhans cells are important immunomodulatory cells with close contacts to epidermal nerves, and studies have shown modulation of their function by these contacts, it would be reasonable to hypothesise that they may well play a role in regulation of nociceptor function also. The clear proximal-

distal gradient seen in the patient, but not healthy control cohort supports other recent animal studies suggesting neuropathy may affect Langerhans' cell density (Dauch et al., 2013, Siau et al., 2006, Bertelsen et al., 2013). The trend to higher LC numbers relative to remaining IENFD suggests that Langerhans' cells may indeed play a role in the modulation of the painfulness of a neuropathy, and is an area that would be very interesting to explore further. Ideally, any further study would examine markers of activation rather than just morphology and linear density, as well as fibre subtypes, as the peptidergic fibres are the ones implicated in maintenance of their tolerogenic phenotype.

Conclusion and future directions:

In summary, this project has demonstrated the utility of the skin as a tool to examine neuropathic mechanisms in neuropathy, confirmed that acute nociceptor activation is insufficient to provoke immune changes in the skin, and opened a new and interesting area of study exploring potential interaction between immune cells and neurons in the skin, particularly the role of Langerhans' cells. Utilising a combination of immunohistochemistry to explore intracellular molecular pathways, dermal microdialysis and ELISA to quantitate small amounts of extracellular proteins of interest and correlation with clinical and neurophysiological phenotype may be useful tools to better understand the complex interplay between disease and host factors in neuropathy, and how best to modulate these to optimize patient outcomes. Markers of inflammation, dedifferentiation, redifferentiation and apoptosis may be useful endpoints in clinical trials.

There are two main sets of limitations of these and possible future studies:

1. The difficulties in controlling for a possibly wide range of interindividual variability across complex molecular pathways, many of which exhibit significant degrees of interaction and redundancy; and
2. The difficulties in standardizing the point of assessment along the continuum of neuropathy progression, as it is likely that pathogenic mechanisms are not constant over time. For example earlier in the disease there may be more evidence of attempts at regeneration, possibly with more inflammation (either as part of the pathogenesis or as part of the repair response), and later apoptosis and clearing of cellular debris as attempts at repair fail. Similarly, mechanisms in the generation of pain may alter between the earlier phases of a painful neuropathy, when molecular changes in the peripheral nerve leading to peripheral nociceptor hyperexcitability and sensitisation may be more important, and later stages when factors such as dorsal horn hyperexcitability leading to central sensitisation and indeed cortical remodeling may play a greater role.

References

ALBERS, K. M., WRIGHT, D. E. & DAVIS, B. M. 1994. Overexpression of nerve growth factor in epidermis of transgenic mice causes hypertrophy of the peripheral nervous system. *The Journal of Neuroscience,* 14**,** 1422-1432.

ANAND, P. & BLEY, K. 2011. Topical capsaicin for pain management: therapeutic potential and mechanisms of action of the new high-concentration capsaicin 8% patch. *British Journal of Anaesthesia,* 107**,** 490-502.

ANDERSON, C., ANDERSSON, T. & WARDELL, K. 1994. Changes in skin circulation after insertion of a microdialysis probe visualized by Laser-Doppler Perfusion Imaging. *Journal of Investigative Dermatology,* 102**,** 807-811.

ANSEL, J., BROWN, J., PAYAN, D. & BROWN, M. 1993. Substance P selectively activates TNF-alpha gene expression in murine mast cells. *The Journal of Immunology,* 150**,** 4478-4485.

AO, X. & STENKEN, J. A. 2006. Microdialysis sampling of cytokines. *Methods,* 38**,** 331-341.

ARMBRUSTER, D. A. & PRY, T. 2008. Limit of Blank, Limit of Detection and Limit of Quantitation. *The Clinical Biochemist: Reviews,* 49**,** S49-S52.

ARTHUR, R. P. & SHELLEY, W. B. 1959. The Innervation of Human Epidermis. *Journal of Investigative Dermatology,* 32**,** 397-411.

ARTHUR-FARRAJ, P., BHASKARAN, A., PARKINSON, D. B., TURMAINE, M., FELTRI, M. L., WRABETZ, L., BEHRENS, A., MIRSKY, R. & JESSEN, K. R. 2007. The transcription factor c-Jun controls Schwann cell demyelination and dedifferentiation after peripheral nerve injury. *Journal of Neuron and Glia Biology,* 3**,** S133.

ARTHUR-FARRAJ, P., LATOUCHE, M., WILTON, D. K., QUINTES, S., CHABROL, E., BANERJEE, A., WOODHOO, A., JENKINS, B., RAHMAN, M., TURMAINE, M., WICHER, G. K., MITTER, R., GREENSMITH, L., BEHRENS, A., RAIVICH, G., MIRSKY, R. & JESSEN, K. R. 2012. c-Jun Reprograms Schwann Cells of Injured Nerves to Generate a Repair Cell Essential for Regeneration. *Neuron,* 75**,** 633-647.

ASAHINA, A., HOSOI, J., BEISSERT, S., STRATIGOS, A. & GRANSTEIN, R. 1995. Inhibition of the induction of delayed-type and contact hypersensitivity by calcitonin gene-related peptide. *The Journal of Immunology,* 154**,** 3056-3061.

ATHERTON, D. D., FACER, P., ROBERTS, K. M., MISRA, V. P., CHIZH, B. A., BOUNTRA, C. & ANAND, P. 2007. Use of the novel contact heat evoked potential stimulator (CHEPS) for the assessment of small fibre neuropathy: correlations with skin flare responses and intra-epidermal nerve fibre counts. *BMC Neurology,* 7.

AVERBECK, M., BEILHARZ, S., BAUER, M., GEBHARDT, C., HARTMANN, A., HOCHLEITNER, K., KAUER, F., VOITH, U., SIMON, J. C. & TERMEER, C. 2006. In situ profiling and quantification of cytokines released during

ultraviolet B-induced inflammation by combining dermal microdialysis and protein microarrays. *Experimental Dermatology,* 15**,** 447-454.

AVERILL, S., MCMAHON, S. B., CLARY, D. O., REICHARDT, L. F. & PRIESTLEY, J. V. 1995. Immunocytochemical Localization of trkA Receptors in Chemically Identified Subgroups of Adult Rat Sensory Neurons. *European Journal of Neuroscience,* 7**,** 1484-1494.

BAKKERS, M., MERKIES, I. S. J., LAURIA, G., DEVIGILI, G., PENZA, P., LOMBARDI, R., HERMANS, M. C. E., VAN NES, S. I., DE BAETS, M. & FABER, C. G. 2009. Intraepidermal nerve fiber density and its application in sarcoidosis. *Neurology,* 73**,** 1142-1148.

BARCLAY, J., PATEL, S., DORN, G., WOTHERSPOON, G., MOFFATT, S., EUNSON, L., ABDEL'AL, S., NATT, F., HALL, J., WINTER, J., BEVAN, S., WISHART, W., FOX, A. & GANJU, P. 2002. Functional downregulation of P2X3 receptor subunit in rat sensory neurons reveals a significant role in chronic neuropathic and inflammatory pain. *The Journal of Neuroscience,* 22**,** 8139-8147.

BASBAUM, A. I. & BRÀZ, J. M. 2010. Transgenic mouse models for the tracing of "pain" pathways. *In:* KRUGER, L. & LIGHT, A. R. (eds.) *Translational pain research: from mouse to man.* Boca Raton: CRC Press.

BASCHANT, U. & TUCKERMANN, J. 2010. The role of the glucocorticoid receptor in inflammation and immunity. *Journal of Steroid Biochemistry and Molecular Biology,* 120**,** 69-75.

BENNETT, D. L. H. 2001. Neurotrophic Factors: Important regulators of nociceptive function. *The Neuroscientist,* 7**,** 13-17.

BENNETT, D. L. H., AVERILL, S., CLARY, D. O., PRIESTLEY, J. V. & MCMAHON, S. B. 1996. Postnatal changes in the expression of the trkA high-affinity NGF receptor in primary sensory neurons. *European Journal of Neuroscience,* 8**,** 2204-2208.

BENNETT, G., AL-RASHED, S., HOULT, J. R. S. & BRAIN, S. D. 1998. Nerve growth factor induced hyperalgesia in the rat hind paw is dependent on circulating neutrophils. *Pain,* 77**,** 315-322.

BERESFORD, L., ORANGE, O., BELL, E. B. & MIYAN, J. A. 2004. Nerve fibres are required to evoke a contact sensitivity response in mice. *Immunology,* 111**,** 118-125.

BERTELSEN, A. K., TÖNDEL, C., KROHN, J., BULL, N., AARSETH, J., HOUGE, G., MELLGREN, S. I. & VEDELER, C. A. 2013. Small fibre neuropathy in Fabry disease. *Journal of Neurology,* 260**,** 917-919.

BHANGOO, S., REN, D., MILLER, R. J., HENRY, K. J., LINESWALA, J., HAMDOUCHI, C., LI, B., MONAHAN, P. E., CHAN, D. M., RIPSCH, M. S. & WHITE, F. A. 2007. Delayed functional expression of neuronal chemokine receptors following focal nerve demyelination in the rat: a mechanism for the development of chronic sensitization of peripheral nociceptors. *Molecular Pain,* 3**,** 38.

BIANCINI, G. B., VANZIN, C. S., RODRIGUES, D. B., DEON, M., RIBAS, G. S., BARSCHAK, A. A. G., MANFREDINI, V., NETTO, C. B. O., JARDIM, L. B., GIUGLIANI, R. & VARGAS, C. R. 2012. Globotriaosylceramide is correlated with oxidative stress and inflammation in Fabry patients treated with

enzyme replacement therapy. *Biochimica et Biophysica Acta (BBA) - Molecular Basis of Disease,* 1822**,** 226-232.

BIEGSTRAATEN, M., BINDERL, A., MAAGL, R., HOLLAKL, C. E. M., BARONL, R. & VAN SCHAIKL, I. N. 2011. The relation between small nerve fibre function, age, disease severity and pain in Fabry disease. *European Journal of Pain,* 15**,** 822-829.

BIEGSTRAATEN, M., HOLLAK, C. E. M., BAKKERS, M., FABER, C. G., AERTS, J. M. F. G. & VAN SCHAIK, I. N. 2012. Small fiber neuropathy in Fabry disease. *Molecular Genetics and Metabolism,* 106**,** 135-141.

BINDER, A., MAY, D., BARON, R., MAIER, C., TÖLLE, T. R., TREEDE, R.-D., BERTHELE, A., FALTRACO, F., FLOR, H., GIERTHMÜHLEN, J., HAENISCH, S., HUGE, V., MAGERL, W., MAIHÖFNER, C., RICHTER, H., ROLKE, R., SCHERENS, A., ÜÇEYLER, N., UFER, M., WASNER, G., ZHU, J. & CASCORBI, I. 2011. Transient Receptor Potential Channel polymorphisms are associated with the somatosensory function in neuropathic pain Patients. *PLoS ONE,* 6**,** e17387.

BIO-RAD. 2012. *Bio-Plex Pro human cytokine, chemokine, and growth factor assays* [Online]. Available: http://www3.bio-rad.com/cmc_upload/Literature/222250/Bulletin_5828A.pdf [Accessed 16.1.12 2012].

BODO, E., KOVACS, I., TELEK, A., VARGA, A., PAUS, R., KOVACS, L. & BIRO, T. 2004. Vanilloid receptor-1 (VR1) is widely expressed on various epithelial and mesenchymal cell types of human skin. *Journal of Investigative Dermatology,* 123**,** 410-413.

BOLTON, C. F., WINKELMANN, R. K. & DYCK, P. J. 1966. A quantitative study of Meissners corpuscles in man. *Neurology,* 16**,** 1-9.

BOS, J. D. 2004. *Skin Immune System: Cutaneous immunology and clinical immunodermatology,* New York, CRC Press.

BOTCHKAREV, V. A., EICHMÖLLER, S., PETERS, E. M. J., PIETSCH, P., JOHANSSON, O., MAURER, M. & PAUS, R. 1997. A simple immunofluorescence technique for simultaneous visualization of mast cells and nerve fibers reveals selectivity and hair cycle ‚Äì dependent changes in mast cell ‚Äì nerve fiber contacts in murine skin. *Archives of Dermatological Research,* 289**,** 292-302.

BOUHASSIRA, D., ATTAL, N., FERMANIAN, J., ALCHAAR, H., GAUTRON, M., MASQUELIER, E., ROSTAING, S., LANTERI-MINET, M., COLLIN, E., GRISART, J. & BOUREAU, F. 2004. Development and validation of the neuropathic pain symptom inventory. *Pain,* 108**,** 248-257.

BOULAIS, N. & MISERY, L. 2008. The epidermis: a sensory tissue. *European Journal of Dermatology,* 18**,** 119-127.

BOWLES, W. R., SABINO, M. Ä., HARDING-ROSE, C. & HARGREAVES, K. M. 2006. Chronic nerve growth factor administration increases the peripheral exocytotic activity of capsaicin-sensitive cutaneous neurons. *Neuroscience Letters,* 403**,** 305-308.

BRADBURY, E. J., BURNSTOCK, G. & MCMAHON, S. B. 1998. The expression of P2X3 purinoreceptors in sensory neurons: effects of axotomy and glial-

derived neurotrophic factor. *Molecular and Cellular Neuroscience,* 12**,** 256-268.
BRENNAN, K. M., BAI, Y. & SHY, M. E. 2015. Demyelinating CMT: what's known, what's new and what's in store? *Neuroscience Letters,* 596**,** 14-26.
BURLINA, A. P., SIMS, K. B., POLITEI, J. M., BENNETT, G. J., BARON, R., SOMMER, C., MOLLER, A. T. & HILZ, M. J. 2011. Early diagnosis of peripheral nervous system involvement in Fabry disease and treatment of neuropathic pain: the report of an expert panel. *BMC Neurology,* 11**,** 61.
BURNSTOCK, G. 2012. Purinergic signalling in healthy and diseased skin. *Journal of Investigative Dermatology,* 132**,** 526-546.
CABLE, W. J., KOLODNY, E. H. & ADAMS, R. D. 1982a. Fabry disease: impaired autonomic function. *Neurology,* 32**,** 498-502.
CABLE, W. J. L., DVORAK, A. M., OSAGE, J. E. & KOLODNY, E. H. 1982b. Fabry disease: significance of ultrastructural localisation of lipid inclusions in dermal nerves. *Neurology,* 32**,** 347-353.
CAMPBELL, J. N. & LAMOTTE, R. H. 1983. Latency to detection of first pain. *Brain Research,* 266**,** 203-208.
CAMPERO, M. & BOSTOCK, H. 2010. Unmyelinated afferents in human skin and their responsiveness to low temperature. *Neuroscience Letters,* 470**,** 188-192.
CAMPRUBÍ-ROBLES, M., PLANELLS-CASES, R. & FERRER-MONTIEL, A. 2009. Differential contribution of SNARE-dependent exocytosis to inflammatory potentiation of TRPV1 in nociceptors. *The FASEB Journal,* 23**,** 3722-3733.
CASANOVA-MOLLA, J., MORALES, M., PLANAS-RIGOL, E., BOSCH, A., CALVO, M., GRAU-JUNYENT, J. M. & JOSEP, V.-S. 2012. Epidermal Langerhans cells in small fiber neuropathies. *Pain,* 153**,** 982-989.
CASTANEDA, J., LIM, M., COOPER, J. & PEARCE, D. 2008. Immune system irregularities in lysosomal storage disorders. *Acta Neuropathologica,* 115**,** 159-174.
CATERINA, M. J. & JULIUS, D. 2001. The vanilloid receptor: A molecular gateway to the pain pathway. *Annual Review of Neuroscience,* 24**,** 487-517.
CATERINA, M. J., SCHUMACHER, M. A., TOMINAGA, M., ROSEN, T. A., LEVINE, J. D. & JULIUS, D. 1997. The capsaicin receptor: a heat-activated ion channel in the pain pathway1. *Nature,* 389**,** 816-824.
CAVANAUGH, D. J., CHESLER, A. T., JACKSON, A. C., SIGAL, Y. M., YAMANAKA, H., GRANT, R., O'DONNELL, D., NICOLL, R. A., SHAH, N. M., JULIUS, D. & BASBAUM, A. I. 2011. TRPV1 reporter mice reveal highly restricted brain distribution and functional expression in arteriolar smooth muscle cells. *The Journal of Neuroscience,* 31**,** 5067-5077.
CHAO, C. C., HSIEH, S. T., CHIU, M. J., TSENG, M. T. & CHANG, Y. C. 2007. Effects of aging on contact heat-evoked potentials: The physiological assessment of thermal perception. *Muscle & Nerve,* 36**,** 30-38.
CHAPMAN, B. P. & MOYNIHAN, J. 2009. The brain-skin connection: role of psychosocial factors and neuropeptides in psoriasis. *Expert Review of Clinical Immunology,* 5**,** 623-627.

CHOI, L., VERNON, J., KOPACH, O., MINETT, M. S., MILLS, K., CLAYTON, P. T., MEERT, T. & WOOD, J. N. 2015. The Fabry disease-associated lipid Lyso-Gb3 enhances voltage-gated calcium currents in sensory neurons and causes pain. *Neuroscience Letters,* 594**,** 163-168.

CHORRO, L. & GEISSMANN, F. 2010. Development and homeostasis of 'resident' myeloid cells: the case of the Langerhans cell. *Trends in Immunology,* 31**,** 438-445.

CLAPHAM, D. E., RUNNELS, L. W. & STRUBING, C. 2001. The trp ion channel family. *Nature Reviews Neuroscience,* 2**,** 387-396.

COCCHIARA, R., LAMPIASI, N., ALBEGGIANI, G., BONGIOVANNI, A., AZZOLINA, A. & GERACI, D. 1999. Mast cell production of TNF-alpha induced by substance P evidence for a modulatory role of substance P-antagonists. *Journal of Neuroimmunology,* 101**,** 128-136.

CUMBERBATCH, M., GRIFFITHS, C. E. M., TUCKER, S. C., DEARMAN, R. J. & KIMBER, I. 1999. Tumour necrosis factor-alpha induces Langerhans cell migration in humans. *British Journal of Dermatology,* 141**,** 192-200.

CZESCHIK, J. C., HAGENACKER, T., SCHAFERS, M. & BUSSELBERG, D. 2008. TNF-alpha differentially modulates ion channels of nociceptive neurons. *Neuroscience Letters,* 434**,** 293-298.

DA SILVA, L., CARVALHO, E. & CRUZ, M. T. 2010. Role of neuropeptides in skin inflammation and its involvement in diabetic wound healing. *Expert Opinion on Biological Therapy,* 10**,** 1427-1439.

DALLOS, A., KISS, M., POLYANKA, H., DOBOZY, A., KEMENY, L. & HUSZ, S. 2006. Effects of the neuropeptides substance P, calcitonin gene-related peptide, vasoactive intestinal polypeptide and galanin on the production of nerve growth factor and inflammatory cytokines in cultured human keratinocytes. *Neuropeptides,* 40**,** 251-263.

DAUCH, J. R., BENDER, D. E., LUNA-WONG, L. A. A., HSIEH, W., YANIK, B. M., KELLY, Z. A. & CHENG, H. T. 2013. Neurogenic factor-induced Langerhans cell activation in diabetic mice with mechanical allodynia. *Journal of Neuroinflammation,* 10**,** 64-64.

DE FRANCESCO, P. N., MUCCI, J. M., CECI, R., FOSSATI, C. A. & ROZENFELD, P. A. Fabry disease peripheral blood immune cells release inflammatory cytokines: Role of globotriaosylceramide. *Molecular Genetics and Metabolism,* 109**,** 93-99.

DE FRANCESCO, P. N., MUCCI, J. M., CECI, R., FOSSATI, C. A. & ROZENFELD, P. A. 2013. Fabry disease peripheral blood immune cells release inflammatory cytokines: Role of globotriaosylceramide. *Molecular Genetics and Metabolism,* 109**,** 93-99.

DELGADO, A. V., MCMANUS, A. T. & CHAMBERS, J. P. 2005. Exogenous Administration of Substance P Enhances Wound Healing in a Novel Skin-Injury Model. *Experimental Biology and Medicine,* 230**,** 271-280.

DENDA, S., DENDA, M., INOUE, K. & HIBINO, T. 2010. Glycolic acid induces keratinocyte proliferation in a skin equivalent model via TRPV1 activation. *Journal of Dermatological Science,* 57**,** 108-113.

DENG, L., DING, W. H. & GRANSTEIN, R. D. 2003. Thalidomide inhibits tumor necrosis factor-alpha production and antigen presentation by Langerhans cells. *Journal of Investigative Dermatology,* 121**,** 1060-1065.

DIAMOND, J., HOLMES, M. & COUGHLIN, M. 1992. Endogenous NGF and nerve impulses regulate the collateral sprouting of sensory axons in the skin of the adult rat. *The Journal of Neuroscience,* 12**,** 1454-1466.

DINARELLO, C. A. 2009. Immunological and Inflammatory Functions of the Interleukin-1 Family. *Annual Review of Immunology,* 27**,** 519-550.

DING, W., WAGNER, J. A. & GRANSTEIN, R. D. 2007. CGRP, PACAP, and VIP modulate Langerhans cell function by inhibiting NF-kappaB activation. *Journal of Investigative Dermatology,* 127**,** 2357-2367.

DING, W. H., STOHL, L. L., WAGNER, J. A. & GRANSTEIN, R. D. 2008. Calcitonin gene-related peptide biases Langerhans cells toward Th2-type immunity. *Journal of Immunology,* 181**,** 6020-6026.

DOCHERTY, R., YEATS, J., BEVAN, S. & BODDEKE, H. 1996. Inhibition of calcineurin inhibits the desensitization of capsaicin-evoked currents in cultured dorsal root ganglion neurones from adult rats. *Pflügers Archiv European Journal of Physiology,* 431**,** 828-837.

DOSS, A. L. N. & SMITH, P. G. 2014. Langerhans cells regulate cutaneous innervation density and mechanical sensitivity in mouse footpad. *Neuroscience Letters,* 0**,** 55-60.

DOUGLAS, S. D. & LEEMAN, S. E. 2011. Neurokinin-1 receptor: functional significance in the immune system in reference to selected infections and inflammation. *Annals of the New York Academy of Sciences,* 1217**,** 83-95.

DUSSOR, G., KOERBER, H. R., OAKLANDER, A. L., RICE, F. L. & MOLLIVER, D. C. 2009. Nucleotide signaling and cutaneous mechanisms of pain transduction. *Brain Research Reviews,* 60**,** 24-35.

DÜTSCH, M., MARTHOL, H., STEMPER, B., BRYS, M., HAENDL, T. & HILZ, M. J. 2002. Small fibre dysfunction predominates in Fabry neuropathy. *Journal of Clinical Neurophysiology,* 19**,** 575-586.

EBENEZER, G. J., MCARTHUR, J. C., THOMAS, D., MURINSON, B., HAUER, P., POLYDEFKIS, M. & GRIFFIN, J. W. 2007. Denervation of skin in neuropathies: the sequence of axonal and Schwann cell changes in skin biopsies. *Brain,* 130**,** 2703-2714.

ELSHAL, M. F. & MCCOY, J. P. 2006. Multiplex bead array assays: Performance evaluation and comparison of sensitivity to ELISA. *Methods,* 38**,** 317-323.

ESSEX, T. J. H. & BYRNE, P. O. 1991. A laser Doppler scanner for imaging blood flow in skin. *Journal of Biomedical Engineering,* 13**,** 189-194.

FARTASCH, M., SUGAR, M., SCHNETZ, E., ESCHER, S. & SCHMELZ, M. 1997. Dynamic measurements of the perculatenous penetration of sodium lauryl sulphate by microdialysis. *Journal of Investigative Dermatology,* 109**,** 459.

FELDMEYER, L., WERNER, S., FRENCH, L. E. & BEER, H. D. 2010. Interleukin-1, inflammasomes and the skin. *European Journal of Cell Biology,* 89**,** 638-644.

FERRARI, D., LA SALA, A., CHIOZZI, P., MORELLI, A., FALZONI, S., GIROLOMONI, G., IDZKO, M., DICHMANN, S., NORGAUER, J. & DI VIRGILIO, F. 2000. The P2 purinergic receptors of human dendritic cells: identification and coupling to cytokine release. *The FASEB Journal,* 14**,** 2466-2476.

FERRARIS, S. E., ISONIEMI, K., TORVALDSON, E., ANCKAR, J., WESTERMARCK, J. & ERIKSSON, J. E. 2012. Nucleolar AATF regulates c-Jun-mediated apoptosis. *Molecular Biology of the Cell,* 23**,** 4323-4332.

FERREIRA, S. H., LORENZETTI, B. B., BRISTOW, A. F. & POOLE, S. 1988. Interleukin-1 beta as a potent hyperalgesic agent antagonized by a tripeptide analogue. *Nature,* 334**,** 698-700.

FINDLAY, J. W. A. & DILLARD, R. F. 2007. Appropriate calibratioin curve fitting in ligand binding assays. *Aaps Journal,* 9**,** 260-267.

FINDLAY, J. W. A., SMITH, W. C., LEE, J. W., NORDBLOM, G. D., DAS, I., DESILVA, B. S., KHAN, M. N. & BOWSHER, R. R. 2000. Validation of immunoassays for bioanalysis: a pharmaceutical industry perspective. *Journal of Pharmaceutical and Biomedical Analysis,* 21**,** 1249-1273.

FLATTERS, S. J. L., FOX, A. J. & DICKENSON, A. H. 2004. Nerve injury alters the effects of interleukin-6 on nociceptive transmission in peripheral afferents. *European Journal of Pharmacology,* 484**,** 183-191.

FOLLENFANT, R. L., NAKAMURA-CRAIG, M., HENDERSON, B. & HIGGS, G. A. 1989. Inhibition by neuropeptides of interleukin-1 beta-induced, prostaglandin-independent hyperalgesia. *British Journal of Pharmacology,* 98**,** 41-43.

FOREMAN, J. C., JORDAN, C. C., OEHME, P. & RENNER, H. 1983. Structure-activity relationships for some substance P-related peptides that cause wheal and flare reactions in human skin. *The Journal of Physiology,* 335**,** 449-465.

FUJITA, H., ASAHINA, A., GAO, P., FUJIWARA, H. & TAMAKI, K. 2004. Expression and Regulation of RANTES/CCL5, MIP-1alpha/CCL3, and MIP-1beta/CCL4 in Mouse Langerhans Cells. *Journal of Investigative Dermatology,* 122**,** 1331-1333.

FUKUHARA, N., SUZUKI, M., FUJITA, N. & TSUBAKI, T. 1975. Fabry's disease on the mechanism of the peripheral nerve involvement. *Acta Neuropathologica,* 33**,** 9-21.

FUKUOKA, H., KAWATANI, M., HISAMITSU, T. & TAKESHIGE, C. 1994. Cutaneous hyperalgesia induced by peripheral injection of interleukin-1-beta in the rat. *Brain Research,* 657**,** 133-140.

GALLUCCI, R. M., SIMEONOVA, P. P., MATHESON, J. M., KOMMINENI, C., GURIEL, J. L., SUGAWARA, T. & LUSTER, M. I. 2000. Impaired cutaneous wound healing in interleukin-6-deficient and immunosuppressed mice. *The FASEB Journal,* 14**,** 2525-2531.

GARCÍA-SANZ, N., FERNÁNDEZ-CARVAJAL, A., MORENILLA-PALAO, C., PLANELLS-CASES, R., FAJARDO-SÁNCHEZ, E., FERNÁNDEZ-BALLESTER, G. & FERRER-MONTIEL, A. 2004. Identification of a tetramerization domain in the C terminus of the Vanilloid receptor. *The Journal of Neuroscience,* 24**,** 5307-5314.

GARDNER, E. P. & MARTIN, J. H. 2000. Coding of sensory information. *In:* KANDEL, E. R., SCHWARTZ, J. H. & JESSELL, T. M. (eds.) *Principles of neural science.* 4 ed. New York: McGraw-Hill.

GAUDILLERE, A., MISERY, L., SOUCHEIR, C., CLAUDY, A. & SCHMITT, D. 1996. Intimate associations between PGP9-5-positive nerve fibres and Langerhans cells. *British Journal of Dermatology,* 135**,** 343-344.

GEEVASINGA, N., TCHAN, M., SILLENCE, D. & VUCIC, S. 2012. Upregulation of inward rectifying currents and Fabry disease neuropathy. *Journal of the Peripheral Nervous System,* 17**,** 399-406.

GILLITZER, R. & GOEBELER, M. 2001. Chemokines in cutaneous wound healing. *Journal of Leukocyte Biology,* 69**,** 513-521.

GIUSTIZIERI, M. L., MASCIA, F., FREZZOLINI, A., DE PITѵ†, O., CHINNI, L. M., GIANNETTI, A., GIROLOMONI, G. & PASTORE, S. 2001. Keratinocytes from patients with atopic dermatitis and psoriasis show a distinct chemokine production profile in response to T cell-derived cytokines. *The Journal of allergy and clinical immunology,* 107**,** 871-877.

GOODNESS, T. P., ALBERS, K. M., DAVIS, F. E. & DAVIS, B. M. 1997. Overexpression of nerve growth factor in skin increases sensory neuron size and modulates Trk receptor expression. *European Journal of Neuroscience,* 9**,** 1574-1585.

GORMAN, S., JUDGE, M. A. & HART, P. H. 2010a. Immune-modifying properties of topical vitamin D: focus on dendritic cells and T-cells. *Journal of Steroid Biochemistry & Molecular Biology,* 121**,** 247-249.

GORMAN, S., JUDGE, M. A. & HART, P. H. 2010b. Topical 1,25-dihydroxyvitamin D(3) subverts the priming ability of draining lymph node dendritic cells. *Immunology*.

GOTTSCHALK, P. G. & DUNN, J. R. 2005. The five-parameter logistic: A characterization and comparison with the four-parameter logistic. *Analytical Biochemistry,* 343**,** 54-65.

GOYARTS, E., MATSUI, M., MAMMONE, T., BENDER, A. M., WAGNER, J. A., MAES, D. & GRANSTEIN, R. D. 2008. Norepinephrine modulates human dendritic cell activation by altering cytokine release. *Experimental Dermatology,* 17**,** 188-196.

GROTH, L. & SERUP, J. 1998. Cutaneous microdialysis in man: Effects of needle insertion trauma and anaesthesia on skin perfusion, erythema and skin thickness. *Acta Dermato-Venereologica,* 78**,** 5-9.

GSCHWANDTNER, M., ROSSBACH, K., DIJKSTRA, D., BAUMER, W., KIETZMANN, M., STARK, H., WERFEL, T. & GUTZMER, R. 2010. Murine and human Langerhans cells express a functional histamine H-4 receptor: modulation of cell migration and function. *Allergy,* 65**,** 840-849.

GUARDA, G. & SO, A. 2010. Regulation of inflammasome activity. *Immunology,* 130**,** 329-336.

HADDEN, R. D. M., NOBILE-ORAZIO, E., SOMMER, C., HAHN, A., ILLA, I., MORRA, E., POLLARD, J., HUGHES, R. A. C., BOUCHE, P., CORNBLATH, D., EVERS, E., KOSKI, C. L., LEGER, J. M., VAN DEN BERGH, P., VAN DOORN, P. & SCHAIK, I. N. 2006. European Federation of Neurological Societies Peripheral Nerve Society guideline on management of paraproteinaemic

demyelinating neuropathies: report of a joint task force of the European Federation of Neurological Societies and the Peripheral Nerve Society2. *European Journal of Neurology,* 13**,** 809-818.

HARVIMA, I. T., NILSSON, G. & NAUKKARINEN, A. 2010. Role of mast cells and sensory nerves in skin inflammation. *Giornale Italiano di Dermatologia e Venereologia,* 145**,** 195-204.

HENDRIX, S., PICKER, B., LIEZMANN, C. & PETERS, E. M. J. 2008. Skin and hair follicle innervation in experimental models: a guide for the exact and reproducible evaluation of neuronal plasticity. *Experimental Dermatology,* 17**,** 214-227.

HONORE, P., KAGE, K., MIKUSA, J., WATT, A. T., JOHNSTON, J. F., WYATT, J. R., FALTYNEK, C. R., JARVIS, M. F. & LYNCH, K. 2002. Analgesic profile of intrathecal P2X3 antisense oligonucleotide treatment in chronic inflammatory and neuropathic pain states in rats. *Pain,* 99**,** 11-19.

HOSOI, J., MURPHY, G. F., EGAN, C. L., LERNER, E. A., GRABBE, S., ASAHINA, A. & GRANSTEIN, R. D. 1993. Regulation of Langerhans cell-function by nerves Containing calcitonin gene-related peptide. *Nature,* 363**,** 159-163.

HOU, L., LI, W. & WANG, X. 2003. Mechanism of interleukin-1β-induced calcitonin gene-related peptide production from dorsal root ganglion neurons of neonatal rats. *Journal of Neuroscience Research,* 73**,** 188-197.

HSIEH, S. T., CHOI, S., LIN, W. M., CHANG, Y. C., MCARTHUR, J. C. & GRIFFIN, J. W. 1996. Epidermal denervation and its effects on keratinocytes and Langerhans cells. *Journal of Neurocytology,* 25**,** 513-524.

HUGHES, R. A. C. & CORNBLATH, D. R. 2005. Guillain-Barre syndrome. *Lancet,* 366**,** 1653-1666.

HUTTON, E. J., CARTY, L., LAURÁ, M., HOULDEN, H., LUNN, M. P. T., BRANDNER, S., MIRSKY, R., JESSEN, K. & REILLY, M. M. 2011. c-Jun expression in human neuropathies: a pilot study. *Journal of the Peripheral Nervous System,* 16**,** 295-303.

JARVIS, M. F., BURGARD, E. C., MCGARAUGHTY, S., HONORE, P., LYNCH, K., BRENNAN, T. J., SUBIETA, A., VAN BIESEN, T., CARTMELL, J., BIANCHI, B., NIFORATOS, W., KAGE, K., YU, H., MIKUSA, J., WISMER, C. T., ZHU, C. Z., CHU, K., LEE, C.-H., STEWART, A. O., POLAKOWSKI, J., COX, B. F., KOWALUK, E., WILLIAMS, M., SULLIVAN, J. & FALTYNEK, C. 2002. A-317491, a novel potent and selective non-nucleotide antagonist of P2X3 and P2X2/3 receptors, reduces chronic inflammatory and neuropathic pain in the rat. *Proceedings of the National Academy of Sciences,* 99**,** 17179-17184.

JERATH, N. U. & SHY, M. E. 2015. Hereditary motor and sensory neuropathies: Understanding molecular pathogenesis could lead to future treatment strategies. *Biochimica et Biophysica Acta (BBA) - Molecular Basis of Disease,* 1852**,** 667-678.

JESSEN, K. R. & MIRSKY, R. 2008. Negative regulation of myelination: relevance for development, injury, and demyelinating disease. *Glia,* 56**,** 1552-1565.

JIN, X. & GEREAU, R. W. 2006. Acute p38-mediated modulation of tetrodotoxin-resistant sodium channels in mouse sensory neurons by tumor necrosis factor-alpha. *The Journal of Neuroscience,* 26**,** 246-255.

JOCHUM, W., PASSEGUE, E. & WAGNER, E. 2001. AP-1 in mouse development and tumorigenesis. *Oncogene,* 20**,** 2401-2412.

JOHNSON, M. S., RYALS, J. M. & WRIGHT, D. E. 2008. Early loss of peptidergic intraepidermal nerve fibers in an STZ-induced mouse model of insensate diabetic neuropathy. *Pain,* 140**,** 35-47.

KAMATA, H., HONDA, S.-I., MAEDA, S., CHANG, L., HIRATA, H. & KARIN, M. 2004. Reactive oxygen species promote TNFalpha-induced death and sustained JNK activation by inhibiting MAP kinase phosphatases. *Cell,* 120**,** 649-661.

KATONA, I., WU, X. Y., FEELY, S. M. E., SOTTILE, S., SISKIND, C. E., MILLER, L. J., SHY, M. E. & LI, J. 2009. PMP22 expression in dermal nerve myelin from patients with CMT1A. *Brain,* 132**,** 1734-1740.

KAYE, E. M., KOLODNY, E. H., LOGIGIAN, E. L. & ULLMAN, M. D. 1988. Nervous system involvement in Fabry's disease: Clinicopathological and biochemical correlation. *Annals of Neurology,* 23**,** 505-509.

KESWANI, S. C., POLLEY, M., PARDO, C. A., GRIFFIN, J. W., MCARTHUR, J. C. & HOKE, A. 2003. Schwann cell chemokine receptors mediate HIV-1 gp120 toxicity to sensory neurons. *Annals of Neurology,* 54**,** 287-296.

KIGUCHI, N., MAEDA, T., KOBAYASHI, Y., FUKAZAWA, Y. & KISHIOKA, S. 2010. Macrophage inflammatory protein-1alpha mediates the development of neuropathic pain following peripheral nerve injury through interleukin-1beta up-regulation. *Pain,* 149**,** 305-315.

KIM, A. Y., TANG, Z., LIU, Q., PATEL, K. N., MAAG, D., GENG, Y. & DONG, X. 2008. Pirt, a Phosphoinositide-Binding Protein, Functions as a Regulatory Subunit of TRPV1. *Cell,* 133**,** 475-485.

KIM, C. F. & MOALEM-TAYLOR, G. 2011. Interleukin-17 contributes to neuroinflammation and neuropathic pain following peripheral nerve injury in mice. *The Journal of Pain,* 12**,** 370-383.

KLEDE, M., HANDWERKER, H. O. & SCHMELZ, M. 2003. Central origin of secondary mechanical hyperalgesia. *Journal of Neurophysiology,* 90**,** 353-359.

KO, Y., LEE, C., MOON, M. H., HONG, G.-R., CHEON, C.-K. & LEE, J.-S. 2015. Unravelling the mechanism of action of enzyme replacement therapy in Fabry disease. *J Hum Genet*.

KOIZUMI, S., FUJISHITA, K., INOUE, K., SHIGEMOTO-MOGAMI, Y. & TSUDA, M. 2004. Ca2+ waves in keratinocytes are transmitted to sensory neurons: the involvement of extracellular ATP and P2Y2 receptor activation. *The Biochemical Journal,* 380**,** 329-338.

KOLTZENBURG, M., LUNDBERG, L. E. R. & TOREBJÖRK, H. E. 1992. Dynamic and static components of mechanical hyperalgesia in human hairy skin. *Pain,* 51**,** 207-219.

KORN, T., BETTELLI, E., OUKKA, M. & KUCHROO, V. K. 2009. IL-17 and Th17 Cells. *Annual Review of Immunology,* 27**,** 485-517.

KULKA, M., SHEEN, C. H., TANCOWNY, B. P., GRAMMER, L. C. & SCHLEIMER, R. P. 2008. Neuropeptides activate human mast cell degranulation and chemokine production. *Immunology,* 123**,** 398-410.

LAAKSONEN, S. M., ROYTTA, M., JAASKELAINEN, S. K., KANTOLA, I., PENTTINEN, M. & FALCK, B. 2008. Neuropathic symptoms and findings in women with Fabry disease. *Clinical Neurophysiology,* 119**,** 1365-1372.

LAKOMÁ, J., RIMONDINI, R., DONADIO, V., LIGUORI, R. & CAPRINI, M. 2014. Pain related channels are differentially expressed in neuronal and non-neuronal cells of glabrous skin of Fabry knockout male mice. *PLoS ONE,* 9**,** e108641.

LAMBRECHT, B. N. 2001. Immunologists getting nervous: neuropeptides, dendritic cells and T cell activation. *Respiratory Research,* 2**,** 133-138.

LANE, N. E., SCHNITZER, T. J., BIRBARA, C. A., MOKHTARANI, M., SHELTON, D. L., SMITH, M. D. & BROWN, M. T. 2010. Tanezumab for the treatment of pain from osteoarthritis of the knee. *New England Journal of Medicine,* 363**,** 1521-1531.

LAURIA, G. 2005. Small fibre neuropathies. *Current Opinion in Neurology,* 18**,** 591-597.

LAURIA, G., BORGNA, M., MORBIN, M., LOMBARDI, R., MAZZOLENI, G., SGHIRLANZONI, A. & PAREYSON, D. 2004. Tubule and neurofilament immunoreactivity in human hairy skin: Markers for intraepidermal nerve fibers. *Muscle & Nerve,* 30**,** 310-316.

LAURIA, G., LOMBARDI, R., BORGNA, M., PENZA, P., BIANCHI, R., SAVINO, C., CANTA, A., NICOLINI, G., MARMIROLI, P. & CAVALETTI, G. 2005. Intraepidermal nerve fiber density in rat foot pad: neuropathologic–neurophysiologic correlation. *Journal of the Peripheral Nervous System,* 10**,** 202-208.

LEDEBOER, A., JEKICH, B. M., SLOANE, E. M., MAHONEY, J. H., LANGER, S. J., MILLIGAN, E. D., MARTIN, D., MAIER, S. F., JOHNSON, K. W., LEINWAND, L. A., CHAVEZ, R. A. & WATKINS, L. R. 2007. Intrathecal interleukin-10 gene therapy attenuates paclitaxel-induced mechanical allodynia and proinflammatory cytokine expression in dorsal root ganglia in rats. *Brain, Behaviour and Immunity,* 21**,** 686-698.

LEVY, J. A. 2009. The unexpected pleiotropic activities of RANTES. *The Journal of Immunology,* 182**,** 3945-3946.

LEWIN, G. R., RUEFF, A. & MENDELL, L. M. 1994. Peripheral and central hechanisms of NGF-induced Hyperalgesia. *European Journal of Neuroscience,* 6**,** 1903-1912.

LEWIS, C., NEIDHART, S., HOLY, C., NORTH, R., BUELL, G. & SURPRENANT, A. 1995. Coexpression of P2X2 and P2X3 receptor subunits can account for ATP-gated currents in sensory neurons. *Nature,* 377**,** 432-435.

LI, J., BAI, Y. H., GHANDOUR, K., QIN, P., GRANDIS, M., TROSTINSKAIA, A., IANAKOVA, E., WU, X. Y., SCHENONE, A., VALLAT, J. M., KUPSKY, W. J., HATFIELD, J. & SHY, M. E. 2005. Skin biopsies in myelin-related neuropathies: bringing molecular pathology to the bedside. *Brain,* 128**,** 1168-1177.

LI, W. H., LEE, Y. M., KIM, J. Y., KANG, S., KIM, S., KIM, K. H., PARK, C. H. & CHUNG, J. H. 2007. Transient receptor potential vanilloid-1 mediates heat-shock-induced matrix metalloproteinase-1 expression in human

epidermal keratinocytes. *Journal of Investigative Dermatology,* 127**,** 2328-2335.

LIGUORI, R., DI STASI, V., BUGIARDINI, E., MIGNANI, R., BURLINA, A., BORSINI, W., BARUZZI, A., MONTAGNA, P. & DONADIO, V. 2010. Small fiber neuropathy in female patients with fabry disease. *Muscle & Nerve,* 41**,** 409-412.

LINDSAY, R. M. & HARMAR, A. J. 1989. Nerve growth factor regulates expression of neuropeptide genes in adult sensory neurons. *Nature,* 337**,** 362-364.

LISHKO, P. V., PROCKO, E., JIN, X., PHELPS, C. B. & GAUDET, R. 2007. The Ankyrin repeats of TRPV1 bind multiple ligands and modulate channel sensitivity. *Neuron,* 54**,** 905-918.

LIU, M., GUO, S., HIBBERT, J. M., JAIN, V., SINGH, N., WILSON, N. O. & STILES, J. K. 2011. CXCL10/IP-10 in infectious diseases pathogenesis and potential therapeutic implications. *Cytokine & Growth Factor Reviews,* 22**,** 121-130.

LUCIANO, C. A., RUSSELL, J. W., BANERJEE, T. K., QUIRK, J. M., SCOTT, L. J. C., DAMBROSIA, J. M., BARTON, N. W. & SCHIFFMANN, R. 2002. Physiological characterization of neuropathy in Fabry's disease. *Muscle & Nerve,* 26**,** 622-629.

LUMPKIN, E. A. & CATERINA, M. J. 2007. Mechanisms of sensory transduction in the skin. *Nature,* 445**,** 858-865.

LUNN, M. P. T. & WILLISON, H. J. 2009. Diagnosis and treatment in inflammatory neuropathies. *Journal of Neurology Neurosurgery and Psychiatry,* 80**,** 249-258.

LUTZ, M. B. & KURTS, C. 2009. Induction of peripheral CD4(+) T-cell tolerance and CD8(+) T-cell cross-tolerance by dendritic cells. *European Journal of Immunology,* 39**,** 2325-2330.

MACEDO, M. F., QUINTA, R., PEREIRA, C. S. & SA MIRANDA, M. C. 2012. Enzyme replacement therapy partially prevents invariant Natural Killer T cell deficiency in the Fabry disease mouse model. *Molecular Genetics and Metabolism,* 106**,** 83-91.

MAGGI, C. A. 1993. The pharmacological modulation of neurotransmitter release. *In:* WOOD, J. (ed.) *Capsaicin in the study of pain.* San Diego: Academic Press.

MANGANELLI, F., NOLANO, M., PISCIOTTA, C., PROVITERA, V., FABRIZI, G. M., CAVALLARO, T., STANCANELLI, A., CAPORASO, G., SHY, M. E. & SANTORO, L. 2015. Charcot-Marie Tooth disease: new insights from skin biopsy. *Neurology,* 85**,** 1202-1208.

MARRIOTT, I. & BOST, K. L. 2001. Expression of authentic substance P receptors in murine and human dendritic cells. *Journal of Neuroimmunology,* 114**,** 131-141.

MARTÍNEZ-MARTINEZ, E., TOSCANO-MÁRQUEZ, B. & GUTIÉRREZ-OSPINA, G. 2011. Long-term effects of neonatal capsaicin treatment on intraepidermal nerve fibers and keratinocyte proliferation in rat glabrous skin. *The Anatomical Record: Advances in Integrative Anatomy and Evolutionary Biology,* 294**,** 173-184.

MATAFORA, V., CUCCURULLO, M., BENEDUCI, A., PETRAZZUOLO, O., SIMEONE, A., ANASTASIO, P., MIGNANI, R., FERIOZZI, S., PISANI, A., COMOTTI, C., BACHI, A. & CAPASSO, G. 2015. Early markers of Fabry disease revealed by proteomics. *Molecular BioSystems,* 11**,** 1543-1551.

MATHERS, A. R., TCKACHEVA, O. A., JANELSINS, B. M., SHUFESKY, W. J., MORELLI, A. E. & LARREGINA, A. T. 2007. In vivo signaling through the neurokinin 1 receptor favors transgene expression by Langerhans cells and promotes the generation of Th1- and Tc1-biased immune responses. *Journal of Immunology,* 178**,** 7006-7017.

MAUHIN, W., LIDOVE, O., MASAT, E., MINGOZZI, F., MARIAMPILLAI, K., ZIZA, J.-M. & BENVENISTE, O. 2015. Innate and adaptive immune response in Fabry disease. *JIMD Reports,* 22**,** 1-10.

MAZZONI, A., SIRAGANIAN, R. P., LEIFER, C. A. & SEGAL, D. M. 2006. Dendritic cell modulation by mast cells controls the Th1/Th2 balance in responding T cells. *Journal of Immunology,* 177**,** 3577-3581.

MCARTHUR, J. C., STOCKS, E. A., HAUER, P., CORNBLATH, D. R. & GRIFFIN, J. W. 1998. Epidermal nerve fiber density - Normative reference range and diagnostic efficiency. *Archives of Neurology,* 55**,** 1513-1520.

MCCARTHY, B. G., HSIEH, S. T., STOCKS, A., HAUER, P., MACKO, C., CORNBLATH, D. R., GRIFFIN, J. W. & MCARTHUR, J. C. 1995. Cutaneous innervation in sensory neuropathies - evaluation by skin biopsy. *Neurology,* 45**,** 1848-1855.

MCGLONE, F. & REILLY, D. 2010. The cutaneous sensory system. *Neuroscience and Biobehavioral Reviews,* 34**,** 148-159.

MERAD, M., GINHOUX, F. & COLLIN, M. 2008. Origin, homeostasis and function of Langerhans cells and other langerin-expressing dendritic cells. *Nature Reviews Immunology,* 8**,** 935-947.

METZ, M. & MAURER, M. 2009. Innate immunity and allergy in the skin. *Current Opinion in Immunology,* 21**,** 687-693.

MEYER, R. & CAMPBELL, J. 1981. Myelinated nociceptive afferents account for the hyperalgesia that follows a burn to the hand. *Science,* 213**,** 1527-1529.

MEYER, R. A., RINGKAMP, M., CAMPBELL, J. N. & RAJA, S. N. 2006. Peripheral mechanisms of cutaneous nociception. *In:* MCMAHON, S. B. & KOLTZENBURG, M. (eds.) *Wall and Melzack's Textbook of pain.* 5 ed. London: Elsevier.

MILLIGAN, E. D., SLOANE, E. M., LANGER, S. J., HUGHES, T. S., JEKICH, B. M., FRANK, M. G., MAHONEY, J. H., LEVKOFF, L. H., MAIER, S. F., CRUZ, P. E., FLOTTE, T. R., JOHNSON, K. W., MAHONEY, M. M., CHAVEZ, R. A., LEINWAND, L. A. & WATKINS, L. R. 2006. Repeated intrathecal injections of plasmid DNA encoding interleukin-10 produce prolonged reversal of neuropathic pain. *Pain,* 126**,** 294-308.

MOLLIVER, D. C., IMMKE, D. C., FIERRO, M., PARÉ, M., RICE, F. L. & MCCLESKY, E. W. 2005. ASIC3, an acid-sensing ion channel, is expressed in metaboreceptive sensory neurons. *Molecular Pain,* 1**,** 35.

MOLLIVER, D. C., RADEKE, M. J., FEINSTEIN, S. C. & SNIDER, W. D. 1995. Presence or absence of TrKA protein distinguishes subsets of small

sensory neurons with unique cytochemical characteristics and dorsal horn projections. *The Journal of Comparative Neurology,* 361**,** 404-416.
MONTELL, C., BIRNBAUMER, L., FLOCKERZI, V., BINDELS, R. J., BRUFORD, E. A., CATERINA, M. J., CLAPHAM, D. E., HARTENECK, C., HELLER, S., JULIUS, D., KOJIMA, I., MORI, Y., PENNER, R., PRAWITT, D., SCHARENBERG, A. M., SCHULTZ, G. N., SHIMIZU, N. & ZHU, M. X. 2002. A Unified Nomenclature for the Superfamily of TRP Cation Channels. *Molecular cell,* 9**,** 229-231.
MOOR INSTRUMENTS. 2012. *Basic Theory and Operating Principles of Laser Doppler Blood Flow Monitoring and Imaging (LDF & LDI), Issue 1.* [Online]. Available: http://gb.moor.co.uk/product/moorldi2-laser-doppler-imager/8 [Accessed 27/2/2012 2012].
MORI, T., KABASHIMA, K., YOSHIKI, R., SUGITA, K., SHIRAISHI, N., ONOUE, A., KURODA, E., KOBAYASHI, M., YAMASHITA, U. & TOKURA, Y. 2008. Cutaneous hypersensitivities to hapten are controlled by IFN-gamma-upregulated keratinocyte Th1 chemokines and IFN-gamma-downregulated Langerhans cell Th2 chemokines. *Journal of Investigative Dermatology,* 128**,** 1719-1727.
MYERS, R. R., SEKIGUCHI, Y., KIKUCHI, S., SCOTT, B., MEDICHERLA, S., PROTTER, A. & CAMPANA, W. M. 2003. Inhibition of p38 MAP kinase activity enhances axonal regeneration. *Experimental Neurology,* 184**,** 606-614.
NAGY, I., SÁNTHA, P., JANCSÓ, G. & URBÁN, L. 2004. The role of the vanilloid (capsaicin) receptor (TRPV1) in physiology and pathology. *European Journal of Pharmacology,* 500**,** 351-369.
NAKAMURA, K., WILLIAMS, I. R. & KUPPER, T. S. 1995. Keratinocyte-derived monocyte chemoattractant protein 1 (MCP-1): analysis in a transgenic model demonstrates MCP-1 can recruit dendritic and Langerhans cells to skin. *Journal of Investigative Dermatology,* 105**,** 635-643.
NAVARRO, X., VIVÓ, M. & VALERO-CABRÉ, A. 2007. Neural plasticity after peripheral nerve injury and regeneration. *Progress in Neurobiology,* 82**,** 163-201.
NEEB, L., HELLEN, P., BOEHNKE, C., HOFFMANN, J., SCHUH-HOFER, S., DIRNAGLE, U. & REUTER, U. 2011. IL-1β stimulates COX-2 dependent PGE2 synthesis and CGRP release in rat trigeminal ganglia cells. *PLoS One,* 6**,** e17360.
NIIZEKI, H., ALARD, P. & STREILEIN, J. 1997. Calcitonin gene-related peptide is necessary for ultraviolet B-impaired induction of contact hypersensitivity. *The Journal of Immunology,* 159**,** 5183-5186.
NOGA, O., PEISER, M., ALTENAEHR, M., KNIELING, H., WANNER, R., HANF, G., GROSSE, R. & SUTTORP, N. 2007. Differential activation of dendritic cells by nerve growth factor and brain-derived neurotrophic factor. *Clinical and Experimental Allergy,* 37**,** 1701-1708.
NOLANO, M., PROVITERA, V., CAPORASO, G., STANCANELLI, A., VITALE, D. F. & SANTORO, L. 2010. Quantification of pilomotor nerves. *Neurology,* 75**,** 1089-1097.
NOMA, N., KHAN, J., CHEN, I. F., MARKMAN, S., BENOLIEL, R., HADLAQ, E., IMAMURA, Y. & ELIAV, E. 2011. Interleukin-17 levels in rat models of nerve damage and neuropathic pain. *Neuroscience Letters,* 493**,** 86-91.

O'CONNELL, P. J., PINGLE, S. C. & AHERN, G. P. 2005. Dendritic cells do not transduce inflammatory stimuli via the capsaicin receptor TRPV1. *Febs Letters,* 579**,** 5135-5139.

O'REILLY, V., ZENG, S. G., BRICARD, G., ATZBERGER, A., HOGAN, A. E., JACKSON, J., FEIGHERY, C., PORCELLI, S. A. & DOHERTY, D. G. 2011. Distinct and overlapping effector functions of expanded human CD4+, CD8α+ and CD4-CD8α- invariant natural killer T cells. *PLoS ONE,* 6**,** e28648.

OAKLANDER, A. L., STOCKS, E. A. & MOUTON, P. R. 2003. Number of Langerhans immune cells in painful and non-painful human skin after shingles. *Archives of Dermatological Research,* 294**,** 529-535.

OKA, T., OKA, K., HOSOI, M. & HORI, T. 1995. Intracerebroventricular injection of interleukin-6 induces thermal hyperalgesia in rats. *Brain Research,* 692**,** 123-128.

OPREE, A. & KRESS, M. 2000. Involvement of the proinflammatory cytokines tumor necrosis factor-alpha, IL-1 beta,and IL-6 but not IL-8 in the development of heat hyperalgesia: Effects on heat-evoked calcitonin gene-related peptide release from rat skin. *Journal of Neuroscience,* 20**,** 6289-6293.

OUWEHAND, K., SCHEPER, R. J., DE GRUIJL, T. D. & GIBBS, S. 2010. Epidermis-to-dermis migration of immature Langerhans cells upon topical irritant exposure is dependent on CCL2 and CCL5. *European Journal of Immunology,* 40**,** 2026-2034.

PARK, K. A., FEHRENBACHER, J. C., THOMPSON, E. L., DUARTE, D. B., HINGTGEN, C. M. & VASKO, M. R. 2010. Signaling pathways that mediate nerve growth factor-induced increase in expression and release of calcitonin gene-related peptide from sensory neurons. *Neuroscience,* 171**,** 910-923.

PARKINSON, D. B., BHASKARAN, A., ARTHUR-FARRAJ, P., NOON, L. A., WOODHOO, A., LLOYD, A. C., FELTRI, M. L., WRABETZ, L., BEHRENS, A., MIRSKY, R. & JESSEN, K. R. 2008. c-Jun is a negative regulator of myelination. *Journal of Cell Biology,* 181**,** 625-637.

PECK, A. & MELLINS, E. D. 2009. Breaking old paradigms: Th17 cells in autoimmune arthritis. *Clinical Immunology,* 132**,** 295-304.

PELESHOK, J. C. & RIBEIRO-DA-SILVA, A. 2011. Delayed reinnervation by nonpeptidergic nociceptive afferents of the glabrous skin of the rat hindpaw in a neuropathic pain model. *The Journal of Comparative Neurology,* 519**,** 49-63.

PEREIRA, C. S., AZEVEDO, O., MAIA, M. L., DIAS, A. F., SA-MIRANDA, C. & MACEDO, M. F. 2013. Invariant natural killer T cells are phenotypically and functionally altered in Fabry disease. *Molecular Genetics and Metabolism,* 108**,** 241-248.

PERRY, M. J. & LAWSON, S. N. 1998. Differences in expression of oligosaccharides, neuropeptides, carbonic anhydrase and neurofilament in rat primary afferent neurons retrogradely labelled via skin, muscle or visceral nerves. *Neuroscience,* 85**,** 293-310.

PERTENS, E., URSCHEL-GYSBERS, B. A., HOLMES, M., PAL, R., FOERSTER, A., KRIL, Y. & DIAMOND, J. 1999. Intraspinal and behavioral consequences of

nerve growth factor-induced nociceptive sprouting and nerve growth factor-induced hyperalgesia compared in adult rats. *The Journal of Comparative Neurology,* 410**,** 73-89.

PETERS, E. M. J., BOTCHKAREV, V. A., BOTCHKAREVA, N. V., TOBIN, D. J. & PAUS, R. 2001. Hair-cycle-associated remodeling of the peptidergic innervation of murine skin, and hair growth modulation by neuropeptides. *Journal of Investigative Dermatology,* 116**,** 236-245.

PETERS, E. M. J., ERICSON, M. E., HOSOI, J., SEIFFERT, K., HORDINSKY, M. K., ANSEL, J. C., PAUS, R. & SCHOLZEN, T. E. 2006. Neuropeptide control mechanisms in cutaneous biology: Physiological and clinical significance. *Journal of Investigative Dermatology,* 126**,** 1937-1947.

PETERSEN, L. J., KRISTENSEN, J. K. & BÜLOW, J. 1992. Microdialysis of the interstitial water space in human skin *in vivo*: quantitative measurement of cutaneous glucose concentrations. *Journal of Investigative Dermatology,* 99**,** 357-360.

PEZET, S. & MCMAHON, S. B. 2006. Neurotrophins: Mediators and modulators of pain. *Annual Review of Neuroscience,* 29**,** 507-538.

PIETRZAK, A., MISIAK-TLOCZEK, A. & BRZEZIŃSKA-BLASZCZYK, E. 2009. Interleukin (IL)-10 inhibits RANTES-, tumour necrosis factor (TNF)- and nerve growth factor (NGF)-induced mast cell migratory response but is not a mast cell chemoattractant. *Immunology Letters,* 123**,** 46-51.

PINCELLI, C., FANTINI, F., GIARDINO, L., ZANNI, M., CALZA, L., SEVIGNANI, C. & GIANNETTI, A. 1993. Autoradiographic detection of substance P receptors in normal and psoriatic skin. *Journal of Investigative Dermatology,* 101**,** 301-304.

PINCELLI, C., SEVIGNANI, C., MANFREDINI, R., GRANDE, A., FANTINI, F., BRACCI-LAUDIERO, L., ALOE, L., FERRARI, S., COSSARIZZA, A. & GIANNETTI, A. 1994. Expression and function of nerve growth factor and nerve growth factor receptor on cultured keratinocytes. *Journal of Investigative Dermatology,* 103**,** 13-18.

PIOTROWSKI, W. & FOREMAN, J. C. 1986. Some effects of calcitonin gene-related peptide in human skin and on histamine release. *British Journal of Dermatology,* 114**,** 37-46.

PIZZIRANI, C., FERRARI, D., CHIOZZI, P., ADINOLFI, E., SANDONv†, D., SAVAGLIO, E. & DI VIRGILIO, F. 2007. Stimulation of P2 receptors causes release of IL-1v ü¬ñloaded microvesicles from human dendritic cells. *Blood,* 109**,** 3856-3864.

PLANELLS-CASES, R. & FERRER-MONTIEL, A. 2007. TRP channel trafficking. *In:* LIEDTKE, W. B. & HELLER, S. (eds.) *TRP ion channel function in sensory transduction and cellular signalling cascades.* Boca Raton: CRC Press.

POOLE, S., CUNHA, F. Q., SELKIRK, S., LORENZETTI, B. B. & FERREIRA, S. H. 1995. Cytokine-mediated iflammatory hyperalgesia limited by interleukin-10. *British Journal of Pharmacology,* 115**,** 684-688.

QIN, X., WAN, Y. & WANG, X. 2005. CCL2 and CXCL1 trigger calcitonin gene-related peptide release by exciting primary nociceptive neurons. *Journal of Neuroscience Research,* 82**,** 51-62.

QIN, Y., HUA, M., DUAN, Y., GAO, Y., SHAO, X., WANG, H., TAO, T., SHEN, A. & CHENG, C. 2012. TNF-α Expression in Schwann Cells is Induced by LPS and NF-κB-Dependent Pathways. *Neurochemical Research***,** 1-10.

RAEDLER, T. J. 2011. Inflammatory mechanisms in major depressive disorder. *Current Opinion in Psychiatry,* 24**,** 519-525.

RAIVICH, G. 2008. c-Jun Expression, activation and function in neural cell death, inflammation and repair. *Journal of Neurochemistry,* 107**,** 898-906.

RAMER, M. S., MURPHY, P. G., RICHARDSON, P. M. & BISBY, M. A. 1998. Spinal nerve lesion-induced mechanoallodynia and adrenergic sprouting in sensory ganglia are attenuated in interleukin-6 knockout mice. *Pain,* 78**,** 115-121.

REYES-ESCOGIDO, M. D., GONZALEZ-MONDRAGON, E. G. & VAZQUEZ-TZOMPANTZI, E. 2011. Chemical and pharmacological aspects of capsaicin. *Molecules,* 16**,** 1253-1270.

RICE, F. L. & ALBRECHT, P. J. 2008. Cutaneous mechanisms of tactile perception: morphological and chemical organisation of innervation to the skin. *In:* KAAS, J. H. & GARDNER, E. (eds.) *The senses: a comprehensive reference.* New York: Elsevier.

ROLKE, R., BARON, R., MAIER, C., TOLLE, T. R., TREEDE, R. D., BEYER, A., BINDER, A., BIRBAUMER, N., BIRKLEIN, F., BOTEFUR, I. C., BRAUNE, S., FLOR, H., HUGE, V., KLUG, R., LANDWEHRMEYER, G. B., MAGERL, W., MAIHOFNER, C., ROLKO, C., SCHAUB, C., SCHERENS, A., SPRENGER, T., VALET, M. & WASSERKA, B. 2006. Quantitative sensory testing in the German Research Network on Neuropathic Pain (DFNS): Standardized protocol and reference values. *Pain,* 123**,** 231-243.

ROOSTERMAN, D., GOERGE, T., SCHNEIDER, S. W., BUNNETT, N. W. & STEINHOFF, M. 2006. Neuronal control of skin function: The skin as a neuroimmunoendocrine organ. *Physiological Reviews,* 86**,** 1309-1379.

ROSENBAUM, T., GORDON-SHAAG, A., MUNARI, M. & GORDON, S. E. 2004. Ca2+/Calmodulin modulates TRPV1 activation by capsaicin. *The Journal of General Physiology,* 123**,** 53-62.

ROSENBAUM, T. & SIMON, S. A. 2007. TRPV1 receptors and signal transduction. *In:* LIEDTKE, W. B. & HELLER, S. (eds.) *TRP ion channel function in sensory transduction and cellular signalling cascades.* Boca Raton: CRC Press.

RUSSELL, F. A., FERNANDES, E. S., COURADE, J. P., KEEBLE, J. E. & BRAIN, S. D. 2009. Tumour necrosis factor alpha mediates transient receptor potential vanilloid 1-dependent bilateral thermal hyperalgesia with distinct peripheral roles of interleukin-1·, protein kinase C and cyclooxygenase-2 signalling. *Pain,* 142**,** 264-274.

SANMIGUEL, J. C., OLARU, F., LI, J., MOHR, E. & JENSEN, L. E. 2009. Interleukin-1 regulates keratinocyte expression of T cell targeting chemokines through interleukin-1 receptor associated kinase-1 (IRAK1) dependent and independent pathways. *Cellular Signalling,* 21**,** 685-694.

SAPORTA, M. A. 2014. Charcot-Marie Tooth disease and other inherited neuropathies. *Continuum,* 20**,** 1208-1225.

SAUERSTEIN, K., KLEDE, M., HILLIGES, M. & SCHMELZ, M. 2000. Electrically evoked neuropeptide release and neurogenic inflammation differ

between rat and human skin. *Journal of Physiology-London,* 529**,** 803-810.

SCHAFERS, M., SVENSSON, C. I., SOMMER, C. & SORKIN, L. S. 2003. Tumor necrosis factor-alpha induces mechanical allodynia after spinal nerve ligation by activation of p38 MAPK in primary sensory neurons. *Journal of Neuroscience,* 23**,** 2517-2521.

SCHIFFMANN, R., FLOETER, M. K., DAMBROSIA, J. M., GUPTA, S., MOORE, D. F., SHARABI, Y., KHURANA, R. K. & BRADY, R. O. 2003. Enzyme replacement therapy improves peripheral nerve and sweat function in Fabry disease. *Muscle & Nerve,* 28**,** 703-710.

SCHIFFMANN, R., HAUER, P., FREEMAN, B., RIES, M., SCOTT, L. J. C., POLYDEFKIS, M., BRADY, R. O., MCARTHUR, J. C. & WAGNER, K. 2006. Enzyme replacement therapy and intraepidermal innervation density in Fabry disease. *Muscle & Nerve,* 34**,** 53-56.

SCHIFFMANN, R., KOPP, J. B., AUSTIN, H. A. R., SABNIS, S., MOORE, D. F., WEIBEL, T., BALOW, J. E. & BRADY, R. O. 2001. Enzyme replacement therapy in fabry disease: A randomized controlled trial. *JAMA: The Journal of the American Medical Association,* 285**,** 2743-2749.

SCHIFFMANN, R. & SCOTT, L. J. C. 2002. Pathophysiology and assessment of neuropathic pain in Fabry disease. *Acta Pædiatrica,* 91**,** 48-52.

SCHMELZ, M. 2009. Translating nociceptive processing into human pain models. *Experimental Brain Research,* 196**,** 173-178.

SCHMELZ, M., LUZ, O., AVERBECK, B. & BICKEL, A. 1997. Plasma extravasation and neuropeptide release in human skin as measured by intradermal microdialysis. *Neuroscience Letters,* 230**,** 117-120.

SCHMELZ, M., MICHAEL, K., WEIDNER, C., SCHMIDT, R., TOREBJÖRK, H. E. & HANDWERKER, H. O. 2000. Which nerve fibres mediate the axon reflex flare in human skin? *Neuroreport***,** 645-648.

SCHMELZ, M. & SCHMIDT, R. 2010. Microneurographic single-unit recordings to assess receptive properties of afferent human C-fibers. *Neuroscience Letters,* 470**,** 158-161.

SCHMELZ, M., SCHMIDT, R., WEIDNER, C., HILLIGES, M., TOREBJÖRK, H. E. & HANDWERKER, H. O. 2003. Chemical response pattern of different classes of C-nociceptors to pruritogens and algogens. *Journal of Neurophysiology,* 89**,** 2441-2448.

SCHMELZ, M., ZECK, S., RAITHEL, M. & RUKWIED, R. 1999. Mast cell tryptase in dermal neurogenic inflammation. *Clinical & Experimental Allergy,* 29**,** 652-659.

SCHMIDT, H. & RATHJEN, F. G. 2011. DiI-Labeling of DRG Neurons to study axonal branching in a whole mount preparation of mouse embryonic spinal cord. *Journal of Visualized Experiments,* 58**,** 3667.

SCHNETZ, E. & FARTASCH, M. 2001. Microdialysis for the evaluation of penetration through the human skin barrier -- a promising tool for future research? *European Journal of Pharmaceutical Sciences,* 12**,** 165-174.

SCHOLZEN, T., ARMSTRONG, C. A., BUNNETT, N. W., LUGER, T. A., OLERUD, J. E. & ANSEL, J. C. 1998. Neuropeptides in the skin: interactions between the

neuroendocrine and the skin immune systems. *Experimental Dermatology,* 7**,** 81-96.

SCOTT, L. J. C., GRIFFIN, J. W., LUCIANO, C. A., BARTON, N. W., BANERJEE, T., CRAWFORD, T., MCARTHUR, J. C., TOURNAY, A. & R., S. 1999. Quantitative analysis of epidermal innervation in Fabry disease. *Neurology,* 52**,** 1249-1254.

SHAMASH, S., REICHERT, F. & ROTSHENKER, S. 2002. The cytokine network of Wallerian degeneration: Tumor necrosis factor-alpha, Interleukin-1 alpha, and Interleukin-1 beta. *The Journal of Neuroscience,* 22**,** 3052-3060.

SHEPHERD, A. J., DOWNING, J. E. G. & MIYAN, J. A. 2005. Without nerves, immunology remains incomplete - in vivo veritas. *Immunology,* 116**,** 145-163.

SHIM, W.-S., TAK, M.-H., LEE, M.-H., KIM, M., KIM, M., KOO, J.-Y., LEE, C.-H., KIM, M. & OH, U. 2007. TRPV1 mediates histamine-induced itching via the activation of phospholipase A2 and 12-lipoxygenase. *The Journal of Neuroscience,* 27**,** 2331-2337.

SHIN, J., CHO, H., HWANG, S. W., JUNG, J., SHIN, C. Y., LEE, S.-Y., KIM, S. H., LEE, M. G., CHOI, Y. H., KIM, J., HABER, N. A., REICHLING, D. B., KHASAR, S., LEVINE, J. D. & OH, U. 2002. Bradykinin-12-lipoxygenase-VR1 signaling pathway for inflammatory hyperalgesia. *Proceedings of the National Academy of Sciences,* 99**,** 10150-10155.

SHIPTON, E. A. 2013. Skin Matters: Identifying pain mechanisms and predicting treatment outcomes. *Neurology Research International,* 2013**,** 329364.

SHU, X.-Q. & MENDELL, L. M. 1999. Neurotrophins and hyperalgesia. *Proceedings of the National Academy of Sciences,* 96**,** 7693-7696.

SHY, M. E., SHI, Y., WRABETZ, L., KAMHOLZ, J. & SCHERER, S. S. 1996. Axon-Schwann cell interactions regulate the expression of c-jun in Schwann cells. *Journal of Neuroscience Research,* 43**,** 511-525.

SIAU, C., XIAO, W. H. & BENNETT, G. J. 2006. Paclitaxel- and vincristine-evoked painful peripheral neuropathies: Loss of epidermal innervation and activation of Langerhans cells. *Experimental Neurology,* 201**,** 507-514.

SIMONE, D. A., BAUMANN, T. K. & LAMOTTE, R. H. 1989. Dose-dependent pain and mechanical hyperalgesia in humans after intradermal injection of capsaicin. *Pain,* 38**,** 99-107.

SJÖGREN, F. & ANDERSON, C. 2009. Sterile trauma to normal human dermis invariably induces IL1beta, IL6 and IL8 in an innate response to "danger". *Acta Dermato-Venereologica,* 89**,** 459-465.

SOMMER, C. & LAURIA, G. 2007. Skin biopsy in the management of peripheral neuropathy. *Lancet Neurology,* 6**,** 632-642.

SOMMER, C. & SCHÄFERS, M. 2004. Mechanisms of neuropathic pain: the role of cytokines. *Drug Discovery Today: Disease Mechanisms,* 1**,** 441-448.

SORKIN, L. S. & DOOM, C. M. 2000. Epineurial application of TNF elicits an acute mechanical hyperalgesia in the awake rat. *Journal of the Peripheral Nervous System,* 5**,** 96-100.

SORKIN, L. S., XIAO, W. H., WAGNER, R. & MYERS, R. R. 1997. Tumour necrosis factor-alpha induces ectopic activity in nociceptive primary afferent fibres. *Neuroscience,* 81**,** 255-262.

SOUSLOVA, V., CESARE, P., DING, Y., AKOPIAN, A. N., STANFA, L., SUZUKI, R., CARPENTER, K., DICKENSON, A., BOYCE, S., HILL, R., NEBENIUS-OOSTHUIZEN, D., SMITH, A. J. H., KIDD, E. J. & WOOD, J. N. 2000. Warm-coding deficits and aberrant inflammatory pain in mice lacking P2X3 receptors. *Nature,* 407**,** 1015-1017.

SOUTHALL, M. D., LI, T., GHARIBOVA, L. S., PEI, Y., NICOL, G. D. & TRAVERS, J. B. 2003. Activation of epidermal vanilloid receptor-1 induces release of proinflammatory mediators in human keratinocytes. *Journal of Pharmacology and Experimental Therapeutics,* 304**,** 217-222.

STÄNDER, S., MOORMANN, C., SCHUMACHER, M., BUDDENKOTTE, J., ARTUC, M., SHPACOVITCH, V., BRZOSKA, T., LIPPERT, U., HENZ, B. M., LUGER, T. A., METZE, D. & STEINHOFF, M. 2004. Expression of vanilloid receptor subtype 1 in cutaneous sensory nerve fibers, mast cells, and epithelial cells of appendage structures. *Experimental Dermatology,* 13**,** 129-139.

STANKOVIC, N., JOHANSSON, O. & HILDEBRAND, C. 1999. Increased occurrence of PGP 9.5-immunoreactive epidermal Langerhans cells in rat plantar skin after sciatic nerve injury. *Cell and Tissue Research,* 298**,** 255-260.

ŠTEMPELJ, M. & FERJAN, I. 2005. Signaling pathway in nerve growth factor induced histamine release from rat mast cells. *Inflammation Research,* 54**,** 344-349.

STUCKY, C. L. & LEWIN, G. R. 1999. Isolectin B4-positive and -negative nociceptors are functionally distinct. *The Journal of Neuroscience,* 19**,** 6497-6505.

SUGIURA, T., TOMINAGA, M., KATSUYA, H. & MIZUMURA, K. 2002. Bradykinin lowers the threshold temperature for heat activation of vanilloid receptor 1. *Journal of Neurophysiology,* 88**,** 544-548.

SUH, Y.-G. & OH, U. 2005. Activation and activators of TRPV1 and their pharmaceutical implication. *Current Pharmaceutical Design,* 11**,** 2687-2698.

SZALLASI, A. & BLUMBERG, P. M. 2007. Complex regulation of TRPV1 by vanilloids. *In:* LIEDTKE, W. B. & HELLER, S. (eds.) *TRP ion channel function in sensory transduction and cellular signalling cascades.* Boca Raton: CRC Press.

SZOLCSÁNYI, J. 1993. Actions of capsaicin on sensory receptors. *In:* WOOD, J. (ed.) *Capsaicin in the study of pain.* London: Acdemic Press.

TAKAHASHI, K., NAKANISHI, S. & IMAMURA, S. 1993. Direct effects of cutaneous neuropeptides on adenylyl cyclase activity and proliferation in a keratinocyte cell line: stimulation of cyclic AMP formation by CGRP and VIP/PHM, and inhibition by NPY through G protein-coupled receptors. *Journal of Investigative Dermatology,* 101**,** 646-651.

TAN, S. V., LEE, P. J., WALTERS, R. J. L., MEHTA, A. & BOSTOCK, H. 2005. Evidence for motor axon depolarization in Fabry disease. *Muscle & Nerve,* 32**,** 548-551.

TAVAKOLI, M., BOULTON, A. J. M., EFRON, N. & MALIK, R. A. 2011. Increased Langerhan cell density and corneal nerve damage in diabetic patients: Role of immune mechanisms in human diabetic neuropathy. *Contact Lens and Anterior Eye,* 34**,** 7-11.

TAYLOR, A. M., PELESHOK, J. C. & RIBEIRO-DA-SILVA, A. 2009. Distribution of P2X(3)-immunoreactive fibers in hairy and glabrous skin of the rat. *Journal of Comparative Neurology,* 514**,** 555-566.

TEUNISSEN, M. B. M. 2004. Langerhans cells and other skin dendritic cells. *In:* BOS, J. D. (ed.) *Skin immune system: Cutaneous immunology and clinical immunodermatology.* CRC Press.

THACKER, M. A., CLARK, A. K., MARCHAND, F. & MCMAHON, S. B. 2007. Pathophysiology of peripheral neuropathic pain: Immune cells and molecules. *Anesthesia & Analgesia,* 05**,** 838-847.

TOEBAK, M. J., ROOIJ, J., MOED, H., STOOD, T. J., VON BLOMBERG, B. M. E., BRUYNZEEL, D. P., SCHEPER, R. J., GIBBS, S. & RUSTEMEYER, T. 2008. Differential suppression of dendritic cell cytokine production by anti-inflammatory drugs. *British Journal of Dermatology,* 158**,** 225-233.

TOMINAGA, M., WADA, M. & MASU, M. 2001. Potentiation of capsaicin receptor activity by metabotropic ATP receptors as a possible mechanism for ATP-evoked pain and hyperalgesia. *Proceedings of the National Academy of Sciences,* 98**,** 6951-6956.

TORVIN MÖLLER, A., WINTHER BACH, F., FELDT-RASMUSSEN, U., RASMUSSEN, Å., HASHOLT, L., LAN, H., SOMMER, C., KØLVRAA, S., BALLEGAARD, M. & STAEHELIN JENSEN, T. 2009. Functional and structural nerve fiber findings in heterozygote patients with Fabry disease. *PAIN¬Æ,* 145**,** 237-245.

TOTH, B. I., BENKO, S., SZOLLOSI, A. G., KOVACS, L., RAJNAVOLGYI, E. & BIRO, T. 2009. Transient receptor potential vanilloid-1 signaling inhibits differentiation and activation of human dendritic cells. *FEBS Letters,* 583**,** 1619-1624.

TOYODA, M., LUO, Y., MAKINO, T., MATSUI, C. & MOROHASHI, M. 1999. Calcitonin gene-related peptide upregulates melanogenesis and enhances melanocyte dendricity via induction of keratinocyte-derived melanotrophic factors. *Journl of Investigative Dermatology Symposium Proceedings,* 4**,** 116-25.

TRAN, J. N. S. N., PUPOVAC, A., TAYLOR, R. M., WILEY, J. S., BYRNE, S. N. & SLUYTER, R. 2010. Murine epidermal Langerhans cells and keratinocytes express functional P2X7 receptors. *Experimental Dermatology,* 19**,** e151-e157.

TREEDE, R.-D., MEYER, R. A., RAJA, S. N. & CAMPBELL, J. N. 1992. Peripheral and central mechanisms of cutaneous hyperalgesia. *Progress in Neurobiology,* 38**,** 397-421.

TROJABORG, W., HAYS, A. P., VAN DEN BERG, L., YOUNGER, D. S. & LATOV, N. 1995. Motor conduction parameters in neuropathies associated with anti-mag antibodies and other types of demyelinating and axonal neuropathies. *Muscle & Nerve,* 18**,** 730-735.

ÜÇEYLER, N., EBERLE, T., ROLKE, R., BIRKLEIN, F. & SOMMER, C. 2007a. Differential expression patterns of cytokines in complex regional pain syndrome. *Pain,* 132**,** 195-205.

ÜÇEYLER, N., HE, L., SCHÖNFELD, D., KAHN, A.-K., REINERS, K., HILZ, M. J., BREUNIG, F. & SOMMER, C. 2011. Small fibers in Fabry disease: baseline and follow-up data under enzyme replacement therapy. *Journal of the Peripheral Nervous System,* 16**,** 304-314.

ÜÇEYLER, N., KAFKE, W., RIEDIGER, N., HE, L., NECULA, G., TOYKA, K. V. & SOMMER, C. 2010. Elevated proinflammatory cytokine expression in affected skin in small fiber neuropathy. *Neurology,* 74**,** 1806-1813.

ÜÇEYLER, N., ROGAUSCH, J. P., TOYKA, K. V. & SOMMER, C. 2007b. Differential expression of cytokines in painful and painless neuropathies. *Neurology,* 69**,** 42-49.

ÜÇEYLER, N., ROGAUSCH, J. P., TOYKA, K. V. & SOMMER, C. 2007c. Differential expression of cytokines in painful and painless neuropathies. *Neurology,* 69**,** 42-49.

ÜÇEYLER, N., SCHAFERS, M. & SOMMER, C. 2009. Mode of action of cytokines on nociceptive neurons. *Experimental Brain Research,* 196**,** 67-78.

ÜÇEYLER, N., TSCHARKE, A. & SOMMER, C. 2007d. Early cytokine expression in mouse sciatic nerve after chronic constriction nerve injury depends on calpain. *Brain Behavior and Immunity,* 21**,** 553-560.

UNGERSTEDT, U. 1984. Measurement of neurotransmitter release by intracranial dialysis. *In:* MARSDEN, C. A. (ed.) *Measurement of neurotransmitter release in vivo.* Chichester: John Wiley & Sons.

URBANOWSKA, T., MANGIALAIO, S., ZICKLER, C., CHEEVAPRUK, S., HASLER, P., REGENASS, S. & LEGAY, F. 2006. Protein microarray platform for the multiplex analysis of biomarkers in human sera. *Journal of Immunological Methods,* 316**,** 1-7.

VAY, L., GU, C. & MCNAUGHTON, P. A. 2012. The thermo-TRP ion channel family: properties and therapeutic implications. *British Journal of Pharmacology,* 165**,** 787-801.

VIGNA, S. R., SHAHID, R. A., NATHAN, J. D., MCVEY, D. C. & LIDDLE, R. A. 2011. Leukotriene B4 mediates inflammation via TRPV1 in duct obstruction-induced pancreatitis in rats. *Pancreas,* 40**,** 708-714.

VINCENT, A. M., CALLAGHAN, B. C., SMITH, A. L. & FELDMAN, E. L. 2011. Diabetic neuropathy: cellular mechanisms as therapeutic targets. *Nature Reviews Neurology,* 7**,** 573-583.

VITAL, A., VITAL, C. & MALEVILLE, J. 1984. Fabry's disease: an ultrastructural study of muscle and peripheral nerve. *Clinical Neuropathology,* 3**,** 168-72.

VULCHANOVA, L., OLSON, T. H., STONE, L. S., RIEDL, M. S., ELDE, R. & HONDA, C. N. 2001. Cytotoxic targeting of isolectin IB4-binding sensory neurons. *Neuroscience,* 108**,** 143-155.

WAGNER, R., JANJIGIAN, M. & MYERS, R. R. 1998. Anti-inflammatory interleukin-10 therapy in CCI neuropathy decreases thermal hyperalgesia, macrophage recruitment, and endoneurial TNF-alpha expression. *Pain,* 74**,** 35-42.

WAGNER, R. & MYERS, R. R. 1996. Endoneurial injection of TNF-alpha produces neuropathic pain behaviors. *NeuroReport,* 7**,** 2897-2901.

WALLENGREN, J. & SUNDLER, F. 2004. Phototherapy reduces the number of epidermal and CGRP-positive dermal nerve fibres. *Acta Dermato-Venereologica,* 84**,** 111-115.

WANG, L. X., HILLIGES, M., JERNBERG, T., WIEGLEBEDSTROM, D. & JOHANSSON, O. 1990. Protein gene-product 9.5-immunoreactive nerve-fibers and cells in human skin. *Cell and Tissue Research,* 261**,** 25-33.

WEIDNER, C., KLEDE, M., RUKWIED, R., LISCHETZKI, G., NEISIUS, U., SKOV, P. S., PETERSEN, L. J. & SCHMELZ, M. 2000. Acute effects of Substance P and calcitonin gene-related peptide in human skin - A Microdialysis Study. *Journal of Investigative Dermatology,* 115**,** 1015-1020.

WHITE, F. A., FELDMAN, P. & MILLER, R. J. 2009. Chemokine signaling and the management of neuropathic pain. *Molecular Interventions,* 9**,** 188-195.

WHITTON, J. T. & EVERALL, J. D. 1973. The thickness of the epidermis. *British Journal of Dermatology,* 89**,** 467-476.

WILCOX, W. R., OLIVEIRA, J. O. P., HOPKIN, R. J., ORTIZ, A., BANIKAZEMI, M., FELDT-RASMUSSEN, U., SIMS, K., WALDEK, S., PASTORES, G. M., LEE, P., ENG, C. M., MARODI, L., STANFORD, K. E., BREUNIG, F., WANNER, C., WARNOCK, D. G., LEMAY, R. M. & GERMAIN, D. P. 2008. Females with Fabry disease frequently have major organ involvement: Lessons from the Fabry Registry. *Molecular Genetics and Metabolism,* 93**,** 112-128.

WOLF, G., GABAY, E., TAL, M., YIRMIYA, R. & SHAVIT, Y. 2006. Genetic impairment of interleukin-1 signaling attenuates neuropathic pain, autotomy, and spontaneous ectopic neuronal activity, following nerve injury in mice. *Pain,* 120**,** 315-324.

XUE, Q., JONG, B., CHEN, T. & SCHUMACHER, M. A. 2007. Transcription of rat TRPV1 utilizes a dual promoter system that is positively regulated by nerve growth factor. *Journal of Neurochemistry,* 101**,** 212-222.

YAMAMOTO, K., SOBUE, G., IWASE, S., KUMAZAWA, K., MITSUMA, T. & MANO, T. 1996. Possible mechanisms of anhidrosis in a symptomatic female carrier of Fabry's disease: an assessment by skin sympathetic nerve activity and sympathetic skin response. *Clinical Autonomic Research,* 6**,** 107-10.

YOSHIKI, R., KABASHIMA, K., SAKABE, J., SUGITA, K., BITO, T., NAKAMURA, M., MALISSEN, B. & TOKURA, Y. 2010. The mandatory role of IL-10-producing and OX40 ligand-expressing mature Langerhans cells in local UVB-induced immunosuppression. *Journal of Immunology,* 184**,** 5670-5677.

YU, X.-J., LI, C.-Y., XU, Y.-H., CHEN, L.-M. & ZHOU, C.-L. 2009. Calcitonin gene-related peptide increases proliferation of human HaCaT keratinocytes by activation of MAP kinases. *Cell Biology International,* 33**,** 1144-1148.

ZARATE, Y. A. & HOPKIN, R. J. 2008. Lysosomal storage disease 3 - Fabry's disease. *Lancet,* 372**,** 1427-1435.

ZELENKA, M., SCHAFERS, M. & SOMMER, C. 2005. Intraneural injection of interleukin-1 beta and tumor necrosis factor-alpha into rat sciatic nerve

at physiological doses induces signs of neuropathic pain. *Pain,* 116**,** 257-263.

ZHANG, X., DAUGHERTY, S. L. & DE GROAT, W. C. 2011. Activation of CaMKII and ERK1/2 contributes to the time-dependent potentiation of Ca2+ response elicited by repeated application of capsaicin in rat DRG neurons. *American Journal of Physiology - Regulatory, Integrative and Comparative Physiology,* 300**,** R644-R654.

ZHANG, X., HUANG, J. & MCNAUGHTON, P. A. 2005. NGF rapidly increases membrane expression of TRPV1 heat-gated ion channels. *EMBO J,* 24**,** 4211-4223.

ZHU, W., GALOYAN, S. M., PETRUSKA, J. C., OXFORD, G. S. & MENDELL, L. M. 2004. A developmental switch in acute sensitization of small dorsal root ganglion (DRG) neurons to capsaicin or noxious heating by NGF. *Journal of Neurophysiology,* 92**,** 3148-3152.

ZHU, W. & OXFORD, G. S. 2011. Differential gene expression of neonatal and adult DRG neurons correlates with the differential sensitization of TRPV1 responses to nerve growth factor. *Neuroscience Letters,* 500**,** 192-196.

ZIGMOND, A. S. & SNAITH, R. P. 1983. The Hospital Anxiety and Depression Scale. *Acta Psychiatrica Scandinavica,* 67**,** 361-370.

ZWICK, M., DAVIS, B. M., WOODBURY, C. J., BURKETT, J. N., KOERBER, H. R., SIMPSON, J. F. & ALBERS, K. M. 2002. Glial cell line-derived neurotrophic factor is a survival factor for isolectin B4-positive, but not vanilloid receptor 1-positive, neurons in the mouse. *The Journal of Neuroscience,* 22**,** 4057-4065.

ZYLKA, M. J., RICE, F. L. & ANDERSON, D. J. 2005. Topographically distinct epidermal nociceptive circuits revealed by axonal tracers targeted to Mrgprd. *Neuron,* 45**,** 17-25.

Appendix 1: Scores and Scales used in Anderson-Fabry study

Neuropathic Pain Symptom Inventory (**NPSI)**

Q1. Does your pain feel like burning?

No burning 0 1 2 3 4 5 6 7 8 9 10 Worst burning imaginable

Q2. Does your pain feel like squeezing?

No squeezing 0 1 2 3 4 5 6 7 8 9 10 Worst squeezing imaginable

Q3. Does your pain feel like pressure?

No pressure 0 1 2 3 4 5 6 7 8 9 10 Worst pressure imaginable

Q4. During the past 24 h, your spontaneous pain has been present:

Select the response that best describes your case:

- Permanently □
- Between 8 and 12 h □
- Between 4 and 7 h □
- Between 1 and 3 h □
- Less than 1 h □

We wish to know if you have brief attacks of pain. For each of the following questions, please select the number that best describes the average severity of your painful attacks during the past 24 h. Select the number 0 if you have not felt such pain (circle one number only).

Q5. Does your pain feel like electric shocks?

No electric shocks 0 1 2 3 4 5 6 7 8 9 10 Worst electric shocks imaginable

Q6. Does your pain feel like stabbing?

No stabbing 0 1 2 3 4 5 6 7 8 9 10 Worst stabbing imaginable

Q7. During the past 24 h, how many of these pain attacks have you had?

Select the response that best describes your case

More than 20 □

Between 11 and 20 □

Between 6 and 10 □

Between 1 and 5 □

No pain attack □

We wish to know if you feel pain provoked or increased by brushing, pressure, contact with cold or warmth on the painful area. For each of the following questions, please select the number that best describes the average severity of your provoked pain during the past 24 h. Select the number 0 if you have not felt such pain (circle one number only).

Q8. Is your pain provoked or increased by brushing on the painful area?

No pain 0 1 2 3 4 5 6 7 8 9 10 Worst pain imaginable

Q9. Is your pain provoked or increased by pressure on the painful area?

No pain 0 1 2 3 4 5 6 7 8 9 10 Worst pain imaginable

Q10. Is your pain provoked or increased by contact with something cold on the painful area?

No pain 0 1 2 3 4 5 6 7 8 9 10 Worst pain imaginable

We wish to know if you feel abnormal sensations in the painful area. For each of the following questions, please select the number that best describes the average severity of your abnormal sensations during the past 24 h. Select the number 0 if your have not felt such sensation (circle one number only).

Q11. Do you feel pins and needles?

No pins & needles 0 1 2 3 4 5 6 7 8 9 10 Worst pins & needles imaginable

Q12. Do you feel tingling?

No tingling 0 1 2 3 4 5 6 7 8 9 10 Worst tingling imaginable

RESULTS

Total intensity score	Subscores
	Burning (superficial) spontaneous pain:
1. Q1 =	Q1 = /10
	Pressing (deep) spontaneous pain:
2. (Q2 + Q3) = /10	(Q2 + Q3)/2 =
	Paroxysmal pain:
3. (Q5 + Q6) = /10	(Q5 + Q6)/2 =
	Evoked pain:
4. (Q8 + Q9 + Q10) = /10	(Q8 + Q9 + Q10)/3 =
	Paraesthesia/dysaesthesia:
5. (Q11 + Q12) =	(Q11 + Q12)/2 = /10

(1 + 2 + 3 + 4 + 5) = /100

Hospital Anxiety and Depression Score (HAD)

Emotions play an important part in most illnesses. This questionnaire is designed to help us know how you feel.

Read each item and tick the reply which comes closest to how you have been feeling in the past week.

Don't take too long over each response; your immediate reaction to each item will probably be more accurate than a long thought out response.

A. I feel tense or 'wound up':

3 ☐ Most of the time
2 ☐ A lot of the time
1 ☐ From time to time, occasionally
0 ☐ Not at all

D. I still enjoy the things I used to enjoy:

0 ☐ Definitely as much
1 ☐ Not quite so much
2 ☐ Only a little
3 ☐ Hardly at all

A. I get a sort of frightened feeling as if something awful is about to happen:

3 ☐ Very definitely and quite badly
2 ☐ Yes, but not too badly
1 ☐ A little, but it doesn't worry me
0 ☐ Not at all

D. I can laugh and see the funny side of things:

0 ☐ As much as I always could
1 ☐ Not quite so much now
2 ☐ Definitely not so much now
3 ☐ Not at all

A. Worrying thoughts go through my mind:

3 ☐ A great deal of the time
2 ☐ A lot of the time
1 ☐ From time to time, but not too often
0 ☐ Only occasionally

D. I feel cheerful:

3 ☐ Not at all

2 ☐ Not often

1 ☐ Sometimes

0 ☐ Most of the time

A. I can sit at ease and feel relaxed:

0 ☐ Definitely

1 ☐ Usually

2 ☐ Not often

3 ☐ Not at all

D. I feel as if I am slowed down:

3 ☐ Nearly all the time

2 ☐ Very often

1 ☐ Sometimes

0 ☐ Not at all

A. I get a sort of frightened feeling like 'butterflies' in the stomach:

0 ☐ Not at all

1 ☐ Occasionally

2 ☐ Quite often

3 ☐ Very often

D. I have lost interest in my appearance:

3 ☐ Definitely

2 ☐ I don't care as much as I should

1 ☐ I may not take quite as much care

0 ☐ I take as much care as ever

A. I feel restless as if I have to be on the move:

3 ☐ Very much indeed

2 ☐ Quite a lot

1 ☐ Not very much

0 ☐ Not at all

D. I look forward with enjoyment to things:

0 ☐ As much as I ever did

1 ☐ Rather less than I used to

2 ☐ Definitely less than I used to

3 ☐ Hardly at all

A. I get sudden feelings of panic:

3 ☐ Very often indeed

2 ☐ Quite often

1 ☐ Not very often

0 ☐ Not at all

D. I can enjoy a good book or radio or TV program:

0 ☐ Often

1 ☐ Sometimes

2 ☐ Not often

3 ☐ Very seldom

A: _____ D: _____

0-7: normal; 8-10: borderline; 11-21: Abnormal

Pain Ratings:

The visual analogue scale (VAS) is used to rate the intensity and the unpleasantness of the pain. The examiner should ask the patient how intense and how unpleasant is the pain in a scale between 0 (= no pain; = no unpleasant sensation) and 10 (= worst pain imaginable; = as unpleasant sensation as you can imagine).

Pain Now:

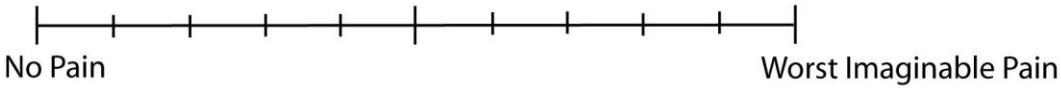

Average Pain score in Last Month:

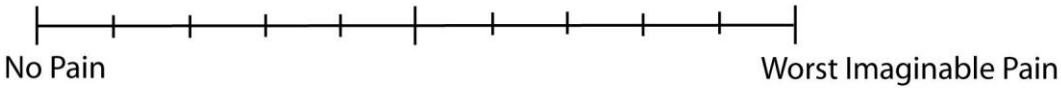

Worst Pain score in Last Month:

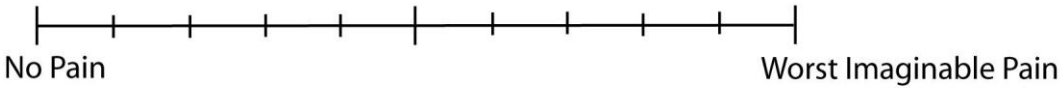

Lowest Pain score in the Last Month:

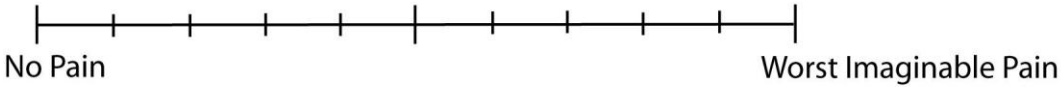

Inconvenience due to Pain: